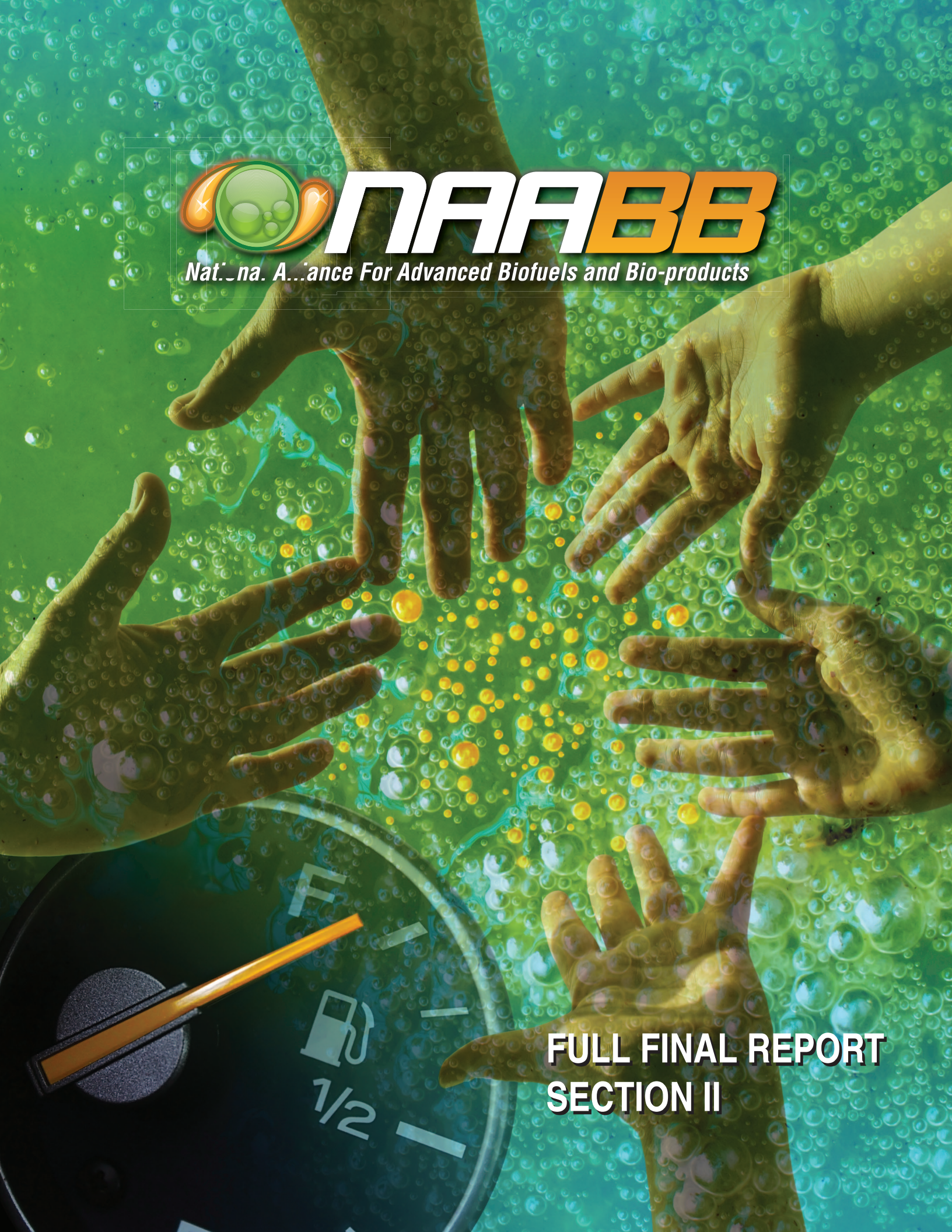




NAAABB

National Alliance For Advanced Biofuels and Bio-products



**FULL FINAL REPORT
SECTION II**

FULL FINAL REPORT
SECTION II
Team R&D Overview

Table of Contents

Algal Biology3

Cultivation60

Harvesting and Extraction89

Fuel Conversion 114

Agricultural Coproducts 144

Sustainability 167

ALGAL BIOLOGY



Introduction

Team Leads

Richard T. Sayre, Los Alamos National Laboratory and the New Mexico Consortium

Jon K. Magnuson, Pacific Northwest National Laboratory

Clifford J. Unkefer, Los Alamos National Laboratory

Preface

Unlike competing renewable energy production systems (wind, solar, or hydroelectric), biomass has the advantage that it can be converted into an energy-dense, liquid fuel feedstock (biocrude) that is compatible with current petroleum refinery technology. Recently, there has been substantial interest in the use of microalgae for sustainable production of biofuels. This is attributed to the ability of algae to produce 2- to 10-fold greater annual aerial biomass than terrestrial crops.¹⁻⁵ In addition, algae have the potential to capture inorganic carbon injected into ponds as CO₂ and hydrated to nongaseous bicarbonate, substantially reducing the potential residence time of CO₂ emitted from point sources in the atmosphere. With respect to fuel conversion technologies, algae are particularly attractive since many are facultatively capable of accumulating between 4% and 60% lipids by dry weight, making them one of the most efficient biofuel feedstock production systems.⁶ Various estimates indicate that potential oil and biomass yields from algal ponds range from 20,000–60,500 L/ha/year or 50,000–15,000 kgdw/ha/year, respectively³. Emerging developments in genetically modified algae promise to increase production yields by as much as 2- to 3-fold.⁷

In 2010, at the start of the National Alliance for Advanced Biofuels and Bioproducts (NAABB) consortium, little was known about the molecular basis of algal biomass or oil production. Very few algal genome sequences were available and efforts to identify the best-producing wild species through bioprospecting approaches had largely stalled since the efforts of the U.S. Department of Energy's Aquatic Species Program. Furthermore, algal genetic transformation and metabolic engineering approaches to improve biomass and oil yields were in their infancy. Genome sequencing and transcriptional profiling was becoming less expensive, however; and the tools to annotate gene expression profiles under various growth and engineered conditions were just starting to be developed for algae. It was in this context that an integrated Algal Biology task was developed for NAABB to address the greatest constraints limiting algal biomass yield. In the following sections, we describe our hypotheses, research objectives, and strategies to move algal biology into the 21st century and to realize the greatest potential of algae biomass systems to produce biofuels.

Approach

Our approach is outlined in Figure 1.1. Two potentially complementary approaches were explored to achieve these objectives, including bioprospecting algal diversity and/or genetic modification of algae to increase both yield and robustness while reducing energy and material inputs. Clearly, given the tremendous biological diversity of algae (>100,000 species) tremendous advantages can be achieved in meeting these objectives by identifying the most robust and productive strains that could be further improved through genetic engineering. Thus, our bioprospecting efforts focused on surveying the natural diversity of wild algal strains for production-relevant traits. Independently, substantial efforts were also focused on targeted transformations and directed engineering of high performance algae, which required a greater understanding of the molecular basis for the observed traits. Our systems biology and bioinformatics efforts included genome sequencing and transcriptomic, proteomic, and phenomic analyses. At each step in the process, we often found it necessary to develop new technologies or tools to address the unique biology of algae. To develop and test these tools, we often relied on model strains of algae whose genetics and molecular biology were well known. To meet these needs, we utilized the readily transformable model alga *Chlamydomonas reinhardtii*.

Highlights of our progress are listed below and form an outline of this report.

Algal Biology Task Framework

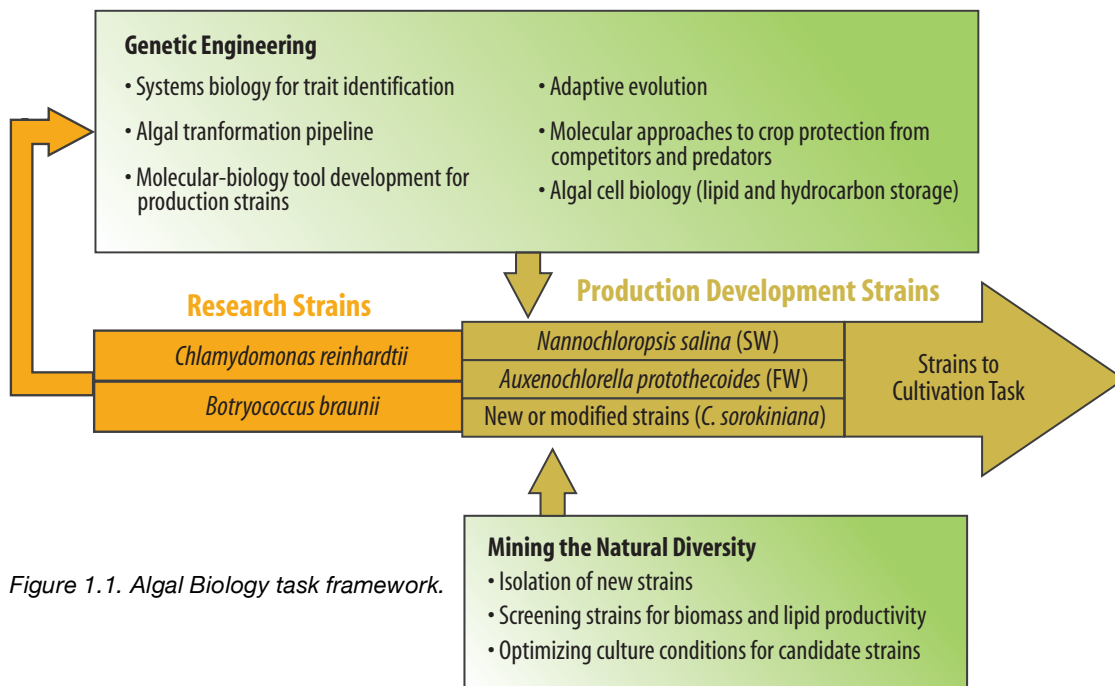


Figure 1.1. Algal Biology task framework.

Mining the Natural Diversity

- Developed a protocol for rapid screening of new strains for biomass accumulation and lipid production.
- Designed large-scale successful cultivation experiments that led to the identification of more robust and productive freshwater production strains than previously existed.
- Used gas chromatography-mass spectrometry (GC-MS) to characterize lipid profiles in the new strains.

Genome Sequencing and Systems Biology

- Developed robust standard operating procedures for the isolation of DNA, sequencing of genomes/transcriptomes, and bioinformatics analyses of complex algal genomes.
- Sequenced eight unique algal genomes representing three phyla, including broader diversity within green algae and stramenopiles.
- Used RNAseq deep sequencing methods to obtain >200 transcriptomes from different physiological states of the sequenced algae.
- Developed a transcriptome analysis pipeline.
- Developed advanced genetic tools for gene mapping and functional analysis of gene expression in *Chlamydomonas* and *Auxenochlorella protothecoides*.
- Developed a deeper understanding of algal biology, particularly regarding the physiology and biochemistry of lipid production including the identification of genes implicated to be involved in high lipid accumulation and demonstrated that stress genes were associated with lipid remodeling.
- Characterized the biosynthesis of the variety of hydrocarbons produced by *Botryococcus braunii* races.

Algal Transformation Pipeline

- Constructed an environmental photobioreactor (ePBR) array to simulate pond growth conditions and to screen phenotypes of environmental isolates and engineered algae under controlled conditions.
- Engineered over 50 independent gene constructs into *Chlamydomonas* using a standard operating procedure (transgenic pipeline) to transform, genotype, and characterize the transgene expression profiles and to phenotype genetically engineered algae.

Molecular Toolbox for Genetically Engineering Algae

- Enabled rapid development of nuclear transformation systems through genome sequencing in the production strains *A. protothecoides*, *Chlorella sorokiniana*, *Nannochloropsis salina* and *Picochlorum* sp.
- Enabled rapid development of plastid transformation systems through genome sequencing in the production strain *A. protothecoides*.



- Demonstrated that systems biology studies can be used to direct metabolic engineering in complex algal systems.
- Demonstrated improvement in oil accumulation in some cases without a deficit in biomass accumulation using a variety of metabolic engineering strategies in *Chlamydomonas*.
- Demonstrated production of triglycerides in a cyanobacterium.

Adaptive Evolution

- Demonstrated a screening protocol for selecting for high-lipid-content *Picochlorum* using boron-dipyrromethene (BODIPY) lipid staining and flow cytometry.
- Used chemostat selection for faster-growing *A. protothecoides* in lower-phosphate medium.

Crop Protection

- Identified bacterial consortia members present in cultivation ponds under defined growth conditions.
- Identified a biochemical mechanism to enable algae to resist rotifer predation to minimize pond crashes.
- Identified antimicrobial peptides that can minimize bacterial contamination in ponds.

Algal Cell Biology

- Gained a deeper understanding of lipid production in microalgae.
- Developed a clearer understanding of the role of lipid remodeling in triacylglyceride (TAG) accumulation.
- Developed a clearer understanding of the physiology of hydrocarbon accumulation in *Botryococcus*.

Technical Accomplishments

Mining the Natural Diversity

The most intensive NAABB bioprospecting effort focused on a relatively broad temporal and geographic sampling approach. The general flow of the approach is shown in Figure 1.2.

Approximately 400 samples were collected across the continental United States. From these samples, over 2200 independent strains were isolated, and over 1500 of those were subjected to a preliminary screen for oil accumulation. Samples were collected from the summer of 2010 through the spring of 2012 from various habitats, including nonaqueous (e.g., soil) substrates, freshwater, brackish water, marine, and hyper-saline environments. Freshwater habitats included manmade and natural waterways, while saline habitats included estuaries, inland salt lakes, shrimp ponds, algal raceways, and the coastal waters of Texas, California, New York, and Connecticut. The tactic of sampling across seasons from the same geographical sites was intended to isolate strains suitable for winter and summer cultivation.

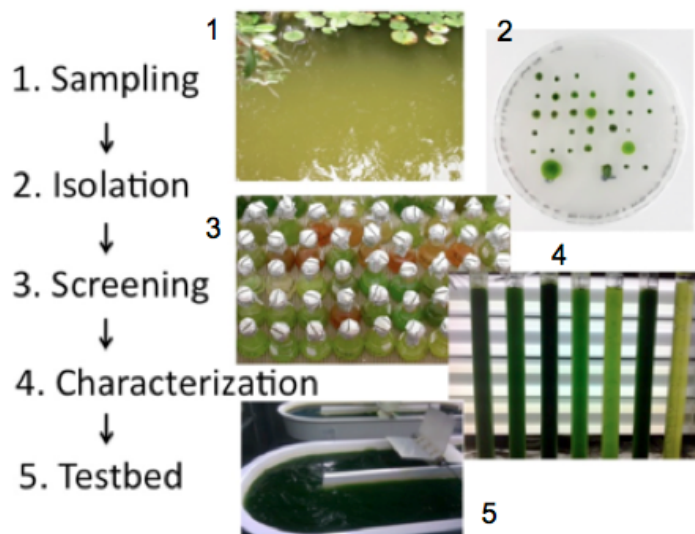


Figure 1.2. Flow diagram of the broad temporal, climatic, and geographic survey approach to isolation and characterization of algal biofuel candidate strains. Panel 1, an example sampling site; Panel 2, isolates from FACS on an agar plate; Panel 3, first-tier screening in traditional flask cultures; Panel 4, 100 mL bubble columns for characterizing the most promising candidates; Panel 5, 200 L NAABB testbeds.

Strains were isolated by traditional culture methods using a variety of growth media for initial plating and by high-throughput fluorescence-activated cell sorting (FACS) to screen for high lipid content. Since any approach introduces biases, screening algal isolates using multiple independent procedures increased the likelihood of recovering a broader diversity of isolates. Previously, it was observed that many strains of microalgae did not survive the cell sorting process; relying on this approach alone would therefore limit the diversity of the strains to be isolated. On the other hand, traditional cell culture techniques using petri dishes and multi-well plates are much slower and would not have provided the large numbers of strains necessary to meet NAABB goals and milestones. Combining these approaches provided wide diversity and large numbers of unialgal (not axenic) isolates.

Once we isolated the strains to apparent homogeneity, we carried out high-throughput screening using 96 well plates to identify strains that grew well autotrophically and that accumulated TAGs. Growth was monitored by optical density at 750 nm and the lipophilic dye Nile Red was used for fluorescence measurements of relative TAG content⁸

Further characterization of the best strains from the high-throughput screen was performed in shake flasks with a limited number of media differing 10-fold in the concentrations of N, P, and Fe to identify the best growth media for the highest oil yield. The best performing strains were then grown in bubble columns using growth media that allowed for the greatest oil yields (Panel 3 of Figure 1.2). Biomass productivity was measured by determining dry weight at a set harvest time and is compared to the biomass productivity of the benchmark strain, *N. salina* CCMP1776, which was a principal cultivated strain used by various NAABB teams. Unialgal strains that approximated or exceeded the biomass productivity of *N. salina* (Table 1.1) were deposited at the University of Texas (UTEX) and considered for large-scale cultivation. A few of these strains were tested on the 4-8 L scale in a greenhouse before final selection for cultivation in the test beds.

Table 1.1. Biomass productivity measured in a bubbling column.

Strain Classification	Initial Strain ID	NAABB Strain ID	Biomass Productivity* (g/L/d)
<i>N. salina</i> **	NA	NA	0.63
Chlorophyceae	DOE0101	NAABB1101	0.73
<i>Scenedesmus</i> sp.	DOE0111	NAABB1111	0.81
<i>Scenedesmus obliquus</i>	DOE0152	NAABB1152	0.89
Chlorophyceae	DOE0202	NAABB1202	0.86
Chlorophyceae	DOE0222	NAABB1222	0.70
<i>Ankistrodesmus</i> sp.	DOE0259	NAABB1259	0.56
Chlorellaceae	DOE0314	NAABB1314	0.61
Chlorophyta	DOE0623	NAABB1623	0.69
Chlorophyta	DOE0686	NAABB1686	0.78
Chlorellaceae	DOE0717	NAABB1717	0.78
Chlorophyta	DOE1044	NAABB2044	0.81
Chlorophyta	DOE1116	NAABB2095	1.00
Chlorophyta	DOE1357	NAABB2116	0.94
<i>Desmodesmus</i> sp.	DOE1357	NAABB2357	0.81
<i>Chlorella</i> sp	DOE1412	NAABB2412	0.65
Chlorophyceae	DOE1426	NAABB2426	0.84
Chlorophyta	DOE1727	NAABB2727	0.72
* Biomass productivity was measured as the ash-free dry weight produced per liter of culture medium per day and is expressed as g/L/d.			
** For comparison, the biomass productivity of <i>N. salina</i> strain CCMP1776 is given.			

Shown in Table 1.2, several strains were examined extensively by other consortium members and cultured in one or more of the NAABB testbed facilities. Cultivation results are discussed in the Algal Cultivation chapter of this report.

Table 1.2. Strains on which NAABB partners obtained significant data.

Classification	Strain ID	Culture Testing*	Sequencing**
<i>Chlorophyceae</i>	DOE0101	L, CS, G, P	G ^(LANL) & T ^(LANL)
<i>Scenedesmus obliquus</i>	DOE0152	L, CS, G, P	G ^(UCLA) & T ^(UCLA)
<i>Chlorella</i> sp.	DOE1412	L, CS, G, P	G ^(LANL) & T ^(LANL)

*Culture Testing: L–Laboratory testing in bubbling columns; CS–Climate-simulated laboratory culturing; G–intermediate scale growth in the green house; P–Growth in algal raceways at the Texas ArgiLife Research, Pecos, Texas site.

**Sequencing G–Genome Sequencing; T–Transcriptome sequencing.

Hundreds of algal strains were assembled into a catalogued culture collection. The 30 best production strains from this task were forwarded to UTEX to ensure that they would be available to the algal research community at large, thus meeting a NAABB final deliverable. This combination of new strain isolation and first testing in the laboratory combined with later testing in outdoor settings using multiple cultivation systems proved successful. Not all strains that were selected after laboratory screening and testing performed well in the testbed cultivation systems, but several algal strains could be successfully grown in testbed facilities. This positive result is in contrast to the previously published Aquatic Species Program report from 1998⁶, which indicated that it would be impossible to identify a successful combination of indoor isolation/screening/testing with outdoor strain performance.

Stramenopile Bioprospecting

A complementary approach to the previously described high-throughput strain isolation protocol was the in-depth characterization of fatty acids in a sampling of 29 oleaginous phototrophs from the under-studied but phylogenetically broad group of stramenopiles that includes *N. salina*. A simple, relatively high-throughput analytical method for the analysis of cellular fatty acid profiles was developed for this screening as well. To facilitate lipid analysis from small algal cultures, a sub-microscale *in situ* (SMIS) method for GC-MS analysis of fatty acids was developed^{9,10}. This method can be performed with less than 250 µg of dry algal biomass. It employs boron trifluoride catalyzed transesterification of lipids in methanol, followed by a two-step phase separation to recover the fatty acid methyl esters (FAMES). GC-MS analysis is performed relative to internal standards by single-ion quantitation.

The utility of this method was demonstrated by generating lipid profiles of 28 algal representatives within the stramenopile clade, the results of which are shown in Figure 1.3. The goal of

this study was to survey the entire chromalveolate cluster, with emphasis on the marginally assayed stramenopiles. The phylogeny represented in Figure 1.3 is based on our modified five-gene (*rnA*, *rbcl*, *psbA*, *psaA*, and *psbC*) phylogeny, which is based on that of Yang and coworkers¹¹. Most revealing is the fact that no distinct fatty acid pattern is immediately obvious at almost any taxonomic level. For example, *Chatonella* and *Heterosigma*, members of the small class Raphididophyceae, exhibit markedly different lipid profiles. Similarly, five members of the

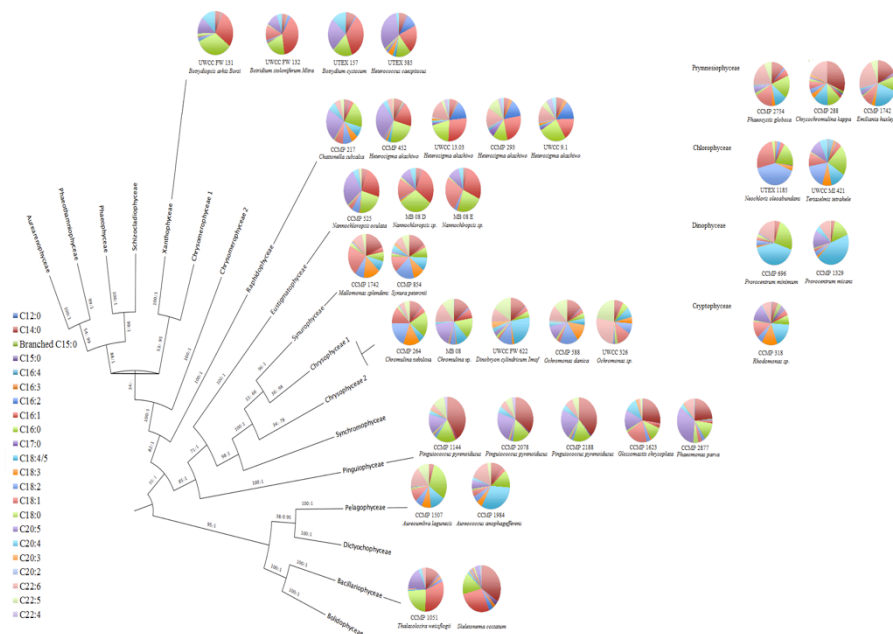


Figure 1.3. Lipid profiles determined using the micro-GC-MS technique of representative taxa appended to a modified stramenopile phylogeny based on our five-gene phylogeny¹.

Pinguiophyceae class exhibit different lipid profiles. Though cultures were grown identically and harvested at the stationary phase, the lack of fatty acid pattern reproducibility is also seen at the strain level. When phyla outside the stramenopile cluster (see insert to Figure 1.3) are examined, differences in fatty acid profiles among classes (with rare exception) show little taxonomic affinity. Comparative analysis does show indicate that algal representatives within the chromalveolate cluster (Stramenopiles, Primmnesiophuceae, Dinophyceae, and Cryptophyceae) contain a much broader and often higher polyunsaturated fatty acid complement than do green algae (Chlorophyta). However, as genetic modification becomes more routine, those organisms with unique products or low productivity of a desirable product could potentially provide targets for molecular harvesting or engineering.

Genome Sequencing and Systems Biology

At the outset of NAABB, it was recognized that it would be necessary to increase algal biomass and lipid accumulation rates substantially to make algal biofuel production economically sustainable. At the time the project was initiated, significant effort had already been expended to characterize growth phenotypes and the lipid-generation potential of a variety of algal species. Furthermore, it was known that under certain growth conditions including nutrient limitation or stress, many algae accumulate large concentrations of lipids, terpenoids (hydrocarbons), or carbohydrates that could be used for fuel production. However, very little was known about the fundamental physiology, genomics, metabolism, and regulation of metabolic pathways that contributed to these phenotypes. Only a few genomes of the model organisms including *C. reinhardtii* had been sequenced well and annotated. While it was known that a starchless mutant of *Chlamydomonas* could be induced to produce lipids, changes in gene expression had not been correlated with lipid production. Due to the high degree of evolutionary diversity in algae, it was not clear that it would be possible to extrapolate genetic, physiologic, and biochemical properties observed in *Chlamydomonas* to produce commercializable strains of algae. Also high-quality genome sequences of production strains would be necessary to transfer the genetic tools (transformation vectors and expression systems) developed for engineering model strains like *Chlamydomonas* rapidly to production strains. At the outset of NAABB, the fundamental knowledge necessary for engineering more efficient production strains of algae was lacking.

Genome Sequencing

For these reasons, NAABB took advantage of new genome sequencing technologies including the Illumina¹², 454¹³, and Pacific Biosciences¹⁴ platforms, which were complemented by the development of novel computational tools¹⁵⁻²³, to sequence, assemble, and annotate high-quality algal genomes and transcriptomes quickly. A major accomplishment of the NAABB consortium was the sequencing and assembly of eight high-quality algal genomes from three independent phyla, the greatest biodiversity of algae sequences at that time (Table 1.3). To develop gene models and correlate algal gene expression to phylogenetic profiling, 220 RNAseq transcriptome samples were sequenced. Many of the gene expression studies were completed under nitrogen deprivation or other stress or growth conditions to monitor changes in gene expression during lipid induction.

Table 1.3. NAABB genome projects.

Genome	Assembly Quality	Size, Mbp
<i>Picochlorum</i> sp.	Improved High Quality Draft	15.2
<i>A. protothecoides</i> UTEX25	Improved High Quality Draft	21.4
<i>Chrysochromulina tobin</i>	High Quality Draft	75.9
<i>N. salina</i> 1776	Improved High Quality Draft	27.7
<i>Tetraselmis</i> sp. LANL1001	Standard Draft	220
<i>Chlorococcum</i> sp. DOE101	Standard Draft	120
<i>Chlorella</i> sp. DOE1412	Standard Draft	55
<i>Chlorella sorokiniana</i> <i>Phycal1228</i>	Standard Draft	55

Discussed in detail below, we provided extensive transcriptome sequences to analyze genes involved in lipid production in *C. reinhardtii*. The RNAseq data were also used to generate gene models and functional annotations for *N. salina*, *Picochlorum* sp., and *A. protothecoides*. This information enabled construction of metabolic pathways. Simultaneously, the NAABB team used similar genomic and RNAseq transcriptome data produced by the U.S. Department of Energy Joint Genome Institute to analyze the production of nonlipid hydrocarbons by *B. braunii*.

Annotation and comparative genomics analyses of the data continue. Using the sequence data developed by NAABB, we carried out a pangenomic comparison of the chloroplast and mitochondrial genomes of *Nannochloropsis* with other stramenopiles.²⁴ This analysis revealed an extreme divergence in several key metabolic genes/systems including the regulation of branched chain amino synthesis (acetoxyacid synthase), carbon fixation (RuBisCO activase), energy conservation (ATP synthase), and protein synthesis and homeostasis (Clp protease, and the ribosome). Many of the organellar gene modifications in *Nannochloropsis* are novel and deviate from conserved orthologs found across the tree of life.

These observations and further discovery of currently unidentified genetic and structural modifications to critical cellular components will be required to help explain (and exploit) the unique physiological properties found in the genus *Nannochloropsis*. It is also worth noting that the high degree of divergence in the amino acid sequences of many *Nannochloropsis* proteins led to false annotations when based on gene homology, thus requiring further optimization of the gene annotation tools. Finally, the extraordinary similarity of the *N. salina* and *N. gaditana* organellar genomes suggested that these two isolates should be reclassified as different strains of the same species. The availability and consequent comparative analyses of the nuclear genomes of both isolates are required, however, to provide verification to support the proposed reclassification.

Systems Biology

To gain a further understanding of the molecular control of oil accumulation, we used a combination of RNAseq transcriptomics, proteomics, and metabolomics studies to characterize changes in gene expression associated with

nitrogen-deprivation and lipid production in *Chlamydomonas*, *Picochlorum*, and *Nannochloropsis*. To ensure that the investigation of deep-sequencing projects was meaningful, it was necessary to develop systematic procedures for analysis. Towards this goal, we constructed an in-house pipeline for algal genomics/transcriptomics, as shown in the Figure 1.4.

Transcriptome Analysis of Lipid Production in *C. reinhardtii*

C. reinhardtii is capable of accumulating intracellular lipids, which can be converted to biofuel, under conditions in which the cells experience physiological stress such as nutrient deprivation^{26,27} or salt stress.²⁸ Furthermore, starchless mutants, such as *sta6*, hyperaccumulate lipids when stressed.²⁹ The generation of “obese” cells containing a higher TAG content per dry weight in *sta6* represents either a remodeling of existing lipids and/or a channeling of fixed carbon into lipid production.³⁰ In the context of NAABB’s objectives, we sought to gain a better understanding of the global response to N-deprivation in the starchless mutant, *sta6*, using RNA-Seq transcriptomics. Our intention was to compare gene expression in wild-type and the *sta6* mutant to deduce the specific metabolic pathways that enable the *sta6* mutant to produce more lipids, potentially identifying genes that may regulate oil accumulation and paving the way for future metabolic engineering projects.

Comparative phenotype of wild type (*cw15*) and mutant (*sta6*) under nitrogen deprivation—The onset of nitrogen deprivation induces starch and lipid accumulation, in addition to provoking gametogenesis, chlorophyll degradation, down-regulation of photosystems, and ribosomal proteins. To investigate in more depth the physiological changes of *cw15* and *sta6* following nitrogen deprivation, we assayed the two strains and the *STA6*-complemented strains (*STA6-C2*, *STA6-C4* and *STA6-C6*). The complemented strains were obtained by transformation of *sta6* with a plasmid carrying a genomic copy of the wild-type *STA6* gene and a paromomycin resistance cassette.²⁹ All five strains were assayed for cell counts and chlorophyll, starch, and lipid contents. Upon nitrogen limitation, the cell counts of all strains remained unchanged, indicating that cell division had been arrested. The chlorophyll content per cell decreased in both strains, as has previously been noted, although the losses appeared to be more rapid in the *sta6* mutant than in the parent strain, and the chlorophyll content was restored to the wild-type level in the complemented strains. Near zero starch was accumulated in the *sta6* mutant strain, but rapidly accumulated in the parent and complemented strains. Although no significant difference between TAG content in *cw15* and *sta6* was observed in the first 48 h of nitrogen deprivation, at 96 h, the TAG content of *sta6* greatly exceeded that of *cw15* and was N-deprivation dependent.

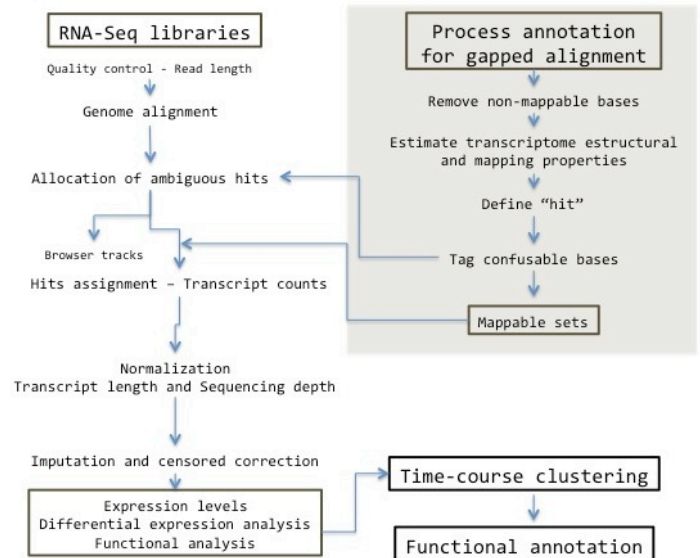


Fig. 1.4. Schematic of the algal genome/transcriptome analysis pipeline. Given the large number of regulated genes in nitrogen-deprived cells and the size of the datasets, we classified the genes according to their temporal expression profiles across individual or combined experiments (time-course clustering). We also performed different model-based clustering analyses by combining responses at early and late time points. Finally, we used our pathways annotation tool to couple genes to function.²⁵

TAG biosynthesis—Given the ability of *sta6* to amass a greater quantity of lipids per cell than the parent strain, we expected that results from the transcriptomes analyses might demonstrate increased transcript abundance of fatty acid and TAG biosynthesis related genes in *sta6* versus *cw15*. However, for most genes associated with lipid biosynthesis, there was no significant difference in reads per kilobase per million (RPKM) between the two strains. *Chlamydomonas* stores lipids as TAGs, which are synthesized by covalent attachment of fatty acids to glycerol by acyltransferases. Of seven putative acyltransferases encoded by the *Chlamydomonas* genome, only two were differentially expressed (Figure 1.5) in *sta6* versus *cw15*: DGTT2, a type-2 diacylglycerol acyltransferase (DGAT)^{31,32} and Cre06.g310200, a putative type-3 acyltransferase^{33,34}. In addition to the acyltransferases, the major lipid droplet associated protein (MLDP1) identified by Moellering and Benning also is differentially expressed in *sta6* versus *cw15* (Figure 1.5). The exact function of MLDP1 is not known, but a knock-down mutant exhibited increased lipid body size suggesting it stabilizes lipid droplets.³⁵ Acyltransferase activity has been postulated to be the rate-limiting step in TAG synthesis, assuming the concentration of acyl-CoA is non-limiting, suggesting that the increased expression of DGTT2 and/or DGAT3 are key mediators of TAG accumulation in *sta6* (Figure 1.6). Unlike many of the genes induced in *sta6* versus *cw15*, there is transcript abundance of both to produce TAGs more rapidly following nutrient stress. DGTT2 and DGAT3 increased early after nitrogen withdrawal (Figure 1.6). Algal production strains engineered to overexpress these genes early may have the potential to produce TAGs more rapidly following nutrient stress.

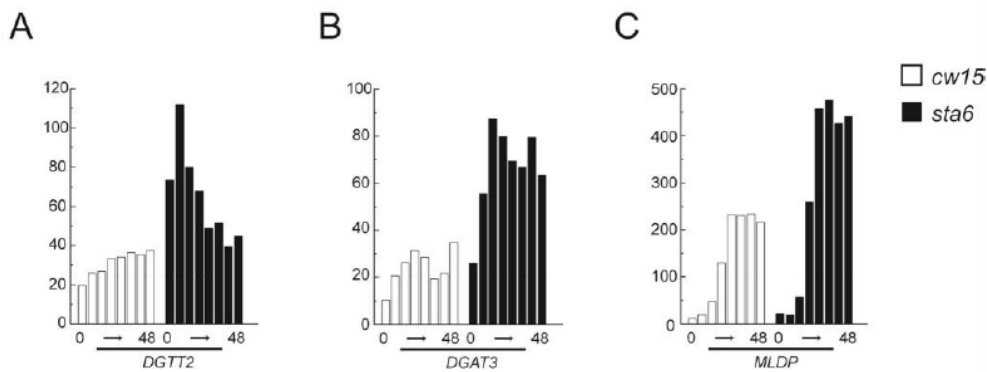


Figure 1.5. Expression profiles of lipid-biosynthesis related genes. (A) DGTT2, (B) DGAT3, putative type-2 and type-3 acyltransferases, and (C) the major lipid droplet protein were expressed about 2-fold higher in *sta6* compared to *cw15*. RPKMs of each gene at 0, 0.5, 4, 8, 12, 24 and 48 h are shown, *cw15* in white and *sta6* in black.

Our transcript analysis also showed that six key genes encoding enzymes involved in pathways associated with central carbon metabolism were up-regulated in *sta6* compared to *cw15* (Figure 1.7). These genes included *ACS1*, which encodes acetyl-CoA synthase, the first step in acetate metabolism; *MAS1* and *ICL1*, which encode malate synthase and isocitrate lyase, respectively, in the glyoxylate fatty acid β -oxidation pathway; and *FBP1* and *PCK1*, which encode fructose-1,6-bisphosphatase and phosphoenolpyruvate carboxykinase involved in primary carbon metabolism. Finally, *TAL1* encodes transaldolase, which is

important for the balance of metabolites in the pentose phosphate pathway, was also overexpressed during N-deprivation. All six genes display highly uniform elevated expression profiles, suggesting metabolic linkage and implying increased metabolic flux through these pathways in the *sta6* mutant (Figure 1.6). These expression patterns are consistent with increased turnover of fatty acids and enhanced carbon scavenging during N-deprivation, processes that may be associated with lipid remodeling.

Although analysis of the transcriptome data showed that the *STA6* deletion was the cause of many of the differentially expressed genes, we sought to independently verify this by analyzing changes in protein and metabolite concentrations. The transcriptome and metabolome data are represented on the metabolic chart in Figure 1.7. Malate synthase and isocitrate lyase activities were assessed in cell extracts from N-deprived cultures. Our enzyme assays showed that the *STA6* mutants had a 2- to 3-fold increase in malate synthase and isocitrate lyase activities 48 h after N-deprivation. Similarly, intracellular concentrations of key metabolites were determined at 48 h with and without nitrogen. As expected, these data demonstrate that in the *STA6* background there was a reduction in ADP-glucose levels. In addition, the *STA6* deletion had significant increases in isocitrate, succinate, malate, and fructose-1,6-bisphosphate levels in N-deprived cultures. These data confirm that the increased mRNA abundance translated into increased enzyme activities and subsequently into increased flux through the glyoxylate cycle and potentially carbon scavenging via the Calvin-Benson cycle as occurs in lipid-accumulating soybean seeds. Significantly, by short-circuiting the Krebs cycle via increased glyoxylate cycle activity, potentially less carbon is lost during respiration.

For algal-derived lipids to realize their potential as a transportation fuel, a complete understanding of the molecular circuitry of algae is essential. The studies described here have taken strides towards this objective by applying transcriptomics and metabolomics approaches to examine the nitrogen-deprivation-induced lipid production in the model organism *C. reinhardtii*. There are a large number of significantly differentially expressed genes between *cw15* and *sta6* including fatty acid acyltransferases involved in the biosynthesis of TAGs. Genes whose expression is substantially altered during oil accumulation are potential targets for genetic regulation to improve lipid production in production strains.

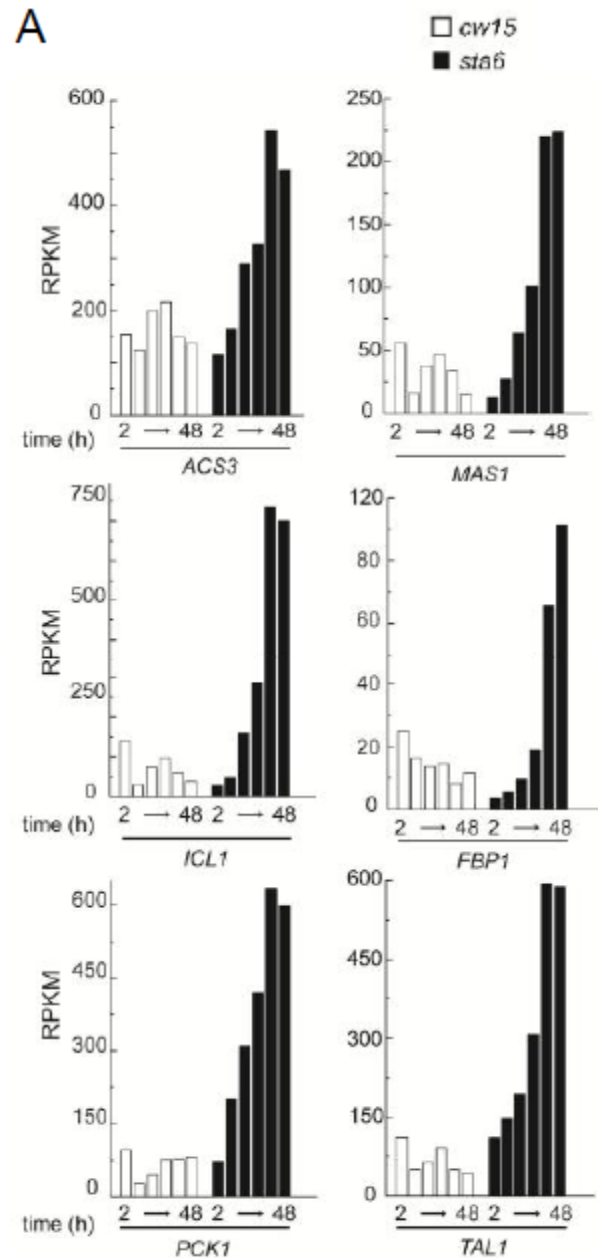


Figure 1.6. Significantly differentially expressed genes involved in central carbon metabolism pathways. Expression profiles of ACS3, ICL1, MAS1, PCK1b, GLPX1, and TAL1 in *cw15* (white) and *sta6* (black) at 2, 4, 8, 12, 24, and 48 hours of nitrogen starvation.

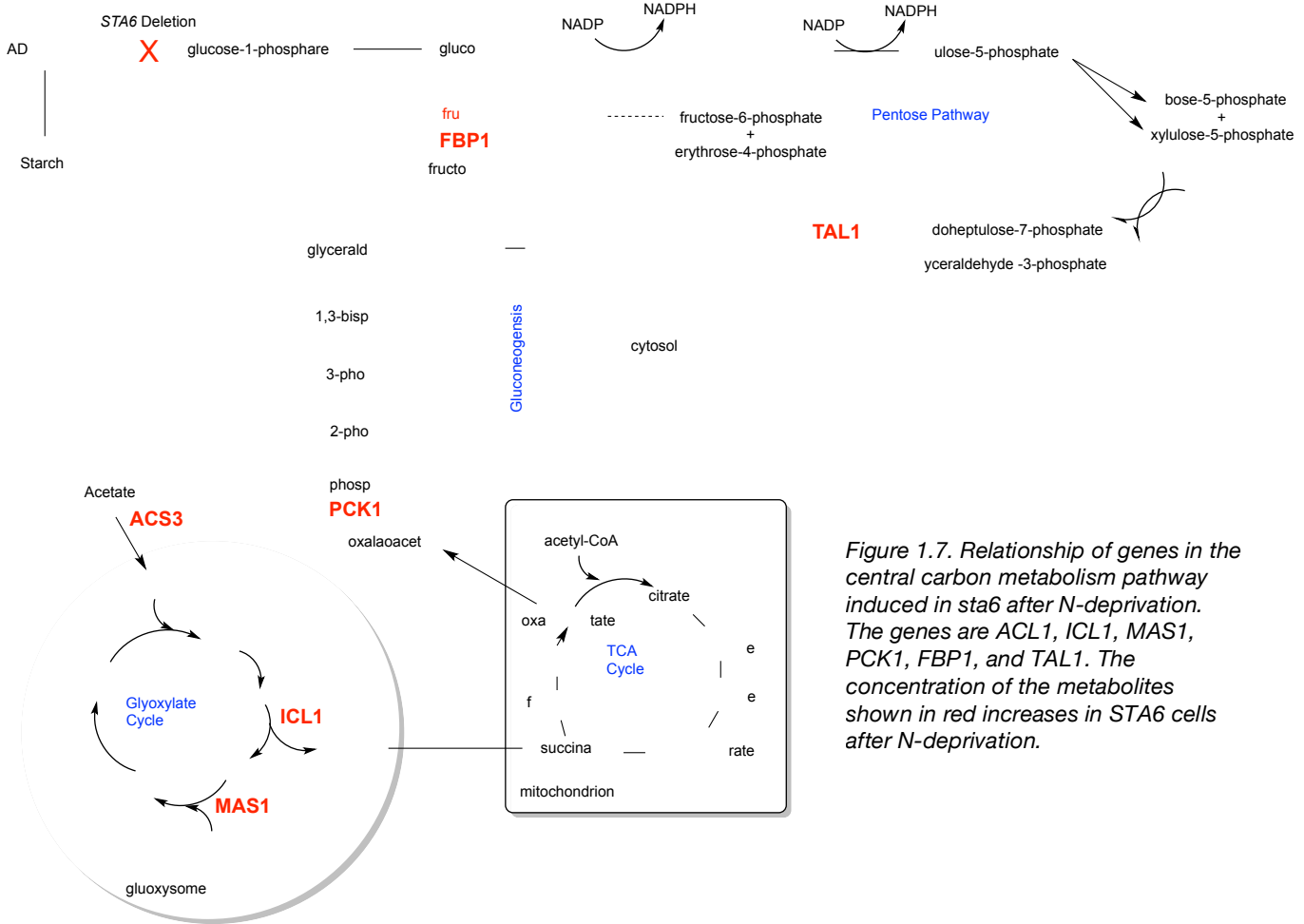


Figure 1.7. Relationship of genes in the central carbon metabolism pathway induced in *sta6* after N-deprivation. The genes are *ACL1*, *ICL1*, *MAS1*, *PCK1*, *FBP1*, and *TAL1*. The concentration of the metabolites shown in red increases in *STA6* cells after N-deprivation.

Transcriptome Analysis of Lipid Production in *A. protothecoides*

To determine the patterns of gene expression associated with oil accumulation induced by various processes, we carried out RNAseq analyses on *A. protothecoides* at various time intervals after a variety of treatments. These treatments included those that induce oil accumulation (glucose or decane addition), stresses (37°C) and cold (4°C), and controls for daylight and at midnight. The transcriptomes were collectively analyzed using the Sequedex program for rapid gene annotation based on kmers of 10 amino acids (Figure 1.8). It can be seen that the transcript abundance for genes encoding enzymes functional in fatty acid synthesis increased with glucose addition, which increase TAG levels from 5-45% (dry weight). In contrast, short exposure (1 h) to decane treatments, which are associated with lipid remodelling and similar levels of TAG accumulation, was associated with increased expression levels of genes associated with stress tolerance and at longer time periods (3 h) with the expression of genes involved in protein metabolism and repair. These results demonstrate that *de novo* TAG synthesis induced by glucose differs substantially from stress-induced (decane) accumulation of TAGs in terms of the patterns of gene expression. These analyses were made possible due to the sequencing and annotation of the *A. protothecoides* genome by NAABB.

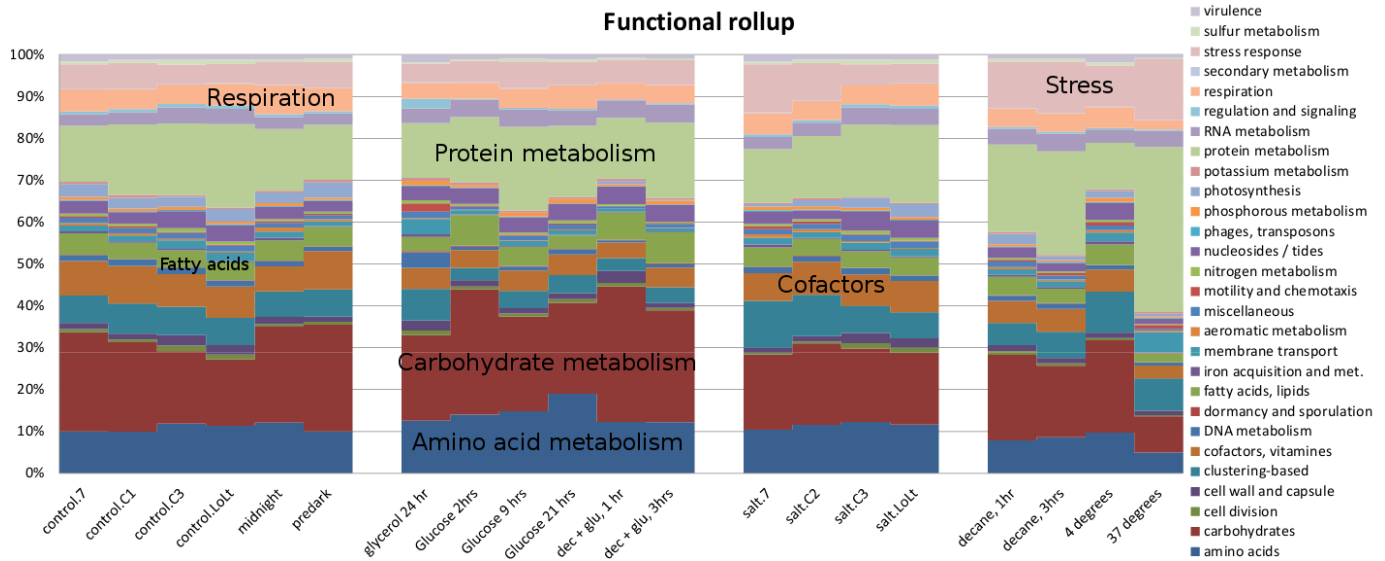


Figure 1.8. Relative transcriptional activity of various functional gene assignments as influenced by various stresses as well as carbohydrate-induced oil accumulation.

Transcriptome Analysis of Lipid Production in *Picochlorum* sp. and *N. salina*

Growth conditions—We cultured *Picochlorum* and *N. salina* in a five-liter cylindrical photobioreactor, which controls and logs the temperature, pH, dissolved $[O_2]$, and rate of addition of CO_2 , O_2 , and N_2 . Algae were grown at saturating light intensities ($400 \mu E/m^2/s$) for 16 h/day at pH 8.2. The pH of the growth medium was 8.2 and during growth, the pH was used to control the addition of CO_2 , which ensured that both the pH and the concentration of the carbon substrate ($[CO_2] + [HCO_3^-] + [CO_3^{2-}]$) were constant throughout the experiment. Cell numbers, (A_{750}), total lipid as FAMES, and nitrate in the medium were monitored. Samples were also analyzed by flow cytometry to measure cell number, cell size, and autofluorescence. The fluorescent dye BODIPY was used to measure total neutral lipids.

Representative data from photobioreactor growth of *Picochlorum* and *N. salina* are shown in Figure 1.9. In the experiments shown, the initial concentration of sodium nitrate was 4 mM for *Picochlorum* and 8 mM for *N. salina*. As the algae grew, nitrate was depleted from the growth medium.

Each of these marine algae increased their lipid accumulation when nitrogen was depleted from the growth medium during growth. Under nitrogen depletion, the rate of lipid accumulation increased 3-fold in the *Picochlorum* cultures (Figure 1.9A). More significantly, when nitrate was depleted from the growth medium of *N. salina* cultures, the lipid accumulation rate increased 6.3-fold from 24 mg/L/d to 151 mg/L/d (Figure 1.9B). Based on analysis by flow cytometry, the cells stopped dividing some time after the nitrate was depleted from the growth medium. However, the biomass continued to increase as the algae accumulated lipids, causing the cells to increase in volume, which resulted in an increased OD at 750 nm. Under these conditions, *N. salina* cultures accumulated lipids to approximately 50–60% of the biomass.

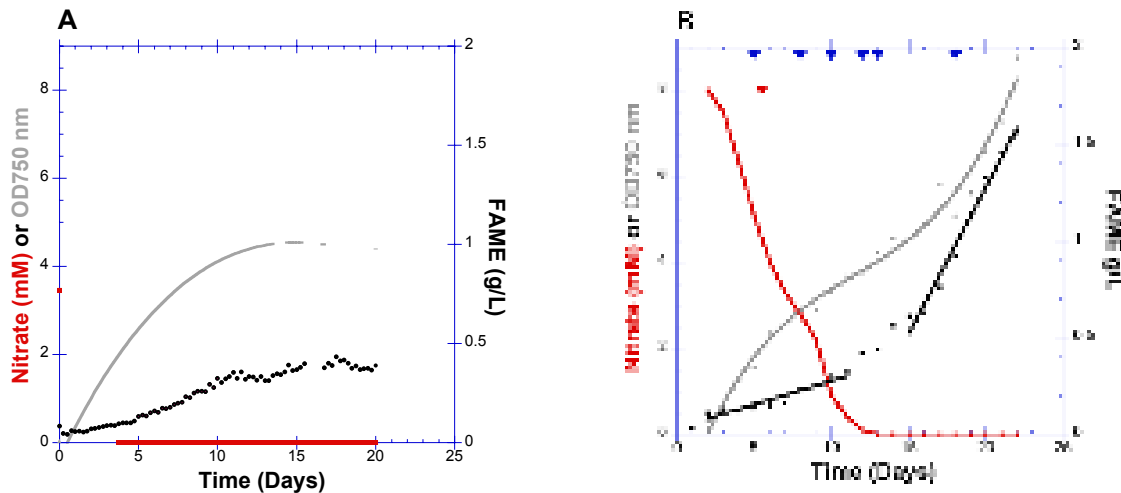


Figure 1.9. (A) Growth of *Picochlorum sp.* in our photobioreactor. When nitrate was depleted from the growth medium, the lipid accumulation rate increased from 12 mg/L/d to 36 mg/L/d. (B) Growth of *N. salina* in our photobioreactor. When nitrate was depleted from the growth medium, the lipid accumulation rate increased from 24 mg/L/d to 151 mg/L/d. The cells stopped dividing some time after nitrate was depleted from the growth medium, but the OD₇₅₀ continued to increase during rapid lipid accumulation because the cells increased in volume. Transcriptomes were analyzed on samples collected on days marked ▼ and nights marked ▼.

Transcriptome Analysis of *Picochlorum sp.*

To examine the changes in gene expression associated with depletion of nitrate (nitrogen) and increased lipid accumulation rate, samples before, during, and after nitrogen depletion were subjected to RNAseq transcriptome analysis. RNA was isolated from samples obtained at four time points: (1) 4 days before nitrate was depleted from the growth medium, (2) the day the nitrate concentration fell to zero, (3) 1 day after nitrogen depletion, and (4) 4 days after nitrogen depletion.

Lipid and TAG biosynthesis—We annotated genes involved in fatty acid biosynthesis including the genes encoding acetylCoA carboxylase 1, AccABCD; acetylCoA carboxylase 3, Acc; malonyl CoA ACP transferase, FabD; 3-ketoacylACP reductase, FabG; 3-ketoacylACP synthase 1, FabB; 3-ketoacylACP synthase 2, FabH; enoylACP reductase, FabI, K, or L; acylACP desaturase; and acylACP thioesterase. The expression of each of these fatty acid biosynthesis genes increased at least two fold as a consequence of nitrogen depletion. We also observed increased expression of genes encoding for enzymes involved in TAG synthesis. Similar to the observation reported above for *Chlamydomonas*, nitrogen depletion induced the expression of acyltransferases including DGAT.

The data are presented as a metabolic pathway in Figure 1.10 where enzymes encoded by genes that were induced upon nitrogen depletion are shown in red; those whose expression was repressed are shown in blue. Genes encoding for enzymes shown in black were not identified in our annotation. Further analysis and experimentation is necessary to identify which of these enzymes are expressed in the chloroplast, the site of fatty acid and triglyceride biosynthesis. However, the overall conclusion is that the increased rate of lipid production results from the induction of the entire lipid biosynthesis pathway. Acetyl-CoA carboxylase (ACCase) catalyzes the conversion of acetyl CoA to malonyl-CoA, the first committed step, and possibly a rate-limiting step, in lipid biosynthesis. It was observed that one of the ACCase gene family members was induced to a greater degree than other gene family members during lipid accumulation.

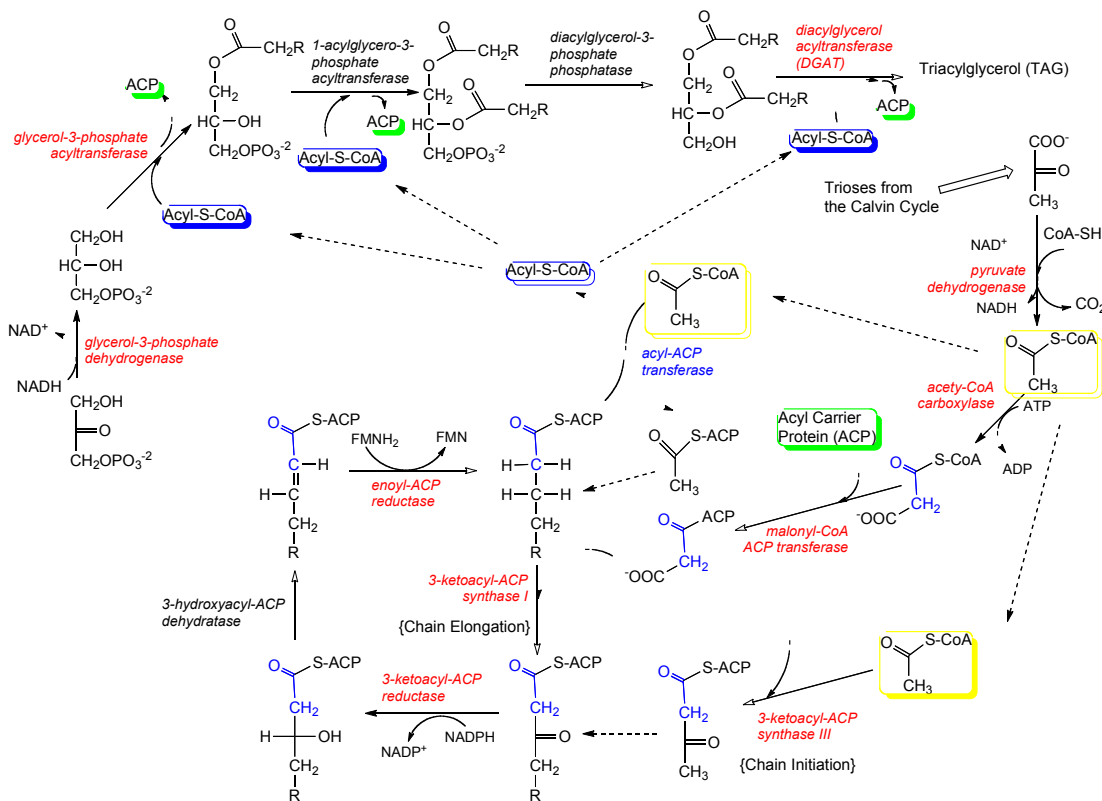


Figure 1.10. Metabolic map of lipid and TAG biosynthesis. Enzymes encoded by genes that are **induced** during the high lipid production phase of growth are lettered in red, **repressed** genes in blue. No genes have been annotated to encode for 2-hydroxyacyl-ACP hydratase, 1-acylglycerol-3P acyltransferase or diacylglycerol-3P phosphatase.

Starch biosynthesis—Nitrogen depletion causes induction of most of the enzymes required for starch biosynthesis. Genes encoding both subunits of the ADP-glucose pyrophosphorylase were induced 2- to 16-fold. One of the isozymes of starch synthase was also induced 4-fold at every time point after nitrogen was depleted. Several enzymes required for production of hexoses from the triose-phosphates produced by the Calvin-Benson Cycle were also induced by nitrogen depletion. This transcriptome profile suggests that upon nitrogen depletion from the growth medium, *Picochlorum* stores energy and carbon transiently as starch, which may provide the substrates for TAG accumulation.

Transcriptome Analysis of *N. salina*

RNA isolated from samples of *N. salina* cultures taken on Days 5, 8, 10, 12, 13, and 18 (Figure 1.9B) were subjected to RNAseq analysis using deep sequencing with a HiSeq sequencer. Proteome analysis was carried out on parallel samples from the *N. salina* culture. RNA was isolated both from the light and mid-dark growth periods (Figure 1.9B).

Expression of tricarboxylic acid (TCA) cycle enzymes during day versus night—

During the day, algae derive their energy and reducing power from photosynthesis and the TCA cycle. At night algae are thought to derive energy primarily via the TCA cycle. Thus, the overall rate of lipid accumulation is the

difference between the rate of biosynthesis of lipids during the day and the rate of oxidation of lipids during the day and night. The enzymes of the TCA cycle also provide essential functions by producing 4- and 5-carbon skeletons required for the biosynthesis of amino acids. We examined the day versus night expression of the mitochondrial TCA cycle enzymes. Consistent with their roles in biosynthesis, all of the TCA cycle enzymes are highly expressed during the day and night. Importantly, 2-oxoglutarate dehydrogenase is induced more than 2-fold at night, consistent with the energy generation role of the TCA cycle and potentially enhanced fatty acid oxidation and lipid turnover at night.

Expression of the lipid droplet protein—The gene encoding for the *Nannochloropsis*-specific lipid droplet protein identified by Benning and coworkers³⁶ is one of the highest expressed genes identified in our transcriptome experiment. The gene encoding for the lipid droplet protein is induced 4.6-fold after nitrogen was depleted from the culture medium (Day 12) consistent with the increase in lipid storage vesicles during lipid accumulation.

Fatty acid biosynthesis and TAG biosynthesis—The expression of the genes encoding for fatty acid biosynthesis in *N. salina* are shown in Figure 1.11. All of the fatty acid biosynthesis genes are expressed in all six transcriptome samples. The only gene in fatty acid biosynthesis that is induced following an initial reduction in expression during nitrogen depletion is *fabH*, which encodes one of the 3-ketoacyl-ACP synthase gene family members.^{37,38} *FabH* is induced 2- to 3-fold after the eighth day of nitrogen deprivation. Similar to the data reported above for *Chlamydomonas* and *Picochlorum*, the expression of the gene encoding DGAT was induced when nitrate was depleted from the growth medium of *N. salina* (data not shown). DGAT catalyzes the last step in TAG biosynthesis.

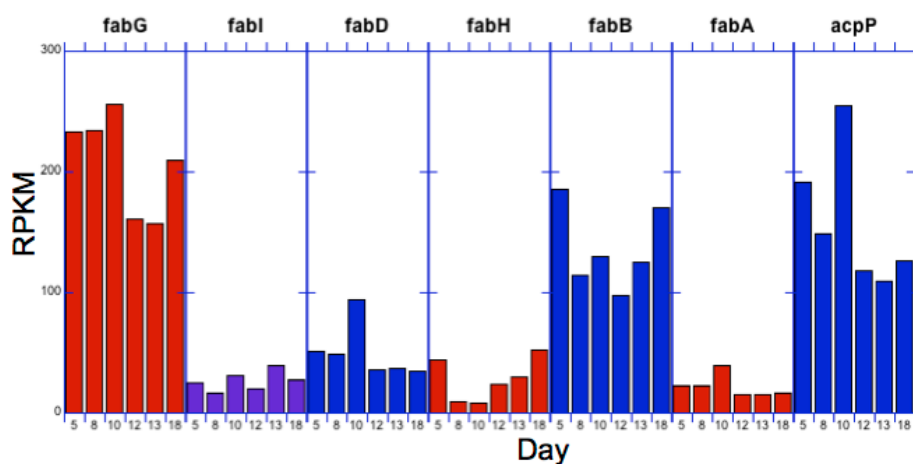


Figure 1.11. Expression of genes encoding for fatty acids biosynthesis in *N. salina*. The genes encode for fatty acid biosynthesis enzymes as follows: *fabA*—3-hydroxyacyl-ACP dehydratase, *fabB*—3-ketoacyl-ACP synthase, *fabD*—malonyl-CoA:ACP transacylase, *fabG*—3-ketoacyl-ACP reductase, *fabH*—3-ketoacyl-ACP synthase, *fabI*—enoyl-ACP reductase, *acpP*—acyl carrier protein.

Expression of genes encoding for acetyl-CoA carboxylase (ACCase)—In bacteria, ACCase is encoded by four genes, *accA*, *accB*, *accC*, and *accD*, that give rise to a four-subunit enzyme. In eukaryotes, ACCase is encoded by a single gene that produces a large single-subunit (1400 amino acids) enzyme. Plants have both bacterial and eukaryote ACCase genes.³⁹ The bacterial-like ACCase is expressed in the plant chloroplast and thought to be responsible in *de novo* lipid biosynthesis. The eukaryote-type ACCase is expressed in the cytoplasm and involved in the biosynthesis of specialized long chain lipids. Algae have two eukaryotic-type ACCase genes and the genes for a four-gene bacterial type ACCase. In *N. salina*, the bacterial ACCase was expressed at very low levels throughout the 18-day nitrogen deprivation period. However, we observed that one of the cytoplasmic ACCase's gene family members was induced 3.3- to 5.6-fold upon nitrogen depletion during the onset of TAG accumulation (Figure 1.12).

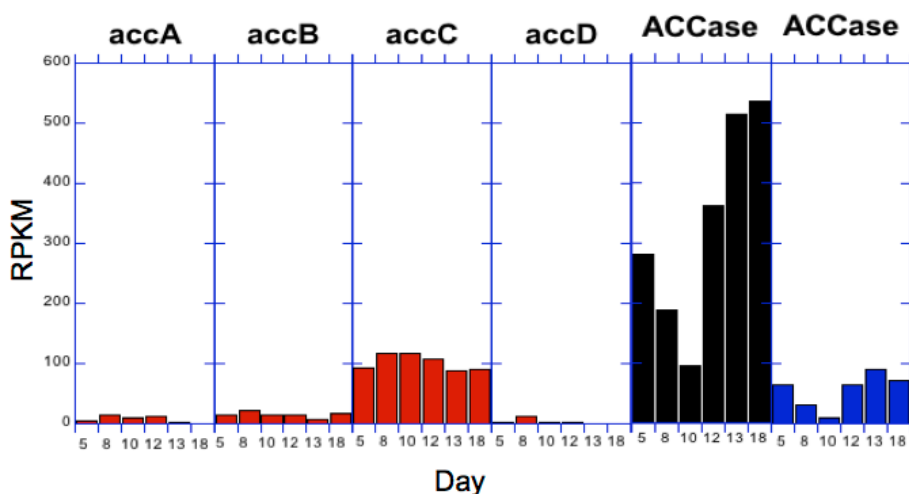


Figure 1.12. Expression of ACCase genes in *N. salina*. Genes labeled *accA*, *accB*, *accC*, and *accD* encode for the four-subunit bacterial enzyme thought to be expressed in the chloroplast. One of the single-subunit eukaryotic ACCase genes is highly expressed and induced upon nitrogen depletion from the growth medium.

Proteomics of *N. salina*

The goal of this task was to utilize liquid-chromatography mass-spectrometry (LC-MS) based proteomics to identify proteins whose abundance changed during the transition to lipid accumulation. For this task, proteomic surveys were carried out on *Nannochloropsis* grown in a laboratory photobioreactor and in an outdoor photobioreactor.

Laboratory photobioreactor—The proteomic survey was carried out in parallel with the *N. salina* transcriptome analysis described above (Figure 1.9B) where cultures were grown in a photobioreactor supplied initially with 8 mM nitrate. By Day 12, the nitrogen was depleted from the growth medium, which led to a 6.3-fold increase in the rate of lipid accumulation. The overall goal was to identify proteins differentially expressed under lipid and nonlipid productive growth states. In the proteomics analysis of the *Nannochloropsis* time course, a total of 6 LC-MS injections were performed for each of six samples of *N. salina* cultures taken on Days 5, 8, 10, 12, 13, and 18. Over 900 proteins and 2150 peptides were identified. In statistical modeling of relative protein abundance levels, 250 proteins were analyzed by spectral counting methods and 375 proteins by mixed-effect statistical modeling of mass spectral abundances. Four proteins associated with stress response, including glutathione reductase, peroxiredoxin, and superoxide dismutase, increased in abundance during nitrogen deprivation.

Peptidyl-prolyl cis-trans isomerase levels also increased in abundance. These enzymes have been shown to have increased abundance in plants under stress⁴⁰ and influence gene expression in eukaryotes⁴¹. A majority of the proteins with reduced abundance at later harvest time points are involved in protein synthesis machinery or regulation of transcription. Interestingly, adenosyl-homocysteinase levels decreased during N-deprivation. In yeast, the reduced expression of this enzyme correlates with an increase in TAGs.⁴² An open reading frame with homology to ketol-acid reductoisomerase also has reduced expression during N-deprivation. This protein is a member of the branched chain amino acid biosynthetic pathway.

Outdoor photobioreactor—*N. salina* cultured in the outdoor reactor were provided replete nitrogen and grown for 22 days. Samples were taken for proteomic surveys at Days 1, 8, 15, and 22. Over 1700 proteins and 4000 peptides were identified. A total of 445 proteins were identified by spectral counting methods and 510 proteins by mixed-effect statistical modeling of mass spectral abundances. Due to the limited amount of genome similarity of *Nannochloropsis* to other annotated model organisms, a significant number of open reading frames that were identified in the proteome analysis did not have a homolog in the UniProt database. The majority of the identified proteins that had increased expression the three-week growth period were those involved in glycolysis, including glyceraldehyde-3-phosphate dehydrogenase, fructose bisphosphate aldolase (also involved in gluconeogenesis and the Calvin cycle), and enolase. The dihydrolipoamide acetyltransferase (E2) subunit of the pyruvate dehydrogenase complex, which converts pyruvate to acetyl-CoA also increased in expression in comparison to the Day 1 sample. Glutamate decarboxylase, which also increased in the Day 22 sample, is a component of the γ -aminobutyrate (GABA) shunt, which in plants has been associated with responses to stress.⁴³ The majority of proteins with decreased abundance levels were involved in photosynthesis, including photosystem II D1 protein (psbA), chlorophyll a-b binding protein, photosystem II reaction center protein, fucoxanthin-chlorophyll a-c binding protein, photosystem II 47 kDa protein (psbB), and chlorophyll a-b binding protein. Ribulose bisphosphate carboxylase oxygenase (RuBisCO) expression was also reduced in comparison to Day 1. On the whole, these results suggest that *Nannochloropsis* metabolism at Day 22 is drastically shifted from the early stage growth as the photosynthesis machinery appears to be down-regulated and enzymes in glycolysis are up-regulated.

Transcriptome Analysis of B. braunii

Among the oleaginous algae, *B. braunii* is unique in producing large amounts of liquid hydrocarbons (polyterpenoids), which are comparable to fossil crude oil.⁴⁴ Biosynthetic engineering of hydrocarbon biocrude production requires identification of genes and reconstruction of metabolic pathways responsible for the production of these hydrocarbons, and mapping the biosynthesis of other metabolites that compete for photosynthetic carbon and energy. Our goal was to use transcriptomic analyses to identify the genes encoding for hydrocarbon biosynthesis.

The three chemical races of *B. braunii* are defined based on the type of hydrocarbon they produce.^{45,46} The A race produces fatty acid derived alkadienes and alkatrienes; the B race produces the isoprenoid derived triterpenes known as botryococenes; and the L race produces the isoprenoid derived tetraterpene known as lycopadiene. All three oils have been found to be major constituents of petroleum deposits, suggesting that *B. braunii* was a large contributor in geologic times to the formation of these deposits. We used next-generation sequencing to assemble essentially complete *de novo* transcriptomes for all three *B. braunii* races. Next, we used a large array of bioinformatics methods to annotate the functions of these transcripts and to reconstruct biosynthetic pathways and biosynthetic networks. Using the dataset for the B race strain that produces triterpenoid hydrocarbons, we manually curated pathways that affect hydrocarbon biosynthesis and export. In particular, we were interested in the biosynthetic pathways that:

- Yield the generalized terpenoid precursors DMAPP and IPP;
- Provide C₃₀ botryococenes and C₄₀ lycopadienes;
- Provide C₂₃-C₃₃ alkadienes and alkatrienes;
- Contribute to the extracellular localization of hydrocarbons; and
- Channel photosynthetic carbon and energy into non-hydrocarbon storage compounds.

Botryococcene biosynthesis—For the B race, the transcriptome was used to reconstruct the entire pathway for botryococcene production through the isoprenoid pathway. Terpenes are biosynthesized from the universal C₅ building blocks of isopentenyl diphosphate (IPP, **13**) (Figure 1.13) and dimethylallyl diphosphate (DMAPP, **14**) (Figure 1.13). These precursors originate from the mevalonate pathway in the cytosol of animal, fungal, archaeal, and higher plant cells, while the methylerythritol 4-phosphate/deoxyxylulose phosphate (MEP/DOXP) pathway is operational in plant plastids and many Gram-positive and Gram-negative Eubacteria.⁴⁷ Experimental evidence from *B. braunii* also argues for the exclusive utilization of the MEP/DOXP pathway. Fittingly, exhaustive searches of the assembled race B transcriptome identified ESTs only for the first two of the six enzymes of the MVA pathway. Because these enzymes are also involved in various catabolic processes, their presence in the race B transcriptome is not an indication for a functional MVA pathway.

In contrast, a complete contingent of deduced enzymes for the MEP/DOXP pathway is well represented in the *B. braunii* race B transcriptome.⁴⁷ The MEP/DOXP pathway uses D-glyceraldehyde 3-phosphate and pyruvate as its metabolic input. Multiple isoforms of the key enzymes for the biosynthesis of these precursors from photosynthetic 3-phospho-D-glycerate (**1**) were identified in the race B transcriptome.⁴⁸ Some of these transcripts are present at very high abundance (>250 reads/kb), suggesting a high metabolic flux in *B. braunii* race B.

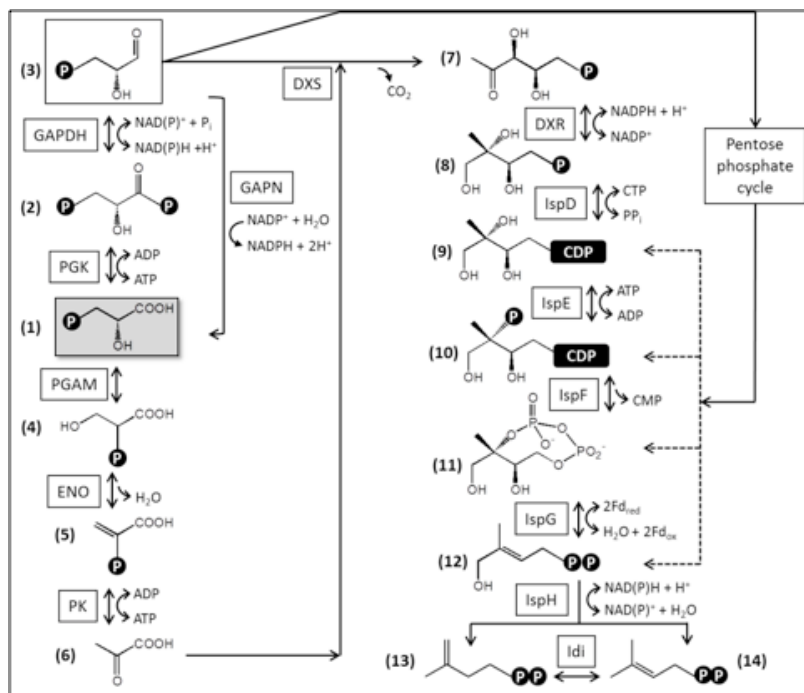


Figure 1.13. *B. braunii* race B genome encodes for a complete MEP/DOXP pathway for terpene biosynthesis. Significantly, three isozymes for 1-deoxy-D-xylulose 5-phosphate synthase (DXS, E.C. 2.2.1.7), the first committed step in the pathway, are expressed.

Of particular interest, genes were identified for three isozymes of the first enzyme of the MEP/DOXP pathway, 1-deoxy-D-xylulose 5-phosphate synthase (DXS). While multiple isozymes of DXS are routinely found in plants,⁴⁹ genomic evidence shows that strains of green algae harbor only a single DXS each. Recently, biochemical characterization of three isozymes of DXS from race B demonstrated that all three isozymes are active and have similar kinetic parameters.⁵⁰ Our data also indicate similar, moderate transcript abundances for all three DXS isozymes of the race B strain. DXS has been described as one of the rate-limiting steps of the MEP/DOXP pathway in plants⁴⁷. The expression of three isoforms of this enzyme in *B. braunii* race B thus might provide an increased metabolic flux for the production of terpenoid precursors.

Curated contigs were also identified in all subsequent steps of the MEP/DOXP pathway. Each of the predicted enzymes for the downstream half of the pathway (IspF and onwards) are encoded by single genes with high to very high sequence coverage, indicating vigorous transcription and perhaps robust metabolic flow through these enzymes.

Terpenoid backbones—Terpenoid backbones were generated by the stepwise addition of IPP (13) with allylic polyprenyl diphosphates catalyzed by prenyl diphosphate synthetases. We identified genes encoding for synthetases for the production of C₁₀ geranyl diphosphate, C₁₅ farnesyl diphosphate, and C₂₀ geranylgeranyl diphosphate. Interestingly, two genes encoding for putative isozymes of farnesyl diphosphate synthase (FDPS) with 72% amino acid identity were identified in the race B transcriptome, both with moderate sequence coverage. We also identified in the race B transcriptome the 3-squalene synthase-like genes that catalyze the condensation of two C₁₅ farnesyl diphosphate molecules to produce the C₃₀ squalene and botryococcene backbones. Finally we

identified six methyl transferases in the transcriptome that are used to mature the methylated C_{31-37} botryococcenes and the methylated C_{31-34} squalenes.

Alkadiene and alkatriene biosynthesis—The A race transcriptome was used to identify potential genes in this race that are involved in alkadiene/triene biosynthesis. This first step in alkadiene/triene production is the elongation of the fatty acid oleic acid (18:1 cis- Δ^9) and/or its isomer elidaic acid (18:1 trans- Δ^9). This elongation is similar to that which takes place in the production of waxes for the leaf cuticle in land plants. Thus, we searched the A race transcriptome for contigs similar to the fatty acid elongation genes from land plants and identified six candidate genes. These genes are currently being cloned for future characterization.

Lycopadiene biosynthesis—For the L race, the biosynthesis of lycopadiene is predicted to require a gene similar to the squalene synthase (SS) gene. Thus, the L race transcriptome was screened for contigs that are similar to SS. Two L race contigs were found that have significant homology to SS and they have been cloned for characterization of the enzyme activity of the encoded protein. For these enzyme characterization studies, an *in vitro* cell free enzyme assay was developed for the production of lycopadiene. This assay entails using an L race protein extract with NADPH, the substrate geranylgeranyl diphosphate (GGPP), and analyzing the reaction products by GC-MS. Two molecules of GGPP were condensed to produce lycopadiene. This assay was successful in production of lycopadiene and was used with bacterial protein extracts from cells expressing the cloned SS-like genes to test the activity of the encoded proteins.

Summary of Systems Biology Experiments

Lipid-producing strains—Analysis of the transcriptome was essential to build gene models and correlate gene expression with each phenotype. We have used transcriptomics to examine nitrogen-deprivation-induced production of lipids by three green algae, *C. reinhardtii*, *A. protothecoides*, *Picochlorum* sp., and a stramenopile *N. salina*. The available annotation of the *Chlamydomonas* genome has facilitated a more complete analysis of the transcriptomics data. While the experimental protocols were distinct for each of the organisms, several trends emerged from comparing these three transcriptomes. First, in all three organisms, several of the acyl transferases, particularly DGAT, are induced during the lipid production phase. Similarly, in *Auxenochlorella* glucose-induced TAG accumulation also induced the expression of genes involved in TAG biosynthesis. In *Picochlorum*, glycerol-3-phosphate dehydrogenase and glycerol-3-phosphate acyltransferase are induced during the lipid production phase. Although structurally unrelated, genes encoding for lipid-droplet-associated proteins were induced in the nitrogen-depleted medium in both *Chlamydomonas* and *Nannochloropsis*. Genes encoding for TAG biosynthesis are important targets for metabolic engineering, which we are testing. In *Auxenochlorella* it was evident that stress genes were also induced during nitrogen deprivation or decane treatments, which rapidly (<48 hrs) induce oil accumulation to maximal levels. We also observed the induction of some stress genes in *Picochlorum*.

In all three organisms, recognizable genes involved in lipid biosynthesis are all expressed, but only in *Picochlorum* are they modestly induced (~about 2-fold) after nitrogen depletion from the growth medium. In *Picochlorum* and particularly in *Nannochloropsis*, the cytoplasmic acetyl-CoA carboxylase gene was induced during lipid production. In *Chlamydomonas* ACCase, expression in

sta6 and *cw15* showed no induction during N-deprivation. However, genes predicted to encode biotin synthase genes were induced in *sta6*.

Interestingly in *Chlamydomonas*, genes encoding for enzymes in the central carbon metabolism pathways are induced during lipid biosynthesis. Enzymes of the pathway for acetate and acetyl-CoA assimilation are induced, including acetyl-CoA synthase, isocitrate lyase, and malate synthase. These genes are all expressed to modest levels in *N. salina* in all of our time points. The isocitrate lyase gene is induced 3-fold during the dark cycle and modestly (1.4-fold) during high lipid production.

In addition, *Chlamydomonas* genes encoding for steps in gluconeogenesis and the pentose pathway, including phosphoenolpyruvate carboxykinase, fructose-1,6-bisphosphate phosphatase, and transaldolase, were all highly induced during lipid production. We have postulated that increasing the carbon flux through these pathways is necessary to generate reducing equivalents in the form of NADPH for lipid biosynthesis. Alternatively, over-expression of these genes may facilitate carbon scavenging. Engineering approaches to increase the flux through gluconeogenesis and pentose pathway flux may be necessary to increase fatty acid biosynthesis.

Hydrocarbon-producing strains—Our study described reconstituted metabolic pathways related to the biosynthesis of terpenoid hydrocarbons. We followed the fate of photosynthetic carbon from 3-phosphoglycerate to the general terpenoid precursors IPP and DMAPP, then onwards to the production of linear polyprenyl backbones and the biosynthesis of triterpenoids, botryococcene, and squalene to yield liquid hydrocarbon compounds, matrix structural materials, and possible routes for the extracellular localization of these compounds. Metabolic pathways leading to other terpenoids have also been reconstructed, and anabolic pathways for competing storage compounds (TAG and polysaccharides) were similarly mapped.

A recurrent theme in the terpenome biosynthesis in *B. braunii* was the expansion of particular gene families. This allows the adaptation of the paralogs to structurally orthogonal substrates (botryococcene methyltransferases), and permits neofunctionalization to support novel biochemical reactions (botryococcene synthase). Paralogs may enhance increased metabolic flux, or they may provide additional flexibility in terms of regulation, compartmentalization, and biochemical properties (deoxyxylulose phosphate synthase and farnesyl diphosphate synthase).

The reconstructed metabolic networks, their participating enzymes and the corresponding cDNA sequences provide a genetic and metabolic framework that should empower biosynthetic engineering approaches targeting the increased production of hydrocarbons in *B. braunii*. Even more relevant to the objectives of NAABB, these pathways/genes may be mobilized into genetically tractable photosynthetic (bacterial, algal, or land plant) hosts or heterotrophic microbial strains.

Algal Transformation

Photobioreactor Array for Phenotype Characterization of Transformants

Because light is the main energy source for algal growth, cultivation of microalgae poses unique challenges. This is particularly true in the laboratory where it is very difficult to reproduce solar light intensity. Previously available laboratory-scale photobioreactors do not attempt to imitate the dynamic environmental conditions found under production conditions in outdoor ponds. This project had three major goals: (1) to produce a new type of environmental photobioreactor (ePBR) that simulated key environmental parameters and could be used in the laboratory to predict the productivity of algal strains under production pond conditions; (2) to produce an ePBR that was small and relatively inexpensive so that it could be arrayed in a laboratory to rapidly test algal strains or growth conditions in parallel; and (3) to use the ePBR to explore the importance of environmental light fluctuations in controlling the efficiency of light capture in algal and cyanobacterial water columns. For the first goal, we designed the ePBR to simulate the abiotic features of a pond that have the greatest influence on algal photosynthesis and growth: light intensity and quality, temperature, gas exchange, and natural dynamics. Shown in the Figure 1.14 is our environmental photobioreactor, a laboratory-scale platform for growing algae under simulated natural environments. We have designed a columnar vessel to mimic a water column in an algal production pond by using collimated white light from a high-power LED to reasonably reproduce both the intensity of sunlight and the light gradient throughout the water column. The ePBR provides programmable computer control over light, mixing, temperature, and gas flow while autonomously measuring optical density and pH. Scripting allows the ePBR to create complex environments and react to its own data. Additionally, the system is scalable for parallel and matrix experiments. We designed, prototyped, and collaborated with Phenometrics Inc. in the production of ePBR arrays. Described below is an array of 24 ePBRs that were used for the phenotype characterization of transgenic *Chlamydomonas*.

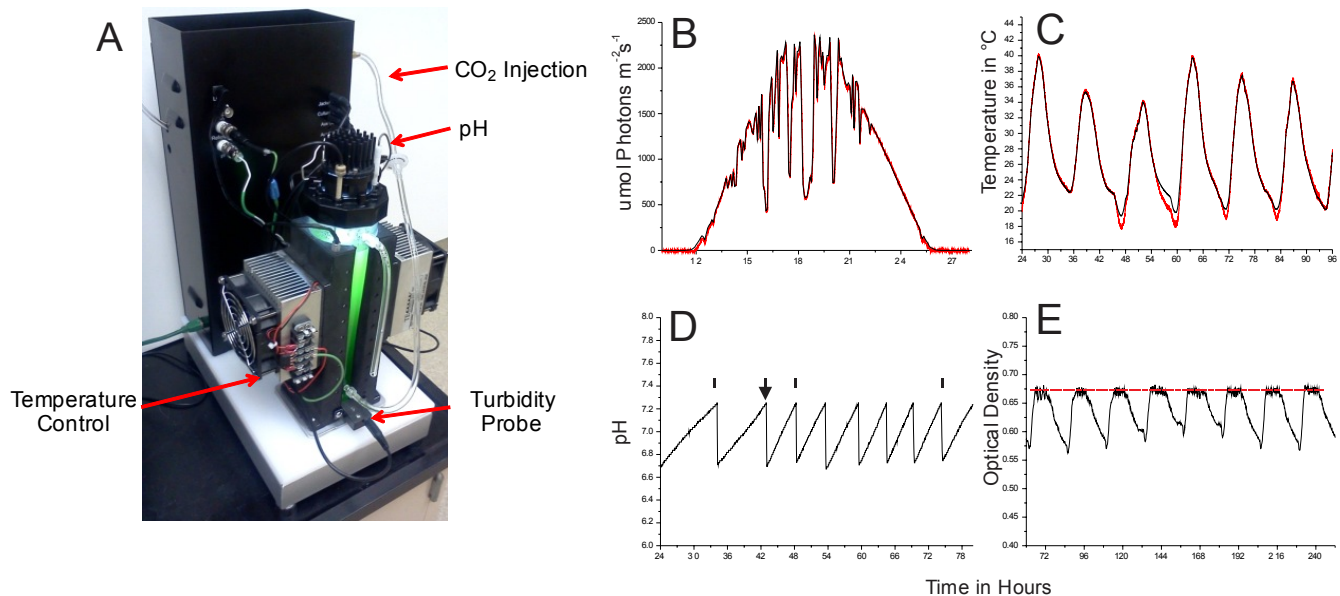


Figure 1.14. The environmental photobioreactor (ePBR) is a modular unit capable of simulating an outdoor water column. Labeled view of a single ePBR unit, Panel A. The ePBR can simulate dynamic environmental conditions within the culture vessel. Solar data from Altus, Oklahoma, was programmed into the ePBR at 5 minute intervals (black line) and actual light intensity output from the reactor was recorded with a data logger connect to a PAR meter, Panel B. Culture temperature as programmed into the reactor (black line) and temperature as recorded by the ePBR (red line), Panel C. The ePBR can control pH via CO₂ injection, as marked by arrows, Panel D. When run in turbidostat mode, the reactors can maintain a constant (or target) optical density as denoted by the red line, Panel E.

Algal Transformation Pipeline

Engineering *Chlamydomonas* for Greater Lipid Production

A major deliverable of the NAABB program was to demonstrate proof-of-concept for advanced biomass and oil accumulation in genetically engineered algae. Two approaches were used for proof-of-concept including: (1) engineering the model fresh-water algae *Chlamydomonas reinhardtii* and (2) engineering new potential production strains of algae that have greater biomass production potential than *Chlamydomonas*. Because these engineering efforts were largely built on the genome sequencing and transcriptomics experiments previously described in this report, the engineering efforts were initiated in the last 14 months of the NAABB program by developing an algal transformation pipeline. Essential to this pipeline was the development of a robust bioreactor array to rapidly test the phenotype of the engineered strains.

Transformation Pipeline

1. *Selection of genes of interest*—The Systems Biology Advisory Committee of NAABB evaluated transcriptomics, proteomics, and metabolomics data from the Algal Biology team partners to identify gene targets that may increase biomass yield, increase oil content, enhance harvestability, or increase the extraction efficiency for harvesting algae or lipids. Candidate genes were prioritized for transgenic expression in targeted algae based primarily on evaluation of their potential impact on biomass productivity and oil yield.



2. *Vector construction*—The team designed and verified the construction of all vectors and plasmids containing genes of interest. All genes of interest were codon-optimized for the relevant algal expression system. For siRNA constructs, an algal intron was often included between the ~200 bp (5' to 3') and ~200 bp (3' to 5') fold-back elements to enhance μ RNA expression. All proposed fold-back constructs were screened against genomic databases to determine if there were potential nontarget hits for any 21- to 24-mer siRNA products. No more than 15 sequential nucleotides can be conserved between the fold-back construct and a nontarget gene. All DNA constructs were also sequenced for quality control purposes. This verification included:
(1) sequencing all constructs to confirm there were no mutations or frame shifts, and that all essential elements (5' and 3' UTR, transit peptides if required, etc.) were present in the construct design; (2) *in silico* translation of all sequenced constructs to ensure proper protein synthesis and no false start sites in the constructs; and (3) cataloguing all constructs with complete restriction and gene maps, DNA sequences, and diagnostic polymerase chain reaction (PCR) primer sets.
3. *Algal transformation*—We developed an algal transformation pipeline. All transformations were repeated at least 3 times for each DNA construct. At least 10 independent transgenes were isolated for each construct. For chloroplast transformation in *Chlamydomonas*, we used a particle gun. For nuclear transformation of *Chlamydomonas*, the glass bead system was used to minimize copy number integration. Molecular characterization of transformants included PCR verification of the presence of an intact transgene in all putative transgenes.
4. *Transformation vectors*—For *Chlamydomonas* transformation, two vector systems were used. For nuclear transformation, we used the PSL18 vector in which the transgenes were driven by the strong *psaD* promoter/terminator pair. These genes were introduced into *Chlamydomonas* using the glass bead procedure for wall-less strains and the particle for walled or chloroplast transformation events. For chloroplast transformation, we linked the transgene of interest to the appropriate promoter-terminator pair or linked the transgene to the *psbA* gene to complement the *psbA* deletion mutants.
5. *Algal phenomics*—Using the PBR array developed by NAABB, we characterized the phenotypes of the transgenes. To demonstrate gene expression, RT-PCR or Q-PCR analyses were carried out and normalized to expression of actin or B-tubulin. All transgenes were to be screened for (1) growth rate by flow cytometry and absorbance at 750 nm, (2) terminal dry weight at the stationary phase, (3) high throughput lipid content analysis by Nile Red fluorescence flow cytometry and gas chromatography–mass spectrometry flame ionization detection (GC-MS-FID). More focused assays were carried out as appropriate including western blots, enzyme assays, metabolomics, etc.

Engineering *Chlamydomonas reinhardtii* with Enhanced Biomass and Oil Yield

Chlamydomonas was chosen for initial surveys of interesting gene targets for several reasons. *Chlamydomonas* was the first algal species that was genetically transformed. It was also the first organism in which the chloroplast and mitochondrial genomes were engineered. In addition, *Chlamydomonas* has two mating types and so it is

possible to introgress transgenes into the progeny resulting from sexual crosses. Importantly, the *Chlamydomonas* genome has been sequenced and a robust array of mutants is available, including deletion mutants that can be functionally complemented thereby greatly facilitating the selection of transgenics. One challenge for *Chlamydomonas*, however, is that it stores energy predominantly in the form of starch rather than oil. Mutants (*sta6*) that are impaired in starch production, however, store TAG as an alternative. Here, we describe the outcomes of the transformation events that increased either biomass or oil yield. Over 50 independent gene constructs were tested either by expression in the nuclear or chloroplast genome. The greatest yield increases observed were 2-fold in biomass and 5-fold in oil levels.

Our initial targets for overexpression were identified in the transcriptomics experiments described previously, including: (1) overexpression of DGAT to increase the rate of triglyceride biosynthesis; (2) overexpression of the glyoxylate cycle enzymes isocitrate lyase and malate synthase; and (3) overexpression of the lipid storage droplet protein. In addition, we developed a strategy to increase biomass production by increasing the rate of carbon assimilation.

Overexpression of DGAT—The enzyme DGAT catalyzes the last step in triglyceride biosynthesis (Figure 1.15). In the transcriptome data we analyzed for *C. reinhardtii*, *Picochlorum* sp., and *N. salina* there was a correlation between increased lipid production and increased transcription of the genes encoding for DGAT. Therefore, we over-expressed the gene DGAT from *Arabidopsis*. The DGAT gene was codon optimized for *Chlamydomonas* and cloned into the PSL18 vector under control of the *psaD* promoter and terminator. We isolated 89 transformant colonies and confirmed 24 as PCR positive for the DGAT gene. We characterized the phenotype of 12 of the PCR positive transformants. We observed a 2.5-fold increase in accumulated lipids in transgenic *Chlamydomonas* overexpressing the plant DGAT relative to wild-type algae. This occurred with or without nitrogen, indicating that nitrogen stress was not required for the additional TAG accumulation and that TAG levels could be further elevated above those achieved by withholding nitrogen alone.

Glyoxylate cycle enzymes—Our transcriptomics studies of *Chlamydomonas* indicated that under nitrogen deprivation conditions, there is a strong induction of the expression of genes encoding for glyoxylate cycle enzymes. This is somewhat surprising because the glyoxylate cycle is thought to play a primary role in the turnover of fatty acids by assimilating acetate (2-carbon) units produced by β -oxidation of lipids (Figure 1.7). However our hypothesis is that the glyoxylate cycle is required to generate reducing equivalents under nitrogen-deprivation conditions. To test the effects of glyoxylate enzymes on lipid production, we both over- and underexpressed the glyoxylate cycle enzymes isocitrate lyase (ICL) and malate synthase (MS). Independently, we constructed

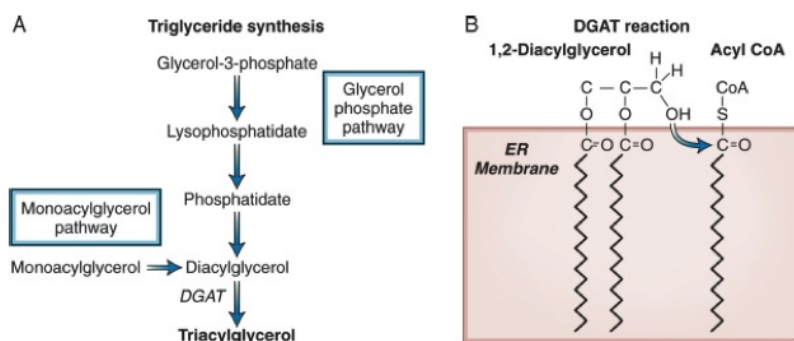


Figure 1.15. TAG biosynthesis (A) and the reaction catalyzed by DGAT (B). By overexpressing DGAT we are increasing the metabolic flux toward triglycerides and increasing the overall lipid yield in algae.

interference RNAs (RNAi) designed to block the expression of ICL (ICL-RNAi) and MS (MS-RNAi). We cloned these RNAi's under control of the *psaD* promoter/terminator pair. Independently, we transformed *Chlamydomonas* with the ICL-RNAi plasmid or the MS-RNAi plasmid. In addition, we cotransformed using both plasmids. Transformants were isolated and confirmed by PCR to harbor the ICL-RNAi, the MS-RNAi, or both ICL-RNAi and MS-RNAi. Interestingly, post-translational gene silencing of isocitrate lyase by ICL-RNAi caused an increase in lipid accumulation in nitrogen-replete growth. RNAi-based repression of both isocitrate lyase and malate synthase caused a 5-fold enhancement of oil accumulation in *Chlamydomonas* grown with nitrogen and 2-fold enhancement after N-deprivation to induce oil accumulation. While the increased lipid accumulation is encouraging, RNAi-based repression of both ICL and MS caused the growth rates to be reduced by 30%.

In contrast, overexpression of a *Euglena* bifunctional ICL/MS gave a 2.6-fold increase in oil content with no impact on growth rate with or without nitrogen. While this result is consistent with our transcriptomics studies, it seems inconsistent with the data presented above because the repression of the *Chlamydomonas* ICL and MS also induced lipid biosynthesis. This observation could be explained, however, by the fact that the bifunctional gene product (ICL/MS) is targeted to the mitochondria in *Euglena*. In *Chlamydomonas*, mistargeting of the ICL/MS protein to the mitochondria rather than the glyoxysome would lead to a competition for the fate of isocitrate. If isocitrate were consumed by the TCA cycle, two carbons would be lost through decarboxylation events. In contrast, the two carbons would not be lost if isocitrate were metabolized by the ICL/MS enzyme, thus increasing the efficiency of carbon utilization from acetyl CoA entering the mitochondria and perhaps allowing for elevated acetyl CoA pools for fatty acid synthesis. Currently, we are confirming the localization of the ICL/MS in *Chlamydomonas* mitochondria and its impact on acetyl CoA pools.

Overexpression of the lipid storage droplet protein—An additional strategy for enhancing end-product (oil) accumulation is to enhance oil storage by overexpressing proteins or enzymes involved in controlling lipid storage or turnover. Previous studies demonstrated that during glucose-induced oil storage in *A. protothecoides*, the levels of lipid storage droplet protein, caleosin, increased substantially. We made a similar observation in our transcriptomics studies, which demonstrated a strong induction of the lipid storage droplet protein during high lipid biosynthesis in *Nannochloropsis*. To mimic this effect, we overexpressed the plant lipid storage droplet protein, oleosin, from *Arabidopsis* in *Chlamydomonas*. We observed a five-fold increase in oil accumulation in nitrogen-replete growth. This was the single largest increase in oil accumulation observed for any single transgene.

Increasing the rate of carbon assimilation—In cyanobacteria and many eukaryotic algae with active inorganic carbon concentrating mechanisms (CCM), the enzyme carbonic anhydrase (CA) is colocalized or concentrated around RuBisCO either in carboxysomes or pyrenoids. CA accelerates the interconversion of bicarbonate and carbon dioxide with a relatively low equilibrium constant. Since bicarbonate is the major form of inorganic carbon that is pumped into cells and since RuBisCO fixes only carbon dioxide,

bicarbonate must be converted back to CO₂ to be fixed by RuBisCO. We hypothesized that linking CA, in this case human carbonic anhydrase II, one of the fastest enzymes in nature, to the C-terminus of the RuBisCO large subunit with linkers of various lengths (3-43 amino acids) would effectively localize CA with RuBisCO, thereby increasing the local concentration of CO₂ and accelerating carbon fixation. These constructs were introduced into an *RbcL* deletion mutant of *Chlamydomonas* and restored autotrophic growth indicating the gene fusions were functional. We are currently evaluating the relative photosynthetic activity of these various constructs.

Optimizing light-harvesting antenna size—Previous studies had demonstrated that intermediate sized peripheral (Chl a/b binding) antenna sizes were optimal for growth in *Chlamydomonas*.⁵¹ In this project we compared the growth rates of algae in which the accumulation of chlorophyll b was light regulated so that it decreased at high light levels. This regulation was achieved by controlling the expression and binding of the NAB1 protein to a 5' light responsive element of the mRNA fused to the *Cao* gene. As shown in Figure 1.16, as much as a 2-fold increase in biomass was achieved with the best performing transgenics when grown in ePBRs mimicking a typical summer day. This gene (trait) conferred the greatest increase in biomass productivity of any tested by the NAABB consortium.

Transgenics with self-adjusting antenna have 2-fold greater biomass yield than wild-type algae!

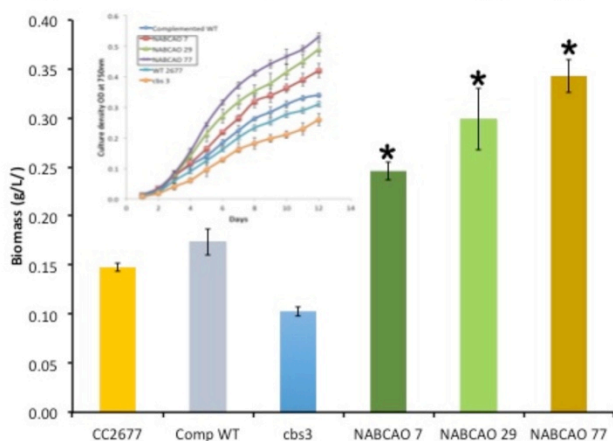


Figure 1.16. Cellular and dry weight productivity of wild-type and transgenic *Chlamydomonas* algae with self-adjusting light-harvesting antenna. The NABCAO lines have been engineered to self-adjust their Chl a/b ratios and hence peripheral light-harvesting antenna size in response to changing light levels or culture densities. Strain **CC2677** is a typical wild-type strain; strain **cbs3** is a mutant in which the chlorophyll a oxygenase (*Cao*) gene, which converts Chl a to Chl b, has been inactivated and is the parent strain for the **NABCAO** lines; strain **Comp WT** is the *cbs3* line complemented with the *Cao* gene. Chlorophyll a/b ratios ranged from 4.2 (day 6) to 3.4 (day 12) for the best performing strain (**NABCAO 77**). Chlorophyll a/b ratios (2.5) did not change over the time course in the complemented wild type strain.

Hydrocarbon production in engineered Chlamydomonas—While much of the NAABB work focused on species that store carbon as lipids, we also examined the potential for developing an autotrophic production system for hydrocarbon-like terpenoids to satisfy the unique requirements for aviation fuels. For example, the monoterpene limonene (Figure 1.17) could be an important component of aviation fuels. Although algae are not known to produce monoterpenes, they make larger terpenoids, such as carotenoids. Thus, they express the biochemical machinery to produce the C5 isoprene precursors as well as the prenyl transferases necessary to produce the C10 geranyl diphosphate in the chloroplast. All that is necessary to produce limonene is to engineer a monoterpene synthase like limonene synthase (Figure 1.17) so that it is expressed in the

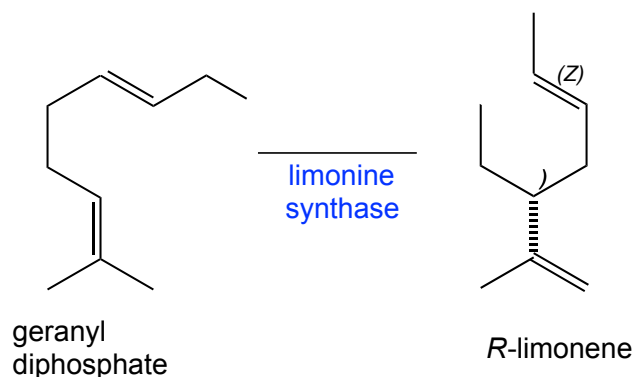


Figure 1.17. The monoterpene synthase from rice catalyzes the cyclization of geranyl diphosphate to yield limonene.

chloroplast. This study demonstrates that the hydrocarbon limonene can be produced by engineering the eukaryotic green algae *Chlamydomonas* to express the rice monoterpene synthase gene (*OsTPS26*). Using a modified nuclear transformation strategy, we engineered stable transformants expressing a functional rice limonene synthase (*OsTPS23*) targeted to the plastid. Our vector was constructed so that expression of limonene synthase is driven by the strong inducible/constitutive Hsp70A/RbcS2 promoter and targeted to the chloroplast using a stroma cTP signal in place of the rice cTP signal. In total, 10 transformant lines were evaluated for limonene production; mRNA abundance was quantified by qPCR and limonene analyte in the headspace of the photobioreactor was quantified by GC-MS analysis. *Chlamydomonas* mutant lines were cultured in enclosed vessels, allowing a purge-and-trap method of trapped volatile limonene in the headspace of the photobioreactor. Limonene was adsorbed onto volatile collection traps, which were subjected to GC-MS for product identification and quantification analyses. We demonstrated limonene production from a single transformant line at $\sim 1 \mu\text{g/g}$ dry biomass in 72 h. We have established a baseline capability of monoterpene production in algae, which will pave the way for advanced autotrophic hydrocarbon production. Additionally, we show that limonene is emitted from the algal biomass into the headspace region of enclosed photobioreactors, eliminating the requirement of cell harvesting, dewatering, and biomass processing.

Advanced autotrophic hydrocarbon production—While we have engineered strains that can produce limonene, our demonstrated production levels are lower by a factor $\sim 10^5$ than the natural lipid production systems discussed in this report. Reported in the systems biology section of this report, we have carried out extensive transcriptomics studies on the colonial microgreen alga, *B. braunii* race B, which is known to be a prolific producer of the highly branched, unsaturated hydrocarbons known as botryococenes. This freshwater alga has been reported to produce greater than 50% of its dry cell weight in botryococenes. Although this alga is attractive as a source of biofuels, the scientific community generally recognizes that this alga grows far too slowly for practical use as a production strain. Our primary goal was therefore to unravel the molecular details associated with hydrocarbon production in *B. braunii* race B and, ultimately, engineer an algal production strain that is fast growing and produces large amounts of hydrocarbons for fuels. Our careful annotation of the *B. braunii* race B transcriptome identified all the genes encoding for the biosynthesis of the enzyme isoprenoid and narrowed in on likely candidates to address bottlenecks. Briefly, gene candidates included *dxs I, II, III* (deoxyxylulose phosphate synthase), *dxr* (MEP synthase), *ispH* (hydroxydimethylallyl diphosphate synthase), *fps* (farnesyl diphosphate synthase) and, importantly, *sqs1, 2, 3* (squalene synthase-like), which were found to be responsible for the head-to-head coupling of two farnesyl units to provide the C30 botryococene. Based on these findings, we are engineering isoprenoid-specific genes into the proof-of-concept green alga, *C. reinhardtii* and the cyanobacterium, *Synechococcus elongatus* PCC7942, to determine the extent of increased hydrocarbon production as a result of overexpression of the respective enzyme. Initially, genes encoding for *dxsI*, *dsxII*, and *dsxIII* were synthesized with codons optimized for expression in *Chlamydomonas*. These genes were cloned into vectors with expression driven by the *psaD* promoter/terminator. These vectors were used to transform *C. reinhardtii* CC4147. We are currently in the process of characterizing these transformants.

Transformation of Nannochloropsis and Picochlorum—As discussed above, we have characterized the growth and lipid production of *Picochlorum* transformed with *BIC A* and *ACCase* genes. *Picochlorum* transformed with *ACCase* show normal growth, but a significant 27% increase in accumulated lipids. Similarly, transformation of *Picochlorum* with the gene encoding for the cyanobacterial bicarbonate transporter gene, *BIC A*, show normal growth, but a 38% increase in accumulated lipids. We are in the process of characterizing *Nannochloropsis* transformed with plasmids designed to express *BIC A* and *ACCase*.

Summary

Our metabolic engineering studies in *Chlamydomonas* are summarized in Table 1.4. Overall, we have demonstrated improvement in oil accumulation without a deficit in biomass accumulation using a variety of metabolic engineering strategies in *Chlamydomonas*. Oil accumulation levels increased as much as 5-fold without affecting growth rates. We have also shown transformants that overexpressed fructose biphosphatase had significantly increased growth. In addition, engineering self-adjusting photosynthetic antenna into *Chlamydomonas* results in a significant 2-fold increase in biomass accumulation. We also demonstrated that engineered *Chlamydomonas* to express rice limonene synthase in the chloroplast of *Chlamydomonas* produces small amounts of limonene.

Table 1.4. Summary of metabolic engineering studies in *Chlamydomonas*.

Gene*	Growth	Lipid Accumulation + nitrogen	-nitrogen
DGAT	No effect	2.5-fold increase	2.5-fold increase
ICL-RNAi	30% decrease	2.5-fold increase	
ICL-RNAi and MS-RNAi	30% decrease	5-fold increase	2-fold increase
Bifunctional ICL/MS	No Effect	2.6 fold increase	2.6 fold increase
Caleosin	No Effect	5 fold increase	
FBPase	1.4X	ND	ND
Self-adjusting Antenna	2.0X	ND	ND

*DGAT, diacylglycerol acyl transferase; ICL-RNAi, RNAi for isocitrate lyase; MS-RNAi, RNAi for malate synthase; bifunctional ICL/MS, bifunctional isocitrate lyase/malate synthase, FBPase, fructose biphosphatase.

Overall, we have demonstrated that systems biology studies can be used to direct metabolic engineering in complex algal systems and that *Chlamydomonas* can be a robust platform for testing novel gene constructs. While our *Chlamydomonas* model is likely to have the greatest implications for engineering closely related production strains such as *Chlorella*, our transcriptomics studies encourage us to test these engineering strategies in other production strains. The increases in lipid production reported here are significant. While it is not known if these improvements are additive, even a 5-fold increase in the rate of lipid biosynthesis caused, for example, by overexpression of caleosin coupled with the increase in biomass yields resulting from engineering overexpression of fructose biphosphatase and expression of self-adjusting antenna into our best production strains could lead to economically viable algal transportation fuels. As discussed in this report, economic models show that with the 2.5-fold increase in biomass

yield predicted here from combining the overexpression of fructose biphosphatase with expression of self-adjusting antenna could enable significant progress toward a sustainable biofuels industry. As discussed elsewhere in this report, we have made significant progress in developing the genetic tools necessary to engineer production strains and are using these tools to engineer the production strains *C. sorokiniana*, *N. salina* and *Picochlorum* sp. We have produced transformants in *Picochlorum* with increased lipid production.

Molecular Biology and Genetic Tool Development in Algae

Gene Identification Strategies for the Model Alga C. reinhardtii

Similar to strategies that have been used for the model plant *Arabidopsis*, developing a library of algal mutants in which particular genes have been silenced using RNA interference in independent isolates could be a useful tool to elucidate the functions of unknown genes and DNA elements or gene products that regulate the expression of other genes. RNA interference (RNAi) is an effective method in most eukaryotic organisms to reduce the expression of specifically targeted genes.⁵² Commonly, RNAi is performed by substituting designed hairpins into natural pre-miRNA genes, where they are converted into microRNAs (miRNAs) by the normal cellular machinery and can lead to down-regulation of the targeted genes.⁵³⁻⁵⁵ A whole genome library of miRNA that targets every gene would provide a tool to identify those genes of interest through an efficient screening procedure. The goal of this project was to develop an inducible RNAi system that contains RNAi targeted against every gene. This was accomplished by generating a random library of genomic DNA that is converted into a precursor, which can be converted by the cell into miRNA. A genomic miRNA library was cloned into the artificial miRNA vector and transformed into *E. coli* where more than 1 million transformants were obtained. That library was sequenced. Over 6 million reads had the expected length and matched exactly to an expected location in the *Chlamydomonas* genome. After removing redundancy, there were about 850,000 unique matches to the *Chlamydomonas* genome. Nearly every gene (more than 95%) had at least one miRNA targeted to it. The library was copied and moved into the *Nit1* promoter vector and transformed into *E. coli*. Again, we obtained over 1 million transformants. That library is now being sequenced to determine its coverage of the *Chlamydomonas* genome and the fraction of genes with at least miRNA targeted to it. We expect the coverage to be the same as for the original vector.

The library exists in two vectors, one in which the miRNA is constitutively expressed and another in which it is driven by the *Nit1* promoter and inducible by nitrogen starvation. We tested the artificial miRNA vector (amiRNA) by designing an amiRNA against the *Chlamydomonas sta6* gene and demonstrated that it effectively reduced expression of that gene, giving rise to the same phenotypes that are observed in strains in which the *sta6* gene mutated. We then tested the new *Nit1* promoter vector using the same amiRNA against *sta6* and demonstrated that it showed the *sta6* phenotype only after being placed in media lacking ammonia. The results show that the two different vector systems we have for expressing amiRNA genes work and can be used to knock down expression of *Chlamydomonas* genes, in one case under specific inducible conditions. Screens

are ongoing to select strains with desired phenotypes from which the miRNA inserts can be sequenced *en masse* to identify the gene knockdowns responsible for those phenotypes. The ultimate goal is to use this system to identify genes that up- or down-regulate the production of TAGs and other lipids.

Gene Mapping in *C. reinhardtii*

Recombinant populations that have been stabilized by single-seed descent are invaluable tools in plant quantitative genetics. *Chlamydomonas*, which is haploid in the vegetative stage, can produce segregating populations with fixed recombination events in the first generation following a cross.^{56,57} In some ways, this makes it ideal for quantitative genetics studies. Once the population is genotyped, the individual lines can be phenotyped for a variety of different traits. Each trait can then be mapped for the underlying genetic architecture. The quality of the mapping improves with greater numbers of lines and greater density of markers. We set out to create a mapping resource for the NAABB consortium and the broader algal biology community.

We created over 800 individual lines, from which we randomly sampled 384 to be the core population. We have distributed the population to the Purugganan lab at NYU and the Niyogi lab at UC Berkeley. We grew out 192 of the lines and made DNA samples and libraries for sequencing. These strains were then screened in various nutrient media for their relative growth rates and mineral composition to identify strains with minimal nutrient requirements as well as to characterize genes involved in nutrient metabolism. We observed a large variation in the phenotypes among the progeny. We are sequencing the libraries we made and the Purugganan lab is sequencing the other 192 in order to generate a genetic map for mapping traits.

Chloroplast Transformation of *A. protothecoides*

The unicellular green alga *A. protothecoides* is a photosynthetic aquatic species that is a member of the Scotielloideae subfamily under the Chlorellaceae family. The alga is considered one of best species for genetic and metabolic engineering to produce biofuels due to the high oil content (< 55% of its dry weight) when heterotrophically cultivated. *Auxenochlorella* synthesizes TAGs as a storage compound that can be converted into renewable fuels. Although TAGs are assembled in the endoplasmic reticulum, their main constituents—fatty acids—are synthesized in the chloroplast.

We sequenced the algal chloroplast genomes and used that information to design chloroplast transformation vectors for *A. protothecoides*. Intact chloroplasts from the green oleaginous microalga were successfully enriched. Quantitative PCR analyses revealed the intact chloroplasts were effectively enriched by 2.36-fold from *C. protothecoides*, compared to the number in control samples. DNA was isolated from the enriched chloroplast fraction and subjected to DNA sequencing using the Illumina platform to yield a total of 3,032,536 reads. The chloroplast genome sequence was determined to be 84.5kb in size and was found to reveal 114 annotated open reading frames (putative coding regions). The genes include 32 tRNAs, 26 rRNAs, 21 photosystem subunit genes, 6 ATP synthesis genes, 6 transcription/translation related genes, 5 cytochrome genes, 4 chlorophyll genes, 2 chloroplast division related-genes, 1 gene encoding RuBisCO, a gene encoding

acetyl CoA reductase (*accD*) involved in the fatty acid biosynthesis as well as 7 others. The size of the cpDNA of *A. protothecoides* is relatively smaller than the cpDNA of *C. variabilis* (124,579bp) and *C. vulgaris* (150,613bp) due to the loss of noncoding regions. Not only are some genes missing, but the cpDNA of *A. protothecoides* shows high gene compactness (only 19% of entire genome is noncoding sequences) while *C. variabilis* cpDNA reveals 46% and 53% in *C. vulgaris* cpDNA. Overall, the three *Chlorella* genomes shared numerous highly conserved genes, while they also contained unique coding and noncoding regions. Gene synteny was primarily conserved, but was variable to some extent among the three genomes. Lastly, phylogenetic analysis revealed a distinct *Chlorella* sp. clade, in relation to the more divergent species included in the analysis.

The presence of introns within target gene sequences can confound the use of gene sequences obtained from one species to transform another species so it was important that we examine these genomes for the presence of introns. Group I/II introns are sporadically distributed in the nuclear, chloroplast, and mitochondrial genomes of a broad range of organisms. Most introns found in the chloroplasts of higher plants and algae belong to group II and are made up of a catalytic RNA (ribozyme; domain I~VI) and intron encoded protein (IEP) composed of four ORFs encoding reverse transcriptase, maturase, DNA binding domain, and endonuclease. The catalytic domain enables introns to self-splice and is promoted by IEP, which allows it to move the fragment into other locations in the genome. Group I and II introns were found in *Chlorella* spp. using two databases, Group I Intron Sequence and Structure Database (GISSD) and Database for Bacterial Group II introns. The GISSD contains 1789 known group I introns, which are classified into 14 subgroups based on the structure. Most group I introns (> 95%) are found in chloroplast *tRNA-leu* gene. To examine the presence of group I introns, the cpDNA of three *Chlorella* spp. were blasted against the GISSD database. We have found only one Group I intron within the *trnL-UUA* gene in *C. variabilis* and two introns within *rrn23* and *trnL-UUA* gene in *C. vulgaris*, while none were found in *A. protothecoides*. In contrast, only partial fragments of Group II introns (16-65nt in size, AT rich) are found in all three species (8 in *C. protothecoides*, 19 in *C. variabilis*, and 45 in *C. vulgaris*) when blasted against a bacterial Group II intron database.

The complete chloroplast genome sequences enabled us to construct three over-expression plasmid vector cassettes flanked with the chloroplast regulatory sequences, *atpA*, *psbD/C*, and *rbcL* and the fluorescent protein, *iLOV* reporter. Each cassette is flanked with chloroplast-derived homologous sequences for chloroplast recombination. Two chloroplast target vector systems were used. The first system used the chloroplast homologous sequences required for transgene integration and three sets of regulatory sequences (5'UTR promoter and 3'UTR terminator) from *atpA*, *psbD/C*, and *rbcL* were selected from resultant data from *C. protothecoides* cpDNA sequences (Figure 1.18, A). As a selectable marker, a paromomycin resistant gene (*aphVIII*; 1.8kb) under regulation of *hsp70/rbc2* promoter was engineered in the T-DNA region of binary vector pGreen plasmid DNA to validate the glass bead transformation method. In addition, a novel reporter gene *iLOV* was conjugated using the over-expression vector system for rapid screening. The second system uses a chloroplast signal peptide (ImapctVctorTM1.4-tag) for chloroplast expression of gene of interests (Figure 1.18, B). The plasmid vector employs the RuBisCO small subunit (*RbcS1*) promoter from *Asteraceous chrysanthemum* and 1 kb of the *RbcS1* terminator

sequence. In addition to the chloroplast targeting signal peptide, the vector has a c-Myc-tag allowing identification of expressed proteins using commercially available monoclonal antibodies and six histidines for protein purification using a nickel column. Chloroplast target vector systems were used for *C. protothecoides* and DOE1412 (a NAABB field isolate of *Chlorella* sp.) transformation.

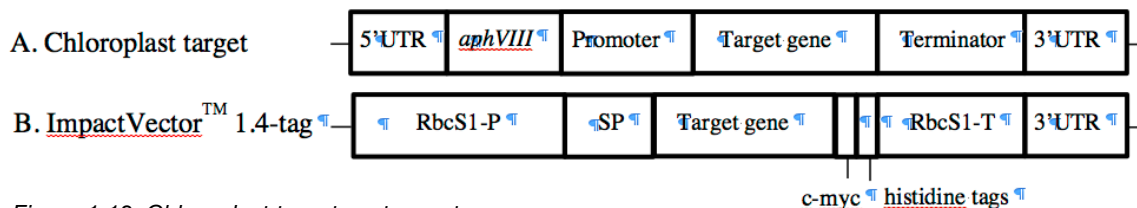


Figure 1.18. Chloroplast target vector systems.

The various constructions were tested using glass bead, electroporation, and particle bombardment transformation. A method that employs algal protoplasts and glass beads was used successfully for nuclear transformation of *A. protothecoides* and *Chlorella* sp. DOE1412 using the pGreen plasmid vector bearing the *aphVIII* gene encoding paromomycin resistance. PCR confirmed transformation efficiencies for the foreign gene of interest were 4/114 clones or 3.5% and 2/96 or 2% for antibiotic resistant colonies for *A. protothecoides* and *Chlorella* sp. DOE1412, respectively.

N. salina CCMP1776 and *Picochlorum* sp. were chosen for transformation studies for several reasons. *N. salina* had persisted and performed well in outdoor ponds during the testing carried out by the DOE EERE Aquatic Species Program⁶ and more recently in additional tests in outdoor ponds. This marine alga has performed well in high-salt-content waters; such waters are not suitable for agricultural or municipal uses. When grown photosynthetically with nitrogen depletion, *N. salina* accumulates triglycerides suitable for fuel to 50–60% of its biomass. No transformation method had been reported for *N. salina* nor had it yielded to transformation methods successfully used to transform a close relative, *N. gaditana*.⁵⁸ We initiated a focused effort to transform *N. salina*. Based on our success with *N. salina*, we also transformed another production alga, *Picochlorum* sp. This second alga was chosen because it has grown vigorously and accumulated significant amounts of lipid (approximately 25% of its dry weight as lipid).

Vector development—The literature on algal transformation is filled with numerous reports of requirements for strain-specific sequences in gene promoters and terminators. No universal promoters for algal gene expression have been reported in contrast to the 35S cauliflower mosaic virus promoter that has worked well in many plants but performs poorly in algae. NAABB obtained the genome sequence of *N. salina*; this information allowed us to design *N. salina*-specific vectors utilizing homologous promoters and codon-optimized sequences. Our goal included incorporation of multiple target genes. We therefore needed to identify and test multiple promoters and selection agents.

Vector backbone—A suitable compact vector backbone was built by modifying the shuttle vector pPha-*T1* (GenBank Accession # AF219942). This shuttle vector had been used successfully in the transformation of the diatom *Phaeodactylum tricornutum*.⁵⁹

Selection agents—Suitable selection agents were identified by testing a set of potential selection agents for their ability to kill *N. salina* 1776 (Table 1.5). Three selection agents were identified as suitable and genes for resistance to these agents were included in the vector construction strategy.

The most suitable selection agents for *N. salina* 1776 were blasticidin, puromycin, and zeocin. Blasticidin was the easiest to use of the three because the molecule itself is stable and robust and was very effective at killing *N. salina* at a concentration of 50 µg/mL. Zeocin was also very effective but it is not as stable as blasticidin and more care must be taken to ensure its performance. Puromycin was somewhat leaky because it allowed some nontransformed cultures to grow, but it can be used if this limitation is kept in mind.

Table 1.5. Potential selection agents of *N. salina*.

Selection Agent	Suitable	Selection Agent	Suitable
Blasticidin	Yes	Chloramphenicol	No
Puromycin	Yes	Spectinomycin	No
Zeocin	Yes	Streptomycin	No

Promoters—Potential suitable promoters were chosen from our results of the transcriptome studies of *N. salina*. Candidate promoters were chosen from those regulating expression of the more highly expressed genes and reports from other algal transformations. The lipid droplet protein was the most highly expressed gene and strongly induced during lipid production (nitrogen depletion); tubulin and the photosystem I subunit protein (*psaD*) genes were also well expressed. Promoters for tubulin and *psaD* protein have also worked well in other transformed alga. These three promoters were tested with the selection agent resistance genes used as the reporter genes. The lipid droplet protein and *psaD* promoters drive strong constitutive expression. The tublin promoter drives moderate constitutive expression.

Terminator—Some algal transformation efforts have reported the need to pair the promoter with a terminator unique to the promoter. We found that the *N. salina* terminator for *fcpa*, the fucoxanthin chlorophyll protein, works well when paired with each of our three promoters. The *fcpa* terminator has been used in each of our vectors. Several vectors were constructed utilizing these components.

Vectors constructed—Four vectors were initially constructed to allow for multiple gene promoters and selectable markers in different combinations to aid the gene stacking activity. In addition, the vector PTY1000 was constructed with the viral linker FMDV 2A so that one promoter drives expression of both the gene of interest and the resistance marker gene.^{60,61} This coupling results in more uniform selection of transformants since the selection agent, blasticidin

resistance, cannot be expressed unless the gene of interest is expressed also. Specifically, the vectors we constructed were as follows:

- PTY100: The gene of interest is under control of the under lipid droplet promoter and *fcpa* terminator and the Zeocin resistance gene is controlled by the tubulin promoter driving and *fcpa* terminator (Figure 1.19A).
- PTY120: The gene of interest is controlled by the lipid droplet promoter and *psaD* (photosystem I subunit protein) terminator separately and the Zeocin resistance gene is under control of a second lipid droplet promoter and *fcpa* terminator pair.
- PTY1000: The gene of interest and blasticidin resistance gene are linked by the FMDV 2A viral linker⁶⁰ and both genes are controlled by the lipid droplet protein promoter and the *fcpa* terminator (Figure 1.19B).
- PTY423: The gene of interest and hygromycin resistance gene (*hph*) are linked by the FMDV 2A viral linker, and both genes are driven by the lipid droplet protein promoter and the *fcpa* terminator.

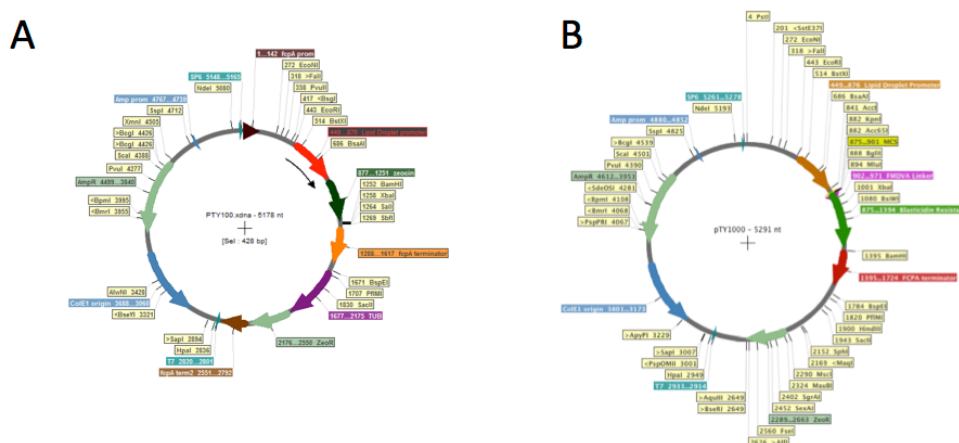


Figure 1.19. Panel A: Vector pTY100, the basic early generation *N. salina*-specific vector. These PTY vectors (100, 110, 120, and 320) provide different combinations of genes for resistance to zeocin, puromycin, or blasticidin in combinations with strong constitutive *psaD*, tubulin, or lipid droplet gene promoters. Panel B: Vector pTY1000, a later generation of our *N. salina*-specific vector, utilizes the FMDV 2A linker to allow easier insertion of target genes.

Transformation method —The preparation of competent cells began with *N. salina* or *Picochlorum* grown with 100 µg/mL kanamycin to assure the absence of the bacterial contamination that is frequently a problem in algal cultures. Cells were grown in *f/2* media with 5% CO₂ and protoplasts were generated using macerozyme and cellulose for electroporation with the plasmid DNA. Cells were then cultivated in the dark overnight followed by growth in flasks in media supplemented with sorbitol and mannitol. Live cultures were then placed on antibiotic selection plates to identify transformants followed by PCR confirmation of the transgene. Using this procedure and the plasmids discussed above, we have successfully transformed *N. salina* and *Picochlorum* based on the single colony PCR, showing, for example the incorporation of cyanobacterial bicarbonate transporter gene (Figure 1.20) into *N. salina*. To date, we have validated the transformation of both *Picochlorum* and *N. salina* by PCR with a cyanobacterial bicarbonate transporter gene, BIC A. Using western blots we have confirmed the

expression of BIC A in both *Picochlorum* and *N. salina*. In addition we have PCR-verified transformation with the gene for acetyl-CoA carboxylase, ACCase, the gene encoding the acyl-carrier protein, the gene encoding the lipid droplet protein, and the gene for diacylglycerol acyltransferase (DGAT) in *Picochlorum*.

We have characterized the growth and lipid production of *Picochlorum* transformed with BIC A and ACCase genes. *Picochlorum* transformed with ACCase show normal growth, but a significant 27% increase in accumulated lipids. Similarly, transformation of *Picochlorum* with the gene encoding for the cyanobacterial bicarbonate transporter gene, BIC A, show normal growth, but a 38% increase in accumulated lipids. At present we are characterizing the phenotype of the BIC A transgene in *N. salina*.

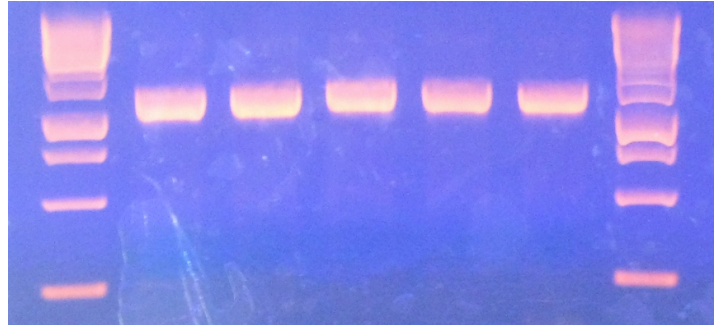


Figure 1.20. Single-colony PCR analysis showing transformation of *N. salina* with a cyanobacterial bicarbonate transporter gene.

Adaptive Evolution

Algal lipid production must be improved for algae to become a cost effective fuel feedstock. Reducing the cost per barrel of algal lipids can be approached by two strategies: increase the production/unit area and reduce the inputs. Our adaptive evolution efforts considered each of these two strategies. Greater lipid production on a per cell basis was achieved by flow cytometry sorting to isolate stable algal lines with greater lipid production while other efforts worked to reduce phosphate requirements.

Selecting for High-lipid Content *Picochlorum* Using BODIPY Lipid Staining and Flow Cytometry

Picochlorum is a marine microalgae of industrial interest due to its high lipid accumulation and its ability to grow under nonideal conditions. It is closely related to *Nannochloris*. We used flow cytometry techniques to isolate and characterize algal strains and subpopulations of interest. The flow cytometry assays were validated using more traditional monitoring methods, such as optical density for culture density and GC-MS for lipid content.

Algal cultures with varying levels of neutral lipids showed distinct separation in the stained samples (Figure 1.21). Sample work-up involved a simple dilution.

This rapid flow cytometry-based assay was used to isolate a hyperperforming subpopulation of *Picochlorum* sp. A *Picochlorum* culture was starved of nitrogen, stained with BODIPY, and subjected to multiple rounds of fluorescence activated cell sorting (FACS) (Figure 1.21). Hyperperforming and hypoperforming cells (as defined by BODIPY fluorescence) were isolated and cultured. After characterization, the parent and hyperperforming (“sorted-high”) cultures were subjected to genome and transcriptome sequencing in order to identify genes related to hyperperformance.

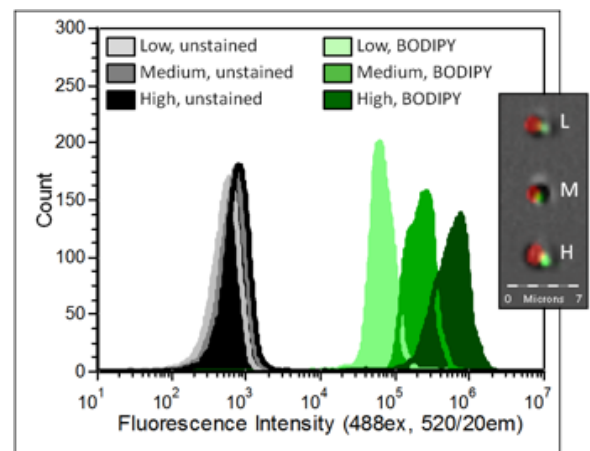


Figure 1.21. BODIPY staining of *Picochlorum* sp. Samples with *varying* levels of lipids show *varying* fluorescence intensities. Inset: Images from the Amnis ImagestreamX flow cytometer show a single lipid body of *varying* fluorescence intensity (green fluorescence staining). Low = lipid content ~10%, Med = lipid content ~25%, and High= lipid content ~45%. Red fluorescence is chlorophyll.

Basic Characterization

Characterization was first conducted using nitrogen-depletion experiments, where lipid accumulation was expected to be the highest. Histograms of BODIPY fluorescence of the parent and sorted populations showed that the sorted-high lipid population had a distinctly improved level of BODIPY fluorescence. When monitored over time, the sorted-high population showed consistently better performance than the parent (Figure 1.22). Interestingly, the sorted-low population showed the same performance as the parent. Overall, the lipid accumulation was 70% greater than the parent strain. Closer examination revealed that not only was the level of lipid content higher in the sorted-high population, but also the rate of accumulation during nitrogen depletion was increased relative to the parent line (140%). An improved rate of accumulation could reduce culture turnaround time in an industrial setting. Further, the cell size as determined by forward light scatter (a correlate of cell size in flow cytometry) was increased in the sorted-high population.

□

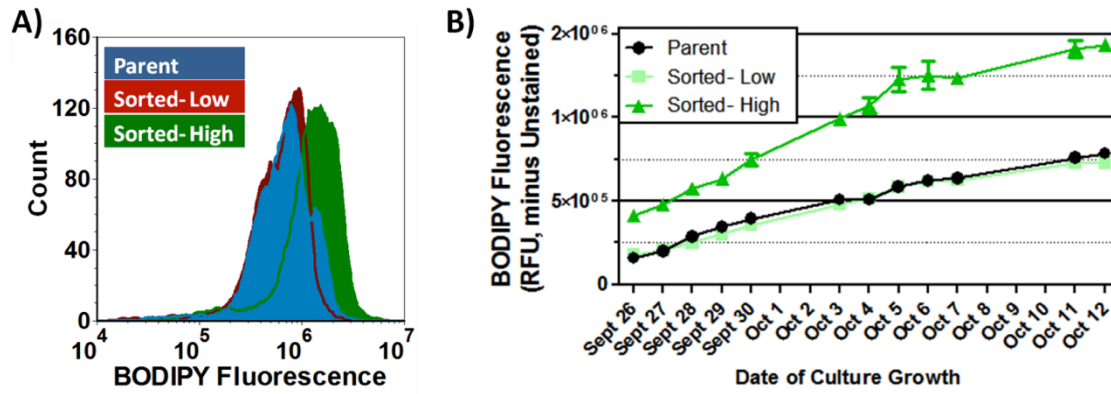


Figure 1.22. Panel A: Histograms of BODIPY fluorescence of *Picochlorum* parent and sorted populations. Panel B: During nitrogen starvation, all cultures accumulate lipids, with the sorted-high population outperforming the parent on all days (avg 2x improvement).

In order to ensure that the isolated subpopulation did not just have improved dye uptake and therefore show an increase in BODIPY fluorescence, sorted and parent populations were examined by microscopy and GC-MS. Microscopy validated that the parent population had smaller cells with an average of one (sometimes two) lipid bodies per cell. The sorted-high population cells were larger and had an average of two (sometimes three) lipid bodies per cell. These lipid bodies were also larger in size. Analysis by GC-MS confirmed an increase in lipid content in the sorted-high population. Our isolated strain has been stable in its greater lipid production phenotype for more than 100 generations (over a year).

Genomics and Transcriptomics

We sequenced the genome and transcriptome of the sorted and parent populations under nitrogen replete and deplete conditions. Very few changes in protein coding genes were observed between the parent and sorted cultures.

Many changes in the nearly 7000 gene transcriptome were observed, however. Our analysis focused largely on gene IDs that have an associated KEGG assignment (891 genes). The largest number of genes showing a greater than 2-fold change in the sorted-high population relative to the parent population was under nutrient replete conditions. Fewer changes were observed during depletion. This result may suggest that the improved performance under depletion is a property achieved by significant changes in expression level prior to depletion; i.e., changes in baseline expression may have a greater effect on lipid accumulation response than changes during the actual response.

Initial analysis of metabolic pathways showing differences in expression between the sorted-high and parent populations are underway. We observed increases in gene expression (sorted strain relative to parent) in the lipid biosynthesis, glycolysis, and TCA cycle pathways over the time course as the algae moved from the replete nitrogen growth phase and well into the depleted nitrogen lipid production phase. Changes are also observed in the following pathways, among others: amino acid metabolism, starch and sucrose metabolism, purine metabolism, pyrimidine metabolism, and carbon fixation in photosynthetic pathways. Much work remains in better understanding the differences in regulation between the hyperperforming strain and the parent. Future work will include mining the genome and transcriptome data to generate a list of gene candidates for genetic modification. These genetically modified organism (GMO) strains will ideally (1) also be hyperproducers and (2) validate proposed mechanisms of hyperproduction suggested by the sequencing data.

Adaptation for Low-phosphorous-requiring Strains

Growing algae under suboptimal conditions can induce adaptation and therefore create optimized strains that will outperform the native algal strain under the selected target conditions. A prime target for adaptation is low-media-phosphate concentrations because of anticipated future limitations in phosphate supply that could be expected to impact large-scale algal production. Prolonged growth (>2 months) of *A protothecoides* in a chemostat with a constant selective pressure of low phosphate shows initial signs of adaptation. The adapted strain appears to outperform the wild type under low-phosphate growth with a ~25% higher biomass yield. The robustness of this potentially adapted strain is currently being tested. Populations that show significant, robust improvement will be used for follow-on proteomics and transcriptomics to identify the biochemical basis for adaptation.

Crop Protection

Cultivation of algae in algal raceways and open ponds is envisioned as the most economical route for algal biomass and biofuels production. In the coming decades, if the projected scales of biofuels are to be generated, algae have to be cultured in several thousand acres of land for the desired biomass yields. Like most plant crops, algal cultures in open ponds are susceptible to a number of environmental factors, including biological agents that gain entry into ponds. Our goal was to examine and understand the nature of biotic factors such as bacteria, viruses, invasive algal species, fungi, and herbivores in algal ponds that impact the algal biomass yields. It is broadly accepted that the biological agents that are present in the algal ponds could be (1) beneficial to algal growth, (2) harmful to

algal culture, or (3) unobtrusive to the cultivated algal culture. Entry of invasive species into algal culture can have deleterious effects on algal cultivation and could result in lowered biomass yields and even cause pond crashes, resulting in crippling losses to biofuel producers. For instance, it has been documented that certain bacteria, viruses, fungi, or herbivores such as rotifers can cause demonstrable losses to an algal crop. One of the major and imminent challenges in cultivating algal crops in an open environment is therefore protection of algal crops from invaders. Furthermore, our investigations are also important because we hope to determine if any potential human, livestock, or plant pathogens can propagate in an algal pond ecosystem that could cause serious problems to cultivators and the environment. If this is not addressed actively, in the long run it could pose serious sustainability problems for the algae production industry. Other challenges undertaken include identifying economically viable strategies to reduce and eliminate contaminants without incurring additional cost in mitigating biomass losses. Furthermore, we proposed to investigate molecular approaches to contain genetically modified algae propagation outside the algal ponds.

As part of the Algal Biology Team in the NAABB consortium, we carried out census analysis on organisms that enter and possibly thrive in algal ponds. With this knowledge, it was also our aim to determine economically viable alternatives for algal crop protection from harmful contaminants through bioengineering approaches. To understand the biological agents that co-inhabit algal ponds, we designed and conducted experiments with both laboratory-grown cultures of *C. reinhardtii* and *A. protothecoides* UTEX25 (representative fresh water cultures grown in nutrient-rich media) and raceway-grown cultures of *N. salina* (a representative marine species grown at Texas AgriLife Research, Corpus Christi, provided by Dr. Tzachi Samocha). Based on the ribosomal RNA (rRNA) gene-based identification of species of contaminants in a *Chlorella* UTEX25 culture, we identified more than 50 different bacterial and fungal species, with bacterial populations reaching one-tenth of the algal culture at the end of seven days. Importantly, many representative bacteria belonged to the genus *Pseudomonas*, with few of them being opportunistic pathogens. For the *N. salina* contaminant survey, both rRNA sequencing and more extensive chip-based analysis of species distribution (PhyloChip—Lawrence Berkeley National Laboratory) were undertaken. Our surveys indicated that an array of organisms ranging among bacteria, fungi, and viruses inhabit these raceways. Significantly, in our analyses, only one known species of human pathogen was identified. It is unclear if this strain was actively propagating in the open ponds or happened to have entered the pond at the time of sampling.

Agents to minimize bacterial contamination and eliminate rotifers in open ponds—Our pond survey studies conclusively proved that large numbers of bacteria can coexist with algae in open pond cultures and the occurrence of algae-invading opportunistic pathogens is certainly a looming problem. In addition, NAABB observed pond crashes caused by rotifer infestation. To address this, we explored the use of antimicrobial peptides^{62,63} (AMPs) and other biomolecule production in algae for improving their innate defense against bacteria and rotifers. We successfully screened and identified one or more AMPs that kill bacteria and eliminate rotifers but not our algae of choice for biomass production. Sample results on rotifer control are presented here.

Two freshwater rotifers *Philodina acuticornis* and *Adineta vaga* were continuously cultured and maintained under laboratory conditions. Bioassays with rotifers were successfully developed in a multi-well plate format to analyze the effect of tested molecules on these fresh water rotifers. As detailed in the Table 1.6, we determined the efficacy of selected molecules on rotifers (at 0.5 mg/mL concentrations) and also on three species of green algae as detailed previously for AMP assays with algae. Based on the results, we have several candidates that are well tolerated by algae but have detrimental/lethal effects on rotifers (Figure 1.23). We are currently in the process of identifying viable bioengineering routes for developing transgenic algae for studying *in vivo* expression and applicability of these strains in rotifer elimination applications.

Table 1.6. Bioassays of three green algae and *Adineta vaga* and *Philodina acuticornis* with molecules to determine their effect on algal growth and rotifer-killing efficiency.

Compound #	Inhibition of Algal Growth ⁺			Rotifer Sensitivity	
	<i>A. protothecoides</i>	<i>Chlorella sorokiniana</i>	<i>C. reinhardtii</i>	<i>Philodina acuticornis</i>	<i>Adineta vaga</i>
				**Sensitivity	**Sensitivity
1	16 μM	66 μM	33 μM	+++	+++
2	10 μM	20 μM	10 μM	+++	+++
3	44 μM	88 μM	22 μM	+++	+++
4	78 μM	155 μM	20 μM	+++	+++
5	37 μM	37 μM	10 μM	+++	+++
6		79 μM	20 μM	+++/**	+++/**
	158 μM				
7		275 μM	17 μM	+++/**	+++/**
	275 μM				
8	48 μM	97 μM	12 μM	+++	+++
9	23 μM	46 μM	11 μM	+++	+++
10	22 μM	87 μM	5 μM	+++	+++
11	44 μM	87 μM	11 μM	+++	+++
12	12 μM	24 μM	12 μM	+++	+++
13			62 μM	++	++
	NK	492 μM			

⁺ Concentration of compound that inhibits algal growth (μM). Algal growth was assayed for 6 days.
^{**} Rotifer sensitivity: 0.5 mg/mL of each molecule was incubated with the rotifer in spring water and assayed after 24 h; +++ complete kill efficiency (100%); ++ moderate kill efficiency (50–75 % death); + low kill efficiency (< 25% death); NK no kill.

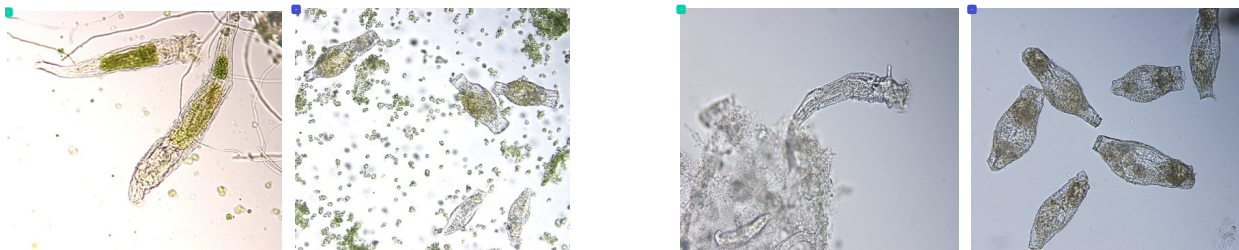


Figure 1.23. Microscopic images of rotifers that are treated with molecules of choice. The left two images are *A. vaga* and the right two images are *P. acuticornis*. Live rotifers can be seen in the green-boxed images, Dead ones are visible in the blue-boxed images.

To achieve economically viable means to employ AMPs for crop protection, we have successfully developed bioengineering tools for expressing these agents in algae. Various lines of algae expressing these biomolecules have been generated to test the viability of these transgenic algae lines in the presence of deleterious bacterial and rotifer species. Based on a similar approach, new biomolecules or gene products can be identified to test their applicability in eliminating other invasive contaminants. Furthermore, we have also undertaken the task of characterizing gene-switch-mediated regulation of chloroplast genes in the model organism *C. reinhardtii* to determine its applicability in genetically modified (GM) algae containment. The regulation of the gene-switch is currently coupled to a small molecule effector that regulates the expression and/or translation of the gene coupled to this element. If this strategy is determined to be successful, we hope to extend this idea into other green algae that are genetically engineered for biofuels or other value added product production, thus averting their proliferation in the natural environment.

Algal Cell Biology

The ability to visualize cell structures and correlate changes in those structures with genetic, species, or culture differences is a powerful approach to making advances in our understanding of algal growth and lipid production. Two complex physiological traits of great interest in regard to the cell biology of algal biofuel production are lipid body formation and cell wall structure. Clearly lipid body formation is of interest with respect to maximizing the amount of biofuel precursors. The structure of cell walls potentially impacts the robustness of the algae in cultivation and the extraction of the lipid during post-culture processing. Being able to observe these processes and correlate them with genetic traits provides valuable information for fundamental understanding of the underlying biology and the potential to implement genetic engineering or process engineering to elicit the desirable traits.

Lipid Bodies in Algae

Quick-freeze deep-etch electron microscopy (QFDEEM)⁶⁴ was used to follow lipid body formation in three strains of special interest to NAABB, *C. reinhardtii*,⁶⁵ *B. braunii*, and *Nannochloropsis* spp., with the goal of uncovering unique and common characteristics in lipid body formation between these diverse species. The three species come from two different families of the green algae and a stramenopile genus (*Nannochloropsis*), so it is not surprising that there are considerable differences in lipid body biogenesis. *C. reinhardtii* normally stores its excess carbon as starch. However, in the *sta6* mutant strain (which also has lesions in genes other than *sta6*), *C. reinhardtii* accumulates substantial amounts of lipid.

C. reinhardtii cells in N-replete media contain small cytoplasmic lipid bodies (α -cyto-LBs) and small chloroplast plastoglobules, as observed by QFDEEM. When starved for N, β -cyto-LB formation is greatly stimulated, apparently resulting in an enlargement of existing α -cyto LBs rather than the formation of new lipid bodies. β -Cyto-LBs are in intimate association with the endoplasmic reticulum (ER) and the outer membrane of the ast envelope (Figure 1.24, cyto-LB), suggesting the active participation of both organelles in β -cyto-LB production/packaging. When *sta6* mutant cells, blocked in starch biosynthesis, are N-starved, they produce β -cyto-LBs and also chloroplast LBs (cpst-LBs) that are much larger than plastoglobules and eventually engorge the chloroplast stroma (Figure 1.24, cpst-LB). Production of β -cyto-LBs and cpst-LBs is dependent on exogenous acetate under our culture conditions and inhibited by darkness. We proposed that the greater LB yield reported for N-starved *sta6* cells can be attributed, at least in part, to its ability to produce cpst-LBs, a capacity lost when the mutant is complemented by *STA6* transgenes.

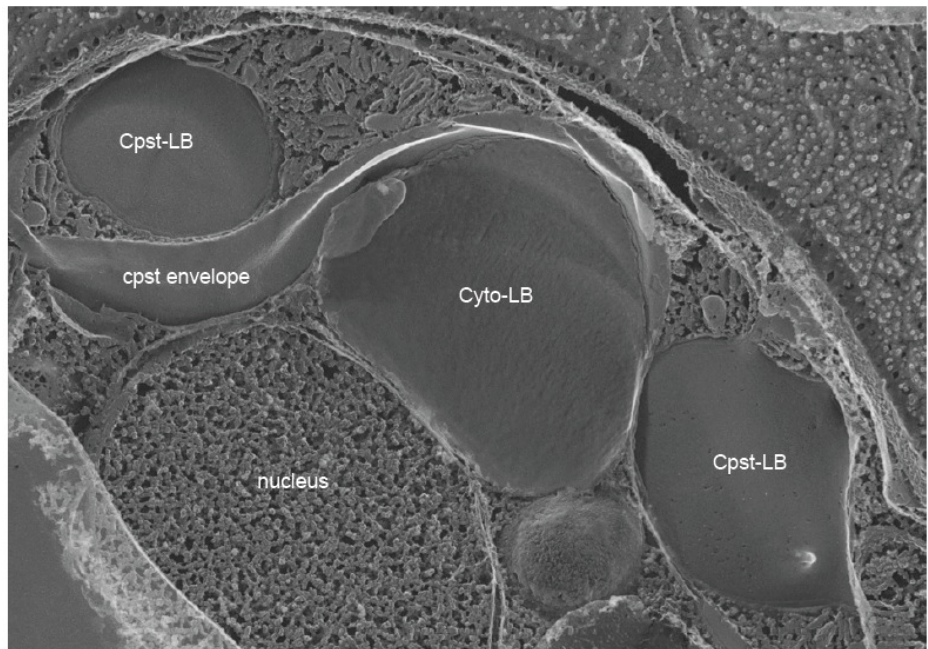


Figure 1.24. Cytoplasmic and chloroplast LBs in the *sta6* strain of *C. reinhardtii*.

In association with external and internal collaborators, NAABB used QFDEEM to investigate four species of the marine stramenopile *Nannochloropsis*: *N. gaditana*, *N. salina*, *N. oceanica*, and *N. oculata*. Compared with the other algae examined in this QFDEEM survey, all *Nannochloropsis* species have many LBs even under N-replete conditions, but like other species, the LBs increase in size upon N-starvation. The log-phase LBs lie in the cell periphery and are oblong in shape, as contrasted with the central and circular LBs of the green algae. They are invariably associated with ER. The direct association between N-stressed LBs and the chloroplast envelope, observed in all green algae examined to date, is not found in *Nannochloropsis*. However, since the ER in stramenopiles completely encloses the chloroplast (the so-called “chloroplast ER”) and makes direct contact with the chloroplast envelope, indirect envelope/LB associations are maintained and possibly have functional significance.

Lipid-body Formation in Stramenopiles

The stramenopile *Chrysochromulina tobin* is a fascinating alga in many regards. This wall-less marine alga is enclosed only by a simple plasma membrane. The organism has a pair of lipid bodies intimately associated with the ER. The ability of NAABB investigators to grow the alga in synchronous culture utilizing a 12 h light/12 h dark photoperiod facilitates observation of the cyclical nature of lipid body volume changes. The lipid bodies reach a maximum volume at the end of the light period and a minimum at the end of the dark period (Figure 1.25).

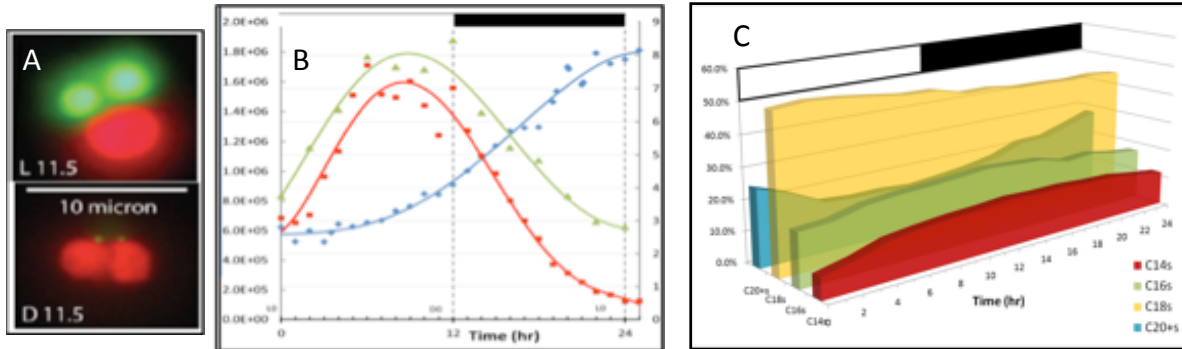


Figure 1.25. Observations of lipid body formation in *Chrysochromulina tobin* during a photoperiod (light: 0-12 hrs; dark: 12-24 hrs). (A) Fluorescent micrographs of cells harvested at the end of the light period (upper panel, L11.5) and end of the dark period (lower panel, D11.5) where red is chlorophyll autofluorescence in chloroplasts; and green is from lipid bodies stained with BODIPY 505/515. (B) Left axis: culture density in cells/ml (blue curve). Right axis: Neutral lipid/BODIPY 505/515 (relative fluorescent units, red) and total fatty acids (pg/cell, green). (C) Diurnal variations in fatty acid profiles of the lipids.

Preliminary transcriptomics analysis of 6 h and 18 h (mid-day and mid-night) cycles showed up-regulation of 3-ketoacyl-ACP synthase and glycerol-3-phosphate dehydrogenase during the day and down-regulation at night, consistent with an increase in TAG synthesis in the light. Differential expression of enoyl reductases was also observed, which begins to give clues to the changes in the fatty acid profiles that were observed through biochemical analysis.

B. braunii

Given that *B. braunii* is known for producing various hydrocarbons from terpene or fatty acid elongation pathways (depending on the race) it was perhaps surprising that it appears to produce lipid bodies that are similar to other green algae. However, *B. braunii* has unique characteristics in regard to the structural organization and composition of the cells, extracellular matrix and shell surrounding this colonial alga. By utilizing fluorescent staining followed by imaging and biochemical analyses, we made major advances in the understanding of this organization and the components involved. The B race of *B. braunii* was used for this study and it produces the triterpenoid botryococenes, which, like TAGs, can be stained with Nile Red. The polysaccharides were stained with a modified periodic acid Schiff (mPAS) reagent system (utilizing the fluorescent dye propidium iodide as the Schiff reagent) for *in situ* visualization. The carbohydrate was isolated and its composition analyzed by derivatization GC-MS, revealing that the extracellular matrix was largely composed of an arabinogalactan with a mixture of unusual linkages. Individual and overlay images of the chloroplasts, polysaccharides, and hydrophobic botryococenes or algaenans are shown in Figure 1.26.

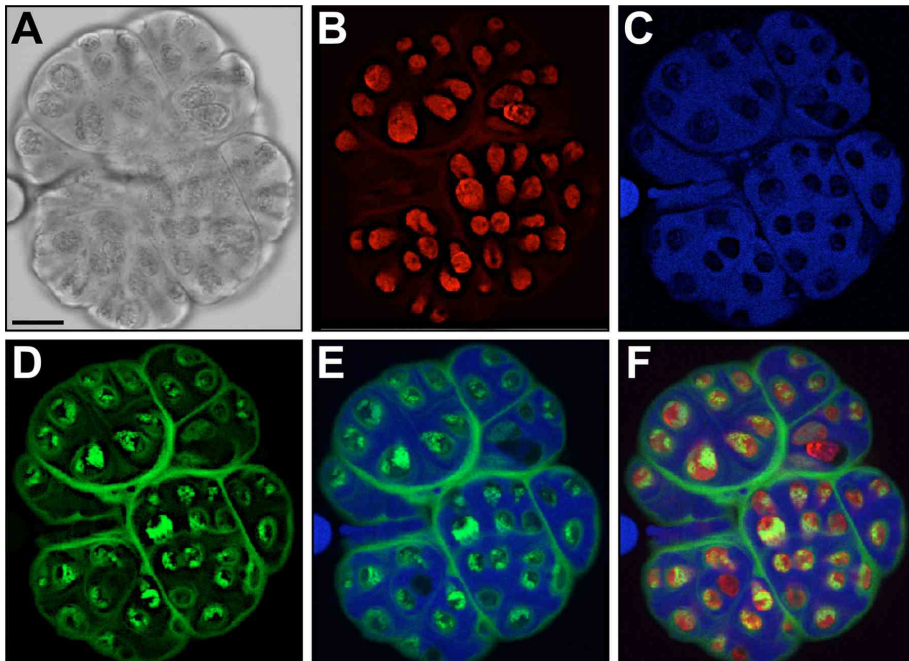


Figure 1.26. AB-V-3. Imaging *B. braunii* race B colonial organization. All images were taken from a single z axis of the same colony. A. DIC image of a single *B. braunii* colony that was stained with Nile Red and mPAS. Bar, 10 μm . B. Chlorophyll autofluorescence channel. C. Nile red channel, false colored blue. D. mPAS channel, false colored green. E. Merge of Nile red and mPAS images. F. Merge of Nile Red, mPAS, and chlorophyll autofluorescence images.

This brief summary covering some of the cell biology studies of various algae conducted within NAABB reveals the power of combining advanced imaging, systems biology methods, and biochemical analyses to understand algal composition, structural organization, diurnal or developmental variation in fatty acid composition, etc. Clearly a greater array of tools is now available and being utilized for meaningful studies of algae that have potential for biofuel production or have characteristics of interest in an engineered biofuel production algal strain. It is equally clear that much remains to be learned from various algal species across the taxonomic breadth of biology.

Conclusions and Recommendations

In the period between the Aquatic Species Program and NAABB, the age of genomics began. This enabled NAABB to take new approaches to studying biofuels production algae, such as systems biology, and led to the development of new genetic tools. NAABB researchers generated a valuable reservoir of information pertaining to potential targets to improve algal growth and lipid productivity that has been tapped but by no means exhausted. The biology of algae for biofuels production is like every other area of biology in the genomics age—there is a wealth of information in the form of systems biology data and resultant gene targets but the hard work of gene deletion and expression analysis to understand and verify the efficacy of individual or stacked genetic variations remains a relatively time-consuming process. NAABB researchers began and continue those studies and have therefore obtained exciting and promising results on strains that have improved growth or lipid productivity. Yet, many interesting gene candidates for improving productivity in various ways

(including crop protection, growth enhancement, and lipid productivity) remain in need of thorough characterization with regard to the impacts of those genetic changes. Further analyses of the systems biology data already collected would be beneficial for understanding the effects of nutrient and physical parameters on growth and lipid production in terms of gene expression and would lead to the identification of additional interesting candidates. The enormity of data sets requires increasingly sophisticated tools for analysis and higher throughput methods for genetic modifications and stacking traits (multiple or recyclable markers in existing and novel systems). The tools for effective analysis of new traits have been developed, including more sophisticated pond-mimicking photobioreactors, many new algal genomes, transcriptomics data sets and analysis tools, proteomics, and lipidomics. Importantly, the team structure of NAABB allowed the development of an efficient conduit for transferring lead algal strains or genetic variants to the Algal Cultivation testbeds for analysis in contained or open pond environment conditions. It is critical going forward that this conduit remains open for analysis of genetic variants that show promise in the lab. The size of the issues and the inter-disciplinary nature of the solutions for algal biofuels production necessitate that the collaborative approach afforded by consortia, such as NAABB, have continued encouragement and support. Overall, the algal strains identified, the greatly expanded genomic resources, the systems biology approaches, and genetic tools developed should enable the broader algal biofuels community to accelerate progress in understanding and implementing existing or developing algal strains for more efficient algal biofuels production.

Accomplishments

Specific accomplishments by the Algal Biology Team are outlined below.

New Strain Isolation

Developed standard screening protocols for identifying high biomass and lipid producing strains from the wild.

- Screened over 2200 environmental isolates and identified 60 strains that outperformed benchmark algal production strains;
- Deposited 30 of these strains at UTEX collection; and
- Developed micro-GC-MS methods for automated analysis of lipid content and fatty acid profiles.

Genome Sequencing and Annotation

Sequenced eight new algal genomes, doubling the number of previously sequenced algal genomes.

- Improved the quality of genome annotation to levels previously not achieved for *N. salina*, *Picochlorum* sp., and *A. Protothecoides*;
- Completed genome annotation for *B. braunii* race B;
- Began genome annotation on four additional strains; and
- Developed two advanced, web-based algal functional genomic annotation and metabolic mapping platforms.

Systems Biology

We sequenced over 250 algal transcriptomes.

Analyzed the transcriptome of *Chlamydomonas cw 15* (wall-less) and *sta6* (CW-15 starch-less) strains grown under +/- N conditions to reveal that gluconeogenesis and glyoxylate cycle genes were most responsive to treatments that increased oil accumulation.

Analyzed the transcriptome of lipid production in *N. salina* and *Picochlorum* sp. to show that N depletion induced oil accumulation and elevated expression of genes involved in lipid, triglyceride, and starch biosynthesis including:

Lipid Biosynthesis:

- Cytoplasmic acetyl CoA carboxylase, catalyzing the first dedicated step in fatty acid synthesis.

Triacylglyceride Biosynthesis:

- Diacylglycerol acyltransferase, catalyzing the last step in TAG synthesis; and
- Genes encoding major lipid droplet proteins involved in TAG storage and accumulation.

Starch Biosynthesis:

- Glyceraldehyde dehydrogenase, 1,6-Fructose bisphosphate aldolase involved in gluconeogenesis; and
- Both subunits of ADP-glucose phosphorylase involved in the first step in starch biosynthesis.

Analyzed transcriptomes that led to the identification and annotation of genes involved in terpenoid biosynthesis in *B. braunii*.

- Multiple genes were identified encoding for key steps in monoterpene biosynthesis potentially accounting for high terpenoid accumulation levels in *B. braunii*.

Transformation and Phenometrics Pipeline

Constructed an ePBR array to simulate pond growth conditions and to screen phenotypes of environmental isolates and engineered algae under controlled conditions.

Engineered over 50-independent gene constructs into *Chlamydomonas* using a standard operating procedure (transgenic pipeline) to transform, genotype, and characterize the transgene expression profiles and phenotyped genetically engineered algae.

- Created and characterized transformants that yielded as much as a 2.5-fold increase in biomass accumulation when grown under outdoor-like conditions in ePBRs; and

- Created and characterized transformants that yielded as much as a 5-fold increase in lipid accumulation when grown under outdoor-like conditions in ePBRs.

Molecular Biology Toolbox

Capitalized on our genomic sequences to develop a molecular toolbox to stably transform the nuclear genomes of key algal production strains including *N. salina*, *Picochlorum* sp., and *A. protothecoides*.

Developed transformation systems for both *Picochlorum* and *N. salina*.

- Demonstrated lipid droplet protein promoter-driven transcription of a bicarbonate transporter in *Picochlorum* and *N. salina*; and.
- Demonstrated increased lipid production on *BIC A* and *ACCase* transformants of *Picochlorum*.

Developed two independent chloroplast genome transformation systems for *A. protothecoides*.

Adaptive Evolution

Utilized FACS coupled with lipid-staining fluorophores to isolate independent *Picochlorum* cell lines with increased (150%) lipid levels.

- Confirmed increased expression of fatty acid synthesis genes in isolates with elevated lipid levels by transcriptome analysis.

Selected for increased growth yield of *A. protothecoides* at lower initial phosphate concentration via chemostat.

Crop Protection

Identified AMPs that kill bacteria and eliminate rotifers from algal production ponds.

Algal Biology

Used QFDEEM to demonstrate lipid-body development and lipid remodeling in a variety of algal strains, including *C. reinhardtii*, *A. protothecoides*, and *Nannochloropsis*.

Team Members

Principal Investigators

Ivan Baxter, USDA at Donald Danforth Plant Science Center

Judith Brown, University of Arizona

Michael Carleton, Matrix Genetics

Rose Anne Cattolico, University of Washington

Taraka Dale, Los Alamos National Laboratory

John C. Detter, Los Alamos National Laboratory

Timothy P. Devarenne, Texas A&M University

Susan K. Dutcher, Washington University

David T. Fox, Los Alamos National Laboratory
Ursula Goodenough, Washington University
Jan Jaworski, Donald Danforth Plant Science Center
David M. Kramer, Michigan State University
Mary S. Lipton, Pacific Northwest National Laboratory
Margret McCormick, Matrix Genetics
Sabeeha Merchant, University of California, Los Angeles
István Molnár, University of Arizona
Ellen A. Panisko, Pacific Northwest National Laboratory
Matteo Pellegrini, University of California, Los Angeles
Juergen Polle, Brooklyn College
Martin Sabarsky, Cellana
Richard T. Sayre, Los Alamos National Laboratory and the
New Mexico Consortium
Shawn R. Starkenburg, Los Alamos National Laboratory
Gary D. Stromo, Washington University
Scott N. Twary, Los Alamos National Laboratory
Clifford J. Unkefer, Los Alamos National Laboratory
Pat J. Unkefer, Los Alamos National Laboratory
Joshua S. Yuan, Texas A&M University

Publications

Full-length, Peer-reviewed Publications

Bigelow, N., W. Hardin, J. Barker, A. MacRay, S. Ryken, and R.A. Cattolico. A comprehensive GC-MS sub-microscale assay for fatty acids and its applications. *Journal of the American Oil Chemists' Society* 88 (2011): 1329–1338.

Bigelow, N., J. Barker, S. Ryken, J. Patterson, W. Hardin, S. Barlow, C. Deodato, and R.A. Cattolico. *Chrysochromulina* sp.: A proposed lipid standard for the algal biofuel industry and its application to diverse taxa for screening lipid content. *Algal Research* 2 (2013): 385–393.

Boyle, N.R., M.D. Page, B. Liu, I.K. Blaby, D. Casero, J. Kropat, S. Cokus, A. Hong-Hermesdorf, J. Shaw, S.J. Karpowicz, S.D. Gallaher, S. Johnson, C. Benning, M. Pellegrini, A.R. Grossman, and S.S. Merchant. Three acyltransferases and nitrogen-responsive regulator are implicated in nitrogen starvation-induced triacylglycerol accumulation in *Chlamydomonas*. *The Journal of Biological Chemistry* 287 (2012): 15811–15825.

Goodson, C., R. Roth, Z.T. Wang, and U.W. Goodenough. Structural correlates of cytoplasmic and chloroplast lipid body synthesis in *Chlamydomonas reinhardtii* and stimulation of lipid body production with acetate boost. *Eukaryotic Cell* 10 (2011): 1592–1606.

Henley, W.J., R.W. Litaker, L. Novoveská, C.S. Duke, H.D. Quemada, and R.T. Sayre. Initial risk assessment of genetically modified (GM) microalgae for commodity-scale biofuel cultivation. *Algal Research* 2 (2013): 66–77.

- Hickman, J.W., K.M. Kotovic, C. Miller, P. Warrener, B. Kaiser, T. Jurista, M. Budde, F. Cross, J.M. Roberts, and M. Carleton. Glycogen synthesis is a required component of the nitrogen stress response in *Synechococcus elongatus* PCC 7942. *Algal Research* 2 (2013): 98–106.
- Hildebrand, M., R.M. Abbriano, J.E.W. Polle, J.C. Traller, E.M. Trentacoste, S.R. Smith, and A.K. Davis. Metabolic and cellular organization in evolutionarily diverse microalgae as related to biofuels production. *Current Opinion in Chemical Biology* 17 (2013): 506–514.
- Jarchow-Choy, S.L., A.T. Koppisch, and D.T. Fox. Synthetic routes to methylerythritol phosphate pathway intermediates and downstream isoprenoids. *Current Organic Chemistry* 18 (2014): 000-000.
- Kaiser, B.K., M. Carleton, J.W. Hickman, C. Miller, D. Lawson, M. Budde, P. Warrener, A. Paredes, S. Mullapudi, P. Navarro, F. Cross, and J.M. Roberts. Fatty aldehydes in cyanobacteria are a metabolically flexible precursor for a diversity of biofuel products. *PLOS ONE* 8 (2013): e58307.
- Kim, H.S., T.L. Weiss, H.R. Thapa, T.P. Devarenne, and A.Han. A microfluidic photobioreactor array demonstrating high-throughput screening for microalgal oil production. *Lab Chip* 14 (2014): 1415.
- Kropat, J., A. Hong-Hermesdorf, D. Casero, P. Ent, M. Pellegrini, S.S. Merchant, and D. Malasarn. A revised mineral nutrient supplement increases biomass and growth rate in *Chlamydomonas reinhardtii*. *The Plant Journal* 66 (2011): 770–780.
- Lohr, M., J. Schwender, and J.E.W. Polle. Isoprenoid biosynthesis in eukaryotic phototrophs: A spotlight on algae. *Plant Science* 185–186 (2012): 9–22.
- Lopez, D., D. Casero, S. Cokus, S.S. Merchant, and M. Pellegrini. Algal Functional Annotation Tool: A web-based analysis suite to functionally interpret large gene lists using integrated annotation and expression data. *BMC Bioinformatics* 12 (2011): 282.
- Lovejoy, K.S., L.E. Davis, L.M. McClellan, A.M. Lillo, J.D. Welsh, E.N. Schmidt, C.K. Sanders, A.J. Lou, D.T. Fox, A.T. Koppisch, and R.E. Del Sesto. Evaluation of ionic liquids on phototrophic microbes and their use in biofuel extraction and isolation. *Journal of Applied Phycology* 25 (2013): 1–9.
- Lucker, B.F., C. C. Hall, R. Zegarac, and D M. Kramer. The environmental photobioreactor (ePBR): An algal culturing platform for simulating dynamic natural environments. *Algal Research* (2014): *In press*.
- Lucker, B. and D. Kramer. Regulation of cyclic electron flow in *Chlamydomonas reinhardtii* under fluctuating carbon availability. *Photosynthesis Research* 117 (2013): 449–459.
- Merchant, S.S., J. Kropat, B. Liu, J. Shaw, and J. Warakanont. TAG, You're It! *Chlamydomonas* as a reference organism for understanding algal triacylglycerol accumulation. *Current Opinion in Biotechnology* 23 (2012): 352–363.
- Molnar, I., D. Lopez, J.H. Wisecaver, T.P.P. Devarenne, T.L. Weiss, M. Pellegrini, and D. Hackett. Bio-crude transcriptomics: Gene discovery and metabolic network reconstruction for the biosynthesis of the terpenome of the hydrocarbon oil-producing green alga, *Botryococcus braunii* Race B (Showa). *BMC Genomics* 13 (2012): 576.

Ramos, A.A., J. Polle, D. Tran, J.C. Cushman, E.S. Jin, and J.C. Varela. The unicellular green alga *Dunaliella salina* Teod. as a model for abiotic stress tolerance: Genetic advances and future perspectives. *Algae* 26 (2011): 3–20.

Starkenburg, S.R., K.J. Kwon, R.K. Jha, C. McKay, O. Chertov, S. Twary, G. Rocap, and R.A. Cattolico. A pangenomic analysis of the *Nannochloropsis* organellar genomes reveals novel genetic variations in key metabolic genes. *BMC Genomics* 15 (2014): 212.

Subramanian, S., A.N. Barry, S. Pieris, and R.T. Sayre. Comparative energetics and kinetics of autotrophic lipid and starch metabolism in chlorophytic microalgae: Implications for biomass and biofuel production. *Biotechnology for Biofuels* 6 (2013): 150.

Tobin, E.D., D. Grünbaum, J. Patterson, and R.A. Cattolico. Behavioral and physiological changes during benthic-pelagic transition in the harmful alga, *Heterosigma akashiwo*: Potential for rapid bloom formation. *PLOS ONE* 8 (2013): e76663.

Weiss, T.L., R. Roth, C. Goodson, S. Vitha, I. Black, P. Azadi, J. Rusch, A. Holzenburg, T.P. Devarenne, and U. Goodenough. Colony organization in the green alga *Botryococcus braunii* (Race B) is specified by a complex extracellular matrix. *Eukaryotic Cell*. 11 (2012): 1424–1440.

Xie, S., S. Sun, S.Y. Dai, and J.S. Yuan. Efficient coagulation of microalgae in cultures with filamentous fungi. *Algal Research* 2 (2013): 28–33.

Other Important Publications

Barker, J.P., R.A. Cattolico, and E. Gatza. Multiparametric analysis of microalgae for biofuels using flow cytometry. *BD Biosciences* (2012): http://www.bdbiosciences.com/br/instruments/accuri/articles/archive/2012_10/index.jsp.

Olivares, J.A. and R.H. Wijffels. Responsible approaches to genetically modified microalgae production. *Algal Research* 2 (2013): 1.

References

1. Chisti, Y. Biodiesel from microalgae beats bioethanol. *Trends in Biotechnology* 26 (2008.): 126–131.
2. Mata, T.M., A.A. Martins, and N.S. Caetano. Microalgae for biodiesel production and other applications: A review. *Renewable & Sustainable Energy Reviews* 14 (2010): 217–232.
3. Weyer, K.M., et al. Theoretical maximum algal oil production. *Bioenergy Research* 3 (2010): 204–213.
4. Sayre, R. Microalgae: The potential for carbon capture. *Bioscience* 60 (2010): 722–727.
5. Wigmosta, M.S., et al. National microalgae biofuel production potential and resource demand. *Water Resources Research* 47 (2011).

6. Sheehan, J., et al. D.o. Energy, editor. A look back at the U.S. Department of Energy's Aquatic Species Program: biodiesel from algae. NREL/TP-580-24190 (1998).
7. Subramanian, S., et al. Comparative energetics and kinetics of autotrophic lipid and starch metabolism in chlorophytic microalgae: implications for biomass and biofuel production. *Biotechnology for Biofuels* (6) 2013).
8. Cooksey, K.E., et al. Fluorometric-determination of the neutral lipid-content of microalgal cells using Nile red. *Journal of Microbiological Methods*. 6 (6) (1987): 333–345.
9. Bigelow, N.W., et al. A Comprehensive GC-MS sub-microscale assay for fatty acids and its applications. *Journal of the American Oil Chemists Society* 88 (2011): 1329–1338.
10. Bigelow, N., et al. A novel, rapid, sub-microscale *in-situ* fatty acid assay and applications to aquatic microorganisms. *Journal of Phycology* 47 (2011): S58–S58.
11. Yang, E.C., et al. Supermatrix data highlight the phylogenetic relationships of photosynthetic stramenopiles. *Protist* 163 (2012): 217–231.
12. Bennett, S. Solexa Ltd. *Pharmacogenomics*. 5 (2004): 433–438.
13. Margulies, M., et al. Genome sequencing in microfabricated high-density picolitre reactors. *Nature*. 437 (2005): 376–380.
14. Eid, J., et al. Real-time DNA sequencing from single polymerase molecules. *Science*. 323 (2009): 133–138.
15. Cantarel, B.L., et al. MAKER: An easy-to-use annotation pipeline designed for emerging model organism genomes. *Genome Research*. 18 (2008): 188–196.
16. Delcher, A.L., et al. Identifying bacterial genes and endosymbiont DNA with Glimmer. *Bioinformatics* 23 (2007): 673–679.
17. Finn, R.D., et al. The Pfam protein families database. *Nucleic Acids Research* 36 (2008): D281–D288.
18. Gotz, S., et al. High-throughput functional annotation and data mining with the Blast2GO suite. *Nucleic Acids Research* 36 (2008): 3420–3435.
19. Grabherr, M.G., et al. Full-length transcriptome assembly from RNA-Seq data without a reference genome. *Nature Biotechnology* 29 (2011): 644–U130.
20. Koren, S., et al. Hybrid error correction and *de novo* assembly of single-molecule sequencing reads. *Nature Biotechnology* 30 (2012): 692–+.

21. Li, B. and C.N. Dewey. RSEM: accurate transcript quantification from RNA-Seq data with or without a reference genome. *BMC Bioinformatics* 12 (2011): 323.
22. Robinson, M.D., D.J. McCarthy, and G.K. Smyth. edgeR: a Bioconductor package for differential expression analysis of digital gene expression data. *Bioinformatics*. 26 (2010): 139–140.
23. Zerbino, D.R. and E. Birney, Velvet: Algorithms for *de novo* short read assembly using de Bruijn graphs. *Genome Research* 18 (2008): 821–829.
24. Starckenburg, S.R., et al. A pangenomic analysis of the *Nannochloropsis* organellar genomes reveals novel genetic variations in key metabolic genes. *BMC Genomics* (2014): in press.
25. Lopez, D., et al. Algal functional annotation Tool: a web-based analysis suite to functionally interpret large gene lists using integrated annotation and expression data. *BMC Bioinformatics* (2011): 12.
26. Kropat, J., et al. A revised mineral nutrient supplement increases biomass and growth rate in *Chlamydomonas reinhardtii*. *Plant Journal* 66 (2011): 770–780.
27. Matthew, T., et al. The Metabolome of *Chlamydomonas reinhardtii* following induction of anaerobic H₂ production by sulfur depletion. *Journal of Biological Chemistry* 284 (2009): 23415–23425.
28. Siaut, M., et al. Oil accumulation in the model green alga *Chlamydomonas reinhardtii*: characterization, variability between common laboratory strains and relationship with starch reserves. *BMC Biotechnology* (2011): 11.
29. Li, Y.T., et al. *Chlamydomonas* starchless mutant defective in ADP-glucose pyrophosphorylase hyper-accumulates triacylglycerol. *Metabolic Engineering* 12 (4) (2010): 387–391.
30. Goodson, C., et al. Structural correlates of cytoplasmic and chloroplast lipid body synthesis in *Chlamydomonas reinhardtii* and stimulation of lipid body production with acetate boost. *Eukaryotic Cell* 10 (2011): 1592–1606.
31. Lardizabal, K.D., et al. DGAT2 is a new diacylglycerol acyltransferase gene family—Purification, cloning, and expression in insect cells of two polypeptides from *Mortierella ramanniana* with diacylglycerol acyltransferase activity. *Journal of Biological Chemistry* 276 (2001): 38862–38869.
32. Sanjaya, et al. Altered lipid composition and enhanced nutritional value of *Arabidopsis* leaves following introduction of an algal diacylglycerol acyltransferase 2. *Plant Cell* 25 (2013): 677–693.

33. Hernandez, M.L., et al. A cytosolic acyltransferase contributes to triacylglycerol synthesis in sucrose-rescued *Arabidopsis* seed oil catabolism mutants. *Plant Physiology* 160 (2012): 215–225.
34. Saha, S., et al. Cytosolic triacylglycerol biosynthetic pathway in oilseeds. Molecular cloning and expression of peanut cytosolic diacylglycerol acyltransferase. *Plant Physiology*, 141 (2006): 1533–1543.
35. Moellering, E.R. and C. Benning Phosphate regulation of lipid biosynthesis in *Arabidopsis* is independent of the mitochondrial outer membrane DGS1 complex. *Plant Physiology* 152 (2010): 1951–1959.
36. Vieler, A., et al. A lipid droplet protein of *Nannochloropsis* with functions partially analogous to plant oleosins. *Plant Physiology* 158 (2012): 1562–1569.
37. Rock, C.O. and J.E. Cronan. *Escherichia coli* as a model for the regulation of dissociable (type II) fatty acid biosynthesis. *Biochimica Et Biophysica Acta-Lipids and Lipid Metabolism* 1302 (1996): 1–16.
38. Rock, C.O. and S. Jackowski. Forty years of bacterial fatty acid synthesis. *Biochemical and Biophysical Research Communications* 292 (2002): 1155–1166.
39. Konishi, T., et al. Acetyl-CoA carboxylase in higher plants: Most plants other than gramineae have both the prokaryotic and the eukaryotic forms of this enzyme. *Plant and Cell Physiology* 37 (1996): 117–122.
40. Gupta, D. and N. Tuteja. Chaperones and foldases in endoplasmic reticulum stress signaling in plants. *Plant Signaling & Behavior* 6 (2011): 232–236.
41. Dilworth, D., et al. The roles of peptidyl-proline isomerases in gene regulation. *Biochemistry and Cell Biology/Biochimie Et Biologie Cellulaire*, 90 (2012): 55–69.
42. Malanovic, N., et al. S-Adenosyl-L-homocysteine hydrolase, key enzyme of methylation metabolism, regulates phosphatidylcholine synthesis and triacylglycerol homeostasis in yeast—Implications for homocysteine as a risk factor of atherosclerosis. *Journal of Biological Chemistry* 283 (2008): 23989–23999.
43. Fait, A., et al. Highway or byway: the metabolic role of the GABA shunt in plants. *Trends in Plant Science* 13 (2008): 14–19.
44. Banerjee, A., et al. *Botryococcus braunii*: A renewable source of hydrocarbons and other chemicals. *Critical Reviews in Biotechnology* 22 (2002): 245–279.
45. Metzger, and C. Largeau. *Botryococcus braunii*: a rich source for hydrocarbons and related ether lipids. *Applied Microbiology and Biotechnology* 66 (2005): 486–496.

46. Brown, A.C., B.A. Knights, and E. Conway. Hydrocarbon content and its relationship to physiological state in green alga *Botryococcus braunii*. *Phytochemistry* 8 (1969): 543–8.
47. Lohr, M., J. Schwender, and J.E.W. Polle. Isoprenoid biosynthesis in eukaryotic phototrophs: A spotlight on algae. *Plant Science* 185 (2012): 9–22.
48. Molnar, I., et al. Bio-crude transcriptomics: Gene discovery and metabolic network reconstruction for the biosynthesis of the terpenome of the hydrocarbon oil-producing green alga, *Botryococcus braunii* race B (Showa). *BMC Genomics* 13 (2012): 576.
49. Cordoba, E., et al. Functional characterization of the three genes encoding 1-deoxy-D-xylulose 5-phosphate synthase in maize. *Journal of Experimental Botany* 62 (2011): 2023–2038.
50. Matsushima, D., et al. The single cellular green microalga *Botryococcus braunii*, race B possesses three distinct 1-deoxy-D-xylulose 5-phosphate synthases. *Plant Science* 185 (2012): 309–320.
51. Perrine, Z., S. Negi, and R.T. Sayre. Optimization of photosynthetic light energy utilization by microalgae. *Algal Research-Biomass Biofuels and Bioproducts* 1 (2012): 134–142.
52. Mohr, S., C. Bakal, and N. Perrimon. Genomic screening with RNAi: results and challenges. *Annual Review of Biochemistry* 79 (2010): 37–64.
53. Bartel, D.P. MicroRNAs: genomics, biogenesis, mechanism, and function. *Cell* 116 (2004): 281–97.
54. Bartel, D. and C.Z. Chen. Micromanagers of gene expression: The potentially widespread influence of metazoan microRNAs. *Nature Reviews Genetics* 5 (2004): 396–400.
55. Jones-Rhoades, M.W., D. Bartel, and B. Bartel. MicroRNAs and their regulatory roles in plants. *Annual Review of Plant Biology* 57 (2006): 19–53.
56. Sager, R. and S. Granick. Nutritional control of sexuality in *Chlamydomonas reinhardtii*. *Journal of General Physiology* 37 (1954): 729–742.
57. Harris, E.H.. The *Chlamydomonas* Sourcebook: Second Edition Introduction to *Chlamydomonas* and Its Laboratory Use. Academic Press (2009).
58. Radakovits, R., et al. Draft genome sequence and genetic transformation of the oleaginous alga *Nannochloropsis gaditana*. *Nature Communications* 3 (2012): doi:10.1038/ncomms1688.

59. Zaslavskaja, L.A., et al. Transformation of the diatom *Phaeodactylum tricornutum* (Bacillariophyceae) with a variety of selectable marker and reporter genes. *Journal of Phycology* 36 (2) (2000): 379–386.
60. Sun, M., et al. Foot-and-mouth disease virus VP1 protein fused with cholera toxin B subunit expressed in *Chlamydomonas reinhardtii* chloroplast. *Biotechnology Letters* 25 (13) (2003): 1087–1092.
61. Rasala, B.A., et al. Robust expression and secretion of Xylanase1 in *Chlamydomonas reinhardtii* by fusion to a selection gene and processing with the FMDV 2A peptide. *PloS One* 7 (8) (2012).
62. Jensen, H., Hamill, and R.E.W. Hancock. Peptide antimicrobial agents. *Clinical Microbiology Reviews* 19 (3) (2006): 491–+.
63. Wang, G.S., X. Li, and Z. Wang. APD2: the updated antimicrobial peptide database and its application in peptide design. *Nucleic Acids Research* 37 (2009): D933–D937.
64. Heuser, J.E., The origins and evolution of freeze-etch electron microscopy. *Journal of Electron Microscopy*, 60 (suppl 1) (2011): S3–S29.
65. Wang, Z.T., et al. Algal lipid bodies: Stress induction, purification, and biochemical characterization in wild-type and starchless *Chlamydomonas reinhardtii*. *Eukaryotic Cell* 8 (2009): 1856–1868.

CULTIVATION



Introduction

Team Leads

Peter Lammers, New Mexico State University

Michael Huesemann, Pacific Northwest National Laboratory

Wiebke Boeing, New Mexico State University

Preface

Economic and environmentally sustainable large-scale cultivation methods must be established to enable the production of algal biofuels. Some of the major challenges associated with large-scale microalgae cultivation are:

- Identifying robust production strains that will perform reliably in specific geographic locations and seasons;
- Developing methods and best practices for preventing large-scale culture crashes due to predators and competitor;
- Developing methods for cultivation in low-cost media using agricultural grade nutrients, wastewater sources, and media recycling; and
- Developing and demonstrating enhanced designs and operational methods that improve productivity of large-scale cultivation systems.

To optimize biomass productivities in outdoor ponds, it is important to identify and select geographic locations that have high annual solar insolation and climatic conditions that can maintain pond water temperatures at elevated levels for most of the year. In addition, microalgae strains must be selected that exhibit high growth rates within the annual temperature range of a potential production site using the available resources (water, nutrients, etc.). Also, there is an urgent need to design relatively simple, cost-effective, and energy-efficient large-scale culture systems that can support high productivity, provide culture stability, and help maintain elevated water temperatures during the cold season to sustain reasonable biomass productivities year round.

Approach

The National Alliance for Advanced Biofuels and Bioproducts (NAABB) developed an R&D framework for the Cultivation Team to begin addressing some of these major challenges and needs. The NAABB Cultivation team employed a variety of capabilities to execute the R&D framework. These include research tools (photobioreactors and specialized laboratory growth systems), small-pond/raceway testbeds and two large-pond testbeds for large-scale cultivation experiments and the production of algal biomass to support downstream processing R&D across NAABB.

Using the above capabilities, our research (Figure 2.1) was conducted across four major thrust areas:

- **Cultivation Tools and Methods:** Focused on developing new strain screening tools, systems, and models; sensors for cultivation; molecular diagnostics tools; and methods to control predators with environmental controls.
- **Nutrient/Water Recycle/Wastewater Cultivation:** Focused on nutrient studies, use of wastewater sources, and media recycle.
- **Cultivation System Innovations:** Focused on new raceway design to extend operation in cold season climates, airlift mixing systems, and computational fluid dynamic (CFD) models to improve raceway performance.
- **Large-pond Cultivation/Biomass Production:** Focused on scale-up of new strains, development of low-cost media, and production of algal biomass.

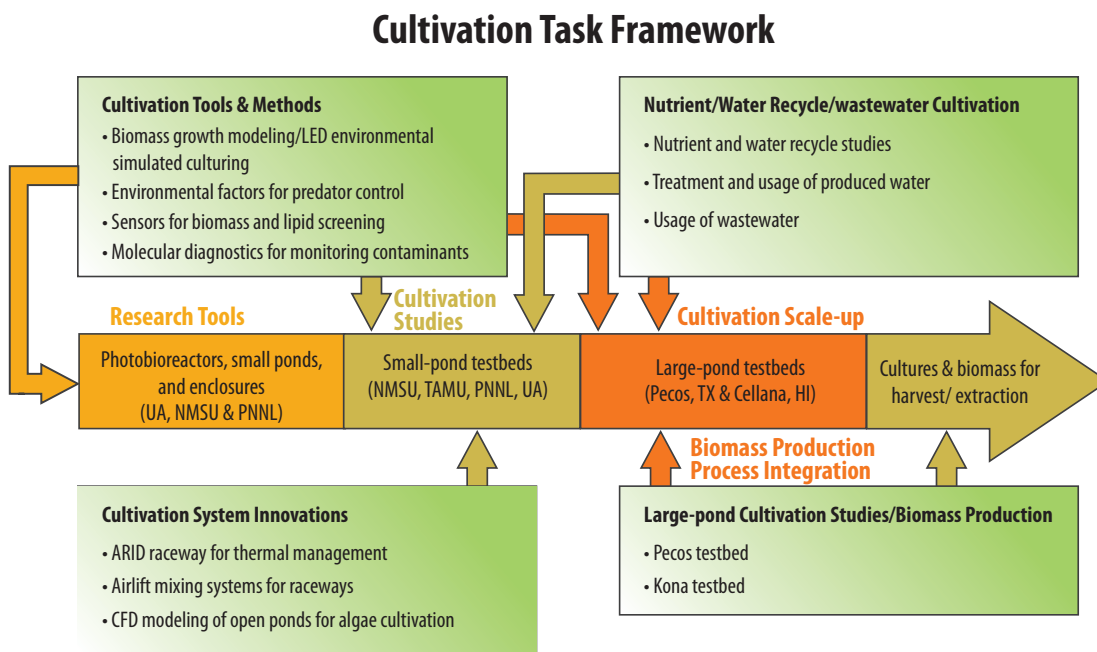


Figure 2.1. The NAABB Cultivation task framework.

Technical Accomplishments

Cultivation Tools and Methods

NAABB focused several efforts on developing new tools and methods for optimizing algal cultivation. These include new models and processes to select strains and cultivation conditions for maximum productivity, methods to control predators using environmental factors and polycultures, and the development of a new molecular monitoring system and sensors.

Biomass Growth Modeling/LED Environmental Simulated Culturing for Strain Screening

Light and temperature are the main determinants of biomass productivity of microalgae in photobioreactors and ponds operated under well-mixed and nutrient-replete conditions. For a pond at a given geographic location, the daily and seasonal fluctuations of sunlight intensity and water temperatures are determined by the prevailing climatic conditions at that site. The biomass productivity of a specific strain grown in this pond culture is then to a large degree determined by how the maximum specific growth rate is affected by sunlight intensity and water temperature. Thus, to optimize biomass productivities in outdoor ponds, it is necessary to identify not only geographic locations that have high annual solar insolation and climatic conditions that maintain pond water temperatures at elevated levels for most of the year, but also microalgae strains that exhibit high growth rates within the annual temperature range of the pond culture.

In order to accelerate the transition of promising microalgae from the laboratory into outdoor ponds, NAABB developed and tested a biomass growth model for determining strains with high biomass productivity potential. For a given strain, the following four biological species-specific input parameters are measured and used as inputs into the biomass growth model:

- Maximum specific growth rate (μ) as a function of temperature;
- Maximum specific growth rate (μ) as a function of light;
- Rate of biomass loss in the dark (μ_{dark}) as a function of temperature and average light intensity; and
- Scatter-corrected biomass light absorption coefficient (k_a).

An example of the data for a maximum specific growth rate matrix (7 light intensities X 7 temperatures) for *Chlorella* sp. DOE1412 is shown in Figure 2.2.

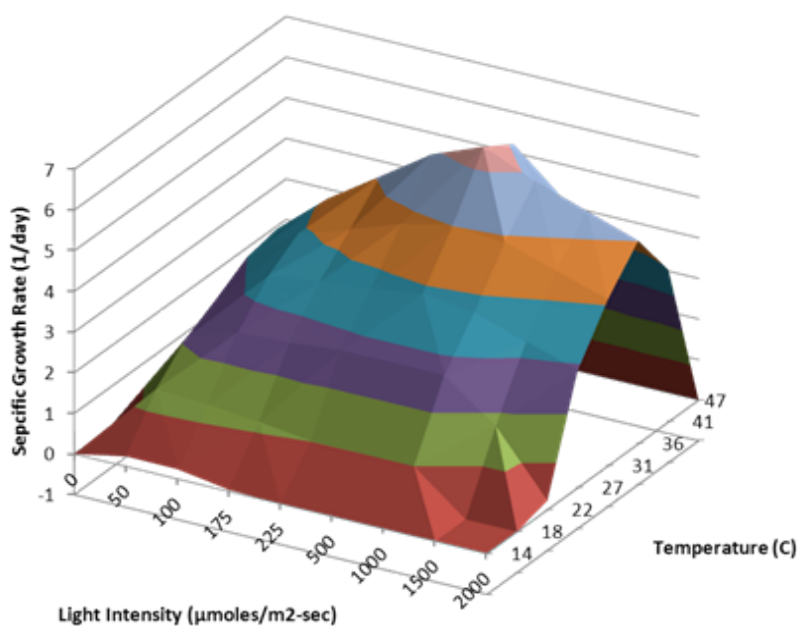


Figure 2.2. Maximum specific growth rate matrix for *Chlorella* sp. DOE1412.

Using *Nannochloropsis salina* and *Chlorella* sp. DOE1412 as the model strains, it was found that *Chlorella* exhibits much higher maximum specific growth rates at the optimal temperature ($\mu = 5.9 \text{ day}^{-1}$ at 31°C) and greater thermal tolerance ($T_{\text{max}} \sim 45^\circ\text{C}$) than *N. salina* ($\mu = 1.1 \text{ day}^{-1}$ at 26°C , $T_{\text{max}} \sim 35^\circ\text{C}$) (Figure 2.3).

Measurement of the maximum specific growth rates as a function of light intensity at different temperatures revealed that *Chlorella* is strongly photo-inhibited at lower temperatures ($\leq 22^{\circ}\text{C}$) and only slightly at higher temperatures. No photo-inhibition was found for *N. salina*.

However, both strains lost about 1% biomass per hour during dark incubation, and the oxygen uptake rate due to dark respiration increased with temperature at comparable rates until approaching the respective T_{max} .

Using these species-specific laboratory measurements together with sunlight intensity and pond water temperature data measured during an outdoor study in Arizona, the model was successful in predicting the biomass growth of *Chlorella* in three outdoor raceways as shown in the Figure 2.4)

Although the biomass growth model is useful for screening strains for the best candidates, it is important to validate the performance of the top strains in pilot-scale ponds simulating the light and water temperature conditions observed in outdoor pond cultures in selected geographic locations and seasons. An indoor LED-lighted and temperature-controlled raceway pond that can be used to measure a strain's seasonal and annual biomass productivity under climate-simulated conditions was designed, built, and validated (Figure 2.5).

Testing in indoor ponds under climate-simulated conditions is a low-risk way to confirm a strain's superior performance before transitioning to cultivation in outdoor ponds. The integrated strategy, consisting of four consecutive steps, for efficiently and cost-effectively screening strains for their potential to exhibit high biomass productivities in outdoor ponds is summarized the Figure 2.6.

The *Chlorella* outdoor pond culture experiment that was conducted in Arizona was repeated using the indoor LED-lighted and temperature-controlled raceway under climate-simulated conditions where scripts were developed to mimic the sunlight and water temperature fluctuations that were recorded during the outdoor study. Preliminary validation results (Figure 2.7) indicate that the indoor LED-lighted and temperature controlled raceway is able to simulate the outdoor cultures using the indoor LED-lighted and temperature-controlled ponds.

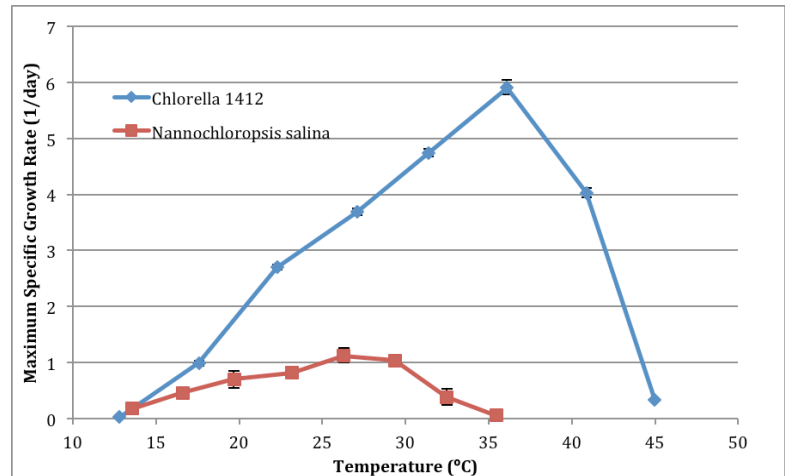


Figure 2.3. Growth rate as a function of temperature for *Chlorella* sp. DOE1412 and *N. salina*.

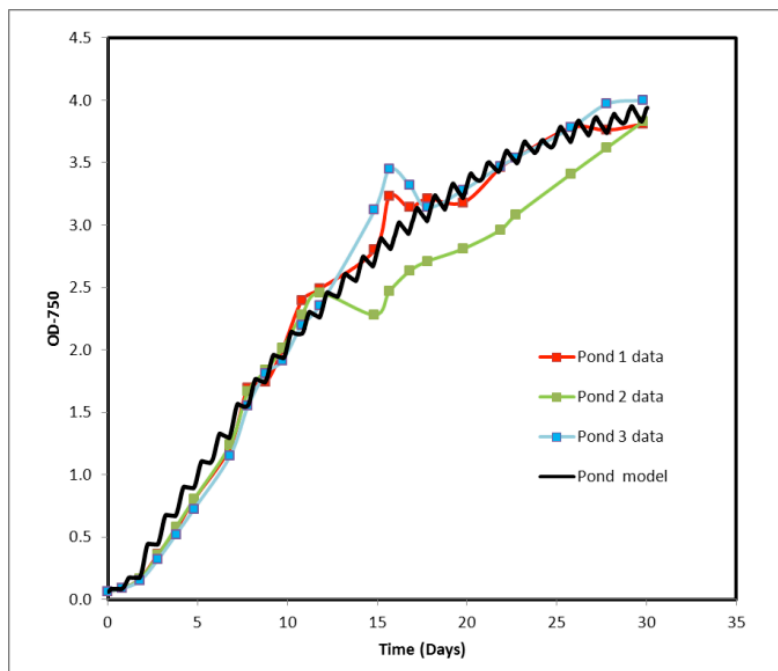


Figure 2.4. Biomass growth model prediction compared to outdoor pond data.

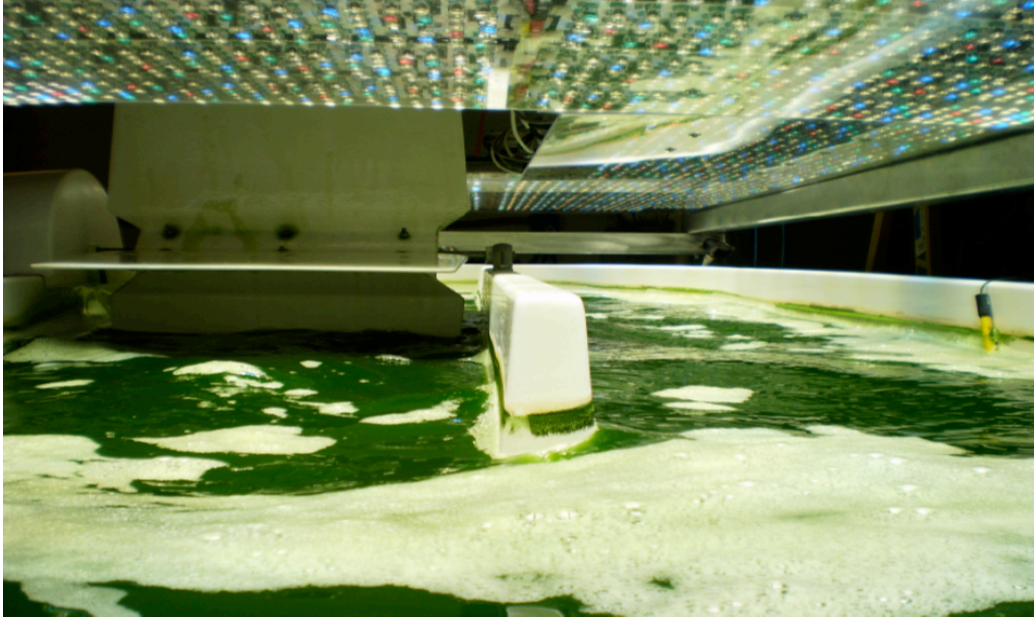


Figure 2.5. LED-lighted and temperature-controlled raceway.

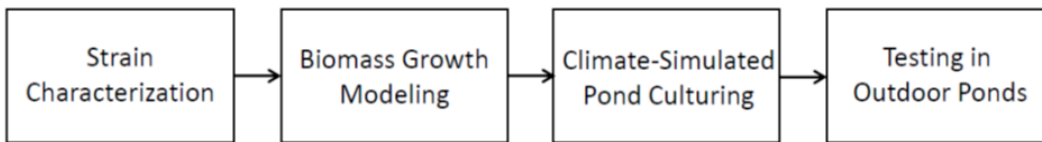


Figure 2.6. New strain screening process.

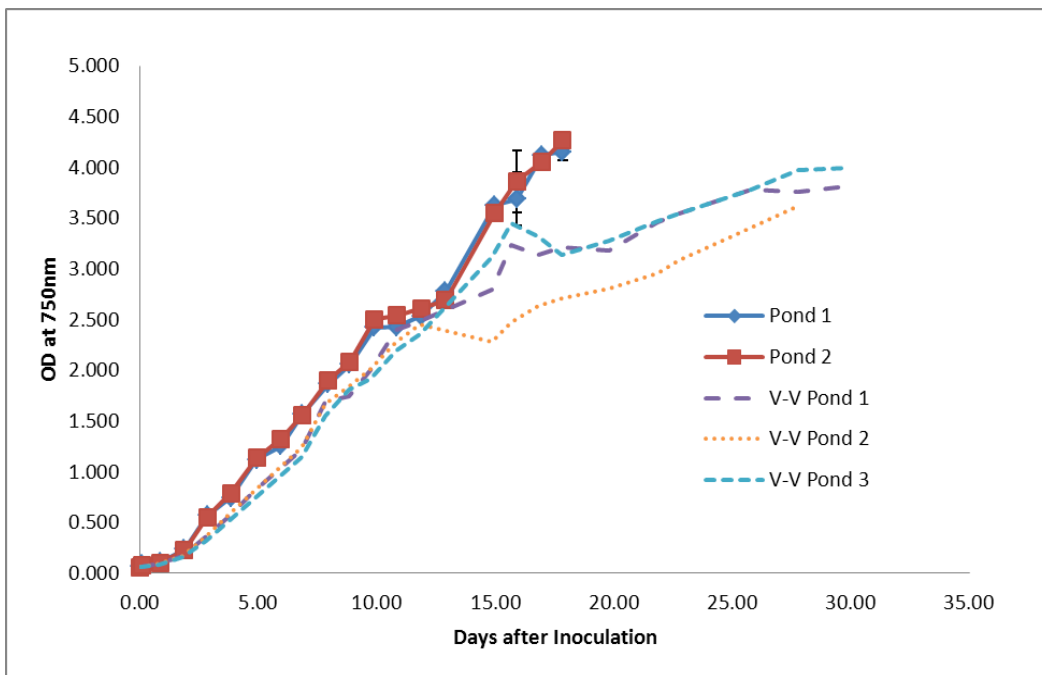


Figure 2.7. Comparison of two LED environmental simulated raceways (Pond 1 and Pond 2) to three outdoor culture ponds replicates.

Environmental Factors for Predator Control

Several limitations impede algal biofuel from attaining cost-effective commercial viability. These include the need for optimized production systems and stable, resilient algae cultures that are resistant to invading organisms. Within these systems, major contaminants have included unwanted bacteria, fungi, algae, and grazers. NAABB examined environmental parameters that promote growth and lipid accumulation of *N. salina* while keeping invading organisms at a minimum. This included testing productivity and stability (resistance and resilience after disturbance by a grazer) of algae polycultures compared to monocultures.

Then, in a series of experiments conducted in open aquaria in a greenhouse, we determined optimum salinity, pH, temperature, and nitrogen source to maximize *N. salina* growth and minimize other algae competitors and predators (rotifers and ciliates). We found that *N. salina* grows fastest at salt concentrations of 22–34 ppt, pH 8–9, temperature 22–27°C, and urea as a nitrogen source. Invaders were reduced at a salinity of 22 ppt, pH above 8, and temperatures above 32°C and using ammonium chloride as a nitrogen source. While *N. salina* still showed optimum growth at 22 ppt salinity and pH above 8, the higher temperatures and ammonium chloride had negative impacts on growth. Table 2.1 shows the effects of salinity on invaders that appeared in *N. salina* cultures.

Table 2.1. Effects of salinity on invaders appearing in *N. salina* cultures.

Salinity	Phytoplankton		Zooplankton	
	Diatoms μL^{-1}	Cyanobacteria mL^{-1}	Ciliates mL^{-1}	Rotifers mL^{-1}
10	410 ± 78	1400 ± 950	2200 ± 900	8.3 ± 6.8
22	450 ± 140	6.7 ± 2.2	630 ± 430	0
34	890 ± 380	0	2500 ± 300	0
46	560 ± 110	0	2000 ± 1000	0
58	810 ± 380	0	970 ± 460	0

In a laboratory experiment, differences in algae monocultures versus polycultures were studied. Polycultures consisted of 2, 4, and 6 species, where each of the 6 species was grown individually in the monocultures. Polycultures were assembled from 3 big (potentially ungrazable) algae species and 3 small, fast-growing species. We demonstrate that growing several algae species together in polycultures (> 4 species) will ensure a doubling of productivity as well as make algae cultures more resistant and resilient to disturbances by predators.

Sensors for Biomass and Lipid Screening

Commercial-scale algae production for biofuels is comparable to crop production in traditional agriculture. Proper decisions concerning media addition, nutrient stressing, harvest, and invasion (by algae grazers, bacteria, or fungi) control should be made in a timely manner, in particular in open-pond conditions. Moreover, unlike traditional agriculture where such decisions are typically made on a time scale of days, algae are very susceptible to environment change; therefore, management decisions should be made on a time scale of hours. Automated sensing and control systems can realize real-time monitoring and cultivation decision-making for production-scale ponds. NAABB developed and evaluated four prototype sensors: (1) an algae optical density (OD) sensor for

biomass concentration measurement; (2) Nile Red-staining-and-fluorescence-based (Nrf-based) algal neutral-lipid quantification and sensor; (3) near-infrared (NIR) and Fourier-transform-infrared (FTIR) analysis to characterize algal biomass composition; and (4) algal thin-film infrared-attenuated total reflectance (IR-ATR) lipid sensor. The field test results of the OD sensor at the Pecos test facility (Figure 2.8) demonstrated that the sensor could accurately measure the OD of the pond, trace algae growth, and pinpoint cultivation events such as media addition and culture transfer.

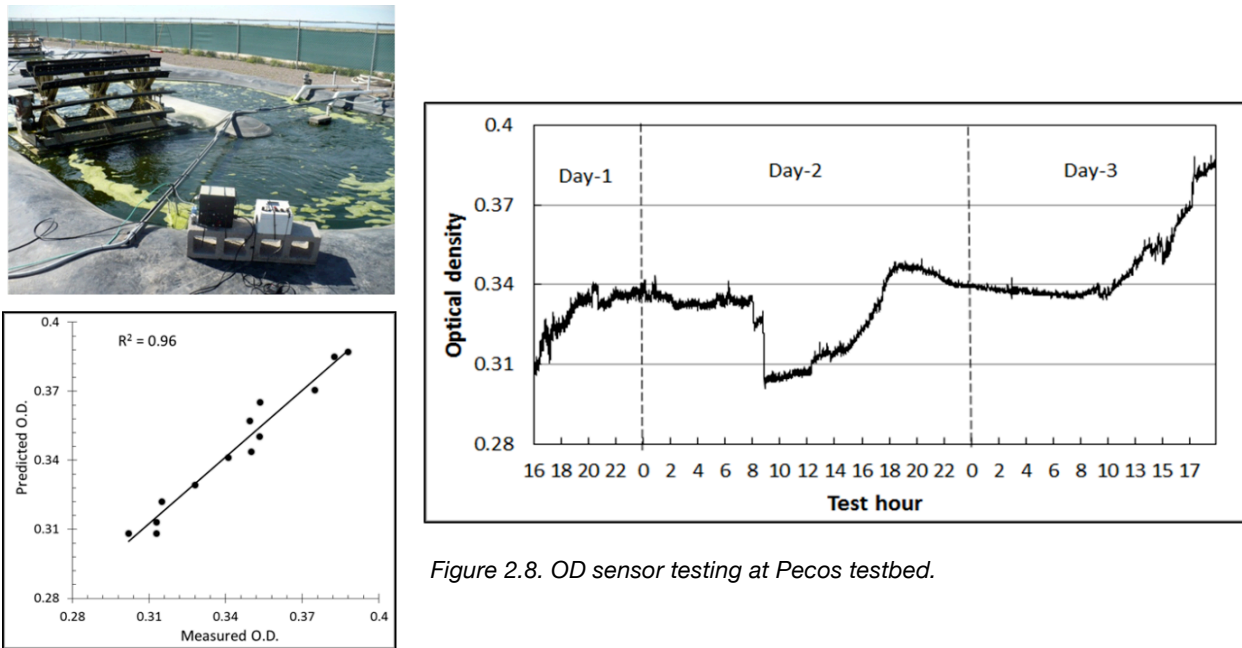


Figure 2.8. OD sensor testing at Pecos testbed.

Algae strains significantly affected Nrf signal intensity. However, within each strain, Nrf signal is highly correlated with lipid content ($R^2 = 0.96$ for *Nannochloropsis* sp. and $R^2 = 0.88$ for *Botryococcus braunii*). Both NIR and FTIR spectroscopy can be used as a rapid and cost-effective technique to quantify several biochemical compositions in dry algal biomass. Crude protein and heating value can be predicted satisfactorily ($R^2 > 0.85$), followed by ash content ($R^2 > 0.57$), and neutral lipids ($R^2 > 0.45$). Finally, the absorption depth at around 2920 cm^{-1} was highly correlated with the total neutral lipid ($R^2 = 0.90$). A prototype IR-ATR sensor was constructed and tested in the lab with vegetable oil as the calibration standard. It showed that the prototype sensor had a satisfactory performance. Additional research and development will be required to make these prototype sensors robust and reliable for commercial applications.

Molecular Diagnostics for Monitoring Contaminants in Algal Cultivation

Sensitive methods for enumeration of elite algal varieties relative to “weedy” invader strains that are ubiquitous in the environment are needed for cultivation management. The ideal monitoring strategy would be inexpensive and identify weedy algae long before they become prominent in cultures of elite varieties. NAABB developed and evaluated polymerase-chain-reaction-based (PCR-based) tools for monitoring contaminants. In this work, primers were designed to amplify an approximately 1500-nucleotide region of the 18S rRNA gene from

three major classes of algae: Bacillariophyceae, Eustigmatophyceae, and Chlorophyceae. These amplicons can be sequenced for definitive identification of strains, or they can be digested with a restriction enzyme to generate allele-specific fragmentation patterns for rapid, inexpensive characterization of strains and cultures. This work provides molecular tools to detect and monitor algal population dynamics and clarifies the utility, strength, and limitations of these assays. These include tools to identify unknown strains, to routinely monitor dominant constituents in cultures, and to detect contaminants constituting as little as 0.000001% of cells in a culture. One of the technologies examined was shown to be 10,000X more sensitive for detecting weeds than flow cytometry. Another NAABB effort looked at developing molecular monitoring tools for tracking bacteria that are associated with the cultivation of different microalgal species as a means of determining the health of the culture and mitigating pond crashes. Algal-associated bacterial communities in one 8 week growth cycle of *C. sorokiniana* in an

Aquaculture Raceway Integrated Design (ARID) cultivation pond are shown in Figure 2.9. The shift in bacterial community observed predicted an eventual crash of the culture due to an infection by *Vampirovibrio chlorellavorus*, a parasitic bacterium known to infect the *Chlorella* genus (particularly *C. sorokiniana* and *C. vulgaris*).

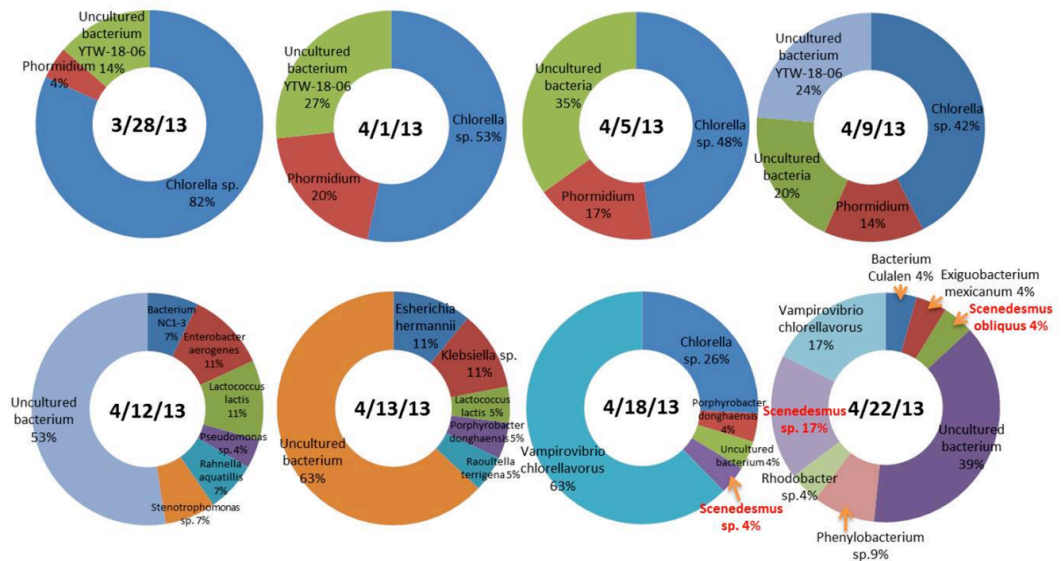


Figure 2.9. Time course community analysis for *C. sorokiniana* in an ARID cultivation pond.

Nutrient/Water Recycle/Wastewater Cultivation Experiments

A variety of bench scale and 1000 L scale cultivation studies were performed to determine strain-specific growth parameters. The scope included investigations of poly versus mono cultures, water recycle strategies and use of impaired waters, including produced water and wastewater. The original NAABB production strain was *N. salina*, hence the majority of the work discussed in this section was done with this strain. The suggested medium for cultivation of *N. salina* is denoted f/2, a well-defined growth medium for marine microalgae; hence the control case for all data presented is growth on f/2 medium.

Small-scale Nutrient and Water-recycle Studies

Initial experiments were done in 12 outdoor 3 m² raceways (Figure 2.10) located at one of the small test-bed locations in Corpus Christi, Texas, to investigate the effects of nitrogen source on productivity for *N. salina* in batch and semicontinuous cultures. Batch culture treatments continued to produce more

biomass over the course of the study than the continuous cultures, with peak growth and time between harvests remaining consistent. Productivity was 12.8 g/m²/d for batch cultures, compared to 10.9 g/m²/d for the continuous cultures. In the nutrient regime study, ODI mix with ammonia as the nitrogen source, f/2, and ODI mix with NO₃ as the N source were compared on an equal N basis for optimal production of *N. salina*. No significant differences in production (afdwt [g/L]) were found between treatments. The ability to get the same production from the ODI mix with ammonia and nitrate compared with the more expensive f/2 media greatly enhances the ability to produce biomass at reduced costs with this strain. Additional experiments were done to compare the productivity of a monoculture of *N. salina* to mixed cultures of *Phaeodactylum tricornutum* and *N. salina*. Results suggest that the mixed culture grew better than or the same as the *N. salina* monoculture. In colder temperatures, the mixed culture did better suggesting that crop rotation strategies require more investigation.



Figure 2.10. Array of outdoor raceways at the Corpus Christi, Texas facility used for media optimization and polyculture experiments.

Another important part of cultivating and characterizing algae is to recycle water. After algal cultures reach stationary phase, the water or spent media is separated from the algae and ideally recycled to the raceway. Recycling of spent media should occur until algal growth is inhibited severely. Figure 2.11 shows growth of *N. salina* as a function of generation. A generation is defined as a batch culture started with fresh inoculum but the water (spent media) is recycled. Hence for this set of experiments 90% of the water was reused 8 times. Each time, sufficient nitrogen and phosphorous were added to the recycled water so that the initial concentration was always the same. When fresh inoculum and additional media are added, the algae grow well with very little change in biomass productivity as a function of generation. Although there is some variation (Figure 2.12), the lipid

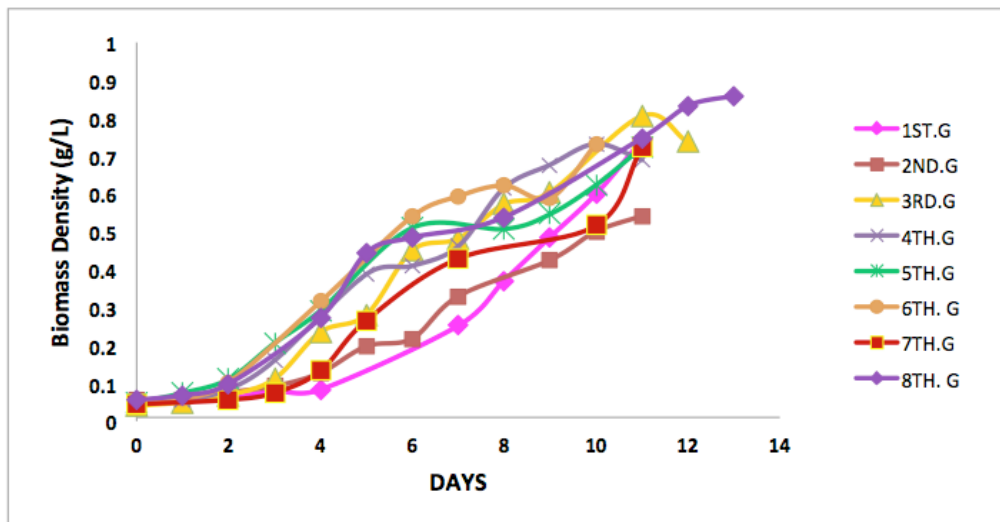


Figure 2.11: Algal growth for *N. salina* as a function of generation of recycling 90% of the spent media using fresh inoculum in batch shake flasks.

percentage also remains consistent at 30% after the first generation. The lipid content in the first generation was significantly higher at 48%.

In the field, some systems operate in fed-batch or semicontinuous mode as opposed to batch mode. In this configuration, a percentage of the culture is removed and dewatered, the water is recycled to the reactor and additional nutrients are added but not additional inoculum. The lipid percentage varied more than when fresh inoculum was used; however, overall, these results demonstrate that water can be effectively recycled multiple times with only small losses in overall lipid productivity.

Produced Water

Since water conservation and nutrient costs are critical determinants in commercial algal biofuel production, impaired water sources were investigated for algal cultivation. One type of impaired water is produced water. Produced water (PW) is a byproduct of oil and gas extraction: it is contained in the same geological formations as the hydrocarbons and is unavoidably brought to the surface along with the oil and gas. Our primary objective was to convert this waste stream into cultivation medium, thereby replacing fresh or brackish ground water consumption and enabling a sustainable algae industry on land that is extraordinarily well-suited for large-scale algae cultivation.

The produced water was first treated in a multistage water treatment system consisting of filtration, flocculation, and oxidation technologies designed by Eldorado Biofuels. The treated water was then discharged to lined, open cultivation ponds (Figure 2.13) and mixed with nutrients to grow algae. Genetic characterization indicates that the native algae growing in the ponds were predominantly *Scenedesmus* sp. and *Tetracystis* sp., with *N. salina* 1776 and *Chlorella* sp. in lesser populations. On average we estimated an annual biomass productivity of 11 g/m²/d in produced water demonstrating that this type of water is suitable for algal cultivation.

Wastewater

Use of wastewater for algal cultivation is the focus of many studies because the use of freshwater is infeasible, especially in arid climates, and because the wastewater treatment industry is interested in additional technologies that can reduce the P and N content in their streams prior to recharging the water. As part of NAABB, three studies were done. The first investigated whether or not the metals found in wastewater would be toxic to algae. The two others investigated different types of wastewater (centrate and secondary) obtained from Southwestern wastewater treatment plants.

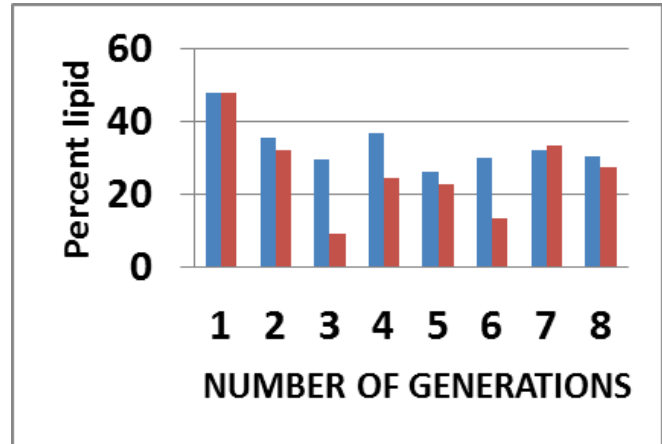


Figure 2.12. Variation in lipid percentage through succeeding generations. Blue bars=media filtered thru 0.2 micron filter. Red bars=unfiltered media.



Figure 2.13: Eldorado algal open pond cultivation system using produced waters.

The metals investigated as potential toxicants included those present at the highest concentrations in regional municipal wastewaters. Compounds and their respective EC₅₀ values (obtained using a particularly sensitive algal species) were as illustrated (Table 2.2). Initial experiments involved *N. salina* in batch cultures that were simultaneously exposed to various multiples of the EC₅₀ concentrations. Subsequent work in this area was designed to determine which metal species was the predominant source of observed toxicity.

Fifty percent inhibition of the *N. salina* growth rate was observed in the culture amended with the Table 2.2 metals at 11X their respective EC₅₀ values (Figure 2.14). That is, zinc and copper were present at concentrations near mg/L levels—exceptionally high relative to their typical concentrations in regional municipal wastewater effluent (Table 2.2).

After determining that *Nannochloropsis* can grow in water that contains more than 10X the amount of heavy metals typically found in wastewater effluent, concentrate was investigated. The basic experimental strategy was to substitute either wastewater effluent or a nutrient-rich sidestream developed during the dewatering of biosolids for the source of macronutrients in the f/2 medium. Effluent or the sidestream flow comprised fractions of the total liquid volume ranging from 5–100%. Salts were added to maintain a near uniform ionic strength. Relative growth rates and lower than normal terminal optical densities were taken as indications of inhibition (Figure 2.15).

Table 2.2. Comparison of continuous flow metals toxicity data to metals levels in concentrated wastewater effluent from the Ina Road Water Pollution Control Facility in Tucson, Arizona.

Metal	EC ₅₀ from Scientific Literature (µg/L)	Actual Conc. in VSEP treated Ina Road wastewater (µg/L)
Copper	50.2 ¹	87.70
Zinc	240 ²	124.00
Cobalt	520 ²	n/a
Lead	680 ²	7.66
Nickel	410 ²	65.54

¹Staub and Florence, 1987 ^{**}Li

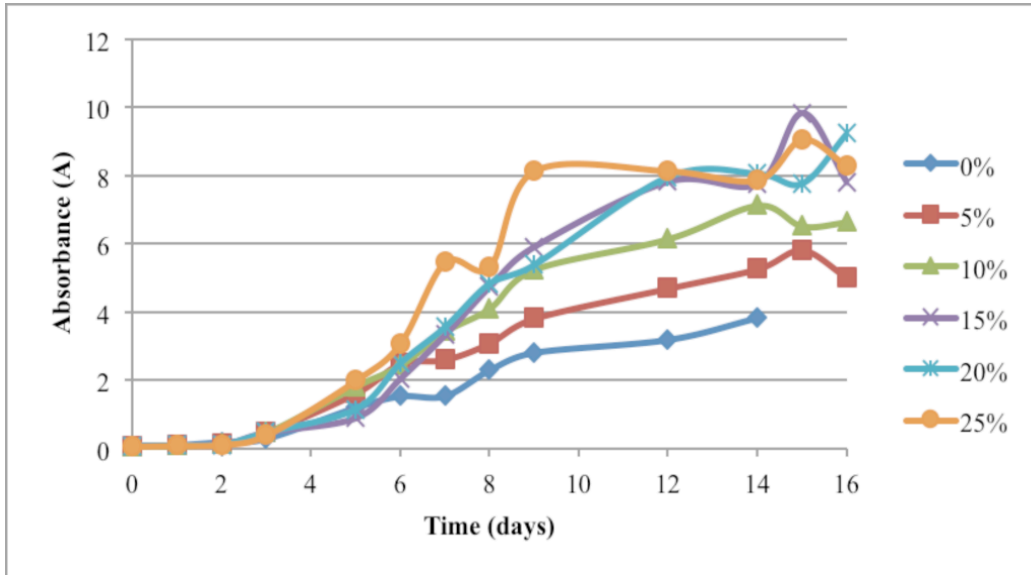


Figure 2.15. Results for *N. salina* growing in normal growth medium with different percentage of centrate derived from the dewatering of digested sludge.

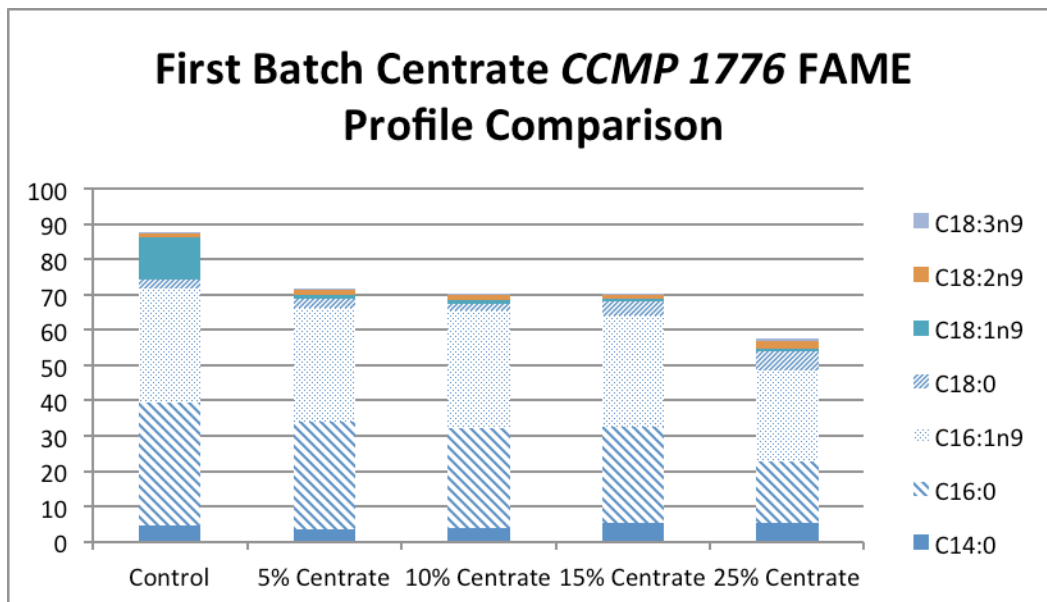


Figure 2.16. FAME profiles for *N. salina* grown in mixtures of f/2 medium and digester centrate.

Results indicate that the addition of centrate derived from biosolids dewatering increased both the rate and extent of growth of *N. salina* at ratios ranging from 5–25% v/v. Higher fractional additions inhibited growth (results not shown). Minor changes were apparent in the lipid compositions of the cells grown in centrate (Figure 2.16). It is apparent that those cells produced a larger percentage of fatty acids that were not recognizable based on the authentic standards utilized here. Furthermore, centrate addition virtually eliminated production of fatty acid C18:1n9 at every level of centrate addition.

Additional tests were carried out using treated wastewater collected at the outflow before discharge or just before the chlorination stage from the Jacob A. Hands municipal wastewater treatment plant in Las Cruces, New Mexico. This plant uses an activated sludge protocol combined with a biological filter pretreatment (trickling filter) and a final chlorination and SO₂-dechlorination. This process produces an advanced secondary treated wastewater effluent. On bench-top shakers, without CO₂ addition, algal growth was significantly slower in the wastewater effluent as compared to the standard substrate (Figure 2.17). The significance of wastewater bacteria on algal productivity and contaminant risk parameters was evaluated by comparing sterile wastewater to raw treated wastewater. As expected, the algae grew to higher cell densities in the sterilized wastewater. For this water source, adding nutrients or fertilizer did not significantly increase the final cell density. We conclude that wastewaters, even partially treated to remove nutrients, are a viable source of nutrients allowing productivity levels similar to the ones obtained on standard growth media.

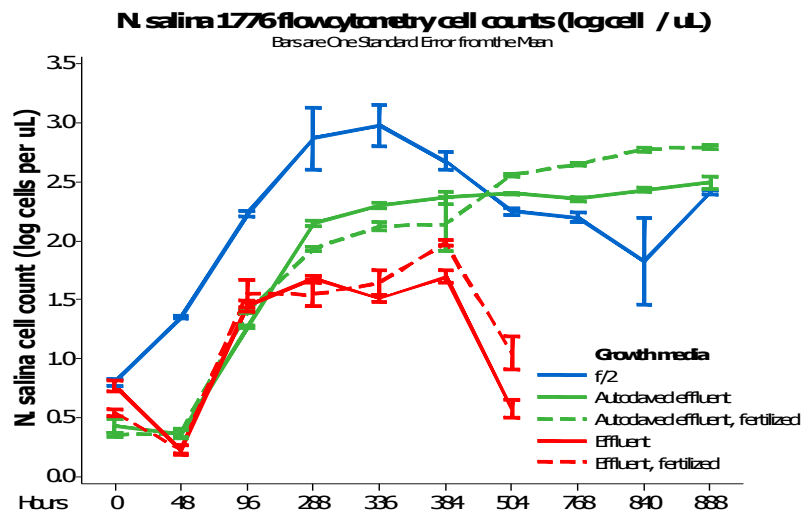


Figure 2.17. Growth of *N. salina* on secondary effluent.

Future Outlook for Wastewater Usage

The research program described has shown that the economic and environmental sustainability of a meaningful algal biofuels industry requires use of CO₂ and fertilizer nutrients that are not derived from fossil fuels³⁻⁵ and that do not reduce the availability of fertilizer for agriculture. Recycling water or using otherwise impaired water can further increase the sustainability of biodiesel production from algae.⁴⁻⁶ One kg biodiesel requires 3726 kg water, 0.33 kg nitrogen, and 0.71 kg phosphate if freshwater is utilized.⁶ Therefore, the use of wastewater as the source of water and nutrients is requisite to the development of algal biofuel technology in Arizona and other parts of the semiarid Southwest. Straightforward calculations indicate that without nutrient recovery and reuse, the supply of municipal wastewater cannot satisfy large scale biofuel nutrient requirements. In their recent report titled *Sustainable Development of Algal Biofuels in the United States* (2012), the National Research Council of the National Academies concluded: “...with current technologies, scaling up production of algal biofuels to meet even 5% of U.S. transportation fuel needs could create unsustainable demands for energy, water, and nutrient resources...” Identification of alternative water and nutrient sources is necessary to make algal biofuels a sustainable energy resource. Municipal wastewater is among the most promising sources of water and nutrients (nitrogen, phosphorus, and trace elements) for algal growth. However, annual production of 39 billion liters of algal biofuel, which is equivalent to 5% of annual U.S. demand for transportation fuels, requires at least 123 billion liters of water, 6 million metric tons of nitrogen (N) and 1 million metric tons of phosphorus (P). Without recycling, it would take over 1X, 4X, and 5X the entire U.S. population, respectively, to generate

sufficient wastewater to provide that much water, N, and P. Therefore, nutrient and water recycling/reuse became fundamentally critical for microalgae to be a sustainable energy source.

Cultivation System Innovations

NAABB had several efforts focused on developing new innovative approaches for the design and operation of the algal cultivation systems to improve algal biomass productivity and the associated capital and operating costs. These include new pond designs, mixing systems, CFD models for improved raceway design and the use of photobioreactor (PBR) systems to produce high-yield inocula for large scale ponds.

ARID Raceway System

One of the causes of decreased algae production in open ponds is diurnal and seasonal temperature variation. The ARID system (Figure 2.18) maintains temperature in the optimal range by changing the water surface area between day and night by draining the culture to a sump.



Figure 2.18. ARID raceway in operation.

A finite-difference temperature model of the ARID raceway was developed in Visual Basic for Applications. The model accurately simulated the temperature changes in the ARID raceway during winter cultivation experiments where the algal growth rate of *N. salina* in ARID and conventional raceways was compared. The ARID raceway remained 7–10°C warmer than conventional raceways throughout the experiments.

NAABB efforts continued to make design improvements and energy evaluations of the ARID system. Although the original ARID system was an effective method to maintain temperature in the optimal growing range, the pumping-energy input was excessive and the flow mixing was poor. Thus, an improved high-velocity raceway design was developed to reduce energy-input requirements (Figure 2.19). This was accomplished by improving pumping efficiency, optimizing the operational hydraulic parameters, and using a serpentine flow pattern in which the water flows through channels instead of over barriers. A second prototype ARID system was installed in Tucson, Arizona, and the constructability, reliability of components, drainage of channels, and flow and energy requirements were evaluated. Each of the energy inputs to the raceway (air sparger, air blower, canal lift

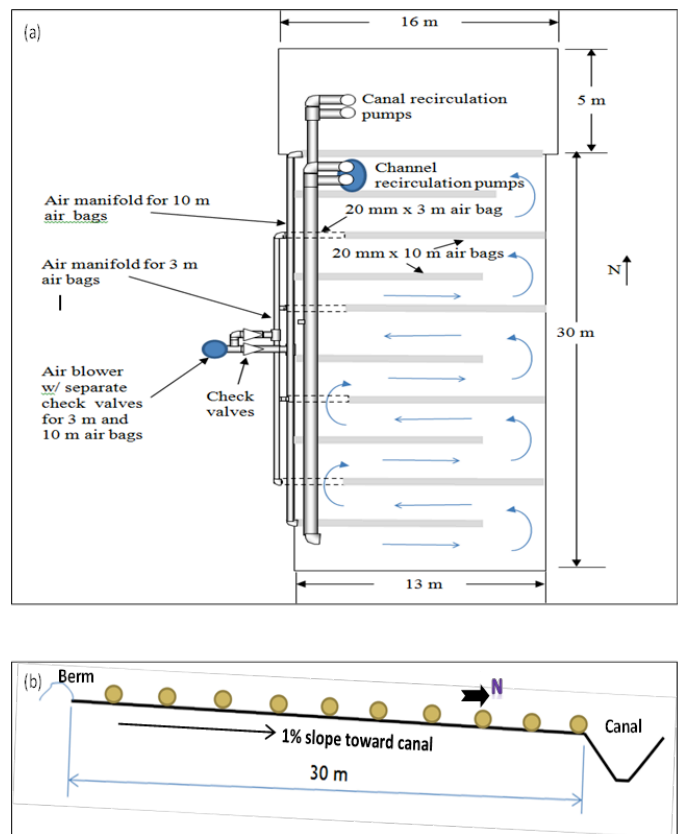


Figure 2.19 (a) ARID dimensions (general view), (b) profile of the channel's cross-section.

pump, and channel recirculation pump) were quantified, some by direct measurement and others by simulation. An algae growth model was used to determine the optimal flow depths as a function of time of year. Then the energy requirement of the most effective flow depth was calculated.

The Biomass Growth Model was added to the ARID raceway model. The accurate estimates of light transmission and temperature enable an accurate prediction of algae growth for various raceway configurations, depths, and operational schemes. The model was used to compare ARID raceway algae growth with conventional raceway algae growth at different flow depths and then to simulate daily and monthly production values for different scenarios. The model was run for Tucson, Arizona, and showed that the ARID raceway had much higher production than a conventional raceway in winter, significantly higher production in spring, the same production in the last month before the monsoon (June), and lower production during the monsoon months (July and August) (Figure 2.20).

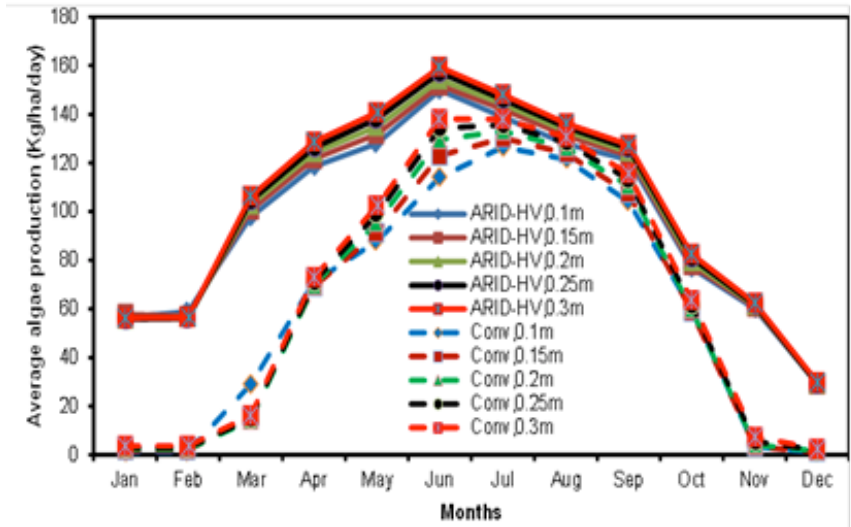


Figure 2.20. Comparisons of ARID and conventional raceway productivities.

Airlift Mixing Systems for Raceways

A new airlift-driven raceway reactor configuration was developed for energy-efficient algal cultivation and high CO₂ utilization efficiency (Figure 2.21). Advantages of this configuration were demonstrated in a 23 L version of the configuration under artificial lighting and laboratory conditions and in an 800 L version under natural light and outdoor conditions.

Results from side-by-side growth studies conducted with *N. salina* in the two raceways, one with the modified air-lift system and the other an identical raceway with a standard paddlewheel (Figure 2.22), are summarized in Figure 2.23. The higher biomass and lipid production due to the efficient CO₂ supply resulted in higher net energy gain in the airlift-driven raceway than in the paddlewheel-driven raceway. The net energy output of the paddlewheel-driven raceway is estimated as 0.03 W/L whereas that in the airlift raceway is 0.15 W/L—an improvement of more than 300%.

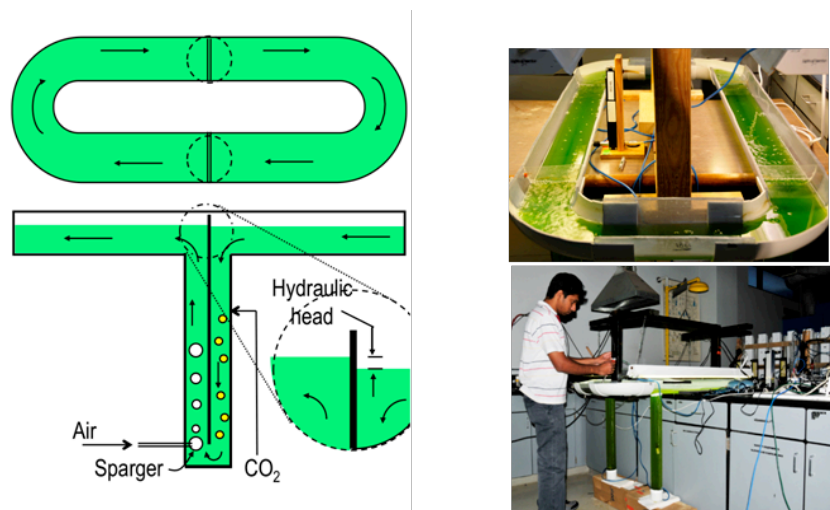


Figure 2.21. Schematic and photograph of laboratory-scale airlift-driven raceway.



Figure 2.22. Outdoor installation of airlift-driven and paddlewheel-driven raceways.



Based on the laboratory tests and the field tests conducted in this research, the proposed airlift-driven raceway can be seen to be more energy-efficient than the traditional paddlewheel-driven raceway. To quantify energy efficiency, this study proposes biomass productivity per unit energy input rather than the traditional measure of volumetric biomass productivity. Based on this measure, performance of the airlift reactor configuration is shown to be comparable to or better than those reported in the literature for different PBR designs. In light of the improved energy-efficiency and the higher CO₂ utilization efficiency demonstrated in this study under laboratory and outdoor conditions, the proposed airlift-driven raceway design holds promise for cost-effective algal cultivation. The mathematical model of the airlift-driven raceway developed as part of this study was validated using growth data on two different algal species under indoor and outdoor conditions. The predictive ability of this model was shown to be high.

CFD Modeling of Open Ponds for Algae Cultivation

Computational Fluid Dynamics (CFD) were employed to obtain the flow pattern in the raceway pond. Once the basic flow pattern is known, many important flow characteristics such as dead zones and velocity channeling can be obtained. CFD can also be employed to obtain or infer pressure drop, hydraulic energy consumption, mass transfer, etc. in the pond. Algae growth can be simulated once the details of growth kinetics are known and are appropriately combined with flow-pattern information from CFD. To

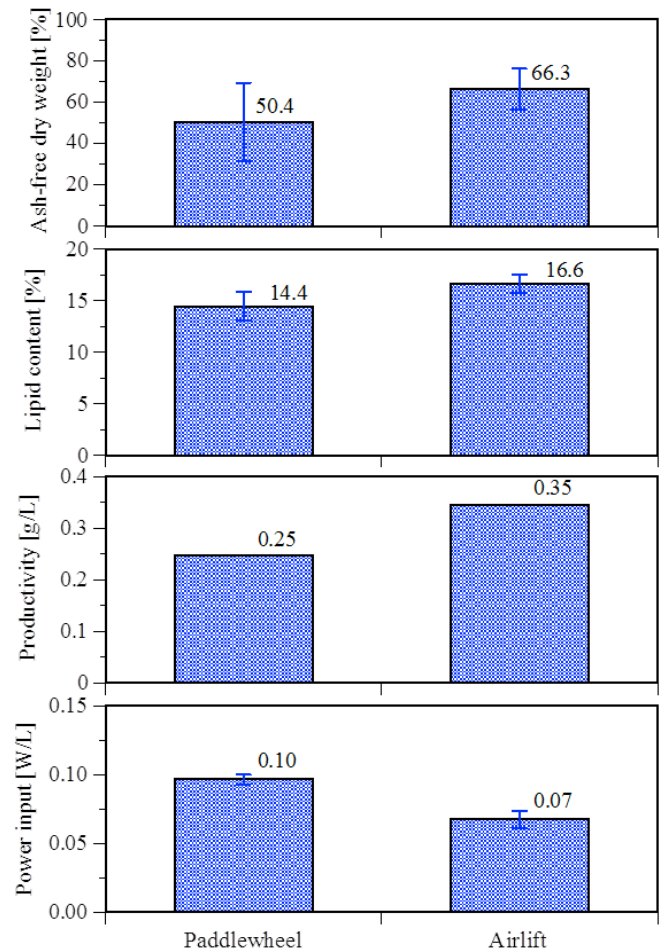


Figure 2.23. Comparison of airlift-raceway versus paddlewheel-driven raceway. Species: *N. salina*. Test duration: 12 days.

this end, NAABB set up an extensive program for CFD simulations of a raceway pond. The geometry and operating details of the 360 m² raceway pond from Samalkota (Andhra Pradesh, India) were obtained. The CFD simulations were carried out for many different cases. The results from CFD must be validated so that they can be used confidently for further analysis. Hence there remains ongoing work on making flow measurements in the raceway pond for CFD validation. Some results of the CFD model of the 360 m² raceway are shown in the Figures 2.24, 2.25, and 2.26.

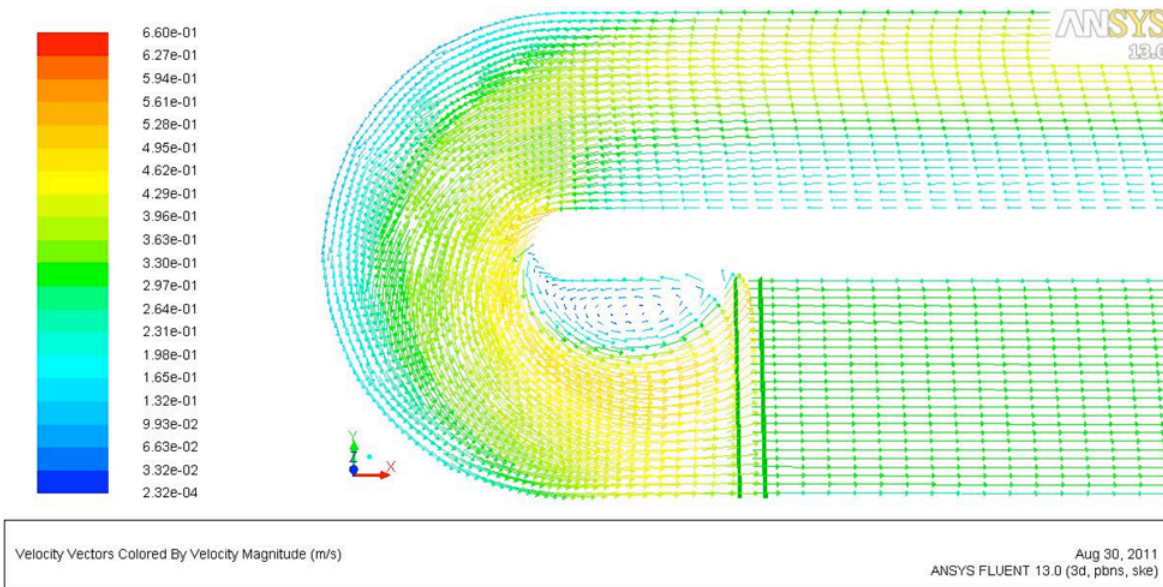


Figure 2.24. Velocity vectors on the free surface at the end of the pond near the paddlewheel. Vectors are color coded as per velocity magnitude.

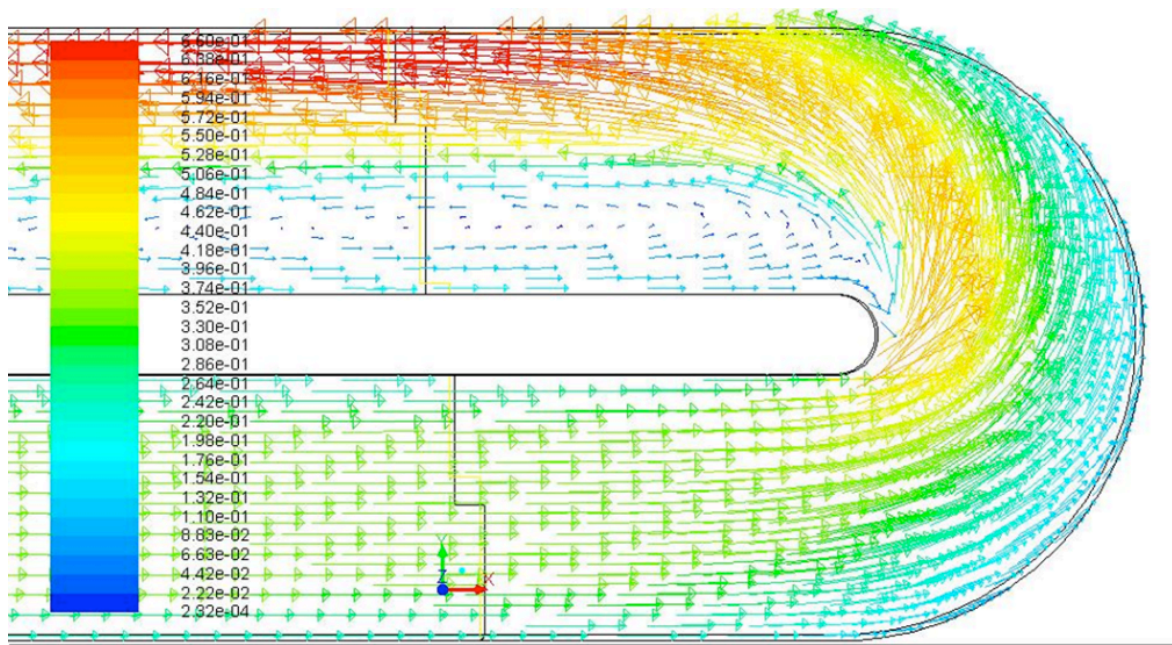


Figure 2.25. Velocity vectors on the free surface at the end of the pond away from the paddlewheel. Note that the bulk flow is from right to left in the upper channel. Flow reversal is seen near the mid-wall of the upper channel.

Line-up-channel

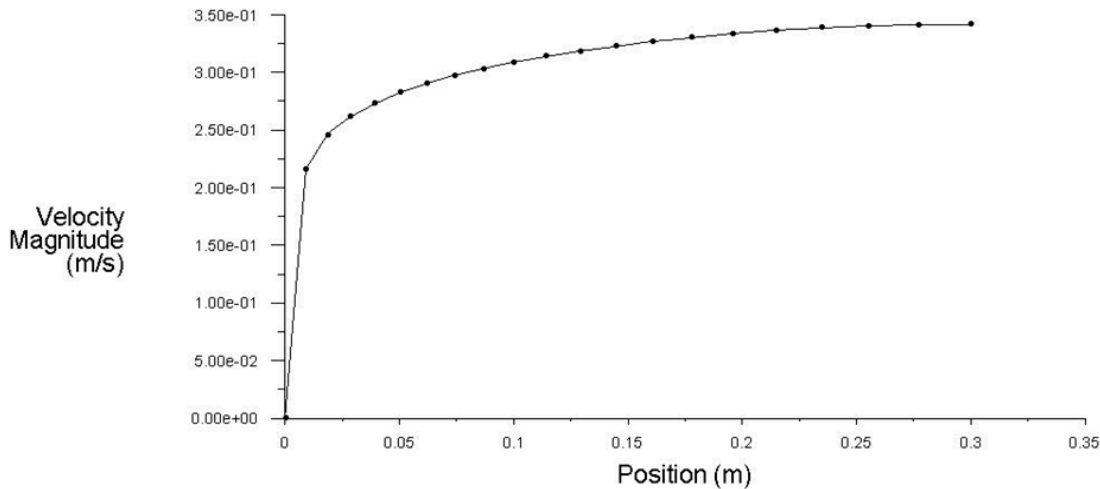


Figure 2.26. The profile of velocity as a function of vertical coordinate (pond depth) at the center of the channel containing paddlewheel (axial location = 30 m from paddlewheel).

The CFD modeling efforts came to the following major conclusions:

- (1) The CFD simulations for flow in the (360 m²) raceway pond showed the overall flow pattern with possible locations of dead zones.
- (2) Vertical mixing in the raceway pond is seen to be very poor from simulations. The same was confirmed through a cold-flow, tracer study conducted on the 360 m² raceway pond.
- (3) The CFD results presented here were obtained for a mean velocity of 0.3 m/s in the raceway pond and need validation using experimental measurements of flow pattern. Similar results were obtained for the mean velocities of 0.1 m/s and 0.2 m/s.
- (4) The top (free) surface of the fluid in the raceway pond is treated as a flat surface in simulations. In reality, the free surface shows a wavy characteristic mainly due to the action of paddlewheel. The turbulent mixing due to the wave interface is difficult to capture using CFD and hence the mixing in the raceway pond captured by CFD simulations is likely to be conservative.
- (5) The pressure drop in the raceway pond obtained from CFD modeling correlates well with the empirical Manning's equation (with Manning's constant ~0.2).

Applications of PBR Systems with High Biomass Yields

Discussions of microalgal cultivation systems have typically focused on either open raceway systems or closed PBRs but this is likely to be a false dichotomy as there are applications best achieved using one or the other or both options in concert. For example, the use of highly efficient PBR systems for quality-controlled inoculum production at maximum rates for open raceway ponds could likely improve yields and cultivation system stability and reliability. PBRs integrated with large-scale open raceway production systems also represent a

risk-mitigation system that can quickly repopulate a large-scale open raceway pond facility after a culture crash. PBR volumetric productivities can be 10-fold higher than open raceway ponds due to the ability to operate at shallower culture depths with better control of culture parameters such as light, temperature, CO₂, and mixing. By using a PBR to produce high yields (5g/L) of clean algal biomass that can be used as an inoculum for open-pond systems one could use 1 L of dense culture from a PBR to seed more than 100 L of media in an open pond.

Data have been collected from operations of the Solix PBR system over the past several years conducted in a serial batch mode with a portion of each harvest used to start the next batch.⁷ Harvest densities ranged between 2 g/L and 3 g/L. Some batches were harvested at lower densities due to low growth rates in low light periods during winter cultivation. A select number of batches were inoculated as low as 0.25 g/L and harvested at 6 g/L.

NAABB tested a newer version of the Solix PBR (AGS4000) with the same media and culture, *N. salina* CCMP1776 from the previously mentioned Solix studies. The lower range of required inoculation densities and upper range of harvest densities was investigated with this system. Harvest densities as high as 6 g/L were observed in the same period. To achieve this growth range the system was fed a second batch of nutrients four days after inoculation. The ability of the system to operate at high linear growth rates over these density ranges supports the use of the system as an industrial scale cultivation technology for both stand-alone production and as an inocula source for large-scale integrated PBR/open-raceway pond systems.

Figure 2.27 shows a data plot for a number of production runs in the Solix PBR over the past several years indicating the relationship between final culture density (x axis) and lipid content (y axis) as a percentage of dry weight. This data plot shows that yields exceeding 5 g/L with 50% lipid have been achieved using the Solix PBR system. Moreover, these results have been confirmed in both small- and large-scale PBR systems with efficient use of nutrients and CO₂. Actual operation of these PBR systems to produce inocula for open ponds would most likely focus on rapid biomass productivity under nutrient-sufficient conditions versus lipid accumulation under nutrient limitation, since this would significantly increase biomass productivity for providing seed for large-scale pond systems.

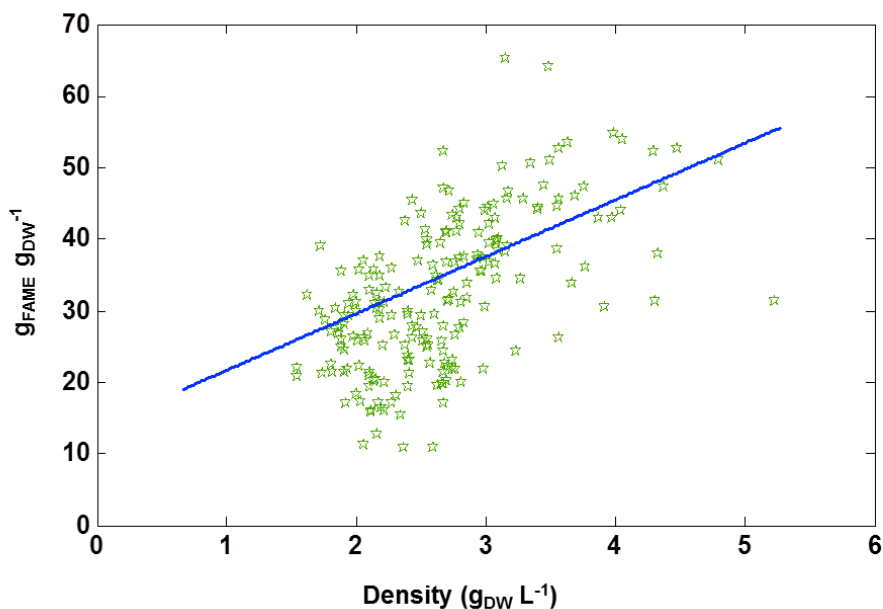


Figure 2.27. Solix PBR data plot for multiple *N. salina* batches with biomass and lipid yield.

Large-pond Cultivation/Biomass Production

An important aspect of the NAABB program was algal cultivation to provide biomass for downstream processing and analysis. Two sites were utilized: the Texas Agrilife facility at Pecos, Texas (Figure 2.28), and the Cellana facility in Kona, Hawaii (Figure 2.29). At Pecos, five algae strains starting with *N. salina* as the baseline strain and four other strains selected by the Algal Biology Team within the NAABB consortium were cultivated. For each alga strain, the medium was optimized, productivity was determined (lipid percentage, ash percentage), and batches were grown in 23,000 L open ponds with paddlewheels. At Kona, Cellana’s ALDUO™ large-scale cultivation “hybrid” system of PBRs and open ponds was utilized. Each production system consists of six 25,000 L PBRs and three 450 m² production ponds. All fluid transfers—including inoculations, nutrient additions, and harvest volumes—were operated and monitored by a remote process-control system.



Figure 2.28. Pecos, TX, testbed facility.

Media and Growth Optimization

The first step done prior to large-scale cultivation was to optimize the media to reduce the costs associated with growing algae at the 23,000 L scale. This was accomplished by replacing the nitrate with urea, the potassium phosphate with a mixture of monoammonium phosphate and potash (potassium source), and the iron citrate with iron chloride. Each component was evaluated separately and the lowest quantity of replacement chemical that did not result in a decreased growth rate was used. The cost and quantity information for a common freshwater *Chlorella* sp. cultivation medium, BG-11 was compared to a much less expensive media developed for use in the field. The new media recipe is 90% lower in cost than the standard BG-11 media.



Covered by US Patents 7,770,322 & 5,541,056, Similar Patents/Patents pending in Europe, Australia, South Africa, Brazil, Japan, Mexico

Figure 2.29. Cellana testbed facility.

Once the species had completed the media optimization testing on the bench scale, intermediate scale tests were conducted in two medium (200 L) raceways located in a greenhouse (Table 2.3). Nine species were tested using this process at the Pecos site. Cultures of *Chlorella* sp. *DOE1412* were scale-up from the bench to 800 L raceways on the traditional versus optimized media. The biomass productivity, lipid productivity, and FAME profile were monitored for both media formulations. Figure 2.30 shows the cultivation data as a function of time. Essentially the amount of media was added slowly, so we started with 5 L of culture in 20 L of media, then 30 additional liters were added, then 30 more. Then the cultures were transferred outdoors and the volume was set to 250 L and then media added up to 800 L. The algae grew as well on the optimized, less expensive media as on the BG-11 media; however, the optimized media (PE-001A) is 10 times cheaper. The lipid content and lipid profile are shown in Figure 2.31. This strain has many unsaturated bonds and primarily consists of C18 compounds that are readily converted to fuels. The lipid profiles are similar for the two media regardless of reactor type.

Table 2.3. Nine species tested at the site at Pecos, Texas.

Strain name	Isolate ID	Suggested Laboratory Scale Media	Growth Rate on Traditional Media g/m ² /d	Growth Rate on Optimized Media g/m ² /d
<i>N. salina</i>	CCMP1776	f/2 10x	15.5	17.9
<i>N. oculata</i>	43-AM	f/2 10x	16.7	18.6
<i>Chlorella</i> sp.	DOE1412	BG-11	20.4	25.2
<i>Desmid</i> sp.	DOE043	BG-11	18.3	17.3
<i>Chlorococcum</i> sp.	DOE0202	BG-11	11.4	11
<i>Chlorococcum</i> sp.	DOE0101	BG-11	14.8	15.6
<i>Scenedesmus obliquus</i>	DOE0152	BG-11	16.9	14.8
<i>Scenedesmus obliquus</i>	EN-0004	BG-11	16.4	15.7
<i>Chlorella</i> sp.	DOE1095	BG-11	21.2	24

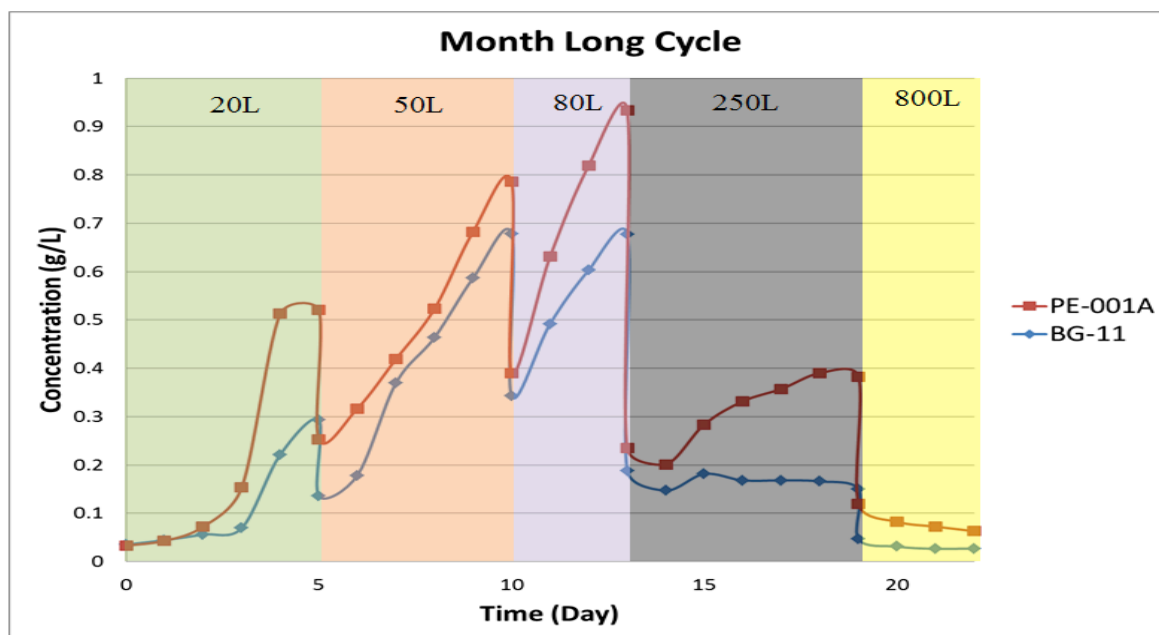


Figure 2.30. Cultivation of *Chlorella* sp. DOE1412 in traditional (blue) and optimized (red) media. The first 80 L of cultivation were done in PBRs, then the cultures were used as inoculum for an 800 L traditional raceway. Two media were compared. The cultures froze shortly after the volume was increased to 800 L.

Additionally, Cellana conducted strain screening and optimization experiments using its midscale cultivation system (Figure 2.29), which is a stand-alone system of 24 PBRs and pond simulators, each of 200 L capacity. Cellana focused on *N. oceanica*, strain KA19 (isolated on the Big Island of Hawaii), and optimized pH, salinity, total nitrogen, and cultivation time.

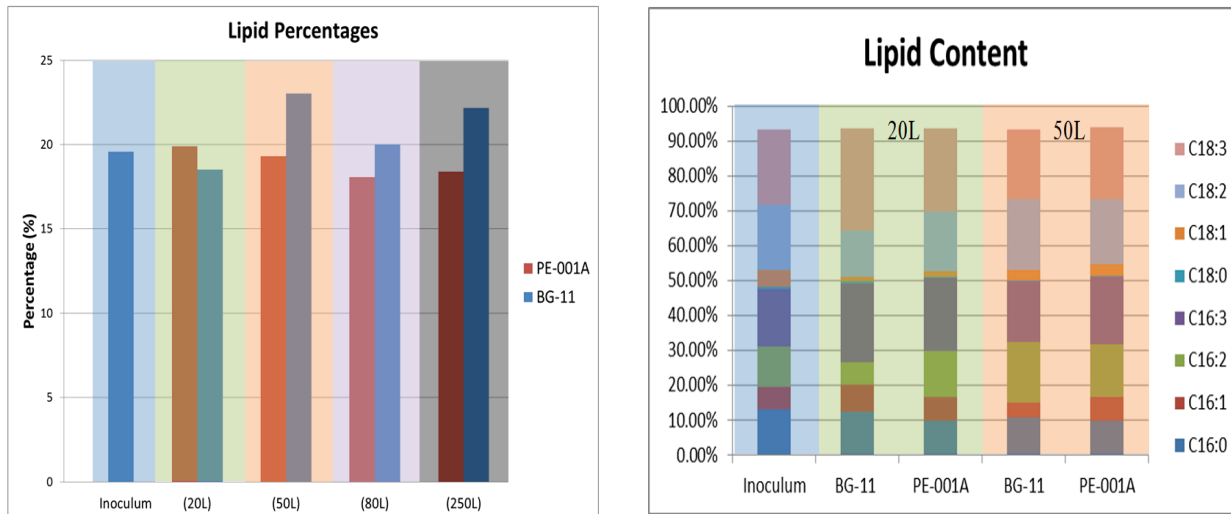


Figure 2.31. Lipid profiles for *Chlorella sp. DOE1412* grown in PBRs and traditional raceways. Two different media were compared for cultivation.

Production

At the large scale, five consortium strains were grown in 23,000 L open pond raceways in Pecos. Additionally, Cellana cultivated three species in their production facility: *N. oceanica* KA19, *Pavlova pinguis* C870 and *Tetraselmis* sp. (strain KA33). Table 2.4 provides the amount of biomass provided to the consortium for downstream processing studies. On average, a productivity of 10 g/m²/day was obtained at both sites. More detail on the long-term and seasonal productivities from the Pecos testbed and other algal cultivation facilities is provided in the Sustainability section. Recycled media showed no adverse effects on media composition, biomass, or lipid yield. However, changes in the concentration of divalent and transition metals over time in the cultivation system and algae remain unaccounted for. These changes appear to be nominally the inverse of total salinity variations. Over 15 cycles of growth using recycled media were accomplished without large increases in salinity. The use of the recycled media reduces the use of new well water and retains salts that would otherwise be purchased for addition, thereby drastically reducing the quantity of water withdrawn from the local shallow aquifer and potentially reducing costs.

Table 2.4. Summary of biomass produced for consortium on a dry weight basis.

Source	Strain	Harvested Biomass (kg)	Average Lipid Percentage
2011 (Pecos)	<i>N. salina</i> (saltwater)	610.0	16.8
2012 (Pecos)	<i>Chlorella sp. DOE1412</i> , <i>Chlorococcum sp.</i> , <i>S. obliquus</i> , <i>Kirchenella sp.</i> (freshwater)	876.0	22.4
2013 (Cellana)	<i>N. oecania</i> (saltwater)	50	35
	<i>Pavlova sp.</i> (saltwater)	4	
	<i>Tetraselmis sp.</i> (saltwater)	50	< 15

Lessons Learned at the Large Scale

There were several lessons learned at the large scale related to scalability, media recycle, pond depth, ash content, contamination, and process integration. Overall, data collected at mid scale matched up very well with that at large scale in terms of the biomass productivity, pond cycle, and the biochemical composition of the biomass. This confirms that mid-scale production systems are useful research tools that simulate microalgae performance in large-scale ponds in a cost-effective manner.

An important aspect of cultivation is the use of media recycling. It is extremely important to reuse as much water for cultivation as possible to reduce input costs. Studies were performed in the lab using ion chromatography (IC) and analysis performed to determine nutrient uptake of each individual alga species as well as to determine the chemical balance of the media after the algae had been removed from suspension. During 2011 and 2012, media was recycled, showing no significant drop in productivity or lipid accumulation. It should also be noted that over time microelements present within the media increased in concentration within the recycled media the more it was reused for cultivation, suggesting a reuse limit. Also, recycled media had to be treated using specific amounts of bleach to remove any potential contaminants that were present over time. Alternative methods for sterilization of the recycled media are ongoing and included UV treatment similar to what is seen in the wastewater and aquaculture industries.

Pond depth depending on the time of year has an effect on the overall performance of the algae cultures. During the summer months, increasing the speed of the paddlewheel and operating at a depth of 4–7 inches can reduce the overall temperature of the algae culture, keeping it more protected from overheating and thus maintaining high growth rates during the more extreme months of the year. Also, slowing the paddlewheel down in the winter to help reduce evaporation and increasing the pond depth to provide more thermal protection helps prevent the culture from getting too cold, allowing the growth rates to stay competitive during the winter months. A reduction in growth rate was observed in the winter months due to temperature fluctuations and lower light levels, but through proper management and culture care, the Pecos facility has been able to stay operational year round.

One other lesson learned at the large scale is related to ash content management. In large open areas, especially in the Southwest, dust frequently blows into the ponds. The dust increases the ash content of the culture and is undesirable in the downstream processes. A strategy was developed to do partial harvests to minimize the amount of dirt in the cultures. However, efficient harvesting methods that minimize dust require further investigation.

Culture contamination is the most prevalent cultivation issue that was observed over the course of the production project. By using a batch cultivation system, contamination issues could be mostly contained, but from time to time either due to older cultures, rain events, or large dust storms, cultures would become contaminated during the production process. Microscope checks were performed on the batches at regular intervals to determine the rate in which each batch was becoming contaminated. A threshold of 20% contamination was established to

provide a decision point when cultures were deemed unusable. Contamination decreased when the ALDUO™ hybrid system, a combination of PBRs and open ponds, was used. Species-specific methods were also developed, such as the addition of salt to freshwater cultivation systems when the algae had some salt tolerance, pH shifts, and nutrient starvation.

The final aspect of large-scale cultivation is gaining an understanding of how changes in cultivation methodologies affect downstream processing. Ash content was one of the most significant issues for processing through harvesting and extraction equipment. Obviously, less is better; however, strategies to mitigate large quantities of ash are still required. Also, the addition of metals and high salt concentrations greatly affect the feed value and may require further cleaning of the bio-oil prior to conversion since these compounds affect catalyst life; hence, process integration is extremely important and crucial as the industry moves forward.

Conclusions and Recommendations

Significant progress was made in all four major thrust areas shown in the Cultivation task framework (Figure 2.1), thereby advancing toward the goal of cost-effective achievement of high annual biomass productivities in robust outdoor pond and hybrid systems in an environmentally sustainable manner.

The key advance in our optimization and modeling was the development of a microalgae biomass growth model. This model utilizes experimentally determined species-specific parameters and was validated using outdoor pond cultivation data. The biomass growth model, in conjunction with the biomass assessment tool, enables the prediction of monthly and annual biomass productivities of a given strain in hypothetical outdoor pond cultures located across the United States. Furthermore, an indoor raceway pond with temperature control and LED lighting to simulate sunlight spectrum and intensity was designed and successfully operated under climate-simulated conditions. This system allows one to simulate the climate conditions of any geographical location and determine how algae will grow in a location of interest. This innovative modeling capability combined with the LED system can be used as a low-risk and cost-effective way of screening strains for their potential of exhibiting high biomass productivities in outdoor ponds, for finding the best match between a given strain and climate (i.e., geographic location), and for identifying the optimum pond operating conditions, thereby accelerating the large-scale cultivation of promising high-productivity strains while quickly eliminating suboptimal candidates.

It was demonstrated that microalgae can be successfully cultivated on municipal wastewater and produced water resulting from oil and gas exploration. Recycling water and media or the nutrients in waste biomass can further reduce the costs of inputs. A water management strategy that includes the use of low-cost impaired waters and recycle strategies for cultivation will be necessary for the anticipated large-scale production of microalgae biofuels.

With respect to the task of developing and operating innovative cultivation systems, the key advance was the modeling, testing, and design improvements of the ARID pond culturing system. This system provides improved temperature

management, i.e., maintaining water temperatures within the optimum range for a given microalgae strain throughout the year. Modeling results and measurements demonstrated that water temperatures during the winter (in Arizona) remained 7–10°C warmer than in conventional raceways. As a result of better temperature management, the ARID system was shown to have significantly higher annual biomass productivities compared to conventional raceways. In conjunction with engineered reductions in the energy use for pumping and mixing (i.e., use of a solar pumping system), cultivation in the ARID system was also shown to have significantly higher energy productivity (biomass produced per unit energy input) than conventional raceways. By extending the growing season and modulating temperatures, the impact of the ARID system could be profound by significantly increasing annual biomass productivities for any microalgae strain of choice. Collectively these improvements result in approximately an 18% reduction in cost of production of algal biomass in comparison to traditional open-pond systems with paddlewheels.

With respect to the task of large-pond cultivation and biomass production, media was optimized for a variety of microalgae species to maximize growth while minimizing cost. Cost reduction of 90% in chemicals was demonstrated over the use of typical laboratory media formulations. More than 1500 kg of biomass from eight different algal species was generated in the large-scale facilities at Pecos, Texas, and Kona, Hawaii for downstream processing and testing. By successfully demonstrating large-scale biomass production, significant progress was made towards the goal of commercial microalgae biofuels generation. A key development was the ability to move strains isolated from the prospecting effort from the laboratory to full production in outdoor pond systems, and subsequent downstream-processing of the strains to fuels and coproducts.

Recommendations

The Cultivation Team offers the following recommendations:

- Continue characterization of new strains using the LED climate-simulation system to optimize conditions for outdoor cultivation and to develop a crop-rotation strategy;
- Conduct long-term cultivation trials in established testbeds at different locations using NAABB strains and various pond designs (i.e., ARID system);
- Provide data to inform DOE harmonized models;
- Scale up and test cultivation in impaired waters with recycle, evaluating the water chemistry, quality, and impact on sustained productivity;
- Begin scale-up cultivation of GMO strains first in the LED climate-simulation system prior to outdoor trials;
- Continue engineering and optimizing pond design to bring down capital and operating costs;
- Develop mitigation strategies to minimize ash content and undesirable metals in algal biomass produced at large scale; and
- Continue to develop and demonstrate crop management strategies at scale.

Team Members

Bob Arnold, University of Arizona
Xuemei Bai, Cellana
Wiebke Boeing, New Mexico State University
Lois Brown, Texas A&M University
N. Gujarathi, Reliance Industries
Michael Huesemann, Pacific Northwest National Laboratory
Pete Lammers, New Mexico State University
Paul Laur, Eldorado Biofuels
N. “Khandan” Nirmalakhandan, New Mexico State University
Ronald Parsons, Solix Biosystems
Tzachi Samocha, Texas A&M University
Alex Thomasson, Texas A&M University
Adrian Unc, New Mexico State University
Pete Waller, University of Arizona

Publications

Full-length, Peer-reviewed Publications

- Arudchelvam, Y. and N. Nirmalakhandan. Energetic optimization of algal lipid production in bubble columns: Part 1: Evaluation of gas sparging. *Biomass and Bioenergy* 46 (2012): 757–764.
- Arudchelvam, Y. and N. Nirmalakhandan. Optimizing net energy gain in algal cultivation for biodiesel production. *Bioresource Technology* 114 (2012): 294–302.
- Arudchelvam, Y. and N. Nirmalakhandan. Energetic optimization of microalgal cultivation in photobioreactors for biodiesel production. *Renewable Energy* 56 (2013): 77–84.
- Arudchelvam, Y. and N. Nirmalakhandan. Energetic optimization of algal lipid production in bubble columns: Part II: Evaluation of CO₂ enrichment. *Biomass and Bioenergy* 46 (2012): 765–772.
- Bartley, M.L., W.J. Boeing, A.A. Corcoran, F.O. Holguin, and T. Schaub. Effects of salinity on growth and lipid accumulation of biofuel microalga *Nannochloropsis salina* and invading organisms. *Biomass Bioenergy* 54 (2013): 83–88.
- Bartley, M.L., W.J. Boeing, B.N. Dungan, F.O. Holguin, and T. Schaub. pH effects on growth and lipid accumulation of the biofuel microalgae *Nannochloropsis salina* and invading organisms. *Journal of Applied Phycology* (2014): *In Press*.
- Cheng, K-C., M. Ren, and K.L. Ogden. Statistical optimization of culture media for growth and lipid production of *Chlorella protothecoides* UTEX 250. *Bioresource Technology* 128 (2013): 44–48.
- Corcoran, A.A. and W.J. Boeing. Biodiversity increases the productivity and stability of phytoplankton communities. *PloS one* 7 (2012): e49397.
- Corcoran, A.A. and W.A. Van Voorhies. Simultaneous measurements of oxygen and carbon dioxide fluxes to assess productivity in phytoplankton cultures. *Journal of Microbiological Methods* 91 (2012): 377–379.

Crowe, B., S. Attalah, S. Agrawal, P. Waller, R. Ryan, J. Van Wagenen, A. Chavis, J. Kyndt, M. Kacira, K.L. Ogden, and M. Huesemann. A comparison of *Nannochloropsis salina* growth performance in two outdoor pond designs: Conventional raceways versus the ARID pond with superior temperature management. *International Journal of Chemical Engineering* (2012): Article ID 920608 9 pages.

Dong, B., N. Ho, K.L. Ogden, and R.G. Arnold. Cultivation of *Nannochloropsis salina* in municipal wastewater or digester centrate. *Ecotoxicology and Environmental Safety* 103 (2014): 45–53.

Fulbright, S.P., M.K. Dean, G. Wardle, P.J. Lammers, and S. Chisholm. Molecular diagnostics for monitoring contaminants in algal cultivation. *Algal Research* 4 (2014): 41-51.

Huesemann, M.H., J. Van Wagenen, T. Miller, A. Chavis, S. Hobbs, and B. Crowe. A screening model to predict microalgae biomass growth in photobioreactors and ponds. *Biotechnology and Bioengineering* 111 (2013): 1583–1594.

Ketheesan, B. and N. Nirmalakhandan. Development of a new airlift-driven raceway reactor for algal cultivation. *Applied Energy* 88 (2011): 3370–3376.

Ketheesan, B. and N. Nirmalakhandan. Feasibility of microalgal cultivation in a pilot-scale airlift-driven raceway reactor. *Bioresource Technology* 108 (2012): 196–202.

Ketheesan, B. and N. Nirmalakhandan. Modeling microalgal growth in an airlift-driven raceway reactor. *Bioresource Technology* 136 (2013): 689–696.

Myint, M.T., A. Ghassemi, and N. Nirmalakhandan. A generic stoichiometric equation for microalgae–microorganism nexus by using clarified domestic wastewater as growth medium. *Desalination and Water Treatment* (2013): 1–9.

Pegallapati, A.K., Y. Arudchelvam, and N. Nirmalakhandan. Energy-efficient photobioreactor configuration for algal biomass production, *Bioresource Technology* 126 (2012): 266–273.

Pegallapati, A.K. and N. Nirmalakhandan. Energetic evaluation of an internally illuminated photobioreactor for algal cultivation. *Biotechnology Letters* 33 (2011): 2161–2167.

Pegallapati, A.K. and N. Nirmalakhandan. Modeling algal growth in bubble columns under sparging with CO₂-enriched air. *Bioresource Technology* 124 (2012): 137–145.

Pegallapati, A.K. and N. Nirmalakhandan. Internally illuminated photobioreactor for algal cultivation under carbon dioxide-supplementation: Performance evaluation. *Renewable Energy* 56 (2013): 129–135.

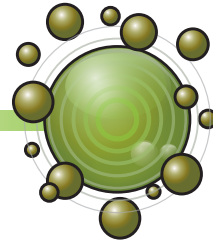
Pegallapati, A. K., N. Nirmalakhandan, B. Dungan, F.O Holguin, and T. Schaub. Evaluation of an internally illuminated photobioreactor for improving energy ratio. *Journal of Bioscience and Bioengineering* 117 (2014): 92–98.

- Quinn, J.C., T. Yates, N. Douglas, K. Weyer, J. Butler, T.H. Bradley, and P.J. Lammers. *Nannochloropsis* production metrics in a scalable outdoor photobioreactor for commercial applications. *Bioresource Technology* 117 (2012): 164–171.
- Ren, M., B. Lian, and K. Ogden. Effect of culture conditions on the growth rate and lipid production of microalgae *Nannochloropsis gaditana*. *Journal of Renewable and Sustainable Energy* (2014): Accepted December 2013.
- Ren, M. and K. Ogden. Cultivation of *Nannochloropsis gaditana* on mixtures of nitrogen sources. *Environmental Progress & Sustainable Energy* (2013): DOI 10.1002/ep.11818.
- Selvaratnam, T., A.K. Pegallapati, F. Montelya, G. Rodriguez, N.Nirmalakhandan, W. Van Voorhies, and P.J. Lammers. Evaluation of a thermo-tolerant acidophilic alga, *Galdieria sulphuraria*, for nutrient removal from urban wastewaters. *Bioresource Technology* 156 (2014): 395-399.
- Sigala, J. and A. Unc. Pyrosequencing estimates of the diversity of antibiotic resistant bacteria in a wastewater system. *Water Science and Technology* 67 (2013): 1534–1543.
- Unnithan, V.V., A. Unc, and G.B. Smith. Mini-review: *A priori* considerations for bacteria-algae interactions in algal biofuel systems receiving municipal wastewaters. *Algal Research* 4 (2014): 35-40.
- Unnithan, V.V., A. Unc, and G.B. Smith. Role of *Nannochloropsis salina* for the recovery and persistence of MS2 virus in wastewater. *Algal Research* 4 (2014): 70-75.
- Van Wagenen, J., T.W. Miller, S. Hobbs, P. Hook, B. Crowe, and M.Huesemann. Effects of light and temperature on fatty acid production in *Nannochloropsis salina*. *Energies* 5 (2012): 731–740.
- Waller, P.M., R. Ryan, M. Kacira, and P. Li. The algae raceway integrated design for optimal temperature management. *Journal of Biomass and Bioenergy* 46 (2012): 702–709.
- Xie, S, S. Sun, S.Y. Dai, and J.S. Yuan. Efficient coagulation of microalgae in cultures with filamentous fungi. *Algal Research* 2 (2013): 28–33.
- Xu, B., P. Li, and P.J. Waller. Study of the flow mixing in a novel ARID raceway for algae production. *Renewable Energy* 62 (2014) 249–257.
- Xu, Y.Y. and W.J. Boeing. Mapping biofuel field: A bibliometric evaluation of research output. *Renewable & Sustainable Energy Reviews* 28 (2013): 82–91.
- Xu, Y.Y. and W.J. Boeing. Modeling maximum lipid productivity of microalgae: Review and next step. *Renewable & Sustainable Energy Reviews* 32 (2014): 29-39.

References

1. Stauber, J.L., and Florence, T.M. Mechanism of toxicity of ionic copper and copper complexes to algae. *Marine Biology* 94 (1987): 511-519.
2. Lin, K.-C., Lee, Y.-L., and Chen, C.-Y. Metal toxicity to *Chlorella pyrenoidosa* assessed by a short-term continuous test. *Journal of Hazardous Materials* 142 (2007): 236-241.
3. Clarens, A. F., E.P. Resurreccion, M.A. White, and L.M. Colosi. Environmental life cycle comparison of algae to other bioenergy feedstocks. *Environmental Science & Technology* 44 (2010): 1813–1819.
4. Handler, R.M., C.E. Canter, T.N. Kalnes, F.S. Lupton, O. Kholiqov, D.R. Shonnard, and P. Blowers. Evaluation of environmental impacts from microalgae cultivation in open-air raceway ponds: Analysis of the prior literature and investigation of wide variance in predicted impacts. *Algal Research* 1 (2012): 83–92.
5. Pfromm, P. H., V. Amanor-Boadu, and R. Nelson. Sustainability of algae derived biodiesel: A mass balance approach. *Bioresource Technology* 102 (2011): 1185–1193.
6. Yang, X., R.C. Flowers, H.S. Weinberg, and P.C. Singer. Occurrence and removal of pharmaceuticals and personal care products (PPCPs) in an advanced wastewater reclamation plant. *Water Research* 45 (2011): 5218–5228.
7. Quinn, J.C., T. Yates, N. Douglas, K. Weyer, J. Butler, T.H. Bradley, and P.J. Lammers. *Nannochloropsis* production metrics in a scalable outdoor photobioreactor for commercial applications. *Bioresource Technology* 117 (2012): 164–171.

HARVESTING AND EXTRACTION



Introduction

Team Leads

Babs Marrone, Los Alamos National Laboratory
Ron Lacey, Texas A&M University

Preface

Harvesting algae and extracting the lipids are significant cost drivers in the biofuel production process.¹⁻³ Therefore, the goal of the Harvesting and Extraction task was to develop low-energy, low-cost harvesting and extraction technologies that could feed lipids into highly efficient fuel-conversion processes.

The new harvesting and extraction technologies developed in this task must have:

- Low capital and operating costs;
- Ease of operation and low maintenance requirements;
- Ease of integration with cultivation facilities to limit pumping and power requirements;
- Compatibility with a broad range of algal species;
- Ability to recycle water;
- Low environmental impact, i.e., low or no hazardous chemical or solvent use;
- Minimum energy requirements that reduce the carbon footprint;

Centrifugation is the industry state of the art for harvesting algae for the production of high-value products. While time-tested and effective, centrifugation has high capital costs, is energy intensive, and can require significant maintenance. Standard centrifuges cannot be deployed directly at the pond, so algae water must be pumped from the pond to the centrifuge station for harvesting.

Algae cells only make up about 0.1% of the total culture volume in a typical outdoor pond. Photobioreactors (PBRs) can produce higher density cultures, but still < 1%. This highly dilute system presents the problem of needing to collect a very small fraction of the total volume for downstream processing. As expected, there are significant energy (and therefore cost) penalties for pumping such large volumes of water.

Therefore, our team aimed to develop methods for harvesting algae that reduce the energy penalty of this step, leading to significant reductions in costs and taking the industry closer to cost-competitive values for a gallon of algae-based oil. We hypothesized that the exploration of a portfolio of innovative methods would provide a path forward for cost-effective algae harvesting. Some methods employed off-the-shelf technology, while at least one method was largely conceptual at the start of the project. In each case, the team demonstrated that algae harvesting could be achieved with these technologies at costs that we projected to be significantly below the baseline case of traditional centrifugation.



HARVESTING AND EXTRACTION

Once the algae are harvested, the oil must be extracted from the cells. This process typically entails drying the algae, treating it with solvent, removing the aqueous fraction (lipid extracted algae, LEA), and distilling the solvent from the remaining oil. This crude oil is then sent for conversion to fuel. This method is energy intensive and wasteful.

There are a number of challenges associated with the lipid-extraction step in the algae biofuels value chain. First, in order for the solvent to effectively remove the oil, the algae must be very dry; drying is a costly and energy-intensive process. Simple air-drying may be incomplete and may result in spoilage of the algae, which may damage the quality of the products. Second, any cell debris (N or S content, for example) or solvent that carries through to the conversion process may affect the quality of the resulting fuel or coproducts.

Thus, an additional objective of this team was to explore effective and inexpensive extraction technologies. Again, a portfolio of innovative lipid extraction technologies was assessed, resulting in an improved understanding of the extraction requirements.

Approach

Our Harvesting and Extraction team comprised physicists, engineers, chemists, and biologists from national laboratories, universities, and industry who had strong track records of developing novel technologies. Our approach focused on minimizing the energy consumption of each technology while maximizing the yield of product (Figure 3.1).

Harvesting & Extraction Task Framework

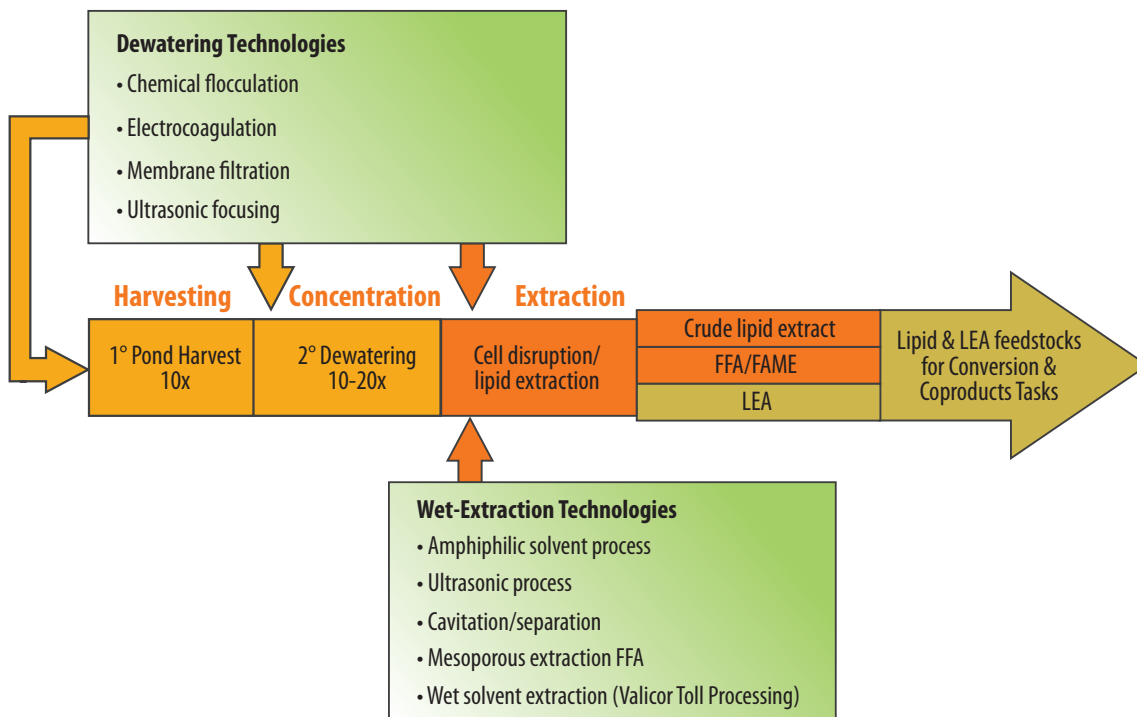


Figure 3.1. The NAABB Harvesting and Extraction task framework.



In this project, harvesting was defined broadly as a 10–20X dewatering/cell concentration process that may include one or more steps. Likewise, extraction was broadly defined to include cell disruption and recovery of lipids and lipid-extracted biomass from the dewatered, cell-concentrated feedstock in one or more steps.

The Harvesting and Extraction Team began the National Alliance for Advanced Biofuels and Bioproducts (NAABB) program effort evaluating five harvesting technologies and four extraction technologies. The initial goal was to develop proofs of concept and scale-up of the technologies leading to a down-selection process and then to move forward with technologies based on a feasibility study.

Multiple harvesting technologies were investigated to find the most energy-efficient, low-maintenance, environmentally friendly alternative. Engineering approaches that were investigated included the following:

- Ultrasonic focusing, in which a standing acoustic wave is applied in a flow-through system to gently aggregate algae cells and concentrate them out of the cultivation water;
- Electrocoagulation or electrolytic aggregation, which uses a commercial unit (used in wastewater treatment) to apply a charge to algae cells, forcing them to aggregate and sediment; and
- Cross -flow membrane filtration, using novel metallic membrane sheets with pore structures and surface properties engineered for algal harvesting.
- In addition, two flocculation approaches were investigated:
aluminum chloride and chitosan.

Multiple extraction techniques were considered based on their potential to eliminate the need for drying the algae and reduce or eliminate the need for solvents. These included:

- Ultrasound technologies, which use ultrasonic cavitation and streaming to lyse the algae cells and release the lipids;
- Mesoporous nanomaterials for selective sequestration of (high-value) free fatty acids (FFAs) in either aqueous media of viable algae cultures or in organic solvent solutions after oil extraction from the algae culture. Once sequestration of the FFAs in the pores of the material is complete, the algae oil can be processed for fuel conversion and the FFAs can be further processed for coproducts;
- Amphiphilic solvents used in a system designed to force algal biomass to move from hydrophilic water phase to a hydrophobic solvent phase and assisted by a pressurized homogenization technique to rupture the algal cells in the process.



Technical Accomplishments

Down-selection

The down-selection process was based on an evaluation of eight algae harvesting and extraction technologies developed and studied within the NAABB program during the first 18 months. Each project submitted a data set to the NAABB Sustainability Team for a formal evaluation, which focused on understanding energy balance, mass balance, operation costs, and parasitic energy losses of each technology as it was envisioned in a test pilot-scale system. The process evaluated a set of minimum criteria for the implementation and development of each harvesting and extraction technology for a 100 L/h culture or 1 L/h concentrate scaled process.

For the down-selection evaluation, each project submitted a process flow diagram (PFD) of its technology that provided information on:

1. All major process equipment, including process vessels and pumps;
2. All energy and mass-flow streams;
3. Comprehensive energy and mass-balance information for all streams leading into and out of the major process equipment;
4. A full account of the fate of chemicals, water, and other materials in the system; and
5. Energy input reported in kWh.

A set of standardized assumptions was developed and used to construct the values provided in each project PFD:

1. Algal water feeding to the harvester:
 - a. Feed rate of 100 L/h;
 - b. Algal content of 1 kg (dry weight)/1000 L algal water;
 - c. Lipid content of 0.5 kg lipid/kg dry weight algae;
2. Algal water feeding to the extractor (i.e., for systems not including a harvester):
 - a. Feed rate of 1 L/h concentrated algal water;
 - b. Algal content of 90 kg (dry weight)/1000 L of concentrated algal water; and
 - c. Lipid content in algae of 0.5 kg lipid/kg dry weight algae.

Based on the evaluation compared to the centrifuge, three of the harvesting technologies showed superior performance on the criteria: electrolytic, membrane filtration, and ultrasonic harvesting. The results for this evaluation are shown on Table 3.1.



Table 3.1. Baseline feasibility assessment of harvesting-extraction technologies.

Technology	Energy Input (kWh/kg)	Chemical Cost (USD/Kg)	Electricity Cost (USD/kg)	OPEX (USD/Kg)	OPEX (USD/Gal)	PEL
BASELINE HARVESTING TECHNOLOGIES						
Centrifuge Baseline	3.300	0.000	0.264	0.264	1.799	56.978
Dissolved Air Floatation	0.250	0.008	0.020	0.028	0.191	4.317
Spiral Plate Separation	1.418	0.000	0.113	0.113	0.773	24.475
NAABB Harvesting Technologies						
Chitosan Flocculation	0.005	0.055	0.000	0.055	0.377	0.093
AlCl ₃ Flocculation	0.120	0.046	0.010	0.056	0.380	2.072
Electrolytic Harvesting	0.039	0.004	0.003	0.007	0.049	0.673
Membrane Filtration	0.046	0.000	0.004	0.004	0.025	0.789
Ultrasonic Harvesting	0.078	0.000	0.006	0.006	0.043	1.347
BASELINE EXTRACTION TECHNOLOGIES						
Pulsed Electric Field	11.520	0.000	0.922	0.922	6.280	198.906
Wet Hexane Extraction	0.110	0.001	0.009	0.010	0.068	1.904
NAABB Extraction Technologies						
Solvent Phase Algal Migration	1.548	0.947	0.132	1.079	7.352	28.446
Ultrasonic Extraction	0.384	0.000	0.031	0.031	0.209	6.630
Nanoparticle Mesoporous	0.008	54.355	0.001	54.356	370.363	0.137
Supercritical	1.174	0.000	0.094	0.094	0.640	20.271

Consequently, these three harvesting technologies were selected for scale-up. The mesoporous nanomaterials sequestration method was also selected for continuation because of the unique contribution of this method to the total economic feasibility of algae biofuels production for high-value product extraction.

The selected technologies were considered to present the best chance for NAABB to make significant impacts in the field and were supported by a vision and state of technology representing a high reduction in operating cost (OPEX) and minimized parasitic energy loss (PEL) when compared to the baseline technologies. In addition, an industry partner (Valicor) using a wet solvent extraction process was added to the extraction task for toll processing of lipids and LEA to consortium members.

Harvesting Field Tests

The three selected harvesting technologies successfully underwent field tests with a target of 100–1000 L/h processing during the third year of the NAABB program. The field tests served to:

- Demonstrate the feasibility of the technology at the target scale;
- Identify technical gaps needing further research and development, particularly with efficient operation of the scaled-up devices; and
- Introduce potentially game-changing harvesting technologies to industry.



HARVESTING AND EXTRACTION

Electrolytic Methods

There are three established electrolytic methods: electrocoagulation, electroflotation, and electroflocculation. Electrically driven methods of harvesting are attractive because they are energy efficient, safe, and cost effective. Electrocoagulation uses reactive metallic electrodes to produce positively charged ions that induce coagulation of the negatively charged microalgae cells. This results in the algae cells being removed from the solution through settling. As more electricity flows through the solution, more metal is dissolved to form ions. Aragon *et al.*⁴ previously examined this method and determined that it was superior to chemical flocculation because of lower cost, a shorter time needed for separation, and a lower probability that the microalgae would be contaminated with metallic hydroxides. Low current strengths were needed to achieve effective coagulation. A direct relationship was determined between the power input and the microalgae removal rate.

Electroflotation uses an inactive metal cathode and a reactive metal anode to create hydrogen bubbles from the electrolysis of water as well as releasing a metal ion from the anode. The ion attracts the negatively charged algae to create flocs and the hydrogen bubbles cling to the flocs, which are then carried to the surface where they can be removed by conventional skimming methods. Alfara *et al.*⁵ conducted a study on removing microalgae using this method where it was determined that increasing the electrical power increased the rate of removal and decreased the time required to remove the algae from solution.

Electroflocculation utilizes an inert anode and cathode and moves negatively charged algal cells to the positively charged anode. Once the cells reach the anode, the negative charge is dropped from the microalgae and the microalgae form flocs without any metal ions. Poelman *et al.*⁶ conducted a study on electrolytic flocculation of microalgae where it was determined that 80–95% of the microalgae solution could be removed from a 100 L vessel in 35 minutes.

Each of these methods has the potential for scale-up. Electrocoagulation is already commercially available in the wastewater treatment industry. Preliminary testing did not demonstrate any advantage of electroflotation over electrocoagulation: both flocs contained metal ions and the sediment from electrocoagulation was more easily recovered and was more concentrated. Thus electroflotation was not evaluated in further studies for this project. Electroflocculation utilizes the same equipment as electrocoagulation with only a change in electrode material. Prior research has demonstrated that the processes are effective when used to harvest or dewater microalgae.

In the laboratory, each electrolytic test was performed in a 400 mL glass beaker serving as the lab-scaled electrolysis unit as shown in Figure 3.2. A commercial bench-scale power supply provided a direct current charge to the electrodes at a measured voltage and current.

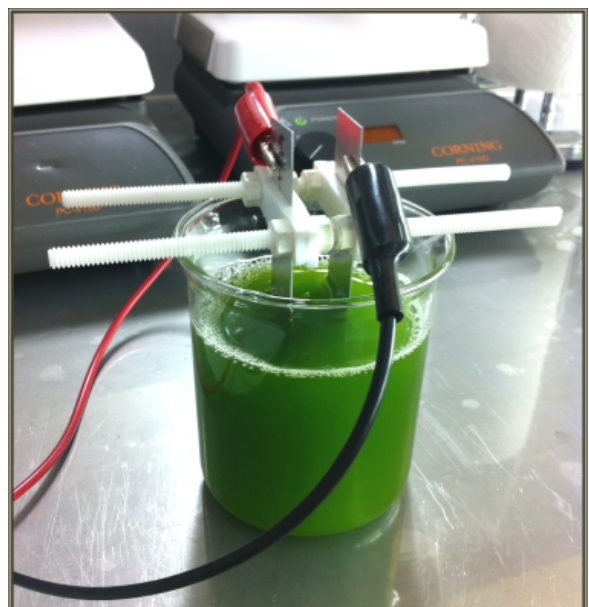


Figure 3.2. Lab-scale (300 mL) electrolysis unit.



The team conducted field tests of their electrocoagulation approach using a commercial electrocoagulation unit loaned from Kaselco (Figure 3.3). The field tests were conducted at the Texas AgriLife Research, Pecos, Texas, facility in the summer of 2011 and 2012. The average percent of solids and biomass of the solution was calculated and is shown in Table 3.2.

A complete harvest of an algal batch was conducted to demonstrate the feasibility of operating the Kaselco electrocoagulation system at pilot scale and over an extended period. The reactor was operated at 15 gpm and 4550 gal were treated with electrocoagulation using stainless steel electrodes. Following overnight settling in a cone-bottom tank, the sediment was separated into two parts and further dewatered using a disc and bowl centrifuge. The centrifuge site glass was used to mark the change between the bottom greenish layer and the lighter, brownish layer. The data are shown in Table 3.3.

The final solids concentration was 8%; the energy consumption was 0.04 kW/m³, and the volumetric loading rate was 270 m³/kg h using *Nannochloropsis salina*. Based on these results and the availability of a commercial unit for calculating the capital (CAPEX) and OPEX costs, the Sustainability Team selected the electrocoagulation approach for their techno-economic forecast analysis.



Figure 3.3. Kaselco reactor testbed.

Table 3.2. Solids concentration and percent biomass after electrocoagulation.

Test	Reactor	Electrode	Average % Solids in the Sediment	% Biomass in the Solids
1	11	SS	2.8%	15.6%
2	11	Al	2.9%	19.9%
3	07/11	SS/Al	3.0%	20.4%
4	11	Al	2.4%	20.1%
5	7	SS	2.2%	18.2%
6	07/11	SS/Al	1.9%	26.0%

Table 3.3. Data from combined electrocoagulation and centrifuge harvest of a 4550 gal batch of *N. salina*.

Process Step	Power Consumed (kWh)	Process Time (h)	Volume Processed (L)	% Ash in the Solids
Primary Dewatering: Electrocoagulation	59	5	17 224	83.8%
Secondary Dewatering: Centrifuge	62	4.2	3785	65.7%
TOTAL	121	9.2	17 244	65.7%



HARVESTING AND EXTRACTION

Depending on the lipid-extraction method to be used, electrocoagulation may serve as a primary dewatering step with a secondary step needed to reach the final desired moisture content. Electrocoagulation allows the majority of the water to be removed (99.97%) prior to secondary dewatering. This greatly reduces the volume that must be processed in the secondary phase and consequently reduces the costs by a large margin. In the example above, if the entire 17,244 L were processed with the centrifuge approximately 282 kWh would be consumed.

Both electrolytic treatments offer robust and economical solutions to harvesting. The electrolytic methods tested in this research had significant operating cost advantages over standard centrifuge technology. The best treatment combinations from the screening experiments are shown in Table 3.4.

Electrocoagulation and electroflocculation offer energy-saving solutions equal to less than 15% of centrifuge requirements. Reduced harvesting costs could reduce the total processing costs from 40% to 3%. The energy savings implied in the findings of this work suggest direct electricity savings and progress towards a renewable energy future.

Table 3.4. Summary of proposed technology compared to centrifuge.

Process	Factor	% Recovery	Current (A)	Power (kWh)	kWh t ⁻¹	% of Centrifuge Energy
Electrocoagulation	Steel	97.2	0.100	0.00004	374	4
	Ni	97.5	0.075	0.00004	344	3
	Al	94.4	0.100	0.00003	239	2
Electroflocculation	Low OD	97.7	0.100	0.00004	432	4
	High OD	95.1	0.150	0.00011	670	6

Membrane Technology

Membrane microfiltration and ultrafiltration are widely used in today's industries, such as wastewater treatment (at the low-value end) and protein concentration (at the high-value end). Reverse osmosis membranes are used for seawater desalination at very large scales. Polymeric membranes are dominant membrane products for these applications, while ceramic and metal membranes only account for a small fraction of the market. Although there are so many industrial membrane processes, application of membranes to algae harvesting and dewatering is new.

No commercial membrane algae harvesting process has been reported. Research and development of membrane technology is needed to address the barriers and/or challenges for practical application to algae harvesting. The first challenge is to significantly enhance filtration flux. Since the algae content in the culture solution is so low, the membrane has to be highly permeable to water. For a given culture production rate, the membrane area required decreases proportionally with increasing flux. The literature review and



preliminary process analysis show that a very large membrane surface area and footprint would be needed for a commercial-scale algae cultivation system, if the algae filtration flux is similar to that currently achieved for wastewater treatment, which may become cost-prohibitive. Another major challenge is membrane stability. Membrane fouling, particularly biological fouling, is a big problem in current wastewater treatment processes. Algae cultures are very rich in biologically active species and hydrocarbon nutrients. Chemical and biofouling of membrane harvesting processes are a serious concern of which little is known.

Polymeric membranes used for wastewater treatment are natural candidates for algae filtration applications. However, fouling has been reported to be a major issue.⁷ Micro- and ultrafiltration flat sheet membranes made of fluoro-polymeric materials were compared for filtration of *Chlorella pyrenoidosa* FACHB-9 algae cells, and no significant difference was shown.⁸ A recent study suggests that algogenic organic matter in *Chlorella zofingiensis* algae culture tends to rapidly plug the pores of hollow-fiber polyvinylchloride (PVC) ultrafiltration membrane (50 kDa MWCO).⁹

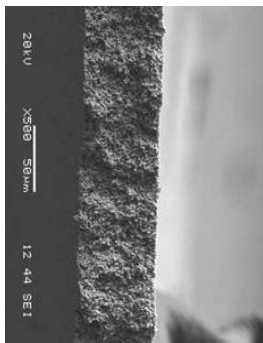
Ceramic and metallic inorganic membranes are viewed as having better biofouling resistance and higher water flux and have received a considerable amount of research interest for the past two decades. However, their widespread application has not happened yet, compared to the large polymeric membrane industry. The high cost per unit of surface area and low surface-area packing are commonly viewed as the main drawbacks. In sharp contrast to fruitful exploration of new membrane materials and/or new applications, research publications on development of new membrane products have been very limited. Recently, developments of ceramic monolithic membrane modules of small channel sizes (~ 1 mm)¹⁰⁻¹¹ and capillary inorganic membrane tubes¹² have been reported. These product concepts show promising progress toward getting the surface area packing density of inorganic membranes close to polymeric hollow-fiber membranes.

The major effort of this work focused on development of novel thin flat-metal-sheet membranes. Our approach was to make porous metal-sheet membranes fabricated with a surface area packing density equal or comparable to flat-sheet polymeric membranes. For this type of membrane product design, manufacturing and engineering capabilities developed in the polymeric-membrane field may be utilized. A variety of metals are made as foams or screen products commercially,¹³ which include aluminum, copper, zinc, nickel, silicon, Inconel, silver, and gold. These structures typically have pore sizes from tens to hundreds of micrometers, which are too large to be effective for microalgae filtration. In addition, the metal foam is mechanically too weak to be used as thin sheets (< 300 μm). Therefore, we considered the desirable properties of a metallic microfiltration membrane sheet to be (1) light, highly permeable, mechanically strong, and flexible; (2) chemically stable—resistant to solvent attack; and (3) thermally stable, enabling membrane processing and/or separation operation at elevated temperatures.

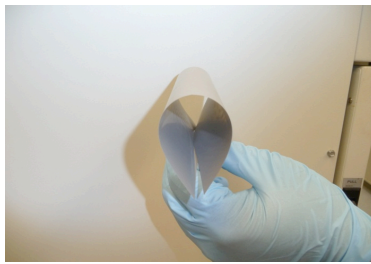


HARVESTING AND EXTRACTION

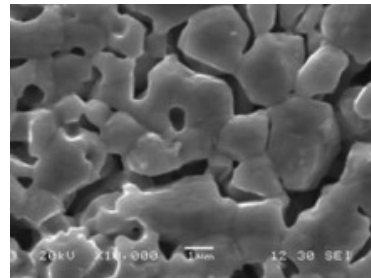
Research and development of membrane harvesting for algae can be approached from different angles, such as obtaining current membrane products and evaluating their performances for algae filtration, modifying current filtration module and/or process designs, and innovation of new membrane and process ideas. We believed that the current membrane producers were better positioned than we were to evaluate their products for new applications. In this project, we focused on innovations of new membrane materials and products. While commercial membrane materials were evaluated briefly to fill the knowledge gap, our research efforts were devoted to development of novel ceramic-modified thin ($\sim 50\ \mu\text{m}$ thick) porous metal sheet membranes (Figure 3.4) for microalgae harvesting applications. The thin metal sheet of uniform pore structures at submicrometer level throughout the thickness is adequately strong and flexible to be self-supported and molded. The pore size and surface chemistry of this metal sheet can be modified by coating with ceramic particles.



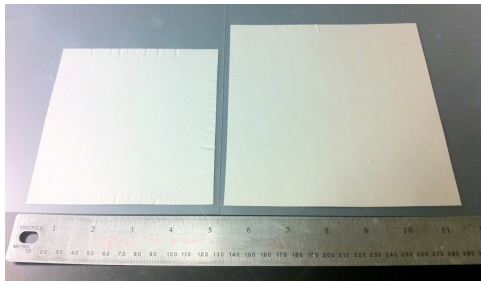
(a) Wall texture



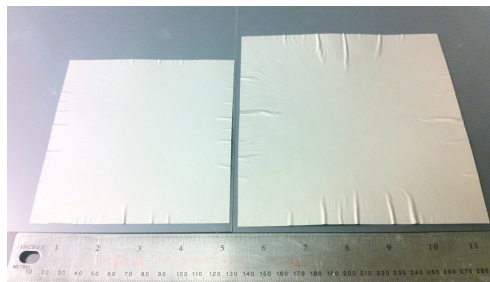
(b) Flexibility of 50 μm sheet



(c) Surface texture



(d) Flat and smooth sheets



(e) Sheets with wrinkles and/or defects

Figure 3.4. 50 μm -thick porous Ni membrane sheets prepared and used in this work.

For the scaled-up membrane filtration field test, we developed a thin porous Ni alloy metal sheet membrane (Figure 3.4d). A cross-flow membrane module (Figure 3.5) was assembled from 18 12 cm x 12 cm membrane sheets on a mobile unit that was tested at the Texas AgriLife Research, Pecos, Texas, facility during the winter of 2012 and early 2013 using *N. salina*. NAABB also worked with Pall, Inc., to test one of their commercial hollow-fiber unit membranes as a baseline, commercially available technology.

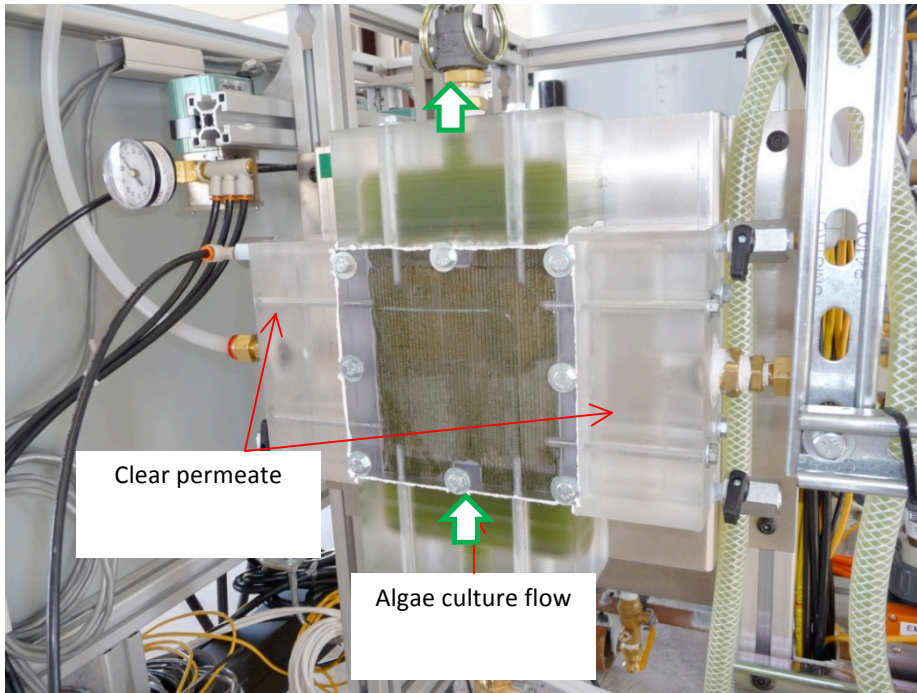


Figure 3.5. Cross-flow-membrane modules assembled for field tests (0.26 m² of membrane area, 1 mm feed flow channel opening).

Figure 3.6 shows variations of operation parameters with time in one representative batch filtration run. The algae from a storage tank was pumped through the membrane module and returned to the tank, while a clear solution was withdrawn from the permeate side of the membrane module under vacuum. The permeate flow direction was perpendicular to the feed flow. Since the liquid velocity inside the feed channel in these runs was fairly low (0.27 m/s) relative to typical cross-flow filtration operation, the liquid feed was aerated by introduction of air pulses to mitigate accumulation of filtration cake layers on the membrane surface. As a result, the module inlet pressure fluctuated over a wide range, while the outlet pressure stayed near atmospheric pressure. The permeate flow fluctuated accordingly. The flux of the present module was about 2 to 3 times of the flux obtained with a commercial PVA membrane plate, which was designed as a bioreactor membrane for wastewater treatment application. However, the flux gradually declined with time. The post examination of the membrane sheet showed no or little deposition of the algae species on the Ni alloy membrane surface as expected, and the membrane pores were intact. The gradual decline of the flux with time was likely due to adsorption of soluble polymers in the culture inside the membrane pores. As a result, the membrane module was cleaned every day during the field tests. A few common chemical cleaning agents were evaluated and found no more effective than physical cleaning by back-flushing. More effective membrane cleaning methods need to be developed for long-time operation.



HARVESTING AND EXTRACTION

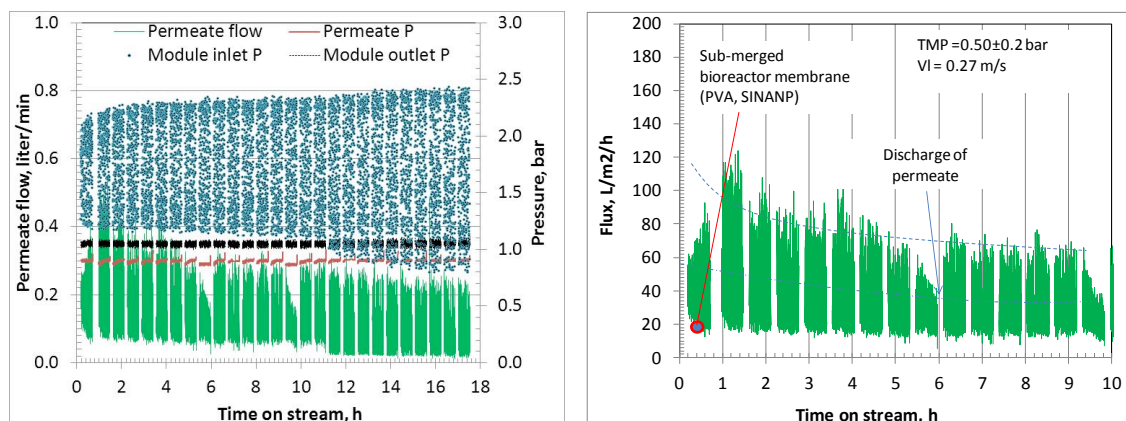


Figure 3.6. Testing results of porous Ni sheet membrane module (Pecos, Texas, January 2013, *Chlorella* sp. DOE1412)

The energy consumption and cost of the membrane technology projected for the commercial scale operation are listed in Table 3.5. We noted that the energy consumption predominantly resulted from the generation of a pressure gradient across the membrane, mainly due to the membrane properties. For a given pressure gradient, the harvesting cost would proportionally decrease with increasing membrane permeability. The energy consumption and cost for dewatering the concentrated sludge was insignificant relative to the cross-flow filtration cost. Thus, concentration of the algae culture should be the main focus for significant reduction to the energy consumption and cost. Overall, the membrane process is an efficient means of harvesting with energy consumption comprising only a small percentage of the algae fuel value. The numbers in Table 3.5 were calculated based on an algae content of 0.04 wt% in the culture. The energy consumption and cost will be reduced proportionally if the algae content in the culture is increased.

Table 3.5. Energy consumption and cost projected at commercial scale (7000 m³/h of culture processing capacity; 0.04 wt% microalgae in the culture solution; TMP= 0.9 bar.

	Cross-flow filtration		Dewatering		
Concentration factor	100	100	6	6	6
Concentrated algae, solid wt%	4.0%	4.0%	24.0%	24.0%	24.0%
Membrane permeability, L/m ² /h/bar	200	400	20	40	80
Electricity consumption ^a , kWh/kg(product) ^b	0.103	0.103	0.001	0.001	0.001
Energy consumption, % of algae fuel value ^c	4.94%	4.94%	0.042%	0.042%	0.042%
Membrane area required, m ²	43,313	21,656	3,646	1,823	911
Membrane cost ^d , \$/t (product)*	\$48.34	\$24.17	\$4.07	\$2.03	\$1.02
Electricity cost ^e , \$/t (product)*	\$10.32	\$10.32	\$0.09	\$0.09	\$0.09
Total cost, \$/t	\$58.66	\$34.49	\$4.16	\$2.12	\$1.11

^aAssume electrical efficiency of pumps is 60%.

^bProduct is based on net algae weight.

^cAssume factor of 3.32 for conversion between the electrical and thermal energy. Assume the algae thermal energy content of 25 MJ/kg.

^dAssume membrane operation time of 16,000 h (two years) and membrane cost of \$50/m².

^eAssume electricity cost of \$0.1/kWh.



In summary, the thin porous Ni sheet membrane showed 100% higher flux (or permeance) than common polymeric (PES, PVA) microfiltration and ultrafiltration membrane products under comparable conditions. The scale-up feasibility of the new membrane sheet from the laboratory bench test unit to a cross-flow membrane module for field tests was shown. A customized, mobile membrane-testing skid was built to conduct further field tests in the future. The feasibility to achieve a 44 to 66 times concentration factor for *Chlorella* sp. DOE1412 was shown through field tests at the Pecos, Texas, facility.

Ultrasonic Technology

We developed the use of ultrasonic fields to harvest¹⁴ and disrupt algae cells¹⁵ to extract lipids and proteins from algae and recover the water. The approach uses ultrasonic-focusing technology and minimal electrical energy to concentrate the algal cells and to fractionate the cells for separation into lipids and proteins. The lipids, or oils, can be refined into biofuel, the proteins used for animal feedstock or other valuable coproduct, and the water recycled. Our vision is to conduct all three operations in one integrated system and reduce the overall costs of harvesting and extraction by several orders of magnitude. The system would be portable and used at the site of algae cultivation to reduce transportation costs.

The use of ultrasonic fields to harvest and extract lipids from algae has several advantages over conventional methods. No chemicals are used to concentrate the algae; therefore, there are no downstream effects on the conversion products or coproducts. The ultrasonic process is a “wet” extraction process, and no drying is needed before cell lysis and lipid extraction. No solvents are used for extraction, therefore eliminating hazardous chemicals and the need to remove them from the downstream processes. Using ultrasound to concentrate cells and to extract and separate lipids from algae allows the water to be recycled and reused at each step. The products of each step are pure, and the process is environmentally benign. Furthermore, the ultrasonic process is expected to be more cost effective than conventional methods.

In the first year of this project, we conducted laboratory-scale experiments to investigate the feasibility of using ultrasonic fields to concentrate and disrupt the algae cells and to separate the lipids from the rest of the biomaterials and water. Different ultrasonic treatment regimes were used: a high-frequency regime to harvest the algae (Figure 3.7) and a low-frequency regime to disrupt the algae cells by cavitation and streaming. A high-frequency regime similar to the harvesting treatment was also used to separate algae oil from water.



Figure 3.7. Concentration lines of N. salina form upon application of power in a laboratory-scale, 5 mL volume ultrasonic harvester. Algae concentrate at nodes of the standing wave and settle spontaneously to the bottom of the harvester where they are available for further processing.



HARVESTING AND EXTRACTION

The properties of the algae, lipids, and proteins were measured after treatment with acoustic fields. Conditions for operation and optimal performance were determined. In Year 2 we continued to gather performance data on the effect of ultrasonic fields on harvesting, cell disruption, and oil separation. These data were used in an economic analysis to establish the efficiency of the ultrasonic technology at the liter scale. After 18 months, a techno-economic analysis of harvesting and extraction technologies was performed and the ultrasonic harvesting process was selected for scale-up to pilot scale. Figure 3.8 shows the PFD of the ultrasonic harvesting process; Table 3.6 shows the corresponding mass and energy balance information for two species of algae. The electrical costs shown in Table 3.6 (based on laboratory-scale studies) are equivalent to 4.3 ¢/gal and 1.1 ¢/gal of lipid for *N. salina* and *Auxenochlorella protothecoides*, respectively. These electrical costs compare to 62–200 ¢/gal of lipid when centrifugation is used at the same feed rate.

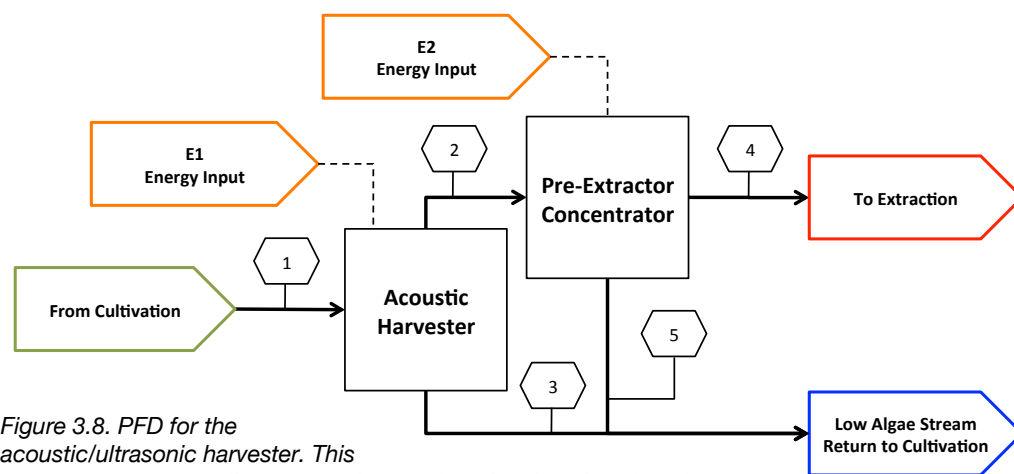


Figure 3.8. PFD for the acoustic/ultrasonic harvester. This two-stage process collects more than 75% of the algae in 1% of the water volume. See summary mass and energy balance information for two species of algae in Table 3.6.

Table 3.6. Mass and energy balance for the ultrasonic harvester process. Flow stream locations 1 through 5 are shown in Figure 3.8. Results are based on laboratory-scale experiments with *N. salina* and *A. protothecoides*. The electrical costs are equivalent to 4.3 ¢/gal and 1.1 ¢/gal of lipid for *N. salina* and *A. protothecoides*, respectively. These electrical costs compare to 62–200 ¢/gallon of lipid when centrifugation is used at the same feed rate.

Flow Stream		1	2	3	4	5
Description	Units					
Total Flow	L/hr	100	10	90	1	9
Water	kg/hr	99.91	9.93	89.98	0.93	8.998
Biomass[§]	kg/hr	0.1	0.0784	0.0216	0.07624	0.00216
Lipid	kg/hr	0.05	0.0392	0.0108	0.03812	0.00108
Electrical Energy Stream		E1		E2		Total Electrical Usage^{§§} (kW)
Algal Species	Units^{§§}					
<i>N. salina</i>	kW	5.41E-03		5.41E-04		
<i>C. protothecoides</i>	kW	1.43E-03		1.43E-04		1.57E-03



In Year 3, we built a pilot-scale harvester and tested it in a field study. The scaled-up ultrasonic harvester unit operated at 45–225 L/hr using 9 modules (Figure 3.9a). The scaled-up device was assembled in a shed outside a laboratory area in Los Alamos, New Mexico, and tested in > 65 experiments during September 2012 using 250 gallons of *Nannochloropsis oculata* feedstock provided by Solix Biosystems from their Coyote Gulch facility. Up to 18X concentration of algae was seen and we routinely observed visual confirmation of algae concentration above the feedstock concentration (Figure 3.9b)



Figure 3.9a. Side view of two scaled modules attached to a customized cart containing 12 modules. Feed into both sides of the distributor tube can be seen on the module on the right. There is a tray between the modules that collects processed (dilute) algal water from the rear of the modules and the concentrate is removed and collected from the bottoms of the modules.



Figure 3.9b. Visual comparison of the dilute feedstock (left tube) and concentrated product (right tube).



HARVESTING AND EXTRACTION

Energy-density measurements showed that the scaled-up harvester module delivered energy to the liquid layer 100-fold more effectively than the laboratory-scale unit. However, over a several-hour trial, we found that there was considerable variability in the harvester performance (Figure 3.10). The removal rates were always higher than the no-power rates, attesting to the effectiveness of the ultrasonic harvester. However, the removal rates measured in the flow experiments quickly dropped to lower than the short-time (1 min) removal rates that were routinely measured in no-flow experiments. Future development of the ultrasonic harvester will focus on improvement in process control to achieve consistent high performance.

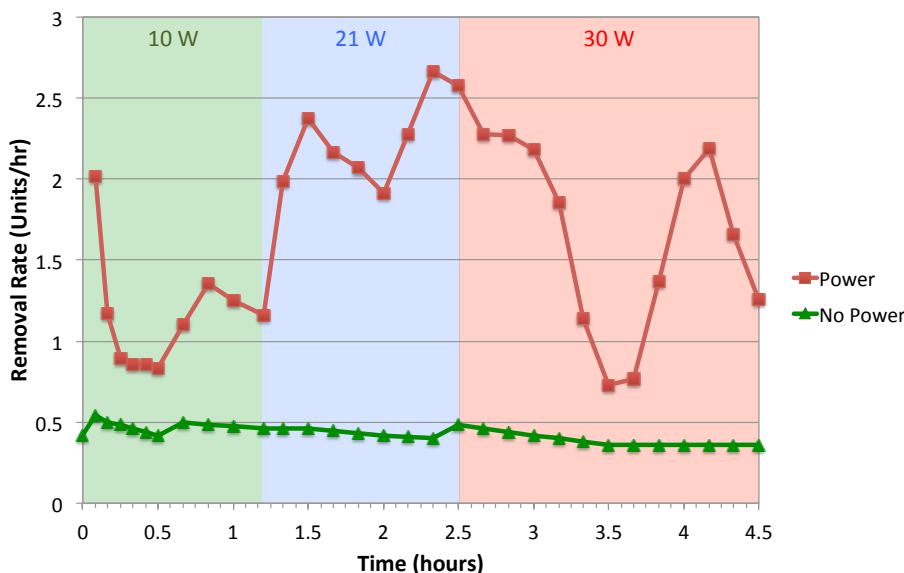


Figure 3.10. Algae (*N. oculata*) removal rates measured in the field at a feed rate of 5 L/h in a scaled-up ultrasonic harvester module. One unit is equivalent to 1.75 g of biomass, which was contained in 1 L of feed. The “no power” values represent the removal rates that were obtained without any concentration effect from the harvester. These values drifted from 0.5 units/h as the product stream flow rate was varied. The “power” values represent the average removal rate measured over a 5- or 10-minute period. Removal rates are shown over time periods where the true power input was periodically increased, as indicated with the different colored regions.

Selective Sequestration of High-value Biomolecules by Mesoporous Nanoparticle Material

Acquiring all possible value out of microalgal oil is imperative to make it an economically viable feedstock for biofuel. Current technologies utilize food-based oils as the feedstock for base catalyzed conversion of triacylglycerides (TAGs) to fatty acid methyl esters (FAMES, or biodiesel). These feedstocks are ideal because they contain >99% TAGs. However, microalgal oil contains a greater variety of lipid and hydrocarbon molecules, some of which are considered high-value or value-added. As such, these biomolecules would contribute to the economics of the microalgal biofuel production if they could be separated from fuel precursors and distributed to the optimal industry (i.e., the industry that gives the naturally produced molecule of interest the greatest value). Current separation and purification techniques for naturally produced lipids, hydrocarbons, and organic acids are challenging and energy-intensive, with extraction and distillation the most common techniques, using organic solvents or supercritical fluids. We developed a high-surface-area, porous-silica-based nanoparticle material for the selective sequestration and removal of these high-value and value-added molecules from microalgal oil. Utilizing our strong synthetic background along with the ability to control the functionalization of these materials, we synthesized and characterized a series of nanomaterials that independently target free fatty



acids (FFAs), polyunsaturated free fatty acids (PUFAs), tocopherol (vitamin E), and microalgal cells from growth media as a magnetic dewatering technology illustrated in Figure 3.11. We identified that pores with an average diameter of 10 nm were optimal to capture FFAs when compared to nanomaterials with smaller pore sizes. Decorating the pore surface with primary amine functional groups selectively targeted FFAs, restricting other molecules normally found in microalgal oil from entering the pores and adsorbing to these porous nanomaterials. By rinsing these nanomaterials with organic

solvents we were able to desorb the FFAs, leaving a solution of highly pure, naturally produced FFAs. Following this discovery, we analyzed the purified FFAs to determine if targeting and removing the high-value FFAs (Omega-3/-6) is possible by adjusting some of the properties of the sequestration materials. Through extensive experimentation, we determined that smaller pore sizes capture PUFAs selectively while limiting the diffusion of saturated and monounsaturated FFAs into the pores. We attribute this to the folding of these organic acids in the microalgal oil. Because all double bonds in naturally produced fatty acids are *cis*, PUFAs will fold into tighter arrangements making the size of Omega-3/-6 the smallest among the different saturations.

Tocopherol is naturally produced by many microalgae strains in concentrations up to 5 wt% lipids. Naturally synthesized tocopherol has considerable advantages over industrially synthesized including higher nutritional value and improved environmental means. By functionalizing the pore surface with a unique organic moiety that reacts noncovalently with functionality on the tocopherol molecules we were able to synthesize and characterize a sequestration nanomaterial that selectively targeted vitamin E. We demonstrated that over 70% of the tocopherol in a simulated microalgal oil solution could be captured and removed while only capturing 15% of the FFAs and 4% terpenes in the same solution. An advancement that we made in this technology was to add magnetic functionality to these materials. This allowed us to separate the sequestration nanomaterials, after the tocopherol molecules were captured, from the microalgal oil by simply utilizing a magnet. We demonstrated, for the first time, that separation of these magnetic, high-surface-area porous nanomaterials can be made possible by including magnetic functionality in the synthesis.

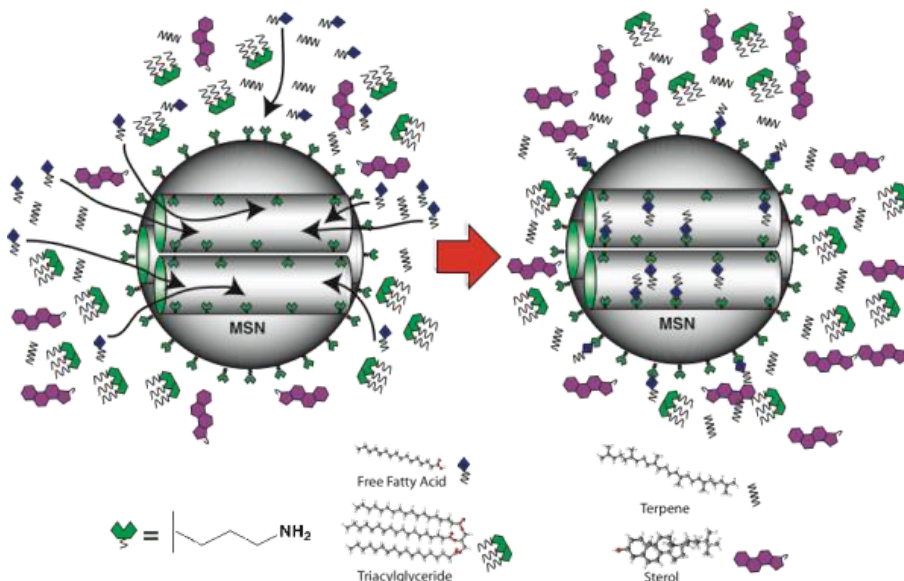


Figure 3.11. Schematic illustrating the selective uptake and sequestration of the FFAs from a solution of lipids and hydrocarbons found in algal oil.



HARVESTING AND EXTRACTION

Table 3.7. Adsorption values (mmol g^{-1}) from simulated microalgal oil for MSN-10 and AP-MSN-10.

	MSN-10 (mmol g^{-1})	MSN-10% Sequestered	AP-MSN-10 (mmol^{-1})	AP-MSN-10% Sequestered
Palmitic Acid	0.0228	100	0.0228	100
Glyceryl tristearate	0.150	93.8	0.012	7.5
Ergosterol	0.0228	100	0.0039	17.1
Squalene	0.0082	17.9	0.0048	10.5

These nanotechnologies not only offer a new method to target and remove molecules of interest from the alphabet soup of molecules that are produced by microalgae, but will likely open the minds of researchers towards other applications for these materials. The relative ease and speed with which these materials can be specifically functionalized along with their biocompatibility and nontoxic nature make them ideal platforms for exploration in biorefinery and biofuel applications.

Wet Algal-biomass Lipid Extraction and LEA Fractionation

Valicor (formerly Solution Recovery Services, or SRS) is a world leader in the recovery and separation of products from industrial process fluids. Valicor formed a wholly owned spin-off, Valicor Renewables, which developed AlgaFrac™, a patent-pending process as a result of five years of R & D.^{16,17} This separation and fractionation technology is capable of recovering and purifying three basic algal biomass fractions suitable for downstream processing to value-added fuels and bioproducts. The three target fractions are a lipid fraction containing glycerides (for downstream fuels and lipid nutraceuticals), a solid residual biomass fraction with proteins (feed and food applications), and an aqueous fraction (soluble sugars and recyclable nutrients).

Whereas more traditional processes require algal cell drying and cell lysis, Valicor Renewables' AlgaFrac™ process is a wet extraction platform. Input algae biomass of 10–20% solids content can be rapidly processed into lipids, residual biomass, and aqueous streams (Figure 3.12). Valicor Renewables' wet extraction platform is cost- and energy-effective, recovering over 80% of the net available energy.

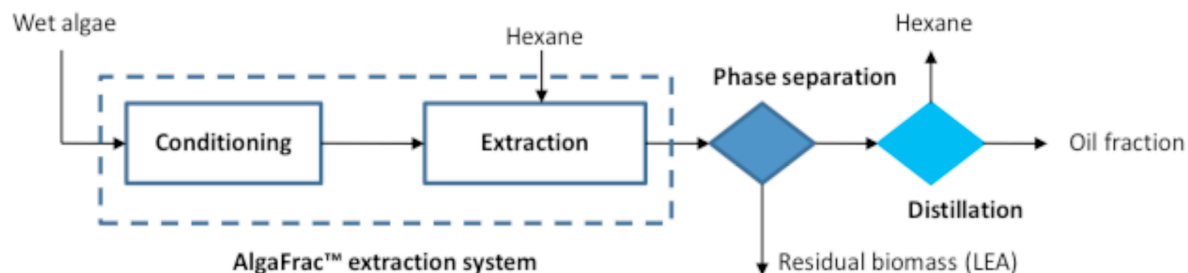


Figure 3.12. Schematic of Valicor's AlgaFrac™ process.



As part of its overall scope, the NAABB project needed extraction services for processing algal biomass to produce lipids and LEA fractions as feedstock for the Conversion and Coproducts tasks. Valicor’s goal was to provide toll processing of wet algal-biomass extraction to satisfy this need. To this end, Valicor conducted a series of bench-scale extraction tests to optimize oil yields for various algae strains and harvests. Findings from bench-scale fractionation were used to define optimal conditions for toll processing of large quantities of algae. Valicor processed NAABB-generated algal biomass in its pilot plant to produce requisite quantities of oil and LEA fractions. Valicor also dried the LEA when necessary in its pilot plant for distribution to NAABB team members. The oil and LEA fractions were supplied to downstream partners for their tasks.

The species processed were *Nannochloropsis* sp., *N. salina*, *N. oculata*, *Desmid* sp., and *Chlorella* sp. These alga strains were extracted at the bench and pilot scale. Figure 3.13 shows oil extracted with the Valicor Renewables process, and Figure 3.14 illustrates a typical analysis of oil samples.



Figure 3.13. Oil extracted with Valicor Renewables process.

		Report: NAABB-Pilot plant extraction	
Sample source	NAABB		
Strain type	Unknown		
Lab No	L2012-2-03		
Oil Compounds			
Compounds by Class	MAG, monoacylglycerides (w/w % AFDW)	1.2	
	DAG, diacylglycerides (w/w % AFDW)	1.9	
	TAG, triacylglycerides (w/w % AFDW)	4.6	
	Free Fatty Acids, Total (w/w % AFDW)	3.7	
	Total Fatty Acids (w/w % AFDW)	11.4	
	Chlorophyll a&b (w/w % AFDW)	0.12	
	carotenoids (w/w % AFDW)	0.09	
	Unidentified material (w/w % AFDW)	5.1	
	Total crude oil yield (w/w% of AFDW)	16.7	
	Fatty Acid Profile		
Fatty Acid Methyl Esters (FAME)		% OF FATTY ACIDS IN THE OIL (w/w %)	% OF TOTAL FATTY ACIDS (w/w %)
	C14:0 Myristic	0.6	0.8
	C14:1 Myristoleic	0.1	0.1
	C16:0 Palmitic	24.8	34.8
	C16:1n7 Palmitoleic	3.4	4.8
	C16:2 hexadecadienoic	6.9	9.7
	C18:0 Stearic	0.9	1.3
	C18:1-cis Methyl Oleate	4.3	6.1
	C18:1-trans Methyl Vaccenate	0.0	0.0
	C18:2 Linoleic	10.7	15.0
	C18:3 Linolenic	17.3	24.2
	C20:0 Arachidic	0.1	0.1
	C20:1 Eicosenoic	0.3	0.4
	C20:2n6 Eicosadienoic	0.1	0.2
	C20:3n6 Homogamma Linolenic	0.0	0.0
	C20:4n6 Arachidonic	0.4	0.5
	C20:3n3 Eicosatrienoic	0.0	0.0
	C20:4n3 Eicosatetraenoic	0.0	0.0
	C20:5n3 Eicosapentaenoic	0.4	0.5
	C22:0 Behenic	0.0	0.1
	C21:5n3 Heneicosapentaenoic	0.0	0.0
	C24 Lignoceric	0.0	0.1
	C24:1 Nervonic	0.0	0.1
	C22:4n6 Docosatetraenoic	0.0	0.0
	C22:5n6 Docosapentaenoic	0.0	0.0
	Other	0.9	1.3
	Total FAME (%) in oil	71.4	100.0

Figure 3.14. Typical analysis of oil samples.



HARVESTING AND EXTRACTION

Good mass balance closure and consistent oil yields were obtained, thereby indicating robustness of the Valicor Renewables process. Two examples of typical mass balance results are shown in Figure 3.15 and 3.16.

AlgaFrac™ was successfully applied to various NAABB algae species. Large quantities of oil and LEA—both dry LEA with dissolved sugars, etc. and dry LEA after dewatering—were provided to NAABB team members. The AlgaFrac™ process is scalable and the quality of the products is high.

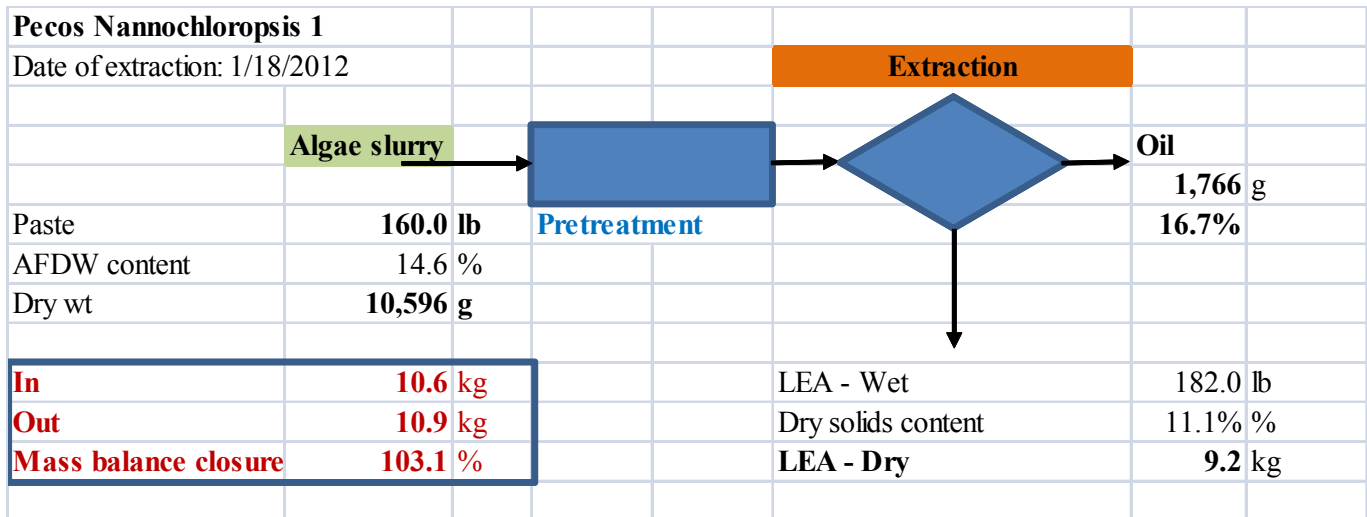


Figure 3.15. Example mass balance of extraction process using *Nannochloropsis* sp. obtained from Pecos, Texas.

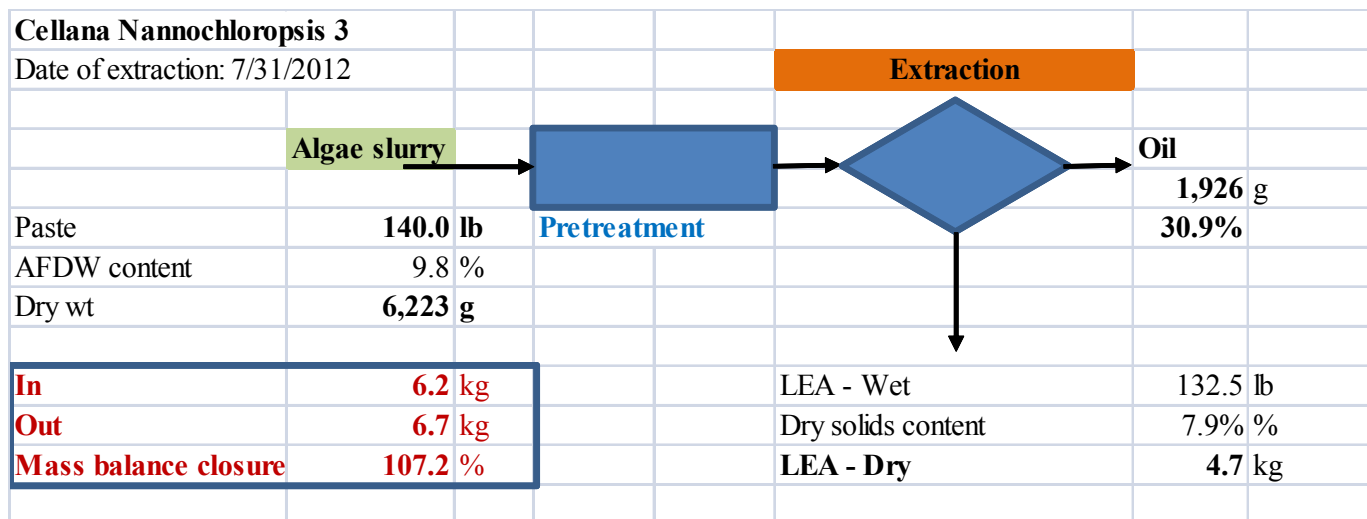


Figure 3.16. Example mass balance of extraction process using *Nannochloropsis* sp. obtained from Cellana.



Conclusions and Recommendations

The NAABB Harvesting and Extraction team made significant progress in the development of innovative technologies for harvesting and extraction of algal biomass and lipids. The projects addressed several key challenges and provided preliminary answers to the potential viability of each approach. Moreover, the new technologies were demonstrated on a range of different algae species and a range of scales.

Specific accomplishments by the team provided a multitude of data sets for continued development and commercialization. Three innovative harvesting approaches were taken from proof of concept at the lab scale to a larger scale with a minimum feedstock-processing rate of 100 L/h:

- The team demonstrated at pilot scale (5000 L/h) at the Texas AgriLife Research facility at Pecos an electrocoagulation method for dewatering. This method reduces the energy demand to 25% of the baseline of centrifugation and resulted in 95% recovery of the biomass.
- The team built a pilot-scale cross-flow membrane filtration system with novel membranes and improved performance over commercially available membrane materials.
- LANL scaled up the ultrasonic harvesting technology 10-fold, thereby demonstrating a 100-fold increase in energy effectiveness compared to the lab-scale device.

All three technologies show promise as primary harvesting techniques. In addition, cross-flow filtration can be used for further dewatering to 24% solids. All show energy savings compared to the baseline technology of centrifugation and may be used in combination with each other to achieve higher concentration factors or higher throughput. Table 3.8 summarizes the results of each NAABB harvesting technology and its impact on energy reduction.

Information about key process parameters previously not available in the public domain was generated. In each case, the field trial provided new insight into the technical challenges of scale-up and identified the gaps needing to be filled to further improve the performance of each technology.

In the extraction area, NAABB demonstrated a lab-scale, selective sequester of polyunsaturated FFAs and tocopherol, value-added algae products from crude lipid extracts. The Valicor process uses wet algae, which reduces the cost of extraction by eliminating the drying step.

NAABB successfully demonstrated >60 wet solvent extraction of >40 algae strains producing crude lipid and LEA samples with mass balance data. These samples were provided to the downstream processing teams.



HARVESTING AND EXTRACTION

Table 3.8. Summary of NAABB harvesting technology and impact on energy reduction.

Technology	Scale	Concentration— Initial, Final, and Factor	Energy Reduction	Recovery	Energy consumption, kwh/m ³ _culture
Electro-coagulation	3445 L per h 17,290 L processed	Initial: 0.8 g/L Final: 40 g/L Factor: 50X	Energy use was 25% (59 kWh) of that used by the centrifuge (236 kWh) under the same conditions	95% of biomass recovered in floc	
Cross-flow filtration with thin-sheet metal membrane	0.4 L/h 10 liter processed in each batch run	0.65 g/L <i>N. salina</i> ; 45- fold concentration to 30 g/L		100%	0.387 @2.0--2.5 m/s velocity demonstrated in this lab run 0.056 @ 0.15--0.5 m/s of velocity targeted for commercial-scale unit and tested at Pecos
Pall membrane filter in tubular form	301 L/h 2334 L processed in this batch run	Initial: 1.31 g/L DW Final: 9.78 g/L; concentration Factor: 7	84.3%	100%	2.14
	300 L/h 2400 L processed in this batch run	Initial: 1.38 g/L DW Final: 69 g/L; concentration Factor: 50	61.3%	100%	5.29
	Pall's engineering calculation	Initial: 0.5 g/L DW Final: 60 g/L; concentration Factor: 120			<0.5
Ultrasonic Harvesting (Lab Scale)	0.9 liters/h	Initial: 3 g/L Final: 27.8 g/L Factor: 9.3	Baseline: 13.65 kWh/m ³ for centrifugation Ultrasonic Harvesting: 0.32 kWh/m ³ Energy Reduction: 97.7%	92.0%	
Ultrasonic Harvesting (Scale-Up)	5 L/h feed Of the 23.3 L total processed in this batch run, 6 L were processed at a power setting of 10 W.	Initial: 1.75 g/L Final (max): 10.1 g/L Final (avg): 4.49 g/L Factor (max): 5.7 Factor (avg): 2.57	Baseline: 13.65 kWh/m ³ for centrifugation Ultrasonic Harvesting: 2 kWh/m ³ Energy Reduction: 85.3%	23.3%	
	5 L/h Of the 23.3 L total processed in this batch run, 6.5 L were processed at a power setting of 21 W.	Initial: 1.75 g/L Final (max): 12.6 g/L Final (avg): 8.7 g/L Factor (max): 7.2 Factor (avg): 5.0	Baseline: 13.65 kWh/m ³ for centrifugation Ultrasonic Harvesting: 4.2 kWh/m ³ Energy Reduction: 69.2%	45.2%	
	5 liters/h Of the 23.3 L total processed in this batch run, 10.8 L were processed at a power setting of 30 W.	Initial: 1.75 g/L Final (max): 10.9 g/L Final (avg): 7.2 g/L Factor (max): 6.2 Factor (avg): 4.13	Baseline: 13.65 kWh/m ³ for centrifugation Ultrasonic Harvesting: 6 kWh/m ³ Energy Reduction: 56%	30.3%	



The team found several important factors that affected the efficiencies of harvesting and extraction technologies. Although we demonstrated new technologies that were compatible with a variety of different algae species, the difference between species proved to be important factors to the efficiency of harvesting and extraction. Likewise, the starting concentration of the cultivation feedstock was important to the overall harvesting and extraction efficiencies. There is an urgent need to collect long-term performance data of new technologies using real-world feedstocks. Finally, each new technology had specific engineering issues that need to be addressed to improve performance and facilitate implementation. For the foreseeable future, achieving scale-up of new technologies while maintaining long-term high performance in the face of variable feedstocks will continue to be the most serious challenge to address.

Harvesting and Extraction Team

James Bonner, Clarkson University
Jim Coons, Los Alamos National Laboratory
Sandun Fernando, Texas A&M University
Brian Goodall, Valicor) (SRS)
Kiran Kadam, Valicor (SRS).
Ronald Lacey, Texas A&M University
Wei Liu, Pacific Northwest National Laboratory
Babs Marrone, Los Alamos National Laboratory
Zivko Nikolov, Texas A&M University
Brian Trewyn, Iowa State University (Colorado School of Mines)

Publications

Full-length, Peer-reviewed Publications

- Garzon-Sanabria, A.J., R.T. Davis, and Z.L. Nikolov. Harvesting *Nannochloris oculata* by inorganic electrolyte flocculation: Effect of initial cell density, ionic strength, coagulant dosage, and media pH. *Bioresource Technology* 118 (2012): 418–424.
- Liu, W., and N. Canfield. Development of thin porous metal sheet as micro-filtration membrane and inorganic membrane support. *Journal of Membrane Science* 409–410 (2012): 113–126.
- Nawaratna, G., R. Lacey, and S.D. Fernando. Effect of hydrocarbon tail-groups of transition metal alkoxide base. *Catalysis Science and Technology* 2 (2012): 364–372.
- Richardson, J.W., M.D. Johnson, R.Lacey, J.Oyler, and S. Capareda. Harvesting and extraction technology contributions to algae biofuels economic viability. *Algal Research* 5 (2014): 70-78.
- Samarasinghe, N., and S. Fernando. Effect of high pressure homogenization on aqueous phase solvent extraction of lipids from *Nannochloris oculata*. *American Society of Agricultural and Biological Engineers Annual International Meeting 2011 2* (2011): 1391–1403.



HARVESTING AND EXTRACTION

Samarasinghe, N., S. Fernando, R. Lacey, and W.B. Faulkner. Algal cell rupture using high pressure homogenization as a prelude to oil extraction. *Renewable Energy* 48 (2012): 300–308.

Valenstein, J.S, K. Kandel, F. Melcher, I.I. Slowing, V.S.-Y. Lin, and B.G. Trewyn. Functional mesoporous silica nanoparticles for the selective sequestration of free fatty acids from microalgal oil. *ACS Applied Materials and Interfaces* 4 (2012): 1003–1009.

Other Important Publications

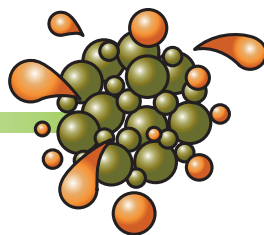
Sullivan, E. The ultrasonic algal biofuels harvest. *Resource: Engineering and Technology for Sustainable World* 18 (2011): 8–9.

References

1. Schenk, P.M., S.R. Thomas-Hall, E. Stephens, U.C. Marx, J.H. Mussgnug, C. Posten, O. Kruse, and B. Hankamer. Second generation biofuels: High-efficiency microalgae for biodiesel production. *BioEnergy Research* 1 (2008): 20–43.
2. Lundquist, T.J., I.C. Woertz, N.W.T. Quinn, and J.R. Benemann. A realistic technology and engineering assessment of algae biofuel production. Energy Biosciences Institute, University of California (2010).
3. Uduman, N, Y. Qi, M.K. Danquah, G.M. Forde, and A. Hoadley. Dewatering of microalgal cultures: A major bottleneck to algae-based fuels. *Journal of Renewable and Sustainable Energy* 2 (2010): 012701-1–012701-15.
4. Aragon, A.B, R.B. Padilla, and J.A.F.R.D. Ursinos. Experimental study of the recovery of algae cultured in effluents from the anaerobic biological treatment of urban wastewaters. *Resources, Conservation and Recycling* 6 (1992): 293–302.
5. Alfafara, G.H., K. Nakano, N. Nomura, T. Igarashi, and M. Matsumura. Operating and scale-up factors for the electrolytic removal of algae from eutrophied lakewater. *Journal of Chemical Technology and Biotechnology* 77 (2002): 871–6.
6. Poelman, E., N. De Pauw, B. Jeurissen. Potential of electrolytic flocculation for recovery of micro-algae. *Resources, Conservation and Recycling* 19 (1997): 1–10.
7. P. Le-Clech, V. Chen, T. and A. G. Fane. Fouling in membrane bioreactors used in wastewater treatment—A review. *Journal of Membrane Science* 284 (2006): 17–53.
8. Sun, X, C. Wang, Y. Tong, W. Wang, and J. Wei. Microalgae filtration by UF membranes: Influence of three membrane materials. *Desalination and Water Treatment* (2013): 1–8.
9. Zhang, W, W. Zhang, X. Zhang, Q. Hu, M. Sommerfeld, P. Amendola, and Y. Chena. Characterization of dissolved organic matters responsible for ultrafiltration membrane fouling. *Algal Research* (2013) 2: 223–229.



10. Williams, J, and W. Liu. High Separation Area Membrane Module. WO2006049940A2 (5/11/2006).
11. Drury, K.J., Y. Gu, and W. Liu. Monolith Membrane Module for Liquid Filtration. WO2009134359A1(11/5/2009).
12. Luiten-Olieman, M.W.J., M. J.T. Raaijmakers, L. Winnubst, M. Wessling, A. Nijmeijer, and N.E. Benes. Porous stainless steel hollow fibers with shrinkage-controlled small radial dimensions. *Scripta Materialia* 65 (2011): 25–28.
13. Ashby, M.F., A.G. Evans, N.A. Fleck, L.J. Gibson, J.W. Hutchinson, and H.N.G. Wadley. *Metal Foams: A Design Guide*. Butterworth Heinemann (2000).
14. Bosma, R., W. A. van Spronsen, J. Tramper, and R. H. Wijffels. Ultrasound, a new separation technique to harvest microalgae. *Journal of Applied Phycology* 15 (2003): 143–153.
15. Gerde, J.A., M. Montalbo-Lomboy, L. Yao, D. Grewell, and T. Wang. Evaluation of microalgae cell disruption by ultrasonic treatment. *Bioresource Technology* 125 (2012): 175–181.
16. Czartoski, T. J., R. Perkins, J.L. Villanueva, and G. Richards. Algae Biomass Fractionation. United States Patent Application 20100233761 (2010).
17. Czartoski, T. J., R. Perkins, J.L. Villanueva, and G. Richards. Algae Biomass Fractionation/Fractionnement D'une Biomasse D'algues. World Patent Application WO 2012/078852 (2012).



FUEL CONVERSION

Introduction

Team Leads

Anthony J. Marchese, Colorado State University
Richard Hallen, Pacific Northwest National Laboratory

Preface

The Fuel Conversion component of the National Alliance for Advanced Biofuels and Bioproducts (NAABB) focused on the development of energy-efficient technologies to convert algae-derived lipids and/or biomass into useful fuels. The Funding Opportunity Announcement by the U.S. Department of Energy (DOE) called out fuel conversion as a requirement for the consortium. Algae produce lipid-rich feedstocks. Therefore, the initial focus was on the production of distillate range fuels (biodiesel, diesel, and jet) from algal oils.

Prior to NAABB, UOP, LLC a Honeywell Company, had developed a catalytic hydrotreating/refining process to deoxygenate and refine a wide range of terrestrially produced lipids into gasoline, diesel, and jet fuel. However, this process had not been demonstrated with the variety of algal lipid feedstocks and extraction processes that would be available through the NAABB consortium. UOP successfully demonstrated via NAABB the production of paraffinic diesel and jet fuel that met both ASTM and military specifications from numerous feedstocks and extraction processes. Albemarle also developed a proprietary process for producing biodiesel prior to NAABB, which was also demonstrated on NAABB algal feedstock.

Effective use of all components of algal biomass is needed in the biorefinery. In addition to lipid utilization, NAABB also had a focus on the development of valuable coproducts from the lipid extracted algae (LEA). LEA is also known as post-extracted algae residue (PEAR). Specifically, the NAABB consortium focused on three potentially large-market coproducts: (1) agricultural (animal feed or fertilizer), (2) chemical feed stocks, and (3) additional power/fuels.

A gap analysis done at 20 months identified the need for conversion processes that (1) combine extraction and conversion steps, thereby removing unit operations; and (2) are effective at producing biocrude oil to be produced directly from whole algae, thus allowing large-scale cultivation R&D to focus purely on algal productivity rather than lipid production. To respond to this gap, NAABB scientists and engineers brought in hydrothermal liquefaction (HTL), a technology under development in NAABB's sister organization, the National Advanced Biofuels Consortium (NABC). HTL combines extraction and conversion into a single step. A limited but sufficient number of studies were done in NAABB to allow the technology to move forward in subsequent projects. In addition, two projects examined biochemical conversion of algae biomass. Finally, limited work was also done on fast pyrolysis. However, the energy consumption required to dry the algal biomass to the level required for pyrolysis can approach or exceed the energy in the algae.



Approach

The science and technology program in NAABB followed the R&D Framework for Conversion (Figure 4.1). Three areas were examined: (1) characterization, (2) lipid conversion, and (3) LEA and biomass conversion. These thrusts allowed NAABB to develop full data sets from algal cultivation through end-product conversion performed in large open ponds from fresh/brackish and sea waters.

Fuel Conversion Task Framework

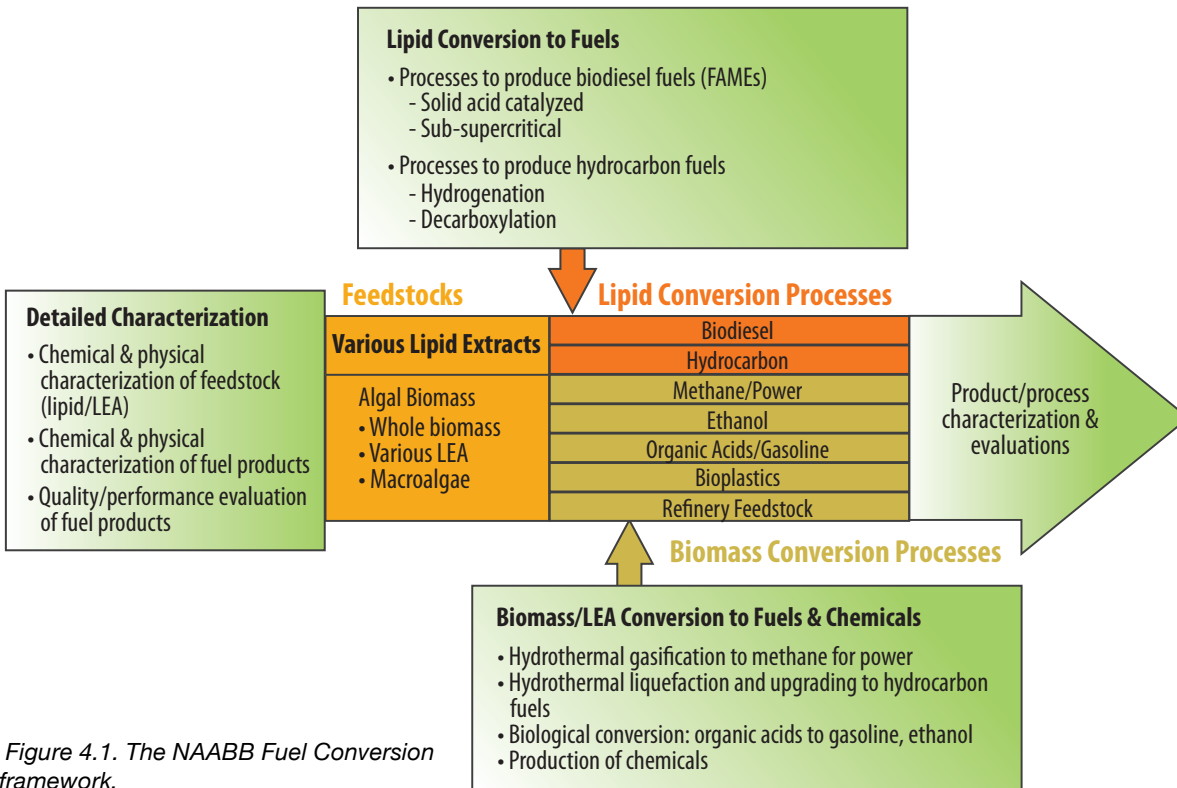


Figure 4.1. The NAABB Fuel Conversion framework.

Technical Accomplishments

Detailed Characterization

A wide variety of algae oils, LEA, and whole-algae feedstocks were characterized to support the Fuel Conversion research program. This included development of new methods not used prior to NAABB and the application of methods to evaluate quality of the material. For this section, it is sufficient to note that feedstocks vary broadly in their composition based on algal strain, growing conditions, and harvesting technologies.

Biochemical Characterization

Considerable variability in algal feedstock is exemplified in Figure 4.2, which illustrates biochemical composition data determined for four algae samples grown and harvested for NAABB. The data set includes stressed (high-lipid) and nonstressed (low-lipid)

Nannochloropsis oceanica, *Pavlova pinguis*, and *Tetraselmis* sp. Ash content in the four samples varied from 13–27%, carbohydrates varied from 12–28%, protein varied from 27–35%, and lipid (gravimetric analysis) varied from 1–36%. The fatty acid content of the lipid (via fatty acid methyl ester, or FAME, analysis) was a fraction of the total lipids. In the high-lipid *N. oceanica* sample, 36% of the dry algae weight was lipid, but the fatty acid content was only 23% of the total algal mass. The FAME content as a ratio of lipids was even lower in the other samples. The FAME analysis for all

other algae species evaluated by the Fuel Conversion team was conducted by one researcher for consistency to determine the relative lipid content as total fatty acids, which are the primary fuel molecules in lipid extracts/oils.

Table 4.1 provides data on other exemplary samples from large-scale cultivation studies in NAABB. This set provides total FAME versus free fatty acid (FFA) in the oil as well as the FAME profile.

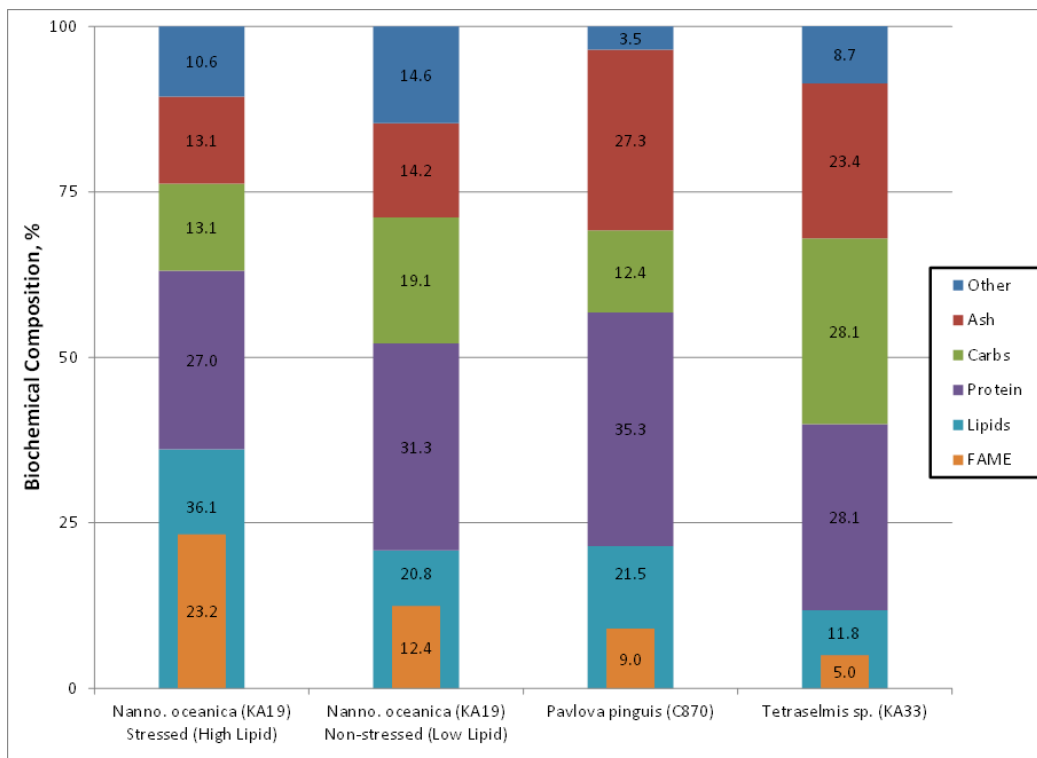


Figure 4.2. Composition for whole algae samples



Table 4.1. Characterization of LEA and Whole Biomass Feedstocks

Algal Species	<i>N. salina</i> (LEA) [*]	<i>N. salina</i> (Whole Algae)	<i>N. salina</i> (High Lipid)	<i>N. oceanica</i> (High Lipid)	<i>N. oceanica</i> (Low Lipid)	<i>Tetraselmis</i> sp.	<i>Pavlova pinguis</i> ^{**}	<i>Chlorella</i> sp.	<i>Chlorella</i> sp.
Source	Solix	Solix	TAMU Pecos	Cellana	Cellana	Cellana	Cellana	U of A and PNNL-Sequim	TAMU Pecos
Dry Basis Biomass Lipid Content as FAMES									
Total FAMES ^{††}	11.4	32.91	11.6 [†]	23.08	16.3	6.98	4.09	10.98	6.65
FFA [‡]	4.8	8.94	1.8	2.33	0.1	2.87	3.03	9.30	4.58
Biomass Lipid Profile, weight fraction of FAMES									
C12:0		0.01							
C14:0	0.02	0.04		0.07	0.09	0.01	0.20		
C15:0					0.01	0.01	0.01		
C16:0	0.26	0.33	0.24	0.36	0.39	0.21	0.16	0.16	0.17
C16:1	0.13	0.33	0.03	0.27	0.26	0.06	0.08	0.03	0.03
C16:2	0.01		0.01					0.03	
C16:3	0.03							0.09	0.01
C16:4									0.17
C18:0	0.01	0.01	0.03	0.01	0.01	0.12	0.01	0.01	
C18:1	0.21	0.08	0.05	0.10	0.08	0.00		0.02	0.06
C18:2	0.04	0.01	0.09	0.02	0.02	0.18	0.03	0.10	0.03
C18:3	0.20	0.02	0.11			0.17	0.03	0.57	0.47
C18:4						0.13	0.10		0.05
C20:0			0.04						
C20:2			0.02						
C20:3						0.02			
C20:4	0.02	0.05	0.02	0.06	0.05	0.01	0.01		
C2:05	0.07	0.10	0.03	0.10	0.09	0.07	0.26		
C22:0			0.06						
C22:1			0.02						
C22:6			0.04				0.11		
C24:0			0.07						

[†]Determined to be 19.9 wt% total lipid via accelerated extraction with 50/50 methanol/chloroform.

^{**}Two separate samples of *Pavlova pinguis* samples, one solar dried and one ring-dryer dried, were mixed to create a single HTL feed slurry.

^{*}Corrected to a dry basis based only on data showing algal biomass that was nominally *N. salina* was 14.3% ash for consistency with other values.

[†]Determined by acid catalyzed esterification.

[‡]Calculated as the difference between acid catalyzed and base catalyzed value.

A few items should be noted. First, the Solix LEA had fairly high lipid content. The ability to recover polar lipid compounds is dependent upon extraction technology. Later solvent extraction processes demonstrated high recovery of both neutral and polar lipids. Many of the samples had a large content of highly unsaturated C20-C24 FAMES, as high as 30% of the fatty acids for *N. salina* and 38% for *Pavlova pinguis*. The large chain lengths are not an issue for the UOP Green Jet Fuel™ process as it includes a cracking step. However, technologies that do not lower acyl chain molecular weights through cracking such as biodiesel and decarboxylation processes would likely produce fuel with poor cold temperature properties. The polyunsaturated lipid content could also be high (e.g., 48% for *Tetraselmis* sp.). The high levels of polyunsaturated lipids decrease the thermal stability of the oils and raise the hydrogen demand in conversion technologies that utilize hydrotreating (e.g., UOP Green Jet Fuel™) or increase the oxidative instability of ester fuels (biodiesel).

Characterization via Fourier Transform Ion Cyclotron Resonance Mass Spectrometry

In addition to the traditional FAME characterization via acid catalyzed esterification, a direct-infusion Fourier transform ion cyclotron resonance mass spectrometry (FT-ICR MS) method was developed for comprehensive characterization of microalgal lipid extracts, produced ester fuel, and HTL products. With this approach, the neutral, polar, and membrane lipid components for several microalgal biofuel candidate strains were determined. For typical algal lipid extracts, the distribution of around 1000 individual lipid compounds per sample was monitored and changes in these compounds were tracked across a sample set. Figure 4.3 shows an example of the positive ion and negative ion mode mass spectra for a single sample.

Typical laboratory-grown algal lipid extracts exhibited 1000 to 1500 peaks per ionization mode. On the other hand, lipid extracts from outdoor cultures were significantly more complex with >2600 peaks (S/N >10) observed in positive ion mode mass spectrometry (MS) (top) and >3300 peaks in negative ion mode MS (bottom). This level of spectral

complexity requires high-resolution FT-ICR MS to discern all component signals. Additionally, sub-part-per-million mass-measurement accuracy allows each ion signal to be converted directly to elemental composition. Following elemental composition assignment, lipid components were sorted to reveal trends in lipid class distribution, degree of alkylation, and number of acyl-double bonds. Lipid class analysis is illustrated for predominant lipid classes observed for two microalgae species in Figure 4.4.

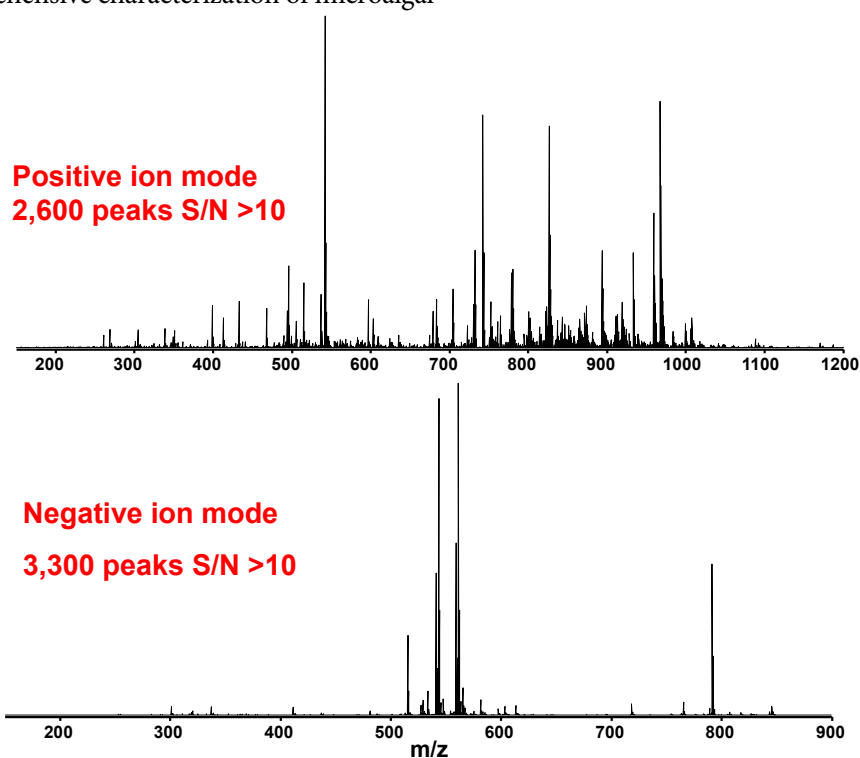


Figure 4.3. Ultra-high resolution FT-ICR mass spectra of extracted *N. salina* grown in outdoor raceways.

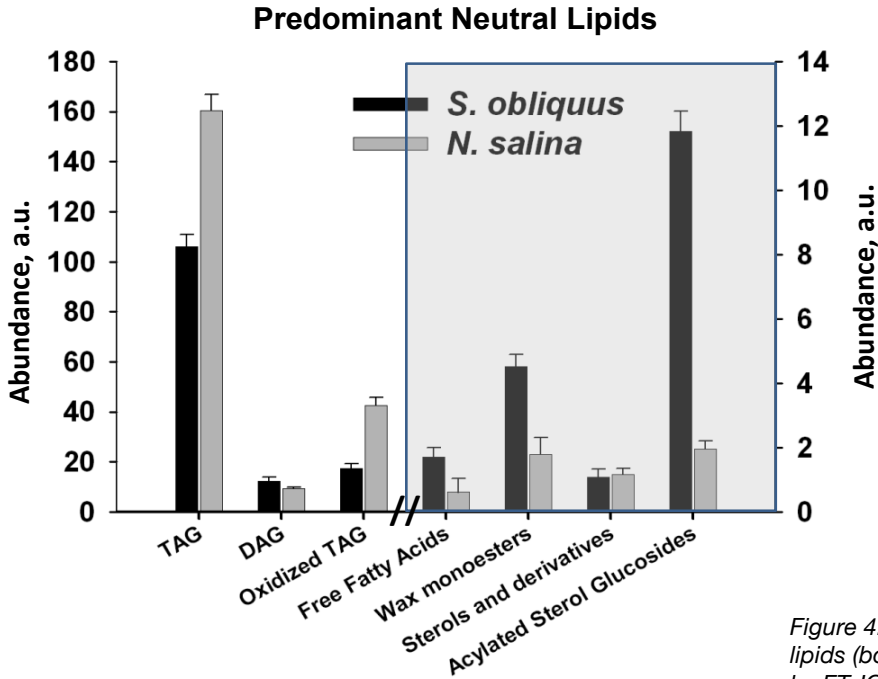
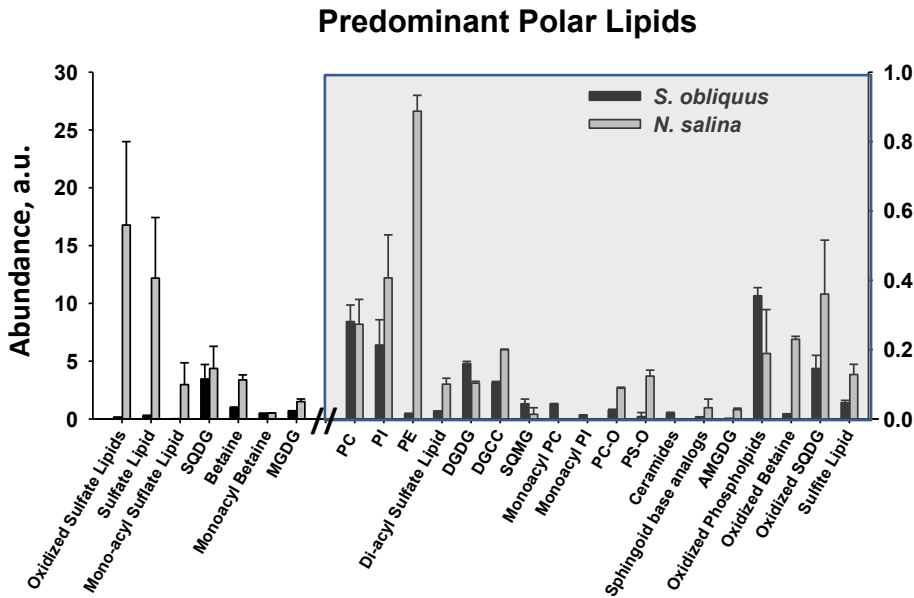


Figure 4.4. Predominant neutral lipids (top) and polar lipids (bottom) of *N. salina* and *S. obliquus* observed by FT-ICR MS.



The lipid chemistries represented in Figure 4.4 are fairly typical for these species and should be considered when choosing conversion and downstream processing approaches. Each lipid class is composed of as many as 60 individual compounds (excluding isomers, which are not resolved by this methodology). These data may be further divided to illuminate change in the distribution of individual molecules within each class. FT-ICR MS was also applied to follow changes in lipid composition during an entire growth cycle for *N. salina* as it transitioned from rapid growth to stationary phase, to monitor the conversion efficiency of intact microalgae lipid species during transesterification and to analyze the compounds resulting from HTL of whole algae cells.

Quantification of Inorganic Compounds and Metals in Lipid Extract

The inorganic components in the feedstock are also important in considering preprocessing and conditioning. Tables 4.2 and 4.3 show characterization data of the algal lipid extracts procured from a number of NAABB-produced algal oil feedstocks. The oils include refined algal oils, crude algal oils, two FAMES-rich algal oils produced via direct methanolysis of algal biomass, and a HTL bio-oil produced via the HTL process. Table 4.2 focuses on acid number and heteroatom content (O, N, S, P, Cl). Table 4.3 focuses on trace metals (Na, K, Ca, Mg, Fe, Cu) concentration.

Table 4.2. Characterization of algal lipid extracts from NAABB consortium producers.

Algal Biomass Supplier and Species	Oil Extractor	Oil Type	Acid Number	Oxygen	Nitrogen	Sulfur	Phosphorous	Chlorine
			mg KOH/g	mass-%	mass-ppm	mass-ppm	mass-ppm	mass-ppm
Eldorado	Eldorado	Refined oil	0.93	10.7	5	6	<0.09	<0.1
Eldorado	Albermarle	Distilled FAME	0.019	11.1	1.5	2	<0.03	<0.1
Inventure	Inventure	FAME	2.6	11	453	158	11.9	62
Cellana <i>N. oceanica</i> (high lipid)	Inventure	Distilled FAME	3.12	11	6000	473	0.18	
Phycal <i>Chlorella protothecoides</i> Sample #1	Phycal	Refined oil	5.74	9.6	9.8	2	4.3	0.7
Phycal <i>C. protothecoides</i> Sample #2	Phycal	Refined oil	2.9	10.2	39	6	2.12	1.7
Solix <i>N. salina</i>	Solix	Crude lipid extract	15.9	11.9	8000	580	303	350
TAMU Pecos <i>N. salina</i> Sample #1	Valicor	Crude lipid extract	41.5	12	2100	1300	71	376
TAMU Pecos <i>N. salina</i> Sample #2	Valicor	Crude lipid extract	91.2	12.8	2800	9007	99	253
Cellana <i>N. oceanica</i> (High Lipid)	Valicor	Crude lipid extract	19.9	12.6	3500	2196	231	519
TAMU Pecos <i>Chlorella</i> sp.	Valicor	Crude lipid extract	114	9.3	3600	2392	436	
Cellana <i>N. oceanica</i> (low lipid)	PNNL	HTL Bio-oil	55.4	19	32,000	2400	3	NR



Table 4.3. Characterization of trace metals in algal lipid extracts from NAABB consortium producers.

Algal-Biomass Supplier and Species	Oil Extractor	Oil Type	Sodium	Potassium	Calcium	Magnesium	Iron	Copper
			ppm	ppm	ppm	ppm	ppm	ppm
Eldorado	Eldorado	Refined Oil	1.58	0.45	0.97	0.27	0.53	<0.05
Eldorado	Albermarle	Distilled FAME	0.04	<0.01	0.03	<0.01	<0.01	<0.01
Inventure	Inventure	FAME	142	5.3	2.31	3.98	37.1	1.52
Cellana <i>N. oceanica</i> (high lipid)	Inventure	Distilled FAME	2.59	0.13	0.03	0.12	1.7	0.06
Phycal <i>C. protothecoides</i> Sample #1	Phycal	Refined Oil	0.9	0.9	0.7	0.4	< 0.2	< 0.2
Phycal <i>C. protothecoides</i> Sample #2	Phycal	Refined Oil	0.46	1.78	0.43	0.43	<0.03	0.11
Solix <i>N. salina</i>	Solix	Crude Lipid Extract	370	426	12.6	106	1.8	28
TAMU Pecos <i>N. salina</i> Sample #1	Valicor	Crude Lipid Extract	178	64	51	34	97	62
TAMU Pecos <i>N. salina</i> Sample #1	Valicor	Crude Lipid Extract	570	192	281	56	49.7	30.3
Cellana <i>N. oceanica</i> (high lipid)	Valicor	Crude Lipid Extract	145	NR	17	10	75	11
TAMU Pecos <i>Chlorella</i> sp.	Valicor	Crude Lipid Extract	58	18	26	6	155	76
Cellana <i>N. oceanica</i> (low lipid)	PNNL	HTL Bio-Oil	1880	637	10.6	6.5	910	13.5



FUEL CONVERSION

The high level of impurities and contaminants in the algal oils pose challenges for the conversion of these oils into fuels due to:

- Catalyst poisoning—Alkali metals, alkaline earth metals, phosphorous, and base metals can neutralize acid sites or bind with active sites on the catalyst surface required for deoxygenation activity.
- Materials of construction—Halogens can lead to stress-corrosion cracking in reactors operating at high temperatures and pressures.
- Final fuel specifications—Fuel specifications require very low levels of nitrogen, sulfur, halogens, and metals in the final product. Hydrotreating can remove heteroatoms at a cost, but transesterification can only be performed on pretreated lipids.

At commercial fuel production scale, the contaminant levels would need to be significantly reduced. NAABB developed and demonstrated proprietary technology to pretreat various NAABB algal lipid extracts to reduce contaminant levels for improved upgrading performance. The level of purification required is not only dependent on downstream processes but also a strong function of the algal species and upstream processing. Refinement of the algal extracts may result in significant loss of yield. For example, only 50 wt% yield of FAMES was obtained when crude lipid extract from *N. salina* was esterified with methanol using sulfuric acid as a catalyst (see the section Transesterification to Produce Biodiesel (Ester-based Fuels), below). Thus, purification and refinement to produce refined TAG lipids from crude algal extract may only yield fuel at around 50% on a mass basis in some cases.

Distillation Profiles of Algal Oils

The organic compositional differences of the samples in Tables 4.2 and 4.3 can be visualized from the simulated distillation profiles of the oils (Figure 4.5). The Eldorado refined oil represents a highly purified triacylglyceride (TAG) and has a similar curve to the highly purified Phycal *C. protothecoides* oil samples. TAG samples have a specific distillation profile. As the TAG content in the oil decreases the distillation profile changes significantly, which is generally to the left (lower boiling point range) in Figure 4.5. The Inventure samples contain no TAGs. The HTL bio-oil sample contains FFAs as well as other oil-types including aromatics and other nonlipid materials. The crude lipid extract samples from various biomass suppliers extracted by Valicor are from a wet-extraction technology that uses a thermal pretreatment and their distillation profiles vary widely.

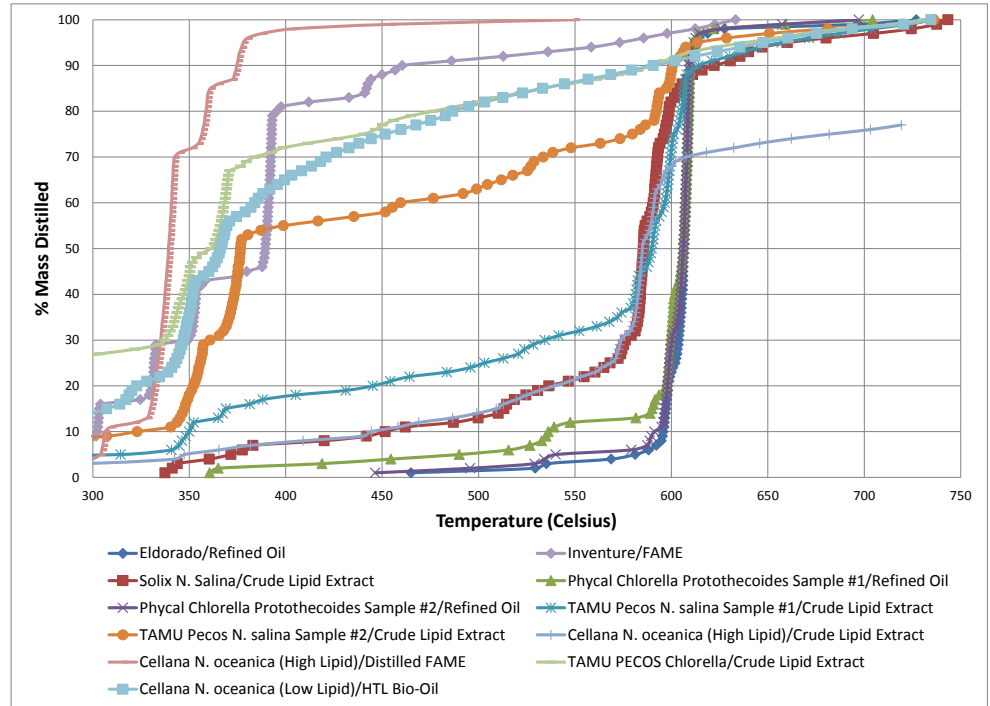


Figure 4.5. Simulated distillation profiles of the various algal lipid and HTL oils.



Characterization of Algal-derived FAME Fuel with Varying EPA and DHA Content

Since the FAME profile for biodiesel derived from algae oil is typically much different from the conventional biodiesel produced from canola or soybean oil, the impact on biodiesel properties was examined using model compound mixtures representing the broad range of compositions expected for algae-derived biodiesel. Several microalgae species that are suitable for large-scale cultivation, such as those in the genus *Nannochloropsis*, produce lipids that contain long-chain polyunsaturated fatty acids (LC-PUFA) such as eicosapentaenoic acid (EPA) and docosahexaenoic acid (DHA). These constituents have high value as nutraceutical coproducts but are problematic in terms of biodiesel properties such as ignition quality, oxidative stability, and other fuel properties.

A major objective of the fuel characterization component of the Fuel Conversion task within NAABB was to examine the effect of varying levels of EPA and DHA on algal-derived FAME fuel properties. Oxidative stability, cetane number, density, viscosity, bulk modulus, cloud point, and cold filter plugging point were measured for algal methyl esters produced from various microalgae feedstocks as well as model algal methyl ester compounds. The model methyl esters were formulated to match the fatty acid composition of *Nannochloropsis* sp., *N. oculata*, and *Isochrysis galbana* and subjected to varying levels of removal of EPA and DHA.

As shown in Figure 4.6, the experimental results showed that the oxidative stability induction period varies exponentially with the bis-allylic position equivalents (BAPE) value of the algal methyl esters. The results of this work also suggest that approximately 50% of the EPA and DHA would need to be removed from the *N. oculata* methyl ester to meet the 3 hour ASTM oxidative stability specification and approximately 80% would need to be removed to meet the European Standard (EN) 6 hour specification. For *I. galbana*, removal of 100% of the EPA and DHA was insufficient for passing either the ASTM or EN oxidative stability requirements. The effect of the presence of EPA and DHA on ignition quality was also found to be quite substantial. Specifically, it was found that nearly 100% of the EPA and DHA would need to be removed from the algal vmethyl esters considered herein to comply with the ASTM D6571 standard for minimum cetane number of 47 for biodiesel. Other fuel properties such as viscosity and density were well within specifications for all the algal methyl ester formulations tested.

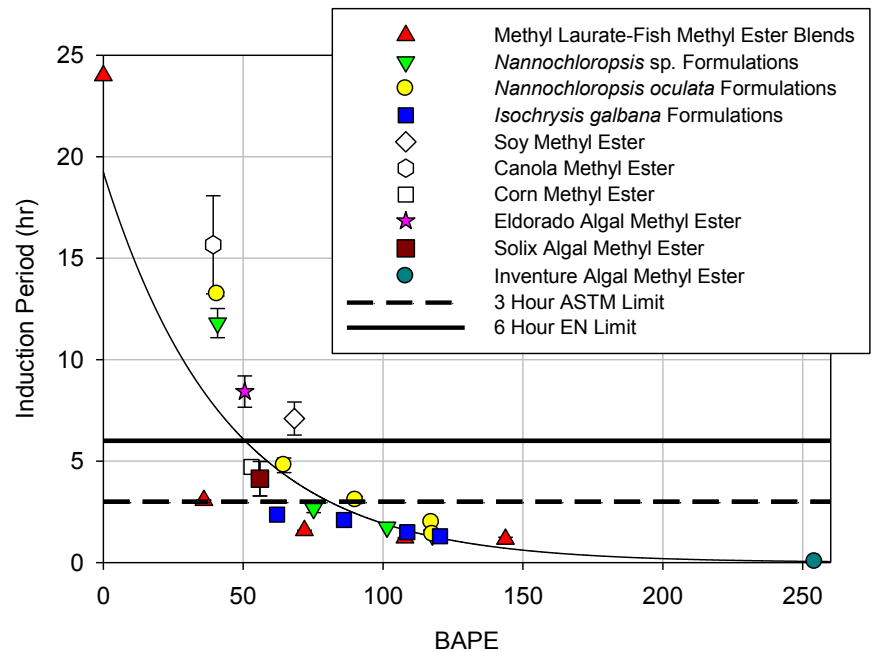


Figure 4.6. Oxidative stability induction period as a function of BAPE for all methyl esters.



In addition to the model algal methyl ester compounds, three algal methyl esters provided by NAABB consortium partners were tested to determine their oxidative stability, ignition quality, viscosity, density, and cold-flow properties. All three of the algal methyl esters proved to perform consistently with the model algal methyl ester formulation results. An algal methyl ester provided by Eldorado Biofuels containing no EPA or DHA passed both the ASTM and EN standards for oxidative stability without the addition of any fuel additives. Conversely, an algal methyl ester sample provided by Inventure, which consisted of nearly 50% DHA, exhibited very poor oxidative stability. The FAME produced from the Solix BioSystems *N. salina* had an oxidative stability induction period that passed the ASTM standard, but did not pass the EN standard.

The cloud point and cold filter plugging point were also found to be sensitive to the level of EPA and DHA present in the algal methyl esters since the balance of the fatty acid profile for algal methyl esters consists of a very high percentage of fully saturated methyl esters. After removal of all of the EPA and DHA from the algal methyl esters considered herein, the remaining product could contain up to 50% saturated methyl esters, which is similar to the saturated content of beef tallow methyl ester, a fuel that is known to have poor cold-flow properties.

In addition to the algal-derived lipids, the LEA and whole-algae samples used to conduct fuel conversion research were characterized by various NAABB partners. NAABB provided biochemical composition data for the whole-algae samples they provided as shown in Figure 4.2. The analysis included both total lipid (gravimetric) and FAMES concentration data for the various species that clearly demonstrates a wide range of composition from high-lipid *N. oceanica* and low-lipid *Tetraselmis* species. Similarly, the FAMES analysis of the *Tetraselmis* illustrated that the fatty acid content was significantly lower than the total lipid content.

In conclusion, characterization is critical for downstream R&D. Algal biomass shows large variability dependent on strain, growth conditions, and processing. The composition, impurity profiles, and properties of the various algal-derived lipids and bio-oil feedstocks vary widely. Many of the samples have high FFA content, which inhibits transesterification catalysts and requires removal or alternative conversion processing schemes. Inorganic and metal impurities also impact processing and end fuel properties. Upstream processes must be developed with the end goal of maximum fuel yield in mind, just as the conversion technology must consider upstream needs for nutrient recycles and reuse.

Algal-derived Lipid and Bio-oil Conversion to Fuel

This section will cover three technologies: (1) hydrotreating lipids or HTL bio-oil to produce diesel and jet fuel (herein referred to as distillate-range hydrocarbons); (2) transesterification of lipids to produce FAMES; and (3) decarboxylation to produce hydrocarbons. All three technologies share a need for feedstocks that are generally of high purity.



Hydrodeoxygenation was the primary pathway examined to convert oils to hydrocarbon fuels. Hydrodeoxygenation technology is commercialized for fat/oil conversion to fuels and uses catalytic hydrotreating technology similar to that used in petroleum refineries. A wide range of oils were upgraded by hydrodeoxygenation to produce hydrocarbon products for further refining and separation to produce the various fuel products. The overall process is illustrated by the UOP Green Jet™ and diesel fuel production process in Figure 4.7. This process successfully produced fuels meeting fuel specification from various oil feedstocks.

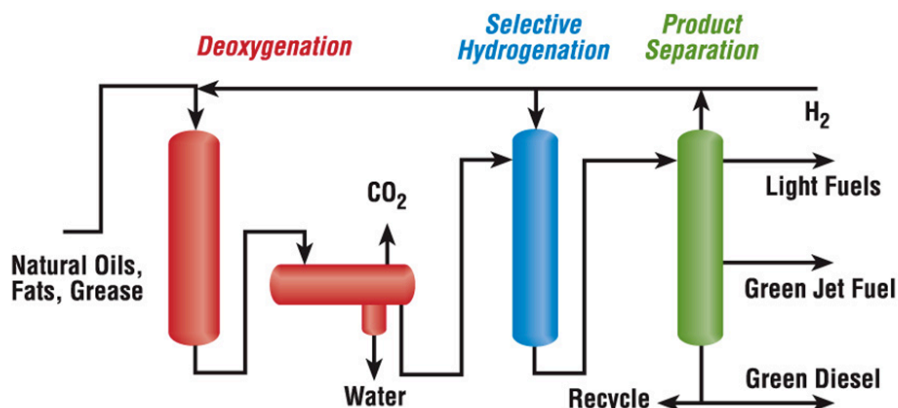


Figure 4.7. UOP Green Jet Fuel™ process for producing synthetic paraffinic kerosene and renewable diesel from biological feedstocks.

The chemistry in the process consists primarily of selective hydrodeoxygenation that converts algal-derived lipids into saturated straight chain hydrocarbons and water. The hydrocarbons are further isomerized and cracked to produce various fuel fractions that include (ordered by boiling point) naphtha, jet fuel (synthetic paraffinic kerosene, or SPK), diesel fuel, and heavies (see Figure 4.8 and Table 4.5).

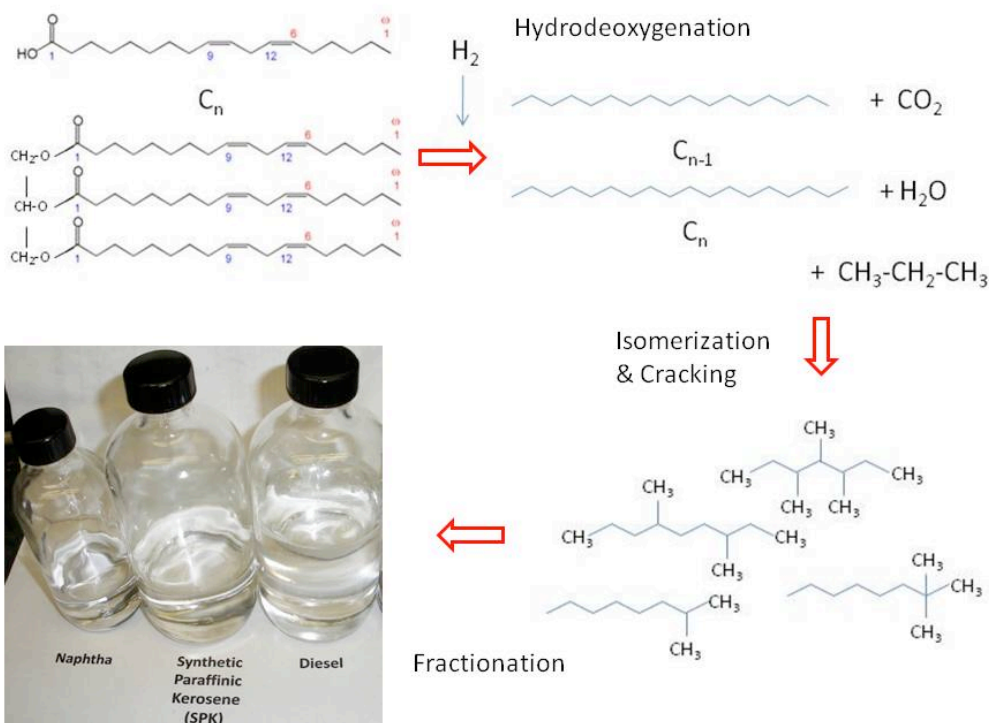


Figure 4.8. Pathway for production of renewable fuels using hydroprocessing technology.

Table 4.5. Fractionation results via spinning-band distillation of hydrotreated and isomerized *N. oceanica* (low lipid) HTL bio-oil.

Fraction	Boiling Range	Mass %
Noncondensable material (gas)	--	6%
Naphtha	IBP–150 °C	4%
Jet (SPK)	150–250 °C	26%
Diesel	250–350 °C	47%
Heavies	350+°C	17%

The UOP Green Jet™ process was used to convert seven NAABB-derived algal oils including FAME, crude lipid from *N. salina*, wet-extracted algal oil from *N. salina* and *N. oceanica* (high lipid), and bio-oil produced via HTL processing of *N. oceanica* (high lipid). During the work, NAABB developed new proprietary conditioning technologies for purifying algal oils. The resulting fuels were fully characterized. The various fuel specifications, including the commercial aviation (D7566 hydroprocessed ester or fatty acid), military (F-76 naval distillate), and commercial ultra-low sulfur diesel (ULSD), are shown in Tables 4.6 and 4.7. The simulated distillation profiles for the jet fuel (Figure 4.9) and renewable diesel (Figure 4.10) fractions were similar regardless of lipid extraction method or whether HTL was utilized as the processing method.

Upgraded HTL bio-oil produced from *N. oceanica* (low lipid) was unique in producing a jet fuel fraction in that it only required hydrodeoxygenation and isomerization but did not require cracking. Two hydrotreating campaigns were performed and the results of both tests with the same bio-oil are tabulated in Table 4.6. The fuel produced was not strictly an SPK, as it contained aromatic and cyclic hydrocarbons that resulted in a higher-density fuel with the potential for a full synthetic jet fuel (Table 4.6). A breakdown of the composition of the hydrotreated HTL bio-oil from the low lipid *N. oceanica* is reported in Table 4.6A. Further research is required to reduce the contaminant level in the crude HTL bio-oil for commercial scale production.



Table 4.6. Properties of renewable jet fuel produced from various algal lipid and HTL oils.

Algal Biomass Origin/Species				<i>N. oceanica</i> (High Lipid)	<i>N. salina</i>	<i>N. salina</i> Sample #1	<i>N. salina</i> Sample #2	<i>N. oceanica</i> (High Lipid)	<i>N. oceanica</i> (Low Lipid)
Oil Extractor				Inventure	Solix	Valicor	Valicor	Valicor	PNNL
Oil Type				Distilled FAME	Crude Lipid Extract	Crude Lipid Extract	Crude Lipid Extract	Crude Lipid Extract	HTL Bio-Oil
Parameter	D7566 HEFA Specifica- tion	<i>Jet A</i>	<i>Jet A1</i>						
	Density (g/L)	730–770	775–840	775–840	755.2	753.1	754.2	756.9	749.4
Freeze Point °C (max)	-47	-40	-47	-48.6	-62.6	-50.4	-61.8	< -80	-57
Flash Point °C (min)	38	38	38	42.5	39.7	44	45	40.2	59.6
Distillation 10% Recovered Temp (T10) °C (max)	205	205	205	156.4	160.2	151.4	150.4	152	167
50% Recovered Temp (T50) °C	Report	Report	Report	192	193.8	191.4	189	180	203.6
90% Recovered Temp (T90) °C	Report	Report	Report	248.8	245.6	252.4	234.8	222.2	242.2
Final Boiling Point °C (max)	300	300	300	279	271.8	293.2	284.2	263.6	272
T50-T10 (min)	15	—	—	35.6	33.6	40	38.6	28	36.6
T90-T10 (min)	40	—	—	92.4	85.4	101	84.4	70.2	75.2

Table 4.6A. Composition of hydrotreated HTL bio-oil produced from low-lipid *N. oceanica* before isomerization and distillation.

Organic Compound Class	Fraction (wt%)
Total n-paraffins	53.304
Total isoparaffins	7.965
Total naphthenes (cycloalkanes)	23.433
Total monoaromatics	10.863
Total diaromatics	3.749
Total triaromatics	0.686
Total 4+ ring aromatics	0
Total	100

Table 4.7. Properties of renewable diesel fuel produced from various algal lipid and HTL oils.

			<i>N. salina</i>	<i>N. salina</i> Sample #1	<i>N. salina</i> Sample #2	<i>N. oceanica</i> (High Lipid)	<i>N. oceanica</i> (Low Lipid)
Oil Type			Crude Lipid Extract	Crude Lipid Extract	Crude Lipid Extract	Distilled FAME	HTL Bio-oil
			Crude Lipid Extract	Crude Lipid Extract	Crude Lipid Extract	Distilled FAME	HTL Bio-oil
Parameter	F-76 Naval Distillate	ULSD Specifications					
Density at 15°C, g/L (max)	876	-	778.2	770	783.2	783.2	784.7
Flash Point, °C (min)	60	52	91.2	62.7	120.9	120.9	118.2
Cetane Number (min)	42	40	92	85	106	109	
Sulfur (max %)	0.15	0.0015	0.0003	0.0001	<0.0001	<0.0001	
Distillation 90% Recovered °C (max) (min)	357	338 282	288.4	305	320	294.8	298
Distillation End Point °C (max)	385		317.8	324.8	345.8	330.4	318.2
Cloud Point °C	-1	By geography	-20.5	-16.2	4.4	-6.9	1.1
Pour Point °C	-6	By geography	-24	-21	3	-12	-3.0
Metals (ppm) max							
Calcium	1	-	<0.009	0.024	0.17		0.77
Lead	0.5	-	<0.01	<0.02	<0.04		<0.2
Sodium + Potassium	1	-	0.29	0.026	0.25		2.17
Vanadium	0.5	-	<0.009	<0.009	<0.01		<0.09

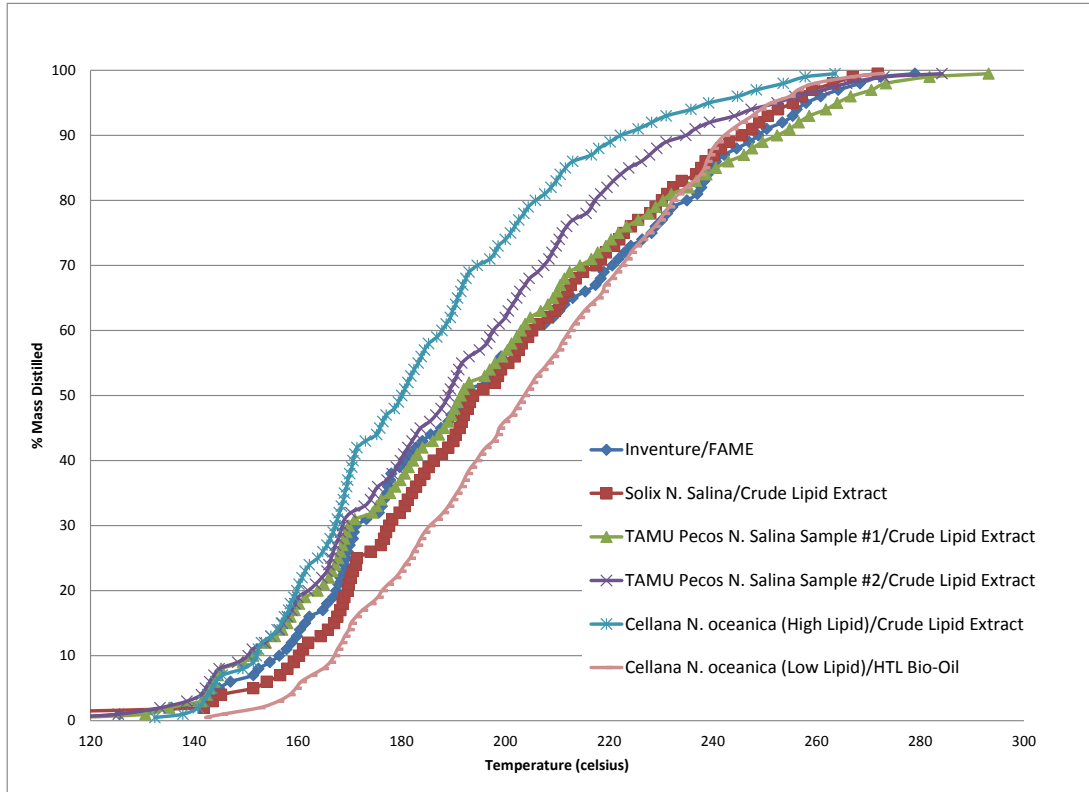


Figure 4.9. Simulated distillation profiles for various lipid and HTL oil derived jet fuels.

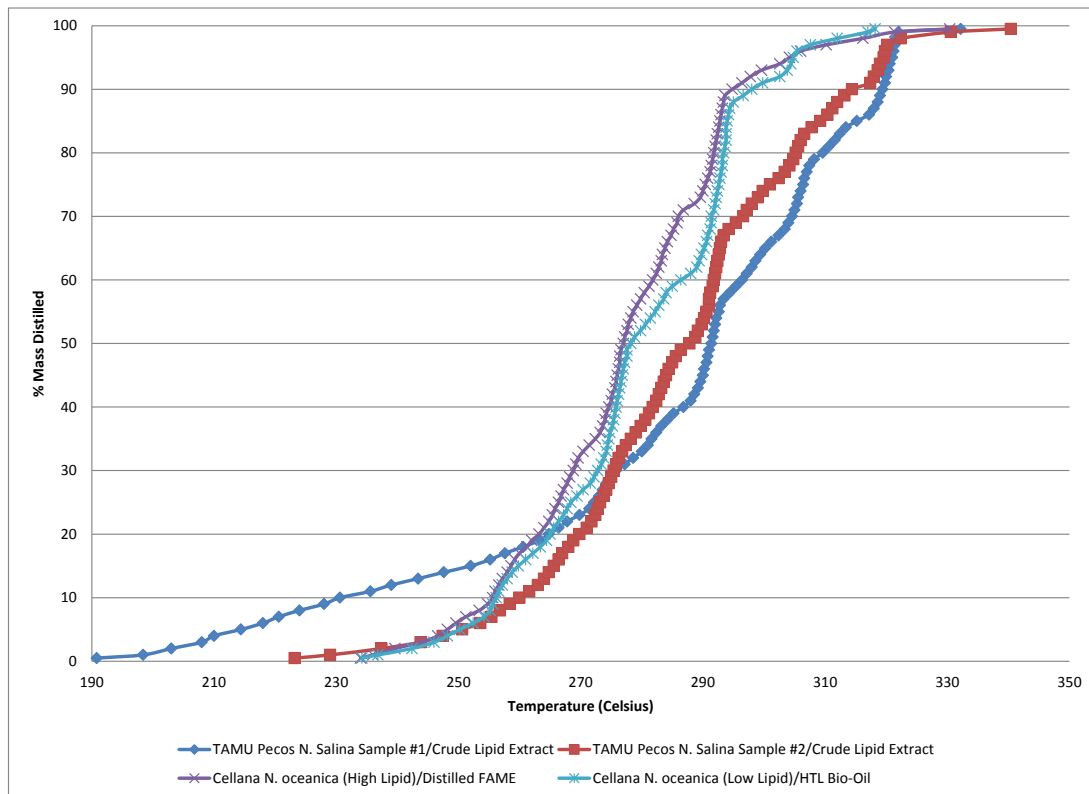


Figure 4.10. Simulated distillation profiles for various lipid and HTL-oil-derived diesel fuel.

Transesterification to Produce Biodiesel (Ester-based Fuels).

NAABB fuel conversion partner Albemarle has a patented process to produce biodiesel based on a heterogeneous (solid) transesterification catalyst. The heterogeneous catalyst, T300, was originally developed at Iowa State University and commercialized by Catilin, a small company that is now part of Albemarle. In 2008 Catilin/Albemarle opened a 300,000 gal/year (1000 mt/year) plant to demonstrate the technology with the capability to operate in either batch or continuous mode. Algal oil adaptation within NAABB was done at the laboratory scale. Pilot-scale work was not done. The catalyst exhibited some flexibility with respect to purity of the feedstock, with no obvious catalyst deactivation with modest metal or phosphorus loading in the feed. The result suggests that certain feedstocks may not require degumming. However, long-term catalyst stability must be performed as a function of phosphorus loading in the oil in order to adequately examine catalyst life with crude algal oil extracts.

While the T300 catalyst exhibited short-term stability in the presence of metals and phosphorus, the fatty acid content must be less than 1%. Under NAABB, a glycerolysis approach for converting FFAs to glycerides was developed. In addition to pretreatment, post-treatment technologies to improve fuel quality were also developed. The coupled systems were optimized, the processes were simulated, and economic analysis performed. In this study, a kinetic model for the transesterification reactions was obtained using nonlinear regression of reaction rate data.¹ A simplified process flow diagram is shown in Figure 4.11.

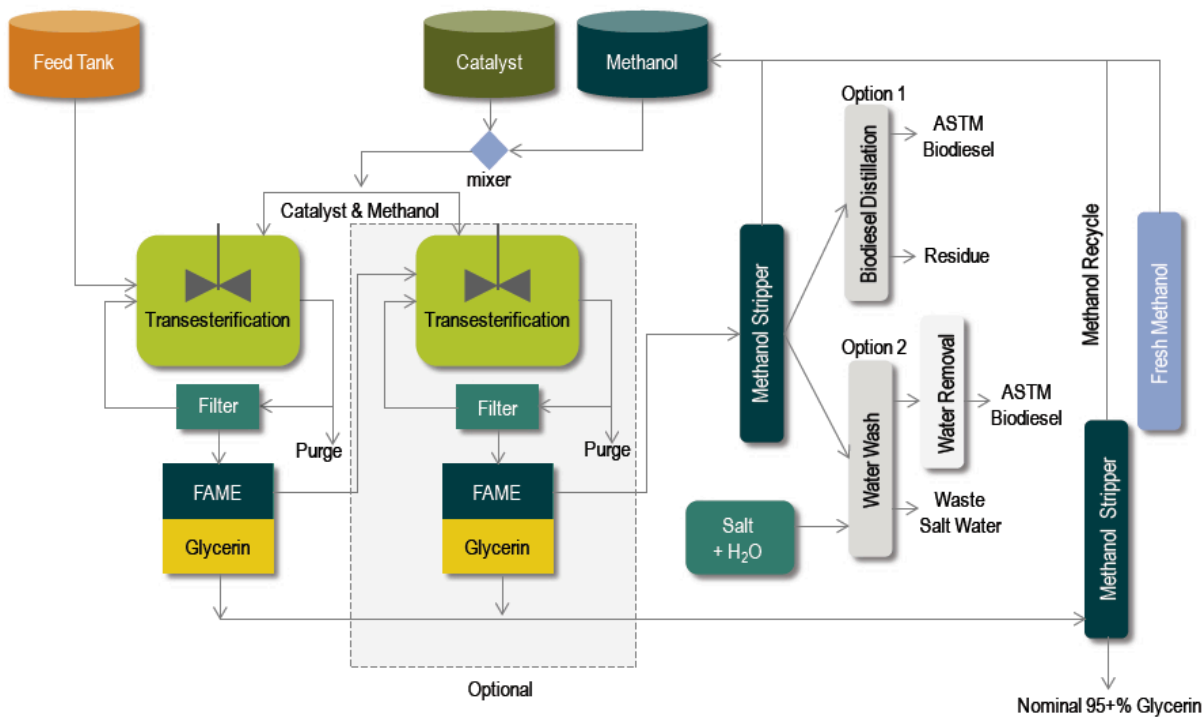


Figure 4.11. Simplified process of the biodiesel process with T300 catalyst.



Trials were performed on five different algal oil feedstocks from NAABB partners. The algal oils that were received varied significantly in quality. Upon receipt, the oils were analyzed and then subsequently pretreated prior to transesterification. Degumming experiments were run on some feedstocks to determine if metals and phosphorus reduction provided improved processing advantages. Through these experiments, it was discovered that T300 is tolerant to moderate metals and phosphorus levels and degumming was not necessary to utilize T300 in transesterification for the short-term conversion of the oils to FAMES. As mentioned previously, greater testing of the effect of concentration of phosphorus levels on the longevity of the T300 catalyst are warranted. FFA reduction technologies were necessary for most feedstocks to reduce the FFA content to the approximate 1% FFA target range suitable for transesterification with T300. Glycerolysis proved to be particularly effective in the FFA reduction of algal oil and surrogate feedstocks. Glycerolysis provides flexibility to treat higher FFA feedstocks than other pretreatment methods, serves as a way to dry feedstocks, and eliminates the need for methanol rectification following pretreatment. The glycerin generated from the T300 transesterification process is of technical grade (nominally 95%) purity, so it is well suited for utilization in glycerolysis pretreatment without further purification. Algal oil feeds were reduced from 35% to 1.9% FFA with glycerolysis. Surrogate feeds with very high FFA content (up to 93%) were similarly reduced with glycerolysis. Albemarle designed and simulated these pretreatment systems to support the T300 solid catalyst transesterification system and determine the T300 technology limits of application. A kinetic model for the glycerolysis reactions using nonlinear regression of reaction rate data was obtained.¹

Processing crude algal lipid extract into refined oil suitable for transesterification will likely impact fuel yield significantly. Generally, more aggressive algal biomass lipid extraction techniques improve overall lipid yield from biomass but result in a crude extract requiring greater purification. In addition to a greater concentration of trace metals and heteroatoms, more non-TAG organic species (especially membrane lipids not suitable for transesterification) will be extracted. On the other hand, less severe extraction techniques may provide algal oil requiring less purification but at the expense of overall lipid yield. For example, the *N. salina* crude lipid extract was converted to FAMES via sulfuric-acid-catalyzed esterification with excess methanol. The sulfuric-acid-catalyzed esterification converted TAGs and FFAs to FAMES. Only about half (by weight) of the original crude oil was successfully converted to FAMES. The balance of the organic material was later determined to primarily consist of membrane lipids not convertible to FAMES. Thus, transesterification would be limited to about 50% yield to fuel from the original crude extract. Hydrotreating, on the other hand, was shown to successfully convert the membrane lipid fraction to hydrocarbons. Further evaluation of the hydrotreating option with crude extracts is also warranted because the heteroatoms present in membrane lipids (e.g., N, P) would likely significantly impact catalyst life. Thus, algal oil purification and the implications of the organic and inorganic species present should be strongly considered for future research.

Decarboxylation

In addition to hydrodeoxygenation, limited research was done in NAABB on an alternative approach based on decarboxylation. Decarboxylation is an emerging technology that has lower (i.e., nonstoichiometric) hydrogen demand. Ideally, the oil would be converted to an FFA stream before catalytic decarboxylation to hydrocarbons allowing glycerol to be used for higher-value chemical conversion.² FAMES have also been demonstrated as suitable feedstocks for decarboxylation processes.³ Decarboxylation produces hydrocarbons with one carbon less than the starting molecule through the removal of CO₂. For production of fuel, the hydrocarbons produced from algae would require further refining via isomerization/cracking to meet fuel specifications such as the cold point unless blended at a relatively low level into the fuel pool.

Generally, saturated fatty acids are preferred as feedstock for decarboxylation but NAABB members demonstrated conversion of both FFAs derived from oils as well as FAME oils to hydrocarbon products suitable for further processing to fuels. Tests focused on algal-derived lipids extracted from the unidentified algae. Based on the nature of the extraction performed, the lipid extract was received as a mixture of FAMES. High-throughput catalyst screening was initiated using the lipid as feedstock but challenges were encountered immediately. The oil had a significant concentration of entrained solids, which could be removed by centrifuging. However, the decanted oil still contained high concentrations of inorganic materials such as sodium and sulfur. Sodium and sulfur are known to poison the state-of-the-art precious metal deoxygenation catalysts that were being screened. To remove the inorganic impurities, purification of the algal-derived lipids through treatment with Grace Davison Trisyl® Silica was investigated. The Trisyl® Silica is used commercially for the removal of phospholipids from edible oils. Processing with the Trisyl® Silica was useful for removing essentially all of the sodium and about 30–50% of the sulfur. However, about 50–60 ppm of sulfur was likely in a form not readily absorbed by the Trisyl® Silica and remained in the oil.

The FAMES were further purified by fractional distillation of the centrifuge- and silica-treated sample. The distilled sample primarily consisted of methyl linolenate (C18:3) and methyl docosaheptaenoate (C22:6) FAMES. This sample was chosen as a feedstock for high-throughput catalyst deoxygenation screening as a “worst-case scenario” feed because previous experience revealed deoxygenation catalysts are less active with unsaturated feedstocks. Of the 17 catalysts screened for deoxygenation activity, none produced more than 15 wt% deoxygenated alkanes after 4 hours at 300°C. Furthermore, a significant portion of the products could not be identified by gas chromatography–flame ionization detection (GC-FID). It was hypothesized that the unaccounted products were high-molecular-weight material formed by bimolecular reaction of two FAMES along points of unsaturation on the acyl chain. The high molecular weight material was likely not volatile enough for analysis on the GC-FID and was therefore not catalogued as a product. While none of the catalysts tested had significant activity, two catalysts did have slightly higher activity than the other catalysts. The second-best catalyst was chosen due to the availability of the catalyst on an engineered (e.g., tableted) support for scale-up testing in a laboratory-scale (20 cm³) fixed-bed reactor. Laboratory fixed-bed reactor testing



commenced using the same silica pretreated FAMES. Low yields of 0.25–0.35 g alkane/g feed were observed. Regardless, about 55–60 wt% of the products were not identified via GC-FID. The likely culprit for the low carbon balance was again thought to be bimolecular reaction of the FAMES at points of unsaturation on the acyl chains, which produced high boiling point (i.e., non-GC-able) material.

Summary of Conversion of Algal Oil to Fuel Projects

Hydrotreating is capable of converting non-TAG organic compounds such as FFAs, FAMES, membrane lipids, carbohydrates, and proteins that may have been extracted with the TAGs. On the other hand, transesterification requires refined TAGs because other organic impurities (especially FFAs) will rapidly foul the catalyst. Furthermore, the high concentration of unsaturated lipids in most algal species results in biodiesel produced from algal-derived TAGs being unsuitable as fuel due to oxidative instability. The unsaturated nature of the lipids is also challenging for decarboxylation, which is typically performed with saturated FFAs or FAMES. Each process requires targeted purification methods. Metals and phosphorus would likely quickly deactivate the hydrotreating and decarboxylation catalysts whereas the transesterification catalyst was tolerant of these metals over the short term. In contrast, hydrotreating and decarboxylation can readily accept the FFAs that rapidly deactivate the transesterification process. Thus, lipid and bio-oil extraction, purification, and catalyst stability testing in the presence of numerous relevant impurities should be a focus of continued future research.

Conversion of Lipid Extracted Algae (LEA) and/or Whole Algal Biomass

A variety of LEA and whole algal biomass conversion technologies were evaluated with various feedstocks provided by the NAABB partners. Two categories of fuel conversion technologies were examined: biological conversion and thermochemical conversion.

Biological Conversion

The biological conversion of LEA to fuel was studied. NAABB utilized one technology whereby the carbohydrates present in LEA were converted biochemically to salts of volatile fatty acids. As shown in Figure 4.12, the fatty acid salts were then treated thermochemically in sequential steps to first form ketones; then they were hydrogenated to alcohols. The alcohols were then dehydrated, oligomerized, and hydrogenated to hydrocarbon fuel.

NAABB also investigated the biological conversion of the carbohydrate/protein fractions of LEA into ethanol using enzymatic and fermentation bioreactors. The goal of this component of NAABB was to develop an engineered process to convert LEA to an additional fuel product, ethanol, which has greater fuel and economic value than biogas.



Figure 4.12. A process flow diagram demonstrating the various stages of the LEA biochemical conversion process to hydrocarbon fuels.

Additional benefits of this conversion process over gasification/liquefaction processes include the ability to produce a wide range of fuel and nonfuel molecules using the same platform and the ability to convert primarily the carbohydrate fraction of LEA, leaving a protein product that can be obtained for use as an animal feed supplement.

A schematic of the conceptual process for converting LEA to ethanol is shown in Figure 4.13. Carbohydrates in LEA are converted to fermentable sugars by either acid hydrolysis or enzymatic hydrolysis, and, optionally, proteins are deconstructed to peptides. The products of those two deconstruction steps are fermented to ethanol. To achieve the project goal of developing this process, experimental and computational tasks were conducted to obtain data on the rates and yields of deconstructing LEA carbohydrates to fermentable sugars. In addition, experiments were done to determine if any fermentation inhibitors were produced during the carbohydrate deconstruction process and to evaluate the effects of process variables such as temperature and pH. Process design methods were used to evaluate the tradeoffs among process options, such as yield versus reagent cost. Furthermore, advanced bioprocessing alternatives, including simultaneous saccharification and fermentation and continuous-flow, immobilized processes were evaluated. A preliminary process design analysis showed that when a batch acid hydrolysis process is used, ethanol production costs are approximately \$2 per gallon. Further analyses of enzymatic and continuous processes are suggested as further work.

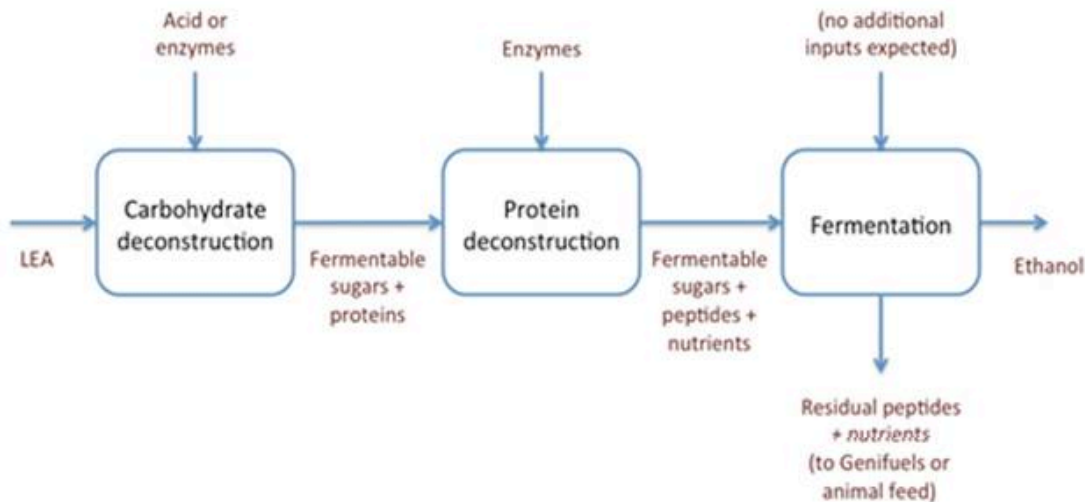


Figure 4.13. Process flow diagram for LEA biochemical conversion route to ethanol.

Thermochemical Conversion

Thermochemical conversion of LEA or whole algae was investigated via various routes. One such route involved the reactive extraction at high temperature and pressure with methanol, which simultaneously extracted lipids and produced a biocrude material rich in FAMES from whole algae. NAABB partners demonstrated that the biocrude could be fractionated/refined to produce FAMES suitable as a biodiesel blend stock. Alternatively, the biocrude could be upgraded via hydrotreating to convert the FAME-rich material into hydrocarbons. A significant



portion of the hydrocarbons produced during hydrotreating consisted of n-alkanes that would be further refined to produce blend stocks for jet and/or diesel fuel. The proteinaceous fraction of the residual material left after reactive extraction with methanol was investigated as a feedstock for a process to produce ethanolamines. Ethanolamines are precursors for the production of detergents, emulsifiers, and other chemicals. The conversion of amino acids derived from algae, parametric studies (reactor temperature and residence time) with different catalysts, and an economic evaluation for scale-up to a continuous version of the aforementioned process were performed. A proposed process flow diagram is shown in Figure 4.14. Chemically, the goal is to convert LEA via catalytic decarbonylation to ethanolamines. Investigations were performed with a fixed-bed catalytic reactor using a 5 wt% Ru on carbon catalyst sample. It was determined the chloride in the LEA must be minimized for optimal catalyst activity and stability. After reaction, the ethanolamines were separated and purified via fractional distillation. A preliminary plant-cost analysis was performed and it was determined that ethanolamines add value as a secondary product from the mass leftover after lipid extraction.

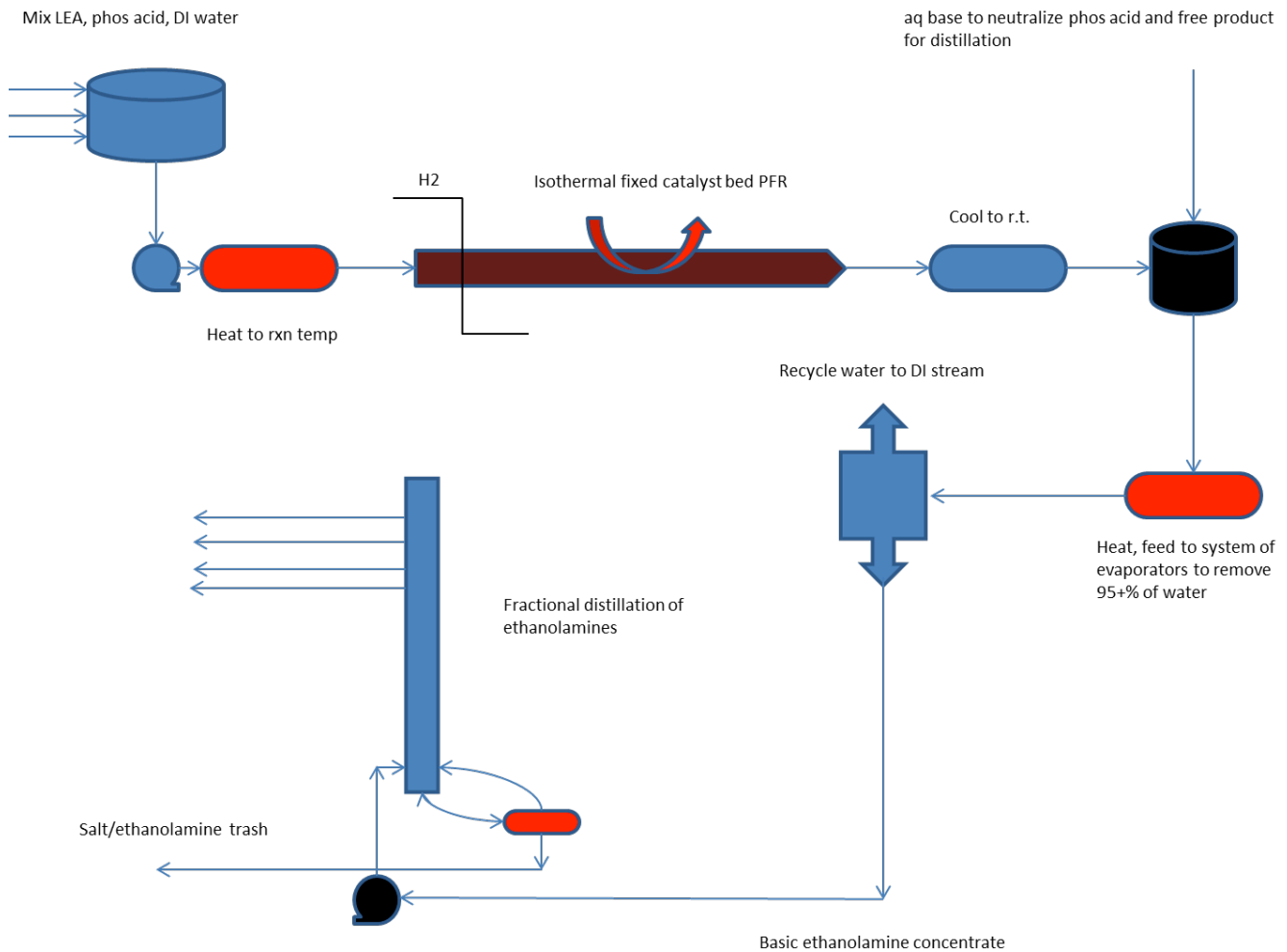


Figure 4.14. Proposed process flow diagram for the production of ethanolamines from LEA produced by reactive methanol extraction of whole algal biomass.

LEA and whole algae were also converted to fuel/energy by hydrothermal processing, utilizing both hydrothermal liquefaction (HTL) and catalytic hydrothermal gasification (CHG) technologies. Figure 4.15 contains schematic diagrams of the HTL process and Figure 4.16 contains photographs of the wet algal paste feedstock, HTL bio-oil, hydrotreated bio-oil, and fractionated cuts. The HTL process converts the lipids present in LEA (leftover from the extraction process) or whole algae to FFAs or fatty acid derivatives. A portion of the carbohydrate and protein fraction of LEA or whole algae is also converted to bio-oil. The bio-oil is subsequently upgraded via hydrotreating to produce hydrocarbons. Because a portion of the nonlipid fraction of the algal biomass is also converted to bio-oil, fuel yields greater than conversion technologies that rely on lipid extraction are possible. For example, HTL conversion and upgrading produced 37% more hydrocarbon fuel than a process whereby lipids were extracted from the same algae and upgraded via hydrotreating.

HTL Processing of LEA at PNNL

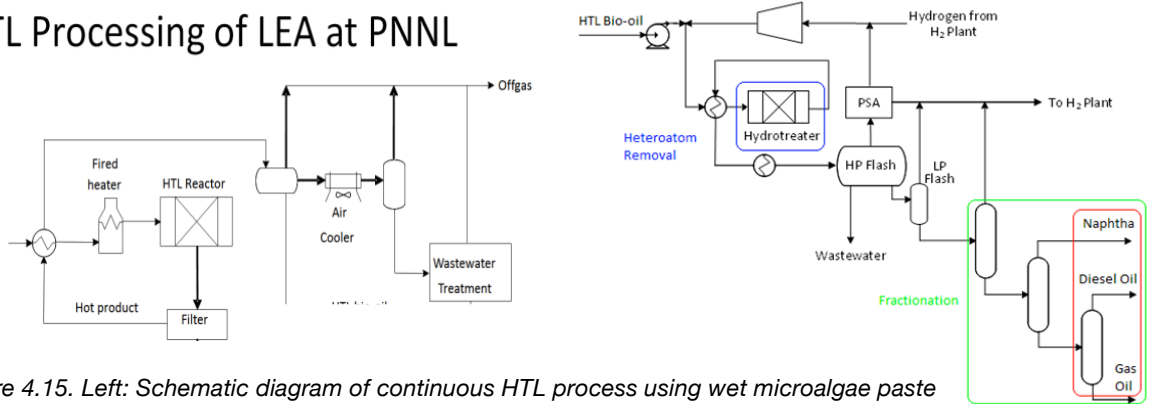


Figure 4.15. Left: Schematic diagram of continuous HTL process using wet microalgae paste as feedstock. Right: schematic diagram of upgrading process, which consists of hydrotreating, hydrocracking/isomeration, and fractionation.

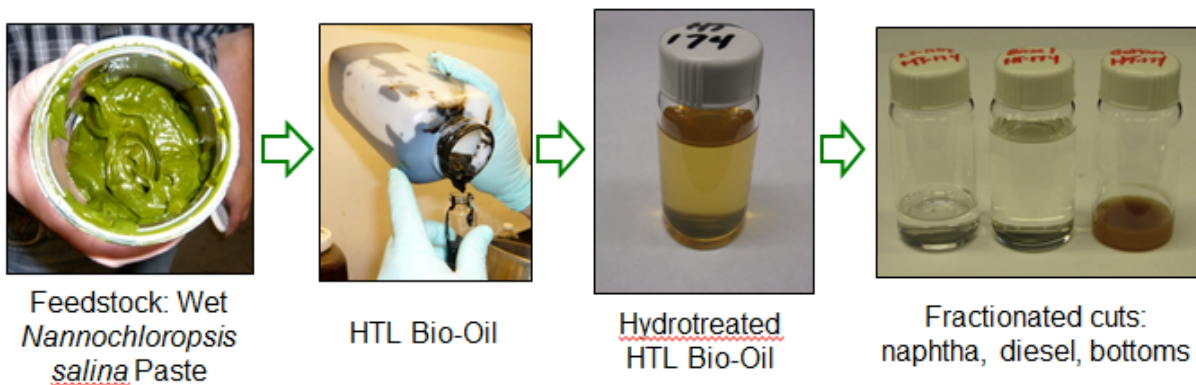


Figure 4.16. HTL process starting with wet algae paste, conversion to HTL bio-oil, upgrading to hydrocarbons, and fractionation. The final process can be readily tailored to create jet fuel and/or diesel fuel cuts.



CHG converts LEA or residual organic contaminated aqueous process streams to methane gas. The methane can be used directly as fuel or be reformed to make hydrogen for upgrading the HTL bio-oil to hydrocarbon fuels. The process is shown in Figure 4.17.

HTL and CHG can be combined into an integrated fuel process that is able to capture 85% of the carbon in algae as fuel-grade components. The hypothetical operation is shown in Figure 4.18. The combined HTL-CHG technology was demonstrated on three algae samples: (1) *N. salina* LEA, (2) *N. oceanica* (low lipid), and (3) *N. oceanica* (high lipid). In each case the algae was first run through HTL, which produced an oil stream and an effluent water stream containing all organic content not converted to oil or gas. The effluent water stream was then processed with CHG to recover additional fuel in the form of a methane gas/carbon dioxide mixture. Table 4.8 below shows key process parameters for the combined HTL-CHG conversions.

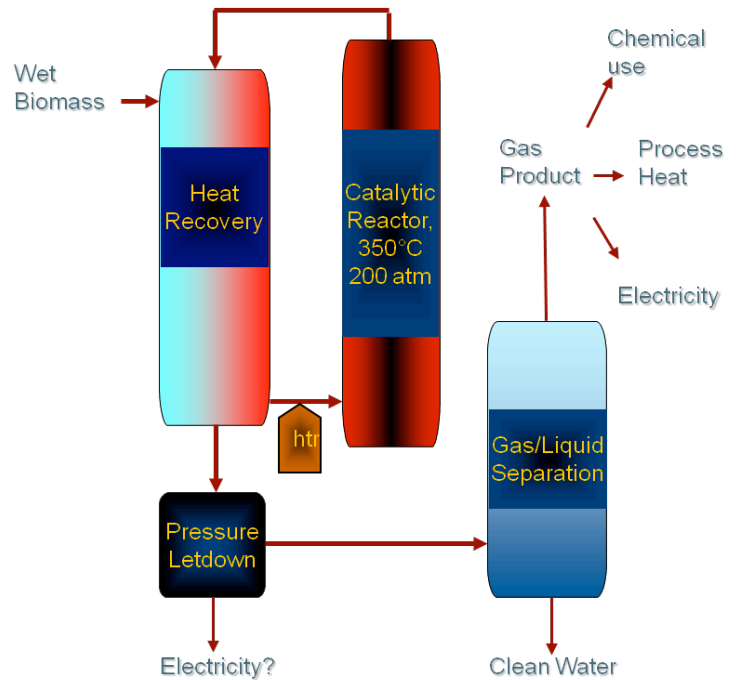


Figure 4.17. CHG converts residual carbon in water to a medium BTU gas (CH + CO).

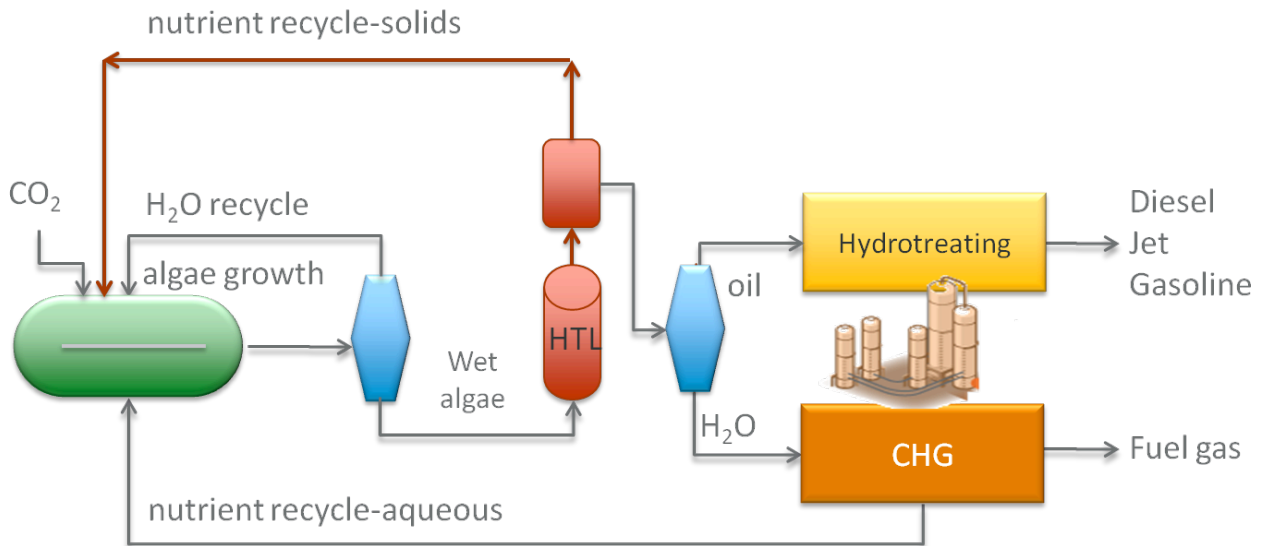


Figure 4.18. Schematic diagram of integrated HTL and CHG process.

Based on the high fuel-conversion efficiency of hydrothermal processing, NAABB is designing and building a 1 ton/day unit capable of performing HTL or CHG processing for continuous outdoor testing with freshly harvested algae. Some specifications of the pilot system are shown in Table 4.9.

Table 4.8. Key parameters and results of combined HTL/CHG testing with LEA and whole algae feedstocks.

Analysis of Biofuel Production from Algae Feedstocks			
Item	<i>N. salina</i> LEA	<i>N. oceanica</i> (Low Lipid)	<i>N. oceanica</i> (High Lipid)
Feedstock converted to bio-crude, ash-free dry weight %	53.2	60.8	63.6
Feedstock carbon converted to biocrude, weight %	72.2	74.5	73.6
Feedstock carbon in effluent water, weight %	26.1	14.0	15.7

Table 4.9. Specifications of the HTL/CHG pilot-scale system.	
Wet feedstock capacity	1 t/d
Solids concentration of feed	20%
Total dry equivalent weight of feed	200 kg/d
Target oil yield as % afdw	50%
Total oil output per day	0.65 bbl/d
Operational date	Q3 2014

In addition to providing additional conversion of feedstock to fuel, the CHG portion of a combined HTL-CHG system also provides effective wastewater treatment by reducing the organic content of the HTL effluent. Reductions in chemical oxygen demand (COD) of 99.9% were reported, with final COD as low as 300 mg O₂/L. The effluent water also contains plant nutrients including nitrogen, potassium, and trace metals. Phosphorus is recovered as a solid precipitate, which can be processed with conventional fertilizer methods to give phosphorus fertilizer. Since the water is sterile, it can be recycled back to the algae growth water for additional production. Nutrient recycle is an important factor in overall cultivation cost.

Thermochemical conversion of dry algal biomass can be accomplished by pyrolysis as well. Research demonstrated a crude bio-oil production by pyrolysis of dry algae. The disadvantages for this route to bio-oil are the need for dry feedstock, the high yield of char product, and the formation of highly condensed nitrogen-containing compounds.

Conclusions and Recommendations

The Fuel Conversion team demonstrated the technical feasibility of fuel production from algae via various pathways, routes, and technologies. These include mid-distillates (jet fuels) and distillates (diesel). The NAABB algae-derived fuels met stringent specifications for jet and military applications.



However, for commercial viability, further work is needed for the pretreatment and removal of impurities contained in algal feedstocks.

Characterization of a wide range of algal-derived oils identified key contaminants that must be removed before upgrading to fuels. This included the algae-derived HTL bio-oils, which contained high levels of metals that would likely lead to catalyst deactivation during the extended operation of a commercial process.

Characterization also demonstrated the wide range of variability in algae composition as a function of species and cultivation conditions. Key to fuel conversion is producing algae or algae-derived oils in large quantities at a competitive price. As techno-economic sensitivity analyses showed, conversion/upgrading costs are most sensitive to feedstock cost, followed by the process scale.

For fuel production, the scale and cost of algae production must be improved. Implementation of alternative direct conversion technology such as HTL allows utilization of all algal biomass components for hydrocarbon fuel production, not just the lipid component.

Processing the LEA is an important part of the algae economics that must be addressed to allow for the recycle of important nutrients and micro-elements back to the algae ponds. Without a process for handling the LEA, the algae production process could not reach scales that would make an important impact in the energy economy.

From the compositional analysis of the LEA, it was clear that most LEA samples were not of good quality for any biological process due to their high ash content. Only one LEA sample had low ash content. In addition, even that LEA had an intrinsic lower digestibility relative to other biomass feedstocks, which was attributed in part to components that were inhibitory to the microorganisms (e.g., residual fatty acids) and also due to innate recalcitrance of certain components (e.g., proteins).

Accomplishments

The specific accomplishments of the Fuel Conversion team include the following:

- Processed seven different algae species to hydrocarbon fuel, including one species developed specifically by NAABB and cultivated and extracted using the Valicor Process from material grown at the Texas AgriLife Pecos test bed.
- From NAABB species, we produced liter quantities of hydrocarbons using the UOP Green Jet™ process treating lipids, FAMES and HTL bio-oil. The hydrotreated material was distilled and the fuels met nearly all specifications for jet and diesel fuel.
- Characterized lipid extracts and bio-oils from a wide range of process technologies, including dry hexane extraction, wet hexane extraction, reactive methanol extraction/ conversion to FAMES, and HTL.



FUEL CONVERSION

- Characterized algae-derived biodiesel demonstrating the correlation of fatty acid profile to important biodiesel fuel stability and internal combustion properties.
- Developed a new characterization technique (FT-ICR mass spectrometry) that provides more detailed information about the extractable components.
- Demonstrated the technical feasibility of eight conversion and upgrading pathways to potential commercial fuel products for a wide range of various algal feedstocks, lipid extracts, and bio-oils.
- Demonstrated the conversion of LEA via biochemical routes to produce ethanol or volatile fatty acids.
- Developed Aspen Plus process models for eight fuel production pathways from lipid, LEA, and whole biomass (Figure 4.19).
- Demonstrated viability of direct conversion of dewatered biomass via HTL that does not require solvent extraction.
- Designed and are building (as of February 2014) a 1 ton/day unit capable of performing HTL or CHG processing.

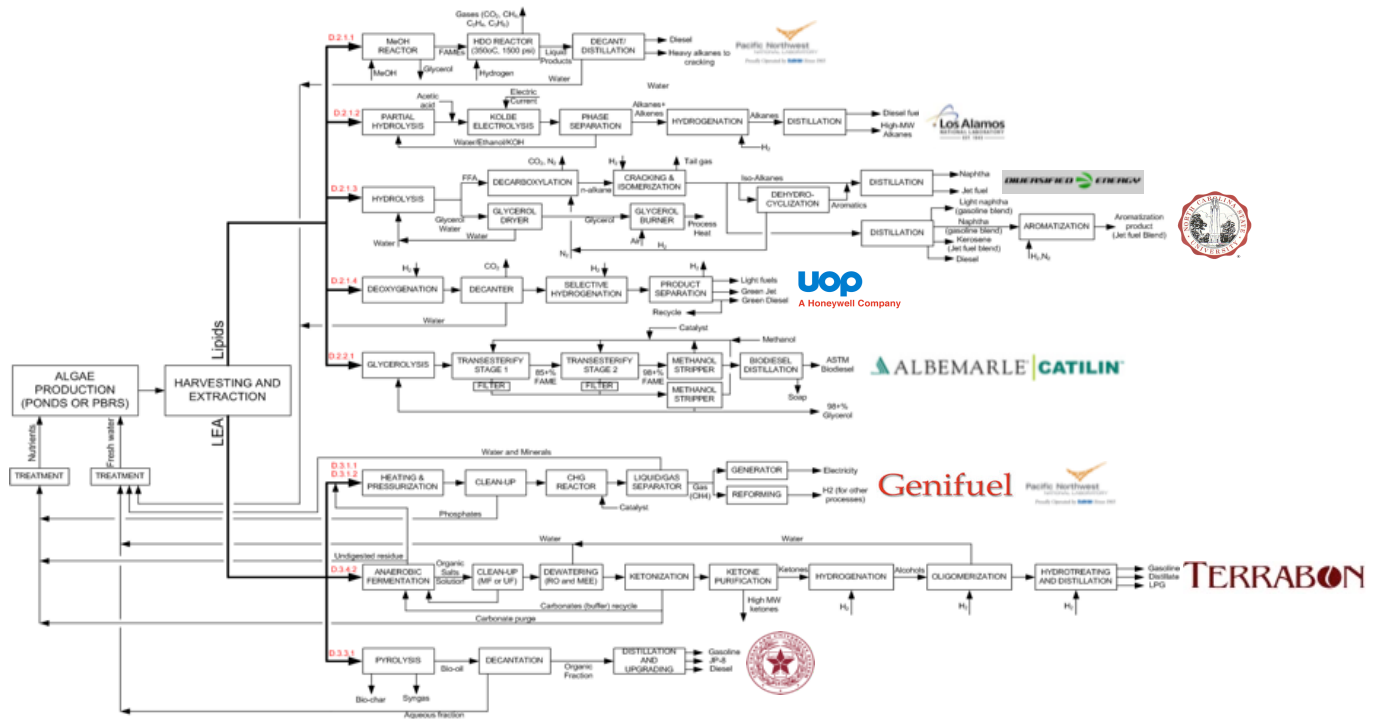


Figure 4.19. Full Aspen simulation models were built on eight process models, including most shown in above. Note: We do not have a model on Kolbe coupling but we do have an Aspen model on ethanol production (not shown).



Team Members

Karl Albrecht, Pacific Northwest National Laboratory
Sergio Capareda, Texas A&M University
Scott Cheney, Diversified Energy
Shuguang Deng, New Mexico State University
Douglas Elliott, Pacific Northwest National Laboratory
Cesar Granda, Terrabon
Richard Hallen, Pacific Northwest National Laboratory
Steve Lupton, UOP
Sharry Lynch, UOP
Anthony Marchese, Colorado State University
Jennifer Nieweg, Albemarle
Kim Ogden, University of Arizona
Jim Oyler, Genifuel
Ken Reardon, Colorado State University
William Roberts, North Carolina State University
Dave Sams, Albemarle
Tanner Schaub, New Mexico State University
Pete Silks, Los Alamos National Laboratory

Publications

Full-length, Peer-reviewed Publications

Bucy, H., M. Baumgardner, and A.J. Marchese. Chemical and physical properties of algal methyl ester biodiesel containing varying levels of methyl eicosapentaenoate and methyl docosahexaenoate. *Algal Research* 1 (2012): 57–69.

Bucy, H. and A.J. Marchese. Oxidative stability of algae derived methyl esters. *Journal of Engineering for Gas Turbines and Power* 134 (2012): 092805.

Crowe, B., S. Attalah, S. Agrawal, P. Waller, R. Ryan, K. Ogden, J. Van Wagenen, M. Kacira, J. Kyndt, and M. Huesemann. A comparison of *Nannochloropsis salina* growth performance in two outdoor pond designs: conventional raceways versus the ARID raceway with superior temperature management. *The International Journal of Chemical Engineering* (2012): Article ID 920608.

Elliott, D.C., T.R. Hart, G.G. Neuenschwander, L.J. Rotness, M.V. Olarte, and A.H. Zacher. Chemical processing in high-pressure aqueous environments. 9. Process development for catalytic gasification of algae feedstocks. *Industrial and Engineering Chemical Research* 51 (2012): 10768–10777.

Elliott, D.C., T.R. Hart, A.J. Schmidt, G.G. Neuenschwander, L.J. Rotness, M.V. Olarte, A.H. Zacher, K.O. Albrecht, R.T. Hallen, and J. E. Holladay. Process development for hydrothermal liquefaction of algae feedstocks in a continuous-flow reactor. *Algal Research* 2 (2013): 445–454.

Fagerstone, K., J.C. Quinn, S. De Long, T. Bradley, and A.J. Marchese. Quantitative measurements of direct nitrous oxide emissions from microalgae cultivation. *Environmental Science and Technology* 45 (2011): 9449–9456.

Gude, V.G., P. Patil, E. Martinez-Guerra, S. Deng, and N. Nirmalakhandan. Microwave energy potential for biodiesel production. *Sustainable Chemical Processes* 1 (2013): 5.

Gude, V.G., P.D. Patil, and S. Deng. Comparison of direct transesterification of algal biomass under supercritical methanol and microwave irradiation conditions. *40th ASES National Solar Conference 2011, SOLAR 2011* 1 (2011): 376–382.

Holguin, F.O. and T. Schaub. Characterization of microalgal lipid feedstock by direct-infusion FT-ICR mass spectrometry. *Algal Research* 2 (2013): 43–50.

Patil, P.D., V.G. Gude, A. Mannarswamy, P. Cooke, S. Munson-McGee, N. Nirmalakhandan, P. Lammers, and S. Deng. Optimization of microwave-assisted transesterification of dry algal biomass using response surface methodology. *Bioresource Technology* 102 (2011): 1399–1405.

Patil, P.D., V.D. Gude, A. Mannarswamy, P. Cooke, S. Munson-McGee, N. Nirmalakhandan, P. Lammers, and S. Deng. Comparison of direct transesterification of algal biomass under supercritical methanol and microwave irradiation conditions. *Fuel* 97 (2012): 822–831.

Patil, P.D., V. Gude, H.K. Reddy, T. Muppaneni, and S. Deng. Biodiesel production from waste cooking oil using sulfuric acid and microwave irradiation processes. *Journal of Environmental Protection* 3 (2012): 107–113.

Patil, P.D., H. Reddy, T. Muppaneni, A. Mannarswamy, T. Schaub, F.O. Holguin, P. Lammers, N. Nirmalakhandan, P. Cooke, and S. Deng. Power dissipation in microwave-enhanced *in situ* transesterification of algal biomass to biodiesel. *Green Chemistry* 14 (2012): 809–818.

Patil, P.D., H. Reddy, H.T. Muppaneni, S. Ponnusamy, P. Cooke, T. Schaub, and S. Deng. Microwave-mediated non-catalytic transesterification of algal biomass under supercritical ethanol conditions. *Journal of Supercritical Fluids* 79 (2013): 67–72.

Patil, P., H. Reddy, T. Muppaneni, S. Ponnusamy, Y. Sun, P. Dailey, P. Cooke, U. Patil, and S. Deng. Optimization of microwave-enhanced methanolysis of algal biomass to biodiesel under temperature controlled conditions. *Bioresource Technology* 137 (2013): 278–285.

Patil, P.D., H. Reddy, T. Muppaneni, T. Schaub, F.O. Holguin, P. Cooke, P. Lammers, N. Nirmalakhandan, Y. Li, X. Lu, and S. Deng. *In-situ* ethyl ester production from wet algal biomass under microwave-mediated supercritical ethanol conditions. *Bioresource Technology* 139 (2013): 308–315.

Sudasinghe, N., B. Dungan, P.J. Lammers, K. Albrecht, D. Elliott, R. Hallen, and T. Schaub. High resolution FT-ICR mass spectral analysis of bio-oil and residual water soluble organics produced by hydrothermal liquefaction of the marine microalga *Nannochloropsis salina*. *Fuel* 119 (2013): 47–56.

Teiseh, E. and S. Capareda. Efficient cycle recovery of hydrogen from a low concentration pyrolysis gas stream by pressure swing adsorption – An experimental evaluation. *Separation Science and Technology* 47 (2012): 1522–1530.

Teiseh, E.A., S. Capareda, and Y.H. Rezenom. Cobalt based hybrid Fischer-Tropsch synthesis catalyst for improved selectivity of hydrocarbons in the JP-8 carbon number range from a synthesis gas obtained from the pyrolysis of the MixAlco process derived sludge. *Applied Catalysis A, General* 437-438 (2012): 63–71.



Teiseh, E.A. and S. Capareda. Maximizing the concentrations of hydrogen, carbon monoxide and methane produced from the pyrolysis of a MixAlco process derived sludge. *Journal of Analytical and Applied Pyrolysis* 102 (2013): 76–82.

Zhu, Y., K.O. Albrecht, D.C. Elliott, R.T. Hallen, and S.B. Jones. Development of hydrothermal liquefaction and upgrading technologies for lipid-extracted algae conversion to liquid fuels. *Algal Research* 2 (2013): 455–464.

Other Important Publications

Albrecht, K.O. and R.T. Hallen. A brief literature overview of various routes to biorenewable fuels from lipids for the National Alliance for Advanced Biofuels and Bioproducts (NAABB) Consortium. PNNL-20279 (2011):

http://www.pnnl.gov/main/publications/external/technical_reports/PNNL-20279.pdf.

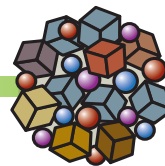
Lupton, F.S. The refining of algal oils into fungible transportation fuels. (2012):

<http://biomassmagazine.com/articles/7672/the-refining-of-algal-oils-into-fungible-transportation-fuels>.

References

1. Silva, C.S., E. Soliman, G. Cameron, L.A. Fabiano, W.D. Seider, E.H. Dunlop, and A.K. Coaldrake. Commercial-scale biodiesel production from algae. *Industrial & Engineering Chemistry Research* (2013): DOI 10.1021/ie403273b.
2. US patents 6841085 and 7038094
3. Kubičková, Iva, Mathias Snåre, Kari Eränen, Päivi Mäki-Arvela, Dmitry Yu. Murzin. Hydrocarbons for diesel fuel via decarboxylation of vegetable oils. *Catalysis Today* 106 (1-4) (2005): 197-200.

AGRICULTURAL COPRODUCTS



Introduction

Team Leads

Shanna Ivey, New Mexico State University
Tryon Wilkersham, Texas A&M University

Preface

The aquaculture market has been the fastest growing sector of agriculture and hence there has been an increase in world demand for fish products and fish meal, which is the traditional ingredient in fish diets.¹ Furthermore, animal nutrition is the most costly component in modern animal production and additional, less expensive sources of protein are attractive to the industry.² Since algal meal has not been approved for feeding livestock, the scientific literature was very limited on the use of algae or lipid extracted algae (LEA) as animal and mariculture feed. However, standard methods for feed evaluation of quality and palatability are widely available and were used in the National Alliance for Advanced Biofuels and Bioproducts (NAABB).

Under ideal conditions, most algal biomass typically contains less than 50% total lipid. When using a lipid extraction processing route to make algal biofuels, the remaining coproduct, LEA, will be produced in excess of the actual product, biofuel. Therefore, the economic and environmental sustainability of algal biofuel production for the lipid extraction route is dependent on identifying markets of sufficient scale and value for the LEA coproduct. Accordingly, NAABB sought to identify and test the ability of LEA to enter various agricultural coproduct markets for feeds and fertilizers. Potential markets for LEA and LEA-derived products must be capable of incorporating LEA without saturating the market such that the value of LEA becomes marginalized. Additionally, the intended market for LEA should enhance environmental sustainability of biofuel production from algae. Livestock and mariculture feeding systems satisfy these criteria. Livestock systems have consistently demonstrated their ability to utilize large quantities of coproducts from biofuel production to provide valuable products to humans.³ At the initiation of the NAABB consortium, the Agricultural Coproducts team identified six potential agricultural markets to research as potential utilizers of LEA: cattle, sheep, swine, shrimp, fish, and fertilizer. Our research focused on evaluating various sources of LEA from different algal strains and processing methods to determine their nutritional value for both feed and fertilizer applications.

Due to potentially diverse sets of algal species types and variations in production methods (cultivation, harvesting, and extraction) it is important to understand how these variables could influence the composition and performance of the various LEA coproducts generated. NAABB was able to secure a large quantity of LEA produced by General Atomics under a Defense Advanced Research Projects Agency (DARPA) program that produced large quantities of lipid extracts using a conventional dry solvent extraction process. These large quantities of LEA were used in large animal feed trials and fertilizer trials. In addition, NAABB produced

multiple batches of smaller quantities of LEA from selected algal species that were cultivated within our cultivation test beds and processed by a wet solvent extraction process developed by Valicor. These smaller LEA batches were used for determining feed values through *in vitro* nutritional analysis methods and for conducting maricultural feeding trials with fish and shrimp, which required much smaller quantities of LEA.

Approach

The research followed the R&D framework for the Agricultural Coproducts task (Figure 5.1). One major thrust was animal-feed development and testing of LEA coproducts. This included *in vitro* and *in vivo* nutritional-value experiments, maricultural-feed studies (fish and shrimp), ruminant-animal-feed studies (cattle and sheep), and nonruminant-animal-feed studies (swine and chickens). The other thrust area was fertilizer evaluations. This included both small greenhouse studies and some limited field trials.

Agricultural Coproducts Task Framework

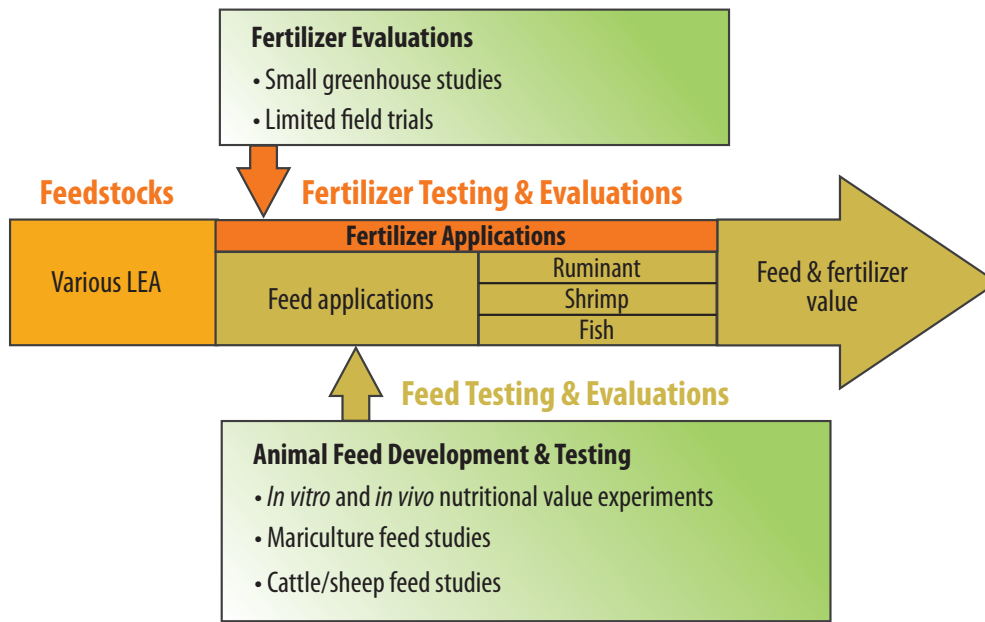


Figure 5.1. Agricultural Coproducts task framework.

Technical Accomplishments

Nutritional Value Determinations for Various LEA Samples

Determinations of feed value were made on three types of algae: *Nannochloris oculata* (marine algae), *Chlorella* sp. (freshwater algae), and *Navicula* sp., (a marine diatom algae). Extraction of both the *Navicula* sp. and the *Chlorella* sp. was completed prior to being received by the Agricultural Coproducts team. In contrast, the *N. oculata* was subjected to various upstream harvesting, drying, and extraction methods as shown in Figure 5.2 in a factorial design in an attempt to quantify the effect of upstream processing on the nutritive value of the resultant LEA. Processing variations include:

- Harvesting with or without chemical flocculants;
- Drying the algal biomass by spray drying (powder);
- Extrusion/pelleting (expanded collets), or drum drying (flakes); and
- Solvent extractions using ethanol, hexane, or methyl pentane at low or high temperature.

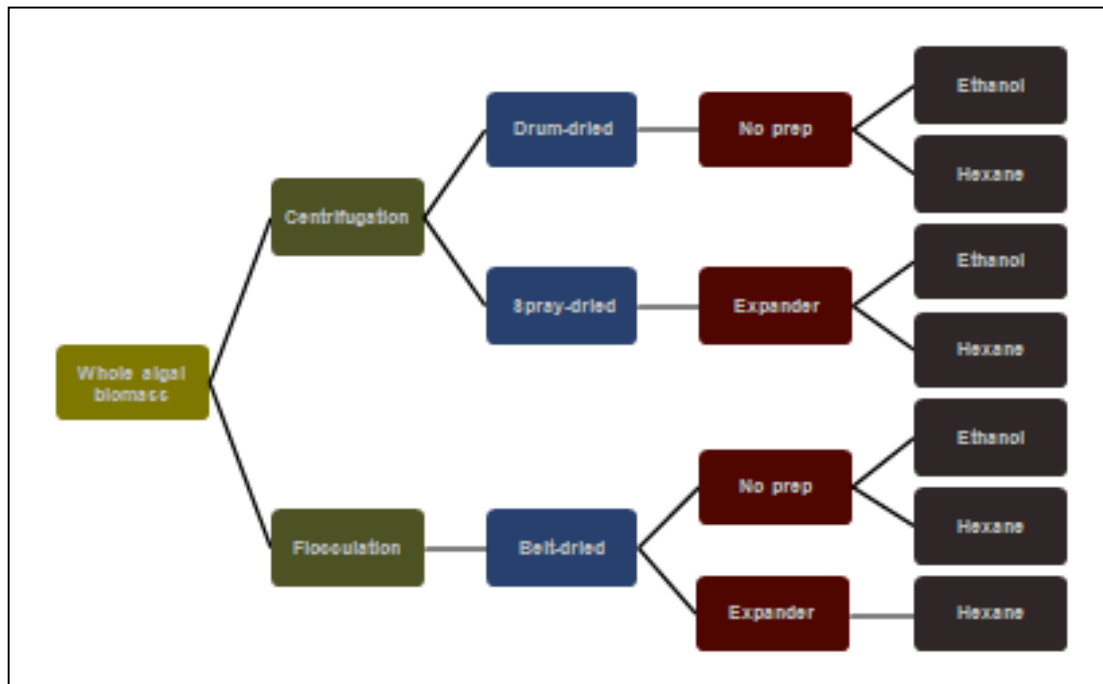


Figure 5.2. LEA Processing methods for *N. oculata*.

The data contained in Tables 5.1 and 5.2 give the results of significant differences found in the nutritive value determinations for proximate analysis and minerals/heavy metals content for these various algal species and processing methods. Ideally, additional replications of the factorial design would have occurred to increase our understanding of how upstream processes impact the effectiveness of lipid extraction and the feeding value of LEA.



Table 5.1. Proximate analysis of LEA from selected species using various cultivation and processing methods.

Species/Process ^a	Dry matter	Organic matter	Crude protein	Fat (EE) ^{**}	Fat (AH) [†]
	%				
<i>Navicula</i> sp.					
Process: S, H	95.3	39.6	11.8	0.31	1.19
<i>N. oculata</i>					
Process: F, E	90.1	75.8	34.2	0.2	2.44
Process: F, H	88.8	50.3	35.5	0.66	5.76
Process: Fl, C, H	92.8	52.2	38.1	1.9	3.63
Process: S, C, E	90.1	56.1	23.6	2.96	9.6
Process: S, C, H	90.8	53.3	23.2	2.93	8.4
Process: Fl, E	94.3	51	21.9	0.31	2.6
Process: Fl, H	92.7	42.4	18.8	0.68	3.61
<i>Chlorella</i> sp.					
Process: Fl, S, M, L	93.8	59	21.3	0.76	4.99
Process: Fl, S, M, Hi	95.8	56.8	20.2	1.56	4.73
Process: Fl, S, M, L, P	91.4	51.6	19.8	2.37	3.34
Process: Fl, S, M, Hi, P	91.6	48.7	20.4	1.93	1.99
^a Fl = flocculated, C = expanded collets, S = spray dried, F = flakes drum-dried, E = ethanol extraction, H = hexane extraction, M = methyl pentane extraction, L = low-temperature extraction, Hi = high-temperature extraction, P = pelleted.					
^{**} EE = ether extract fat. [†] AH = acid hydrolysis fat.					

Based on the analyses of these data, the feed value of LEA is largely driven by:

- Organic matter—The organic matter content ranged from 40% to 76%. Lower organic matter contents are a result of higher ash contents of LEA. This dilutes the valuable components of LEA (protein, lipids, and energy) which, by definition, decreases the price per ton. However, the ash has been shown to be beneficial as a regulator of intake and has the potential to add value to other feedstuffs.
- Crude protein—The protein content ranged from 12% to 38%. The high ash content dilutes the crude protein; however, on a protein basis, there is no data to suggest a discount relative to other feedstuffs.
- Residual lipid:—The residual lipid content ranged from 1% to 10%. Any lipid remaining in the LEA increases the energy content of the LEA and will translate into increased value. Optimization of lipid extraction methods for algae needs to include an assessment of the value of residual lipid in the LEA.
 - Fatty acids: Potential exists for essential fatty acids to further enhance the value of the LEA.

- Mineral content
 - Chemical flocculation significantly impacts the mineral profile of resultant LEA by increasing the concentrations of divalent cations (calcium, aluminum, iron, and manganese) and decreasing sodium levels associated with the algal biomass during harvesting from the addition of alum and/or ferric chloride as flocculants. This highlights the potential influence that upstream processes for harvesting can have on the value of LEA and the potential for toxicity.
 - Pond management: Utilization of toxic metals like copper to control competitors and predators in cultivation systems results in elevated copper concentrations of the LEA. This highlights the potential influence that upstream processes for cultivation pond management can have on the value of LEA and the potential for toxicity.
 - Even though potential metal toxicity issues are present, if the LEA is diluted as part of the total diet it will not likely be a cause for excessive concern and is manageable.

Table 5.2. Significant minerals and heavy metals differences in LEA from selected species using various cultivation and processing methods.

Species/Process*	Calcium	Sodium	Copper	Iron	Manganese	Aluminum
	%	%	ppm	ppm	ppm	ppm
Beef Cattle Toxicity**	—	—	100	1000	1000	1000
<i>Navicula</i> sp. Process: S, H	10.44	3.5	3.8	1510	64.9	191
<i>Nannochloris oculata</i> Process: F, E	3.72	2.55	2920	2260	60.3	2330
Process: F, H	2.99	5.25	2240	1740	46.3	1820
Process: Fl, C, H	10.21	1.17	1540	6890	121	9500
Process: S, C, E	5.7	4.81	2070	1950	57.5	2150
Process: S, C, H	5.28	4.95	2010	1980	55.7	2160
Process: Fl, E	10.76	0.95	1550	7240	132	9800
Process: Fl, H	11.28	1.05	1560	8160	142	11,600
<i>Chlorella</i> sp. Process: Fl, S, M, L	5.28	6.45	16.7	4540	71.7	4310
Process: Fl, S, M, H	6.18	6.61	15.8	5030	85.8	4130
Process: Fl, S, M, L, P	5.22	5.99	15.3	4240	75.4	3950
Process: Fl, S, M, H, P	6.92	5.54	13.4	5410	83.4	3530
*Fl = flocculated, C = expanded collets, S = spray dried, F = flakes drum-dried, E = ethanol extraction, H = hexane extracted, M = methyl pentane extraction, L = low temperature extraction, H = high temperature extraction, P = pelleted.						
**Toxicity is based on the level contained in the total diet not per ingredient.						

***In Vitro* Nutritional Value Determination for Ruminant Feeds**

Experiments were conducted using *in vitro* continuous flow fermentation systems to evaluate the digestibility of LEA derived from multiple algal strains and produced with different cultivation and extraction scenarios as shown in Figure 5.3.



Figure 5.3. *In vitro* fermentation methods.

In these experiments, two different feed types were prepared using six different LEA samples and a soybean meal (SBM) control. One feed-type formulation was for forage diets with approximately 15% LEA and 13% crude protein on a dry matter basis using either SBM or LEA. The other feed-type formulation was for high-starch diets with approximately 7% LEA and 12.5% crude protein on a dry matter basis using either SBM or LEA. The LEA materials were derived from either marine algal strains, *Nannochloropsis* sp., or freshwater algal strains, *Chlorella* sp. Data collected from the *in vitro* fermentation experiments included organic matter digestibility (OM), ammonia production, microbial efficiency, and volatile fatty acid production. Results for *in vitro* nutritional evaluation for forage diets and high-starch diets are shown in Tables 5.3 and 5.4, respectively. The data in Tables 5.3 and 5.4 give the results of differences found in the nutritive value determinations from *in vitro* fermentation studies for these LEA formulations. Based on the analyses of these data:

- Organic matter digestibilities were not influenced by LEA addition to forage diets. Organic matter digestibility increased with *Chlorella* LEA addition to high-starch diets but not with the *Nannochloropsis* LEA.



AGRICULTURAL COPRODUCTS

- Degradation of N was greater for the soy control than LEA treatments with forage diets. However, most LEA treatments were higher for the high starch diets.
- Total volatile fatty acids (VFA) were greatest for soy control in forage diets and increased when LEA was added to high-starch diets.
- Microbial efficiency (MOEFF) did not differ between soy and LEA in forage diets. In the high starch diets *Nannochloropsis* LEA decreased MOEFF. MOEFF results for *Chlorella* were more variable than *Nannochloropsis*. One *Chlorella* sp. LEA increased MOEFF by 36% over soy and the other *Chlorella* sp. decreased MOEFF by approximately 42% compared to soy.

Overall the results from both experiments are promising for LEA as a protein feedstuff in ruminant diets. Further research is necessary to fully understand what roles, interactions, and consequences algal strains and upstream processes play in LEA quality.

Table 5.3. Effects of LEA derived from *Nannochloropsis* sp. and *Chlorella* sp. on digestion and N metabolism in continuous culture fermenters in forage diets.

Measured Parameters	Forage Diet LEA Components						
	Control	<i>Nannochloropsis</i> LEA Formulations			<i>Chlorella</i> LEA Formulations		
	Soy	LEA 1	LEA 2	LEA 3	LEA 4	LEA 5	LEA 6
True OM digestibility, %	54.3	56.4	46.6	50.3	53.8	49.7	51.5
NH ₃ N, mg/100 mL	39.2	27.5	33.4	30.4	31.7	28.9	49.2
N degradation, % of N	84.1	75.4	79.6	66.6	73.7	65.3	82.2
Microbial efficiency	24.8	18.9	44.1	20.1	28.5	33.4	49.3
(g N/kg of OM truly digested)							
Total, mM	111.9	100.6	107.1	107.8	109.9	122.8	77.8
Individual VFA, mol/100 mol							
Acetate	73.3	75.8	71.9	76.9	77.0	76.6	64.2
Propionate	17.7	20.1	18.6	15.7	15.6	16.2	24.9
Butyrate	5.8	2.9	7.2	5	4.5	4.5	6.8
Isobutyrate	0.76	0.55	0.38	0.63	0.75	0.68	0.76
Valerate	1.2	0.6	1	1.1	1.2	1.2	2.6
Isovalerate	1.16	0.4	0.62	0.67	0.92	0.81	0.43
Soy = SBM control							
LEA 1 = <i>N. salina</i> , open pond, Valicor wet solvent extraction							
LEA 2 = <i>N. oceania</i> , photobioreactor/open pond, Valicor wet solvent extraction							
LEA 3 = <i>N. salina</i> , photobioreactor, Valicor wet solvent extraction							
LEA 4 = <i>Chlorella</i> sp. 1, open pond, Valicor wet solvent extraction (high temp)							
LEA 5 = <i>Chlorella</i> sp. 1, open pond, Valicor wet solvent extraction							
LEA 6 = <i>Chlorella</i> sp. 2, open pond, Valicor wet solvent extraction							

Table 5.4. Effects of LEA derived from *Nannochloropsis* and *Chlorella* species on digestion and N metabolism in continuous culture fermenters in high-starch diets.

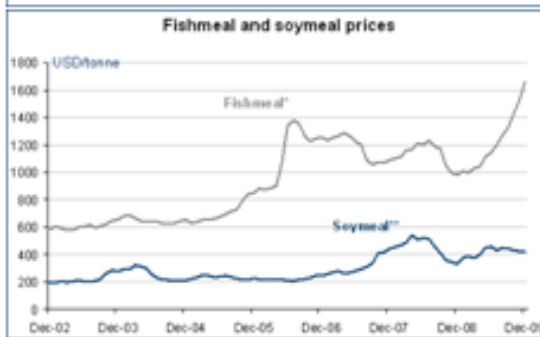
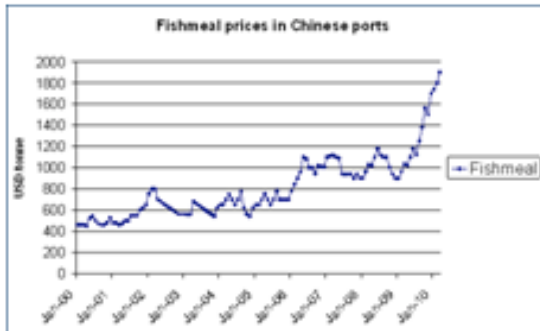
Measured Parameters	Starch Diet LEA Components						
	Control	Nannochloropsis LEA Formulations			Chlorella LEA Formulations		
	Soy	LEA 1	LEA 2	LEA 3	LEA 4	LEA 5	LEA 6
True OM digestibility, %	54.1	45.0	64.4	52.2	62.3	65.6	57.4
NH ₃ N, mg/100 mL	15.4	4.0	4.0	14.4	12.9	13.5	5.8
N degradation, % of N	59.2	36.2	71.3	55.2	64.0	71.3	56.2
Microbial efficiency	22.0	14.6	22.1	14.5	12.7	11.8	34.6
(g N/kg of OM truly digested)							
Total, mM	144.1	172.7	163.3	156.6	154.6	167.9	156.5
Individual VFA, mol/100mol							
Acetate	51.8	55.3	55.7	48.9	50.5	46.8	40.2
Propionate	26.2	14.9	20.1	38.8	34.4	39.5	32.2
Butyrate	15.5	19.8	17.1	6.3	9.4	6.3	17.8
Isobutyrate	0.23	0.33	0.5	0.25	0.29	0.25	0.12
Valerate	4.9	8.9	2.2	4.9	6.9	6.0	9.1
Isovalerate	0.7	0.5	2.5	1.0	1.1	1.1	0.1
Soy = SBM control							
LEA 1 = <i>N. salina</i> , open pond, Valicor wet solvent extraction							
LEA 2 = <i>N. ocellata</i> , photobioreactor/open pond, Valicor wet solvent extraction							
LEA 3 = <i>N. salina</i> , photobioreactor, Valicor wet solvent extraction							
LEA 4 = <i>Chlorella</i> sp. 1, open pond, Valicor wet solvent extraction (high temp)							
LEA 5 = <i>Chlorella</i> sp. 1, open pond, Valicor wet solvent extraction							
LEA 6 = <i>Chlorella</i> sp. 2, open pond, Valicor wet solvent extraction							

Mariculture Feed Studies with Fish and Shrimp

As aquaculture continues to expand, protein sources have become more costly and less available. In fact, the increased use of fish meal and fish oil is not only associated with the tremendous increase in fish and shrimp aquaculture but also the continued use of high levels of fish meal and fish oil in shrimp and fish feeds (Figure 5.4). This has resulted in a major threat to the sustainability of the natural fisheries. By integrating LEA into aquaculture diets and replacing the costly SBM and fish meal, not only could feed prices be lowered but feed nutrient quality also could potentially be increased. A series of nutritional investigations were conducted with red drum, *Sciaenops ocellatus*, as a model marine fish species and the major commercial shrimp species, *Litopenaeus vannamei*, to assess the potential nutritional and economic value of LEA as a protein feedstuff to replace soybean and/or fish meal in aquaculture diets.



Fish Meal, Aquaculture Feed Dilemma



- ✓ Fish meal is a major protein source in aquaculture feeds
- ✓ Cost: \$1,200 to \$1,800/MT
- ✓ Environmentally unsustainable
- ✓ Availability will limit animal aquaculture and agriculture growth in the future
- ✓ Fish oil will also be limiting and expensive (\$800 to \$1,600/MT)



Figure 5.4. Fish meal and soybean trends.

Three separate comparative feeding trials were conducted, each of seven weeks duration, to evaluate five different algal meals as partial replacements for fish meal and soy protein concentrate in reference diets for juvenile red drum. The results of these feeding trials are shown in Table 5.5.

In the first trial, whole-algae meal and LEA derived from *Navicula* sp. could replace 5% and 10% of the crude protein in the reference diet without significantly ($p > 0.05$) reducing weight gain, feed efficiency, hepatosomatic index, or protein and energy retention of the fish. Algal inclusion significantly affected the apparent digestibility coefficients (ADCs) of the various dietary treatments for dry matter, crude protein, and energy. A second feeding trial evaluated LEA derived from *Chlorella* sp. processed at high temperatures replacing 5%, 10%, 20%, and 25% of the crude protein in the reference diet. Weight gain, feed efficiency, survival, and protein efficiency ratio were significantly reduced at substitution levels of 20% and 25%. A third feeding trial evaluated LEA derived from *N. salina* replacing 5%, 7.5%, 10%, and 15% of the crude protein in the reference diet. Weight gain, feed efficiency, survival, and protein efficiency ratio were significantly affected by some dietary treatments, with the 15% substitution level causing significant reductions in weight gain, feed efficiency, intraperitoneal fat ratio, and whole-body lipid.

Table 5.5. Red drum fish feeding trial results with different LEA.

Diet	% Weight Gain	% Survival	Feed efficiency (gain/feed)	Protein efficiency ratio (gain/protein fed)
<i>Navicula</i> sp. LEA				
Reference	203	75.9	0.86	
5% LEA	219	88.9	0.82	
5% Whole Algae	250	85.2	0.89	
10% LEA	212	92.6	0.76	
10% Whole Algae	293	94.4	0.93	
Ref w/ High Ash	256	92.6	0.9	
<i>P</i> > <i>F</i>	0.1699	0.0748	0.0051	
<i>Chlorella</i> sp. LEA				
Reference	580	77.3	0.76	1.73
5% LEA	517	81.8	0.73	1.67
10% LEA	496	66.7	0.69	1.53
20% LEA	271	62.1	0.46	1.01
25% LEA	254	51.5	0.41	0.91
<i>P</i> > <i>F</i>	< 0.0001		< 0.0001	< 0.0001
<i>N. salina</i> LEA				
Reference	720	74.7	0.96	2.5
5% LEA	633	66.7	0.97	2.39
7.5% LEA	798	70.7	0.84	2.86
10% LEA	480	61.3	0.81	1.98
15% LEA	222	42.7	0.49	1.2
<i>P</i> > <i>F</i>	< 0.0001	0.0005	< 0.0001	< 0.0001
Values are means of three replicate groups				

Based on the results of fish feeding experiments:

- Replacement of up to 10% of crude protein from fish meal and soy protein concentrate with LEA was possible without causing substantial reductions in fish performance.
- The whole-algae product provided a more nutritious product than LEA.
- Red drum and hybrid striped bass showed similar responses in their ability to digest crude protein and energy from the various algal products.
- ADCs varied greatly among the different products and processing methods.

Similar feeding trials with some of these same LEA materials were conducted with shrimp. Six growth--and-survival experiments were conducted in which six different algae meals were evaluated as replacements for soybean and/or fish meal in shrimp diets. The first four experiments in which whole and lipid-extracted *Navicula* sp. and processed LEA at low and high temperatures from *Chlorella* sp. were considered preliminary because of the low protein levels of less than 23% in the whole-algae or LEA samples evaluated. Very promising results



AGRICULTURAL COPRODUCTS

were obtained since these four experiments indicated that up to 13.33% for all four batches of whole algae or LEA could be replaced by either soybean and/or fish meal on an equivalent protein basis with no significant reduction in growth and survival. However, the amount of soybean and/or fish meal that was replaced was very small because of the low protein level in the four batches of algae.

The last two growth-and survival-experiments were conducted using two batches (A and B) of LEA from *N. salina* produced at the same facility using the same production method but at different times of the year. The crude fat level in batch A (2.64%) was lower than the crude fat level of batch B (9.92%) while the crude protein levels were similar (41.6% for A and 44.9% for B). The results indicated that even a 5% replacement of soybean or a combination of soybean and fish meals by LEA A with the low crude fat level significantly lowered the growth rate of shrimp. In contrast, the inclusion of 30% of batch B could replace 70% of SBM and 25% of batch B could replace 66.7% of fish meal and 33.3% of SBM in the feed without significantly reducing growth and survival. These data are very significant indicating that large inclusion levels of LEA could replace large levels of soybean and/or fish meals in shrimp diets. However, production, harvesting, extraction, and/or drying methods will be critical in determining the quality and replacement of LEA value in shrimp feeds.

Based on the results of the shrimp-feeding experiments:

- At least a 20% inclusion level of LEA could be used to replace the expensive soybean and/or fish meals in shrimp feed.
- Results from the experiments in which high supplemental levels of Al or Fe were added to shrimp diets indicate that Al or Fe levels in LEA from using Al or Fe as a flocculant will not be limiting.
- Proper production, harvest, extraction, and/or drying methods will be required to produce LEA that can be included into shrimp feeds replacing soybean and fish meals.

Ruminant Animal Feed Studies

Determinations of feeding value were made for cattle and sheep by conducting an *in vivo* feeding trial with feed formulation made with LEA derived from a *Chlorella* sp. that was cultivated in large outdoor ponds, flocculated with alum for harvesting, dried, and solvent-extracted; the LEA was then dried again. Average composition of this LEA was about 20% fat, 45% protein, 20% carbohydrate, 10% various minerals, and vitamins on a dry basis. Large quantities of this LEA were provided to NAABB from General Atomics, who produced the materials as part of a DARPA algal biofuels program.

Three feeding trial experiments were completed to evaluate the use of LEA as a protein supplement to cattle grazing low-quality forage. The objectives of each of these trials were:

1. Evaluate the palatability of LEA in cattle consuming forage.
2. Determine the optimum inclusion rate of LEA in cattle consuming low-quality forage.

3. Compare effects of LEA versus a conventional supplement on nutrient utilization and mineral intake in cattle consuming low-quality forage.

An example of the experimental methods used to determine optimum inclusion rates is shown in Figure 5.5.

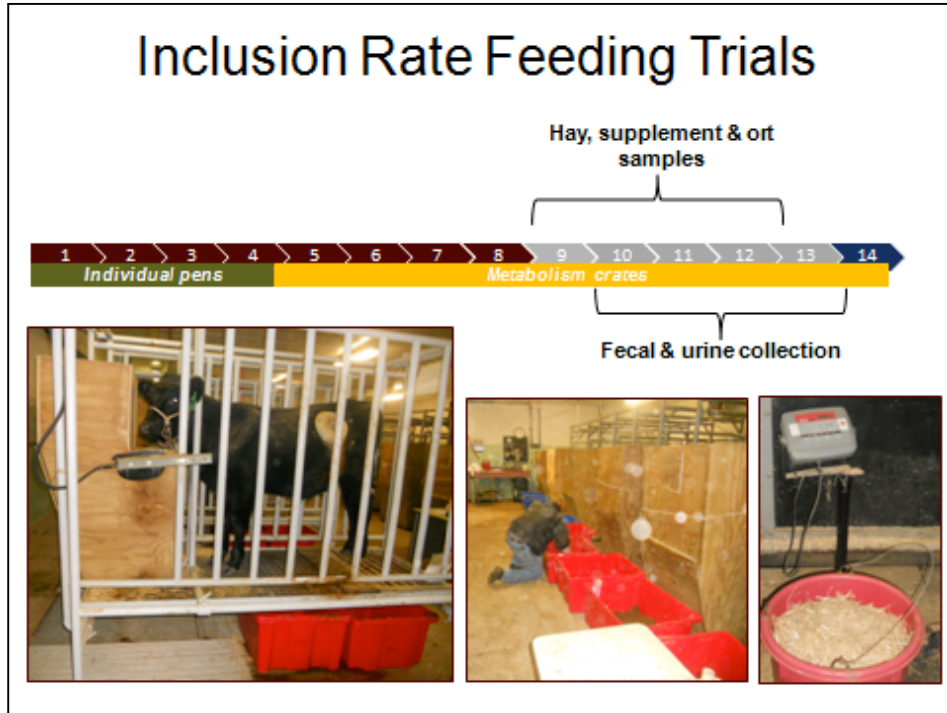


Figure 5.5. Methods used for cattle feeding trials to determine inclusion rate of LEA.

For the palatability test, a small amount, typically less than 1 kg, is provided to a grazing animal per day either in a range cube, in loose feed, or as a liquid supplement; the animal consumes the rest of its diet as grazed grass or fed hay. Under this scenario, palatability is important as there is no mixing with the rest of the diet to mask odor, metabolic limiters, or bad taste. Results from feeding trial 1, summarized in Table 5.6, demonstrate that blending LEA with either dried distillers’ grains (DDG) or cottonseed meal (CSM) resulted in similar intake to those conventional supplements provided in isolation. Additionally, blending works to correct the mineral imbalances observed in LEA and DDG. Provision of LEA as 100% of the supplement decreased the amount consumed and the number of complete consumption events, suggesting some challenges with LEA palatability and intake.

Table 5.6. Palatability of LEA in cattle.

Treatment*	Amount consumed, g**	Complete consumption, %†
100 DDG	1000	100
80 DDG/20 LEA	1000	100
60 DDG/40 LEA	990	94
40 DDG/60 LEA	920	91
100 CSM	970	97
80 CSM/20 LEA	1000	100
60 CSM/40 LEA	1000	100
40 CSM/60 LEA	950	92
100 LS	770	59
66 LS/33 LEA	960	88
33 LS/66 LEA	780	50
100 LEA	780	55

*DDG = dried distillers grains, CSM = cottonseed meal, LS = liquid supplement.
 **Amount consumed = amount of supplement consumed on average out of 1000 g.
 †Complete consumption = % of time entire amount of offered supplement was consumed within 1 h.

For the inclusion rate trials, cattle were fed either oat straw, as a no-supplemental-protein control; mixtures of LEA at 50, 100, or 150 mg N/kg body weight (BW); or cottonseed meal (CSM) at 100 mg N/kg BW. Summary results from this trial for total OM intake and N intake and retention are shown in Figures 5.6 and 5.7 respectively.

Data from these inclusion experiments indicate that LEA acts similarly to CSM in its ability to stimulate forage intake, stimulate total digestible OM intake, and increase nitrogen retention.

The third experimental trial focused on nutrient utilization and mineral intake comparing oat straw, as a no-supplemental-protein control, mixtures of LEA, and CSM at 100 N/kg BW.

Results from these studies shown in Figure 5.8 indicate that the feeding of LEA did increase the excretion of moisture in the urine, an expected result given the increase in sodium consumption and other minerals when LEA is provided. Interestingly, in these experiments the intake of LEA was complete, suggesting that when cattle have access to the LEA throughout the day they are willing to consume it; however, ample water is likely required to support supplement consumption.

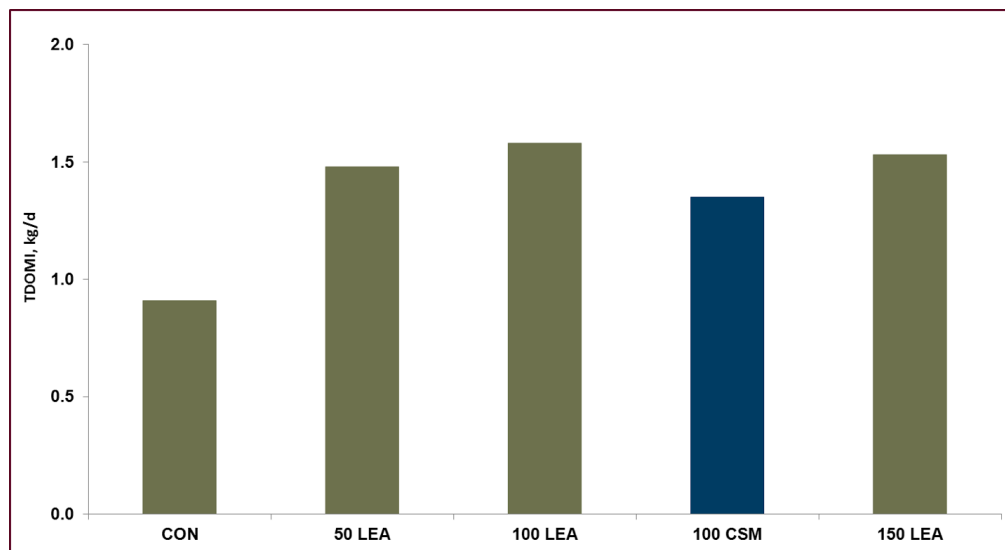


Figure 5.6. Effect of LEA or CSM supplementation on total digestible OM intake.



These data from the cattle feeding trials suggest that LEA could be used as protein supplement and that existing formulation guidelines can be followed when feeding LEA. However, blending of LEA with other coproducts may increase the acceptance by the animal and producer while correcting mineral imbalances. Additional work using other sources of LEA is warranted to more fully elucidate the utility of LEA as protein supplement for grazing cattle.

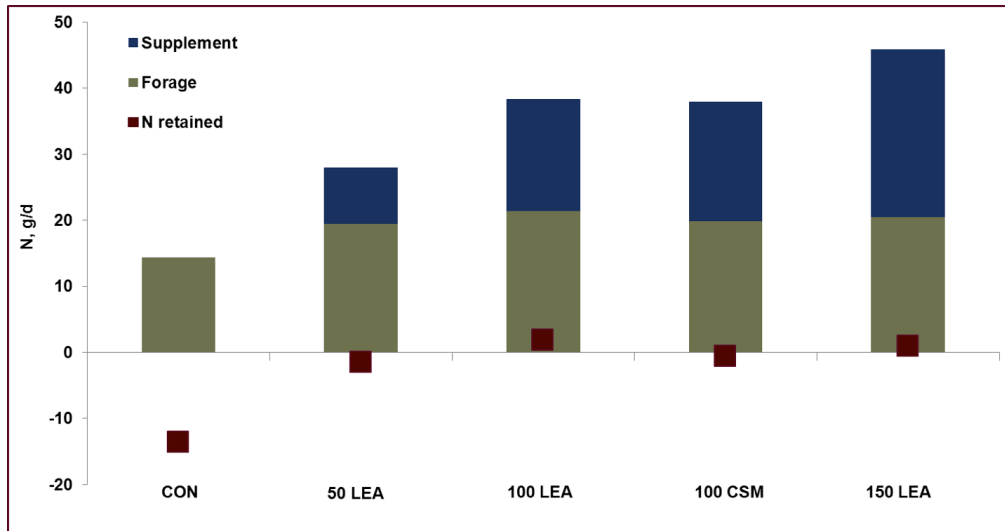


Figure 5.7. Effect of LEA or CSM supplementation on N intake and retention.

A feeding trial was also conducted using the same LEA in growing lambs. The objective of this trial was to determine the effects of varying inclusions of LEA supplementation on performance, blood chemistry, nutrient balance, live health status, and carcass characteristics. Total mixed rations containing between 0% and 20% of the diet as LEA as compared to SBM as the control were fed.

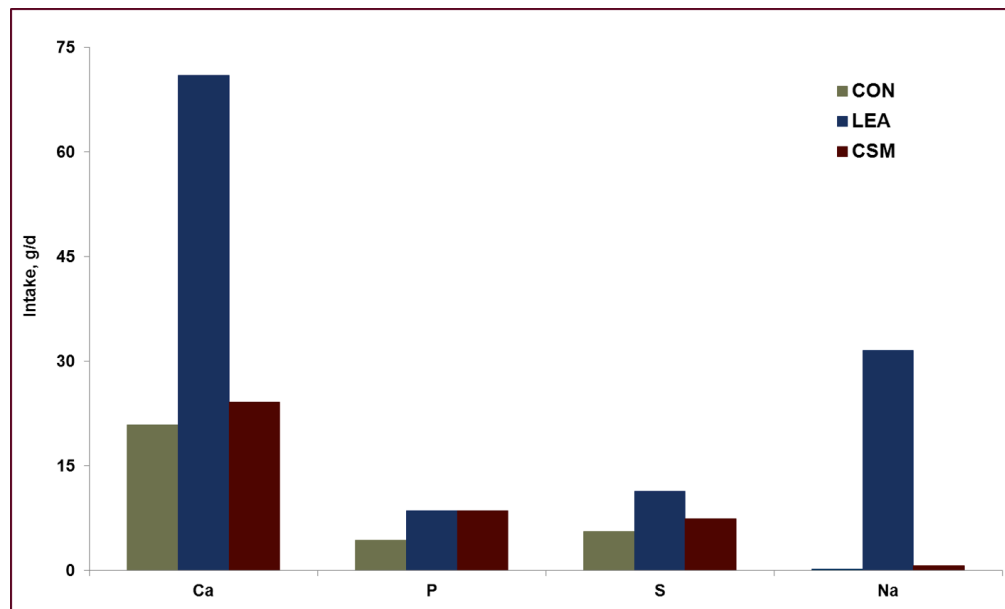


Figure 5.8. Effect of isonitrogenous levels of LEA and CSM on macromineral intake.

Data presented in Table 5.7 show that LEA had no impact on intake, gain, or feed efficiency. These data suggest that sheep diets can be formulated to include 20% of the LEA tested without negatively impacting performance. Further work to investigate improved sources of LEA would validate these results and provide information on how upstream decisions impact feeding value. Inclusion beyond 20% of the diet maybe feasible; however, mineral imbalances, high ash content, and excessive dietary protein likely restricted LEA inclusion to near 20%.

Table 5.7. Sheep LEA inclusion study for live growth performance of yearling wethers.

Item	Treatment				
	Control	5% LEA	10% LEA	15% LEA	20% LEA
Initial BW, kg	46.4	45.2	45.3	44.9	44.6
Final BW, kg	44.6	44.7	45.5	45.1	42.6
ADG adjustment [†] , kg	0.23	0.24	0.27	0.27	0.23
ADG metabolism ^{**} , kg	-0.82	-0.81	-0.79	-0.81	-1.03
G:F [†]	0.16	0.2	0.19	0.21	0.17
Intake, kg/d	1.41	1.26	1.43	1.35	1.38

[†]Average daily gain (ADG) during the 21 days of feedlot pen period.
^{**}ADG during the 7 days of the balance metabolism period.
[†]Gain:Feed (G:F) presented for the whole feeding period.

Based on the results of the ruminant animal feeding experiments:

- Supplementation of LEA stimulates forage utilization to a similar extent as CSM in cattle.
- Supplementation of LEA may be a viable protein and mineral supplement for sheep; however, caution may be advisable for diets containing greater than 20% LEA due to slight reductions in performance.
- Mineral imbalances in LEA can be partially attributed to upstream operations.

Blends of LEA and conventional protein supplements will minimize concerns of palatability and mineral toxicity.

Nonruminant Animal Feed Studies

A feeding trial similar to the aforementioned sheep study was conducted in swine with completely different results. Swine were fed the same LEA as used in the cattle and sheep projects in corn-based rations containing between 0% and 20% of the diet as LEA. In stark contrast to the lamb data, average daily gain, final body weight, and gain:feed was reduced at all levels of LEA inclusion in swine diets. Table 5.8 shows the data for live-growth performance of swine that were fed LEA. Formulation of swine diets containing the *Chlorella* sp. used in this project is not commercially viable and is not recommended. Additional work is required to determine why and to see if this response is unique to this source of LEA.

A small feeding trial was also completed with chickens to determine the maximum feeding level of LEA to young broiler chickens and laying hens. In these studies, LEA was added to feeds for broiler chickens and laying hens at rates of 10% and 20% respectively. The results of these studies are summarized in Figures 5.9 and 5.10.

The conclusions from these data indicate that broilers can tolerate a maximum level of 5% LEA in their feed and layers are largely unaffected by additions of LEA up to 20%.

Table 5.8. Swine LEA inclusion study for live-growth performance of swine.

Item	Treatment				
	Control	5% LEA	10% LEA	15% LEA	20% LEA
Initial BW, kg	46.4	45.2	45.3	44.9	44.6
Final BW, kg	44.6	44.7	45.5	45.1	42.6
ADG adjustment [†] , kg	0.23	0.24	0.27	0.27	0.23
ADG metabolism ^{**} , kg	-0.82	-0.81	-0.79	-0.81	-1.03
G:F [†]	0.16	0.2	0.19	0.21	0.17

[†]Average daily gain (ADG) during the 21 days of feedlot pen period.
^{**}ADG during the 7 days of the balance metabolism period.
[†]Gain:Feed (G:F) presented for the whole feeding period.

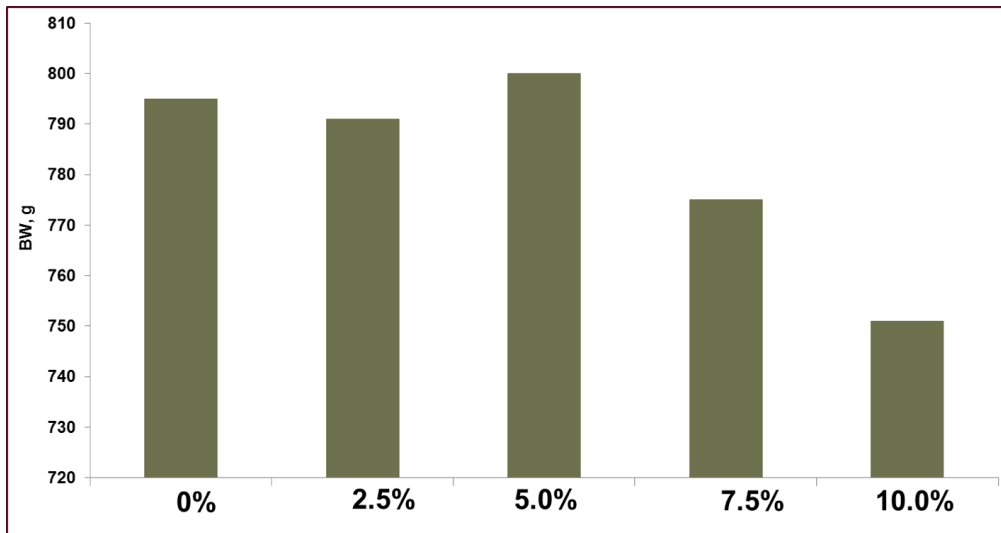


Figure 5.9. LEA Inclusion study for broiler chickens.

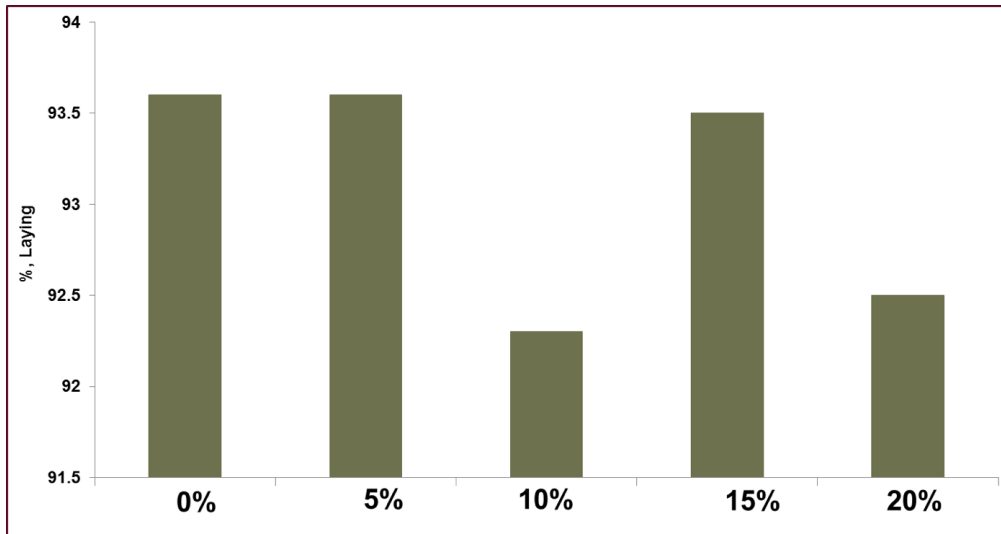


Figure 5.10. LEA inclusion study for layer hens.

Fertilizer Evaluations

The use of algae as a fertilizer is well documented in the scientific literature; however, there is little information regarding the use of LEA for soil fertility and crop production. Therefore, studies were needed to address key concerns regarding the use of LEA as a fertilizer and soil amendment. The key research objectives for this task were to:

1. Quantify chemical constituents and characteristics of LEA that are relevant to soil fertility and fertilization of crops.
2. Determine the mineralization rates of carbon, nitrogen, phosphorus, and other key chemical components of LEA and the effect on soil microbes.
3. Define the application rate and assess the effects of LEA on crops.
4. Conduct field application and determine the effects of LEA application to soil carbon and structure.

Chemical composition of whole and lipid extracted *Navicula* sp. and *N. salina* is similar to the plant nutrients (N, P, K) provided from manure application. The sodium concentration is much greater than that of soil. Application of whole and lipid extracted *Navicula* sp. and LEA of *N. salina* to the soil increased both soil pH and electrical conductivity. Nearly half of the carbon of LEA mineralized after 280 days.

LEA residue is labile and highly mineralizable compared to wheat straw, making it less likely to aid in carbon sequestration but a greater source of plant nutrients as is shown in Figure 5.11 Percent LEA nitrogen mineralized ranged from 30% to 55% for 5% and 1% LEA, respectively, at 56 d of incubation as shown in Figure 5.12. After 56 d of incubation, there is sufficient (350 mg N kg⁻¹ soil) plant-available nitrogen for the 5% LEA amendment level and potential residue for plants in subsequent growing seasons.

Greenhouse plant growth studies were conducted with selected forage species as shown in Figure 5.13. Yields of first cuttings of salt-susceptible and -tolerant crops were not affected by soil treatment with LEA. The yields from ratoon crops of pearl millet and sorghum-Sudangrass were greater for 3.0% LEA and 1.5% LEA amendment level, respectively. The effect of treatments on growth during the ratoon crop and not the first cutting is likely due to the lag time of mineralization of amendment that is required before nutrients become plant available.

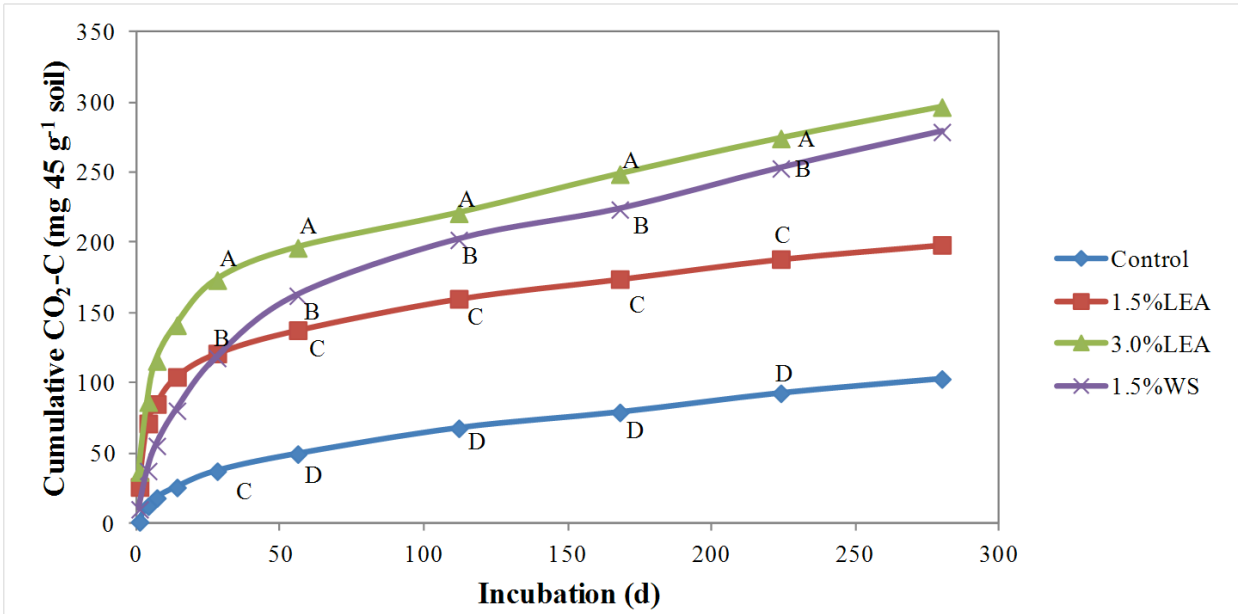


Figure 5.11. Carbon mineralization of LEA.

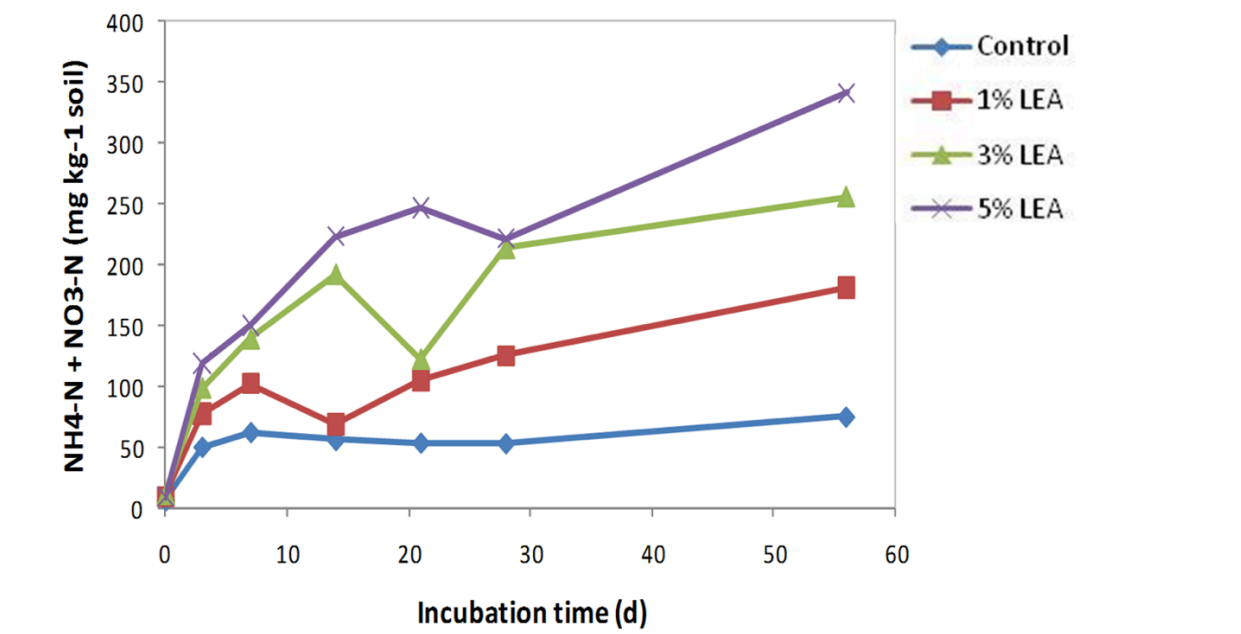


Figure 5.12. Nitrogen mineralization of LEA.

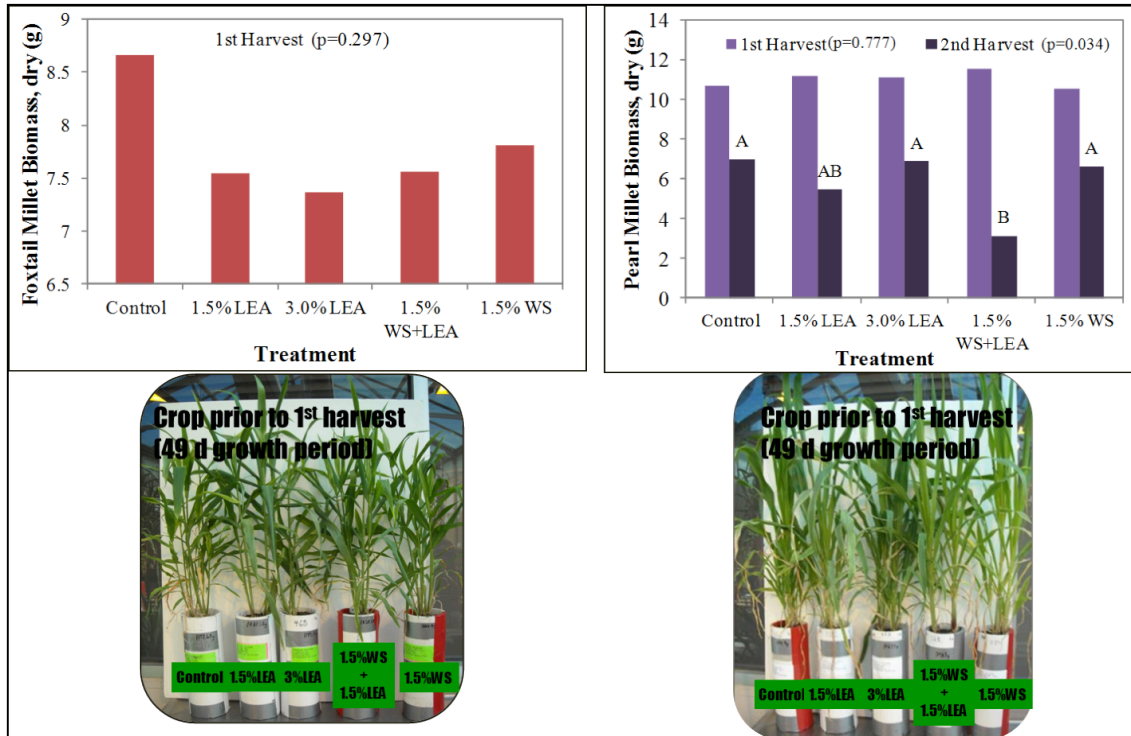


Figure 5.13. Greenhouse plant growth studies with foxtail and pearl millet yield (DM basis).

Addition of LEA has the potential to increase the pH of acidic soils, such as those common in the southeastern USA. Increased soil salinity may have negative effects on plant and soil microbial growth with repeated applications of LEA. Amendment of soil with LEA will not serve as a carbon sink; however, it is a readily available source of plant nutrients with potential for carryover to subsequent growing seasons.

The LEA must mineralize prior to plant uptake and continues to mineralize for at least 280 days post application. Nutrients from LEA can be utilized by plants as a source of fertilizer, and the microminerals provided by LEA may serve as an economical source of these nutrients for agriculture. It is not recommended that LEA be applied annually to soils because of potential toxicity of sodium. Management practices are not yet refined based on this initial evaluation, but would likely warrant application every 3 to 4 years. It is suggested that further research to determine the effects of LEA fertilizer on crop production and soil health be conducted prior to recommending this practice on a large-scale basis.

Based on the results of the fertilizer evaluation experiments:

- LEA is labile and highly mineralizable, compared to wheat straw;
- Neutralizing effect of LEA on soil pH could have potential application;
- LEA is a source of available nitrogen with residual nitrate-nitrogen after growing season;

- Salinity could be an issue so consider using with crops with moderate or better tolerance and avoid repeat application; and
- LEA provided sufficient nutrients to produce greater yield than inorganic fertilizer for at least two growth cycles.

Economic Value Projections for LEA as Feeds and Fertilizers

To leverage the value of these current experimental results, a linkage with members of the NAABB Sustainability Team was formed to assess a dollar value for the LEA based on the feed or fertilizer value. They conducted econometric analyses of value for LEA for animal and mariculture feed and for fertilizer. This analysis considered the chemical composition of LEA and whole algae with a focus on energy, fat, protein, and micronutrients, especially the amino acids. The value of LEA is based on historical values the feed ingredient market has placed on these nutritional attributes.

Hedonic econometric models developed to estimate intrinsic value of LEA based on fractions of energy, protein, fat, etc. in LEA for animal feeds are shown in Figure 5.14. Based on these models, the LEA intrinsic market value is \$100 to \$160 per ton less than SBM or about \$160/ton in 2013. The value could be higher if more oil residue remains in the LEA and this would depend on the alga species, biomass lipid content, harvesting methods, and extraction methods.

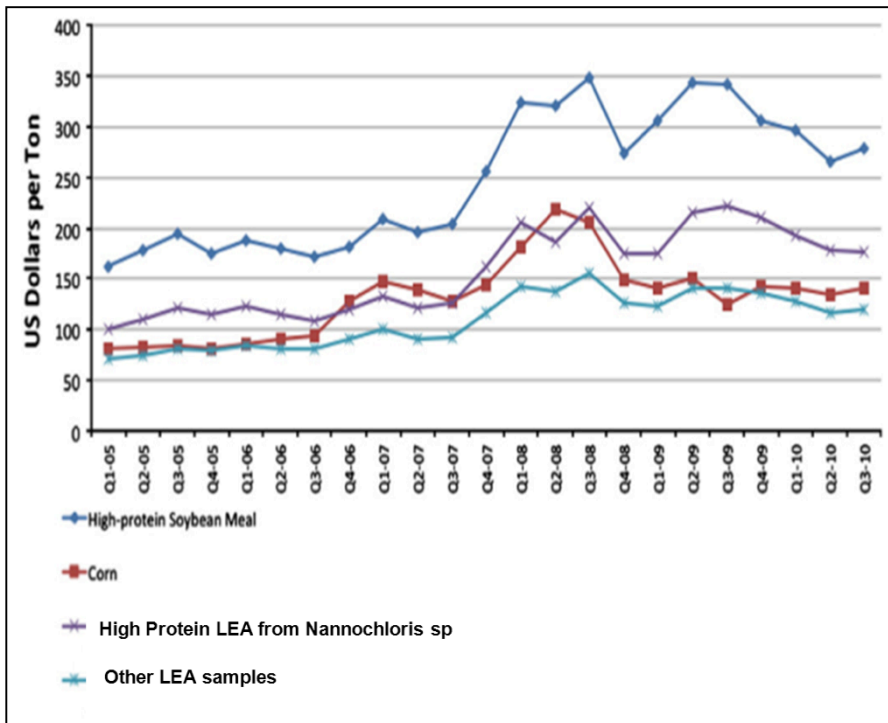


Figure 5.14. Hedonic models for determining intrinsic LEA values for animal feed.



AGRICULTURAL COPRODUCTS

Similar econometric models for determining the value as maricultural feeds were completed for LEA and whole algae as compared to SBM, shown in Figure 5.15. Based on these models, whole-algae intrinsic market value is \$82/ton more than SBM at about \$400/ton in 2013 and LEA intrinsic market value is \$94/ton less than SBM at about \$200/ton in 2013.

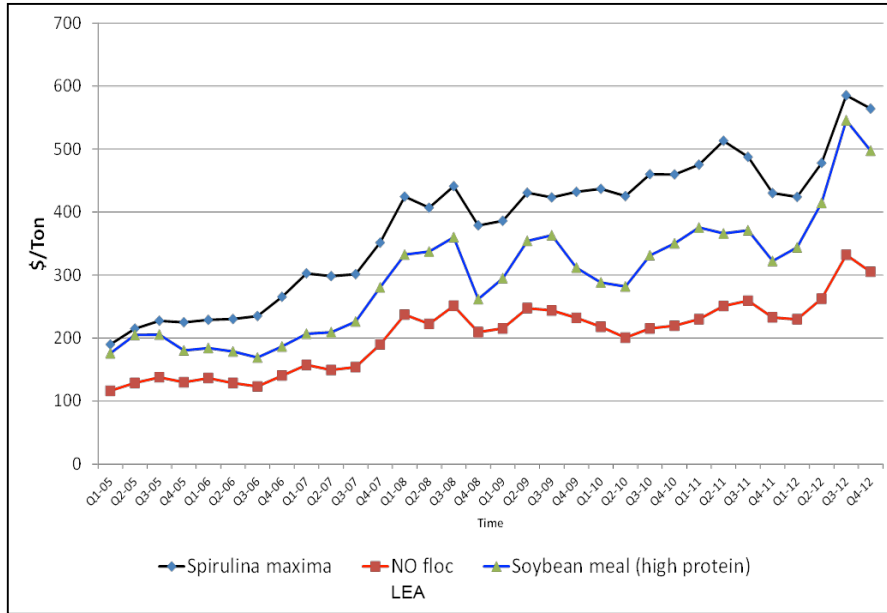


Figure 5.15. Hedonic models for determining intrinsic LEA values for maricultural feed.

Conclusions and Recommendations

As NAABB started this work the scientific literature was very limited on the use of algae as animal and mariculture feed. Collaboration between those involved in developing upstream processes and the end users of the coproduct is essential to optimize LEA value and oil value. Additionally, this could help prevent toxicity concerns and ultimately increase the value of LEA as the end user will have greater confidence in the safety and consistency of the LEA. Determining optimum formulations of feeds containing LEA is complicated and clearly beyond the scope of this NAABB effort.

Feeding studies using LEA were performed with sheep, swine, shrimp, chicken, fish, and cattle. The magnitude of the study using LEA is impressive. Table 5.9 provides a summary of the findings. This is the first set of data on use of LEA in animal and mariculture feed. The major issue is that mineral content must be closely monitored and upstream processes standardized to produce a more consistent biomass. Currently, LEA is valued as a feed supplement for animals at \$160/ton and for mariculture at \$200/ton. Whole algae for mariculture is valued at closer to \$400/ton.

Table 5.9. Summary of the feeding studies conducted on animals and mariculture.

Type of Animal Tested	Performance	Digestibility
Fish (red drum and hybrid striped bass)	Replacement of up to 10% of crude protein from fish meal and soy protein concentrate with LEA without causing substantial reductions in fish performance.	Excellent
Shrimp	At least a 20% inclusion level of LEA could be used to replace the expensive SBM and/or fish meals in shrimp feed.	Excellent
Cattle	Supplementation of LEA stimulates forage utilization to a similar extent of CSM in cattle (100 mg N/kg body weight)	Blends of LEA and conventional protein supplements will minimize concerns of palatability. Does not impair fiber digestion.
Sheep	Supplementation of LEA may be a viable protein and mineral supplement for sheep; however, caution may be advisable for diets containing greater than 20% LEA due to slight reductions in performance.	
Pigs	Use of LEA is not recommended at this time, supplementation with 5–20% LEA tested. Reduction in growth and weight gain.	Not palatable
Chicken	Inclusion of 5% LEA in young broiler chicken and laying hens diets may be viable.	

Fertilizer studies were primarily completed in greenhouses using pearl millet and sorghum-Sudangrass. Based on the results of the fertilizer evaluation experiments, LEA:

- Is labile and highly mineralizable compared to wheat straw.
- Provides a source of available N with residual nitrate-nitrogen after the growing season.
- Provides sufficient nutrients to produce greater yield than inorganic fertilizer for at least two growth cycles.

Based on analysis of the current prices for N, P, K, and char, the value of LEA is about \$30/ton.

Our data and observations suggest that testing a complete system (species, pond management, harvest method, and extraction technology) is required for each LEA developed at commercial scale and formulation cannot be based on the observations of a slightly related product. Our future challenge is collecting data during the development of commercial-scale algal-biofuel production that does three things: (1) provides confidence that the nutrients can be used in human food systems, (2) ensures the system’s capacity to utilize LEA, and (3) operates in a developed market that provides sufficient economic value. Data collected by the NAABB Agricultural Coproducts team supported all three of these objectives. Although LEA does contain protein, in the current market and using existing technologies LEA as a feed or fertilizer does not provide a high enough value to offset the high cost associated with separating the lipid from the LEA.



Team Members

Shawn Archibeque, Colorado State University
Jamie Foster, Texas A&M University
Delbert Gaitlin, Texas A&M University
Addison Lawrence, Texas A&M University
Shanna Lodge-Ivey, New Mexico State University
Tryon Wickersham, Texas A&M University

Publications

Full-length, Peer-reviewed Publications

Fauzi, I. and D.M. Gatlin III. Evaluation of elevated dietary aluminum and iron on Red Drum *Sciaenops ocellatus*. *Journal of the World Aquaculture Society* (2014): *In Press*.

Lodge-Ivey, S.L. L.N. Tracey, and A. Salazar. The utility of lipid extracted algae as a protein source in forage or starch-based ruminant diets. *Journal of Animal Science* 92 (2014): 1331(12).

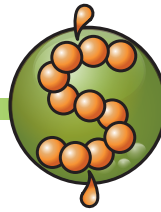
Mendoza-Rodriguez, M.G. and D.M. Gatlin III. Effects of various levels of silica ash in the diet of juvenile red drum (*Sciaenops ocellatus*). *Journal of the World Aquaculture Society* 45 (2014): 199-205.

Patterson, D. and D.M. Gatlin III. Evaluation of whole and lipid-extracted algae meals in the diets of juvenile red drum (*Sciaenops ocellatus*). *Aquaculture* 416-417 (2013): 92-98.

References

1. Tacon, A.G.J. and M. Metian. Global overview of the use of fish meal and fish oil in industrially compounded aquafeeds: trends and future prospects. *Aquaculture* 285 (2008) 146-158.
2. ARS-USDA 2012.
http://www.ars.usda.gov/research/program/programs.htm?np_code=102&pf=1
Accessed on August 12, 2012.
3. Klopfenstein, T. J., G. E. Erickson, and V.R. Bremer. Board invited review: use of distiller's by-products in the beef cattle feeding industry. *Journal of Animal Science* 86 (2008) 619-626.

SUSTAINABILITY



Introduction

Team Leads

Cara Meghan Downes, New Mexico State University.
James W. Richardson, Texas A&M University.

Preface

The National Alliance for Advanced Biofuels and Bioproducts (NAABB) Sustainability team brought together researchers from multiple institutions to integrate their models to provide a unique analysis framework that combined spatial, life-cycle, techno-economic, and financial assessments to quantify a broad range of algal-fuel sustainability issues using experimental data sourced from NAABB partners (Figure 6.1).

Sustainability Task Framework

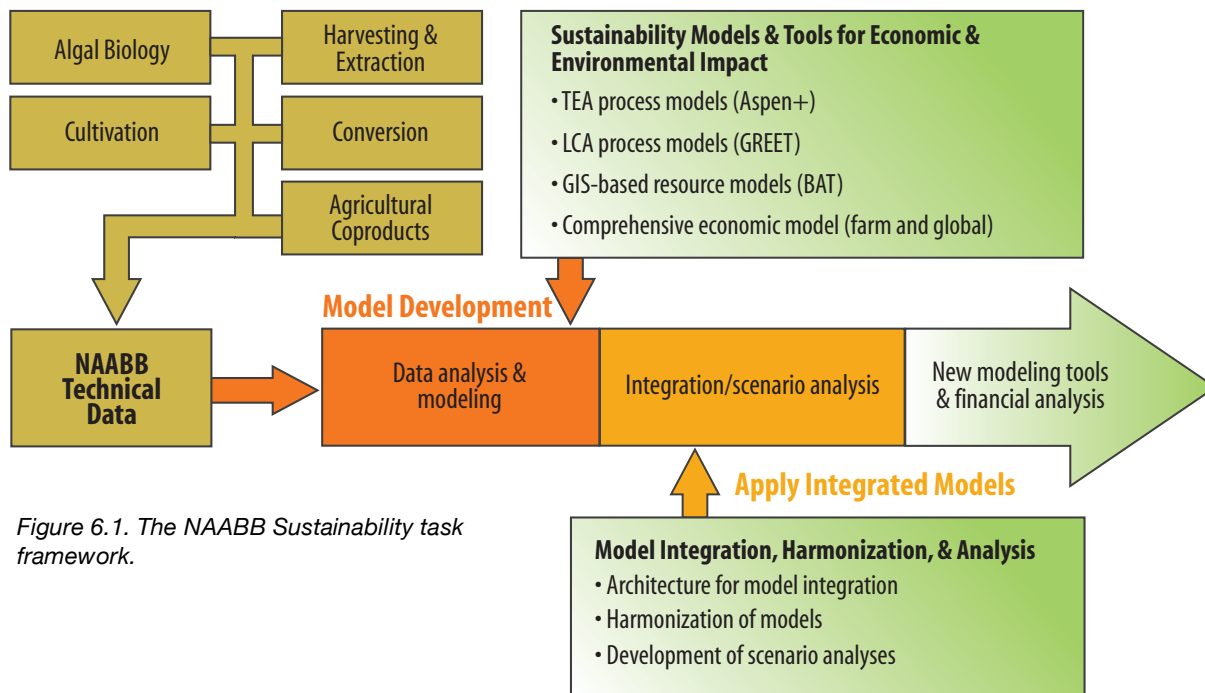


Figure 6.1. The NAABB Sustainability task framework.

Approach

Given the complexity of the NAABB project, the Sustainability team broke the process down into a series of modeling projects (Figure 6.2). The Sustainability team was tasked with analyzing the data developed by other NAABB members. NAABB partners developed estimates of the energy, economic, and environmental impacts for algae-based biofuels, using multiple platforms to address sustainability. A unique aspect of the NAABB effort was the integration of several modeling platforms to address sustainability based on the same set of

assumptions and operational scales. As an extension of the DOE's harmonization effort, experimental data from NAABB was used to update and modify the models in the harmonization series. In all of these modeling efforts the Sustainability team used data from a series of innovative efforts and findings achieved by NAABB investigators. From the NAABB upstream Algal Biology and Cultivation efforts, these include the following:

1. Increased biomass productivity of 2.5 times for a genetically modified organism (GMO) laboratory strain;
2. The sustainability profile of fuels using the NAABB-identified strain *Chlorella* sp. *DOE1412*;
3. The temperature photosynthetic active radiation (PAR) model to update the life-cycle and economic parameters used for the integrated modeling;
4. Outdoor production of *Chlorella* and *Nannochloropsis* as well as our media cost for open-pond cultivation; and
5. The inclusion of the lower-energy-cost/higher-productivity pond system ARID.

For the downstream processes we included model assumptions around lower-cost/higher-throughput harvesting and extraction technologies, as well as technologies that do not require separation of lipid from the biomass.

NAABB's efforts helped bring together the life-cycle-analysis (LCA) and techno-economic-analysis community to develop a harmonized set of assumptions and agree on a baseline comparison for algal fuel production. In this report, this baseline serves as a basis for comparison of the effectiveness of improvements listed above in the overall economic and life-cycle process of developing crude oil from algae.

Technical Accomplishments

Observations from Field Cultivation Data

To measure the environmental, economic, and energy characteristics of algal-fuel production, it is important to have accurate estimates of biomass production. One significant limitation of the current models and literature on algal production are the extrapolations of productivity and yield from lab-based experiments. It is well known that the productivity values measured in the lab do

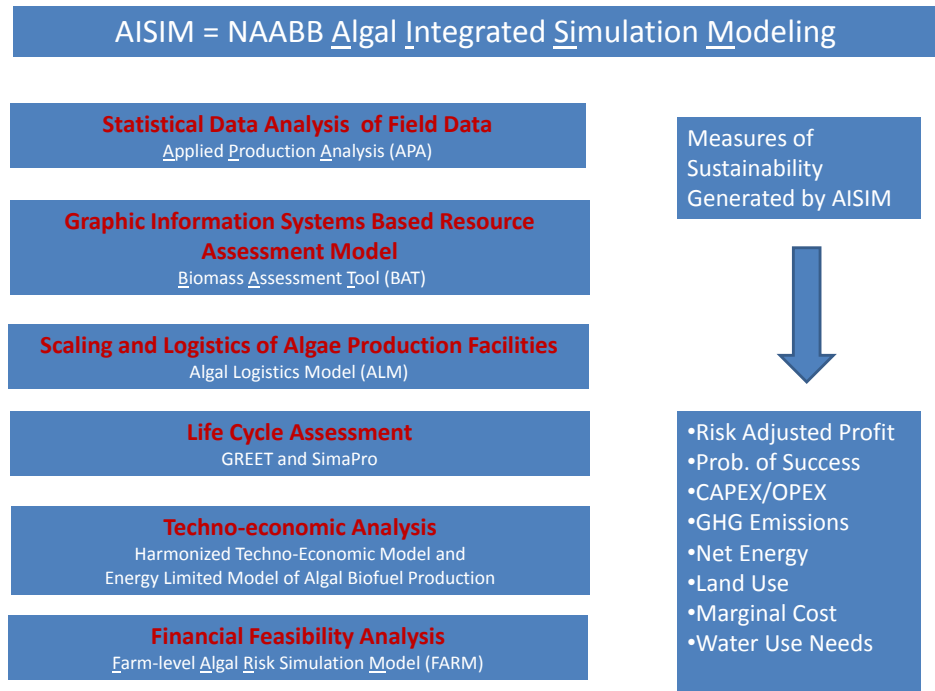


Figure 6.2. NAABB modeling components.

not translate into production in the field. Production data were collected from five different outdoor algal cultivation facilities over a multi-year time period to gain a better understanding of production of algae in the field and to address this significant limitation of the literature on the economic and environmental profile of algal fuels.

The combined data set contains 355 observations on PAR, weather, cell mass by optical density, salinity, pH, temperature, nutrient feeding, select water-chemistry characteristics, and harvest information. From these data the productivity of open-pond outdoor cultivation is calculated using the applied production analysis (APA) modeling system, which consists of advanced econometric techniques. What is unique about this approach to estimating productivity is that it (1) is based on actual experience over a four-year time span, (2) was collected from ponds with cultivation volume between 3000 and 150,000 liters, and (3) was collected year round across multiple seasons.

One of the most interesting aspects of the data is the variance in productivity by season. Figure 6.3 shows the variability in production across seasons using a

histogram plot for each season. The vertical axis of each plot is the percentage of observations falling into that “bin” range and the horizontal axis is grams afdw in $g/m^2/day$. As expected, the changes in solar irradiance and temperature affect algal productivity. We observe lower productivity in spring and fall. In both these seasons a spike in daily productivity with a long right-hand tail on the distribution is observed. Lower overall productivity in the fall is observed. The data on production in the winter is a bit surprising, as production is smoother with a more normal distribution. For this sample, winter production was better than fall. Spring and summer had the highest daily productivity values. The data show that a simple average is not an appropriate assumption for productivity measures. Thus, economic and life cycle analyses should explicitly incorporate the seasonal risk of biomass production.

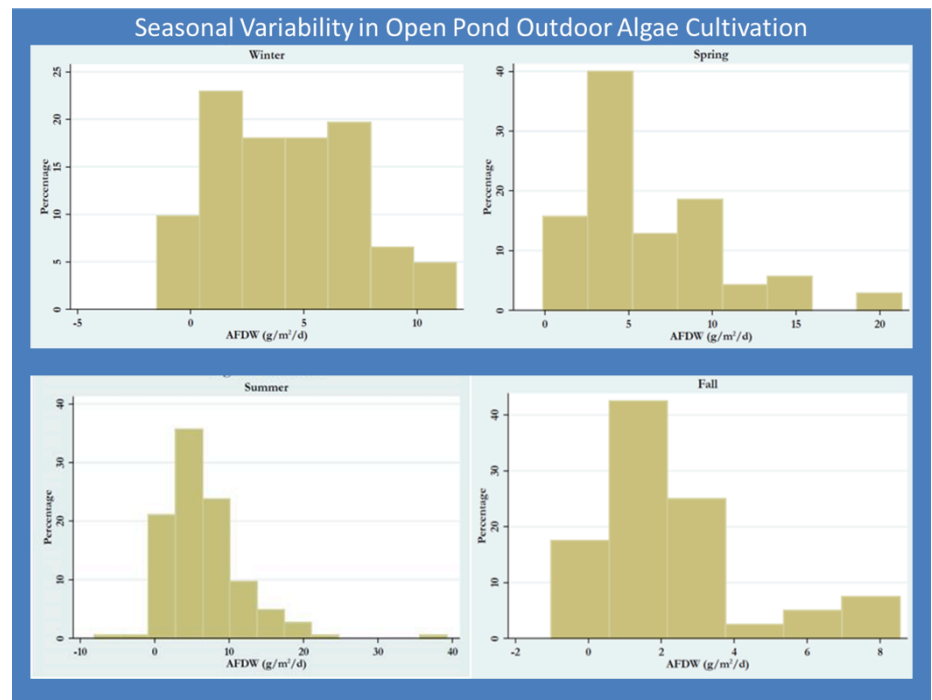


Figure 6.3. Histograms demonstrating the seasonal variability of biomass productivity in open ponds.

Regional Feasibility of Algae Production

The biomass assessment tool (BAT) model¹ was used to analyze a large number of resource-feasible algae production sites in the United States (Figure 6.4) for the production of 5 BGY of algal biofuel for three organism-based scenarios: BAT generic (freshwater) strain, freshwater strain (*Chlorella*), and a salt water strain

(*N. salina*). Overall, the site selection results show remarkable similarity between the freshwater scenarios. The productivity values and number of sites required to meet the 5 BGY target are essentially the same in the states along the Gulf of Mexico and South Atlantic (Figure 6.5). However, the organism chosen for the saltwater scenario (*N. salina*) had a much lower biomass production rate and, despite the higher lipid content, required nearly twice the number of farm sites to reach the 5 BGY target. In addition, the average cost for providing saltwater to a site is over \$1 million. It is doubtful that there are enough economical saltwater sites in the study area to meet the 5 BGY target based on *N. salina*. The results show that it is especially important to maximize production when utilizing saline waters to offset the added supply costs.

The BAT production results were used in the farm-level algae risk simulation model (FARM)² to estimate the economic and financial sustainability of algae farms in each of the regions highlighted by the BAT analysis (Figure 6.5). For each region the BAT model reported 30 years of monthly biomass production that were used to estimate probability distributions for stochastic monthly biomass production.

The biomass probability distributions are used in the FARM model to simulate the economic sustainability of a 4850 hectare farm in each of nine regions along the Gulf of Mexico. The economic and financial analyses showed that *Chlorella* was the best performing algae species and the South Florida region was the most profitable³

LCA Analyses

A variety of LCA analyses for production of biofuels from algae were completed prior to the initiation of NAABB and continue to develop as technical information becomes available. Information in the literature, however, lacks a common basis for comparison and therefore is difficult to interpret. Hence, initially NAABB examined the energy and material results of nine authors with 24 different growth scenarios and put all information into the same functional unit of 1 kg of biomass⁴ The greenhouse-gas emissions for the six scenarios ranged between 0.1–4.4 kg CO_{2eq}/kg biomass, with the fossil energy demand of 1-48 MJ/kg biomass (Table 6.1). Based on this large variation, the potential for algal biofuels to reduce greenhouse-gas emissions depends on the design of the complete algal-fuel production pathway. NAABB performed LCA analyses for a variety of production strategies as data became available throughout the project. GREET and SimaPRO software packages were used.

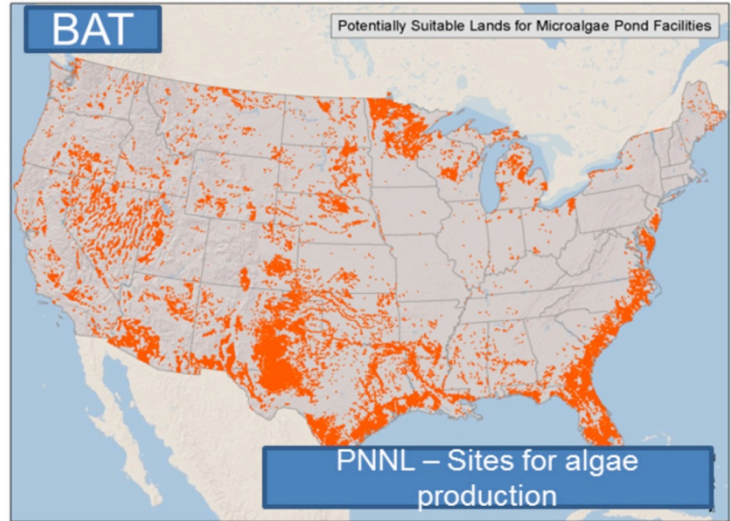


Figure 6.4. Sites for BAT model analysis of algae production.

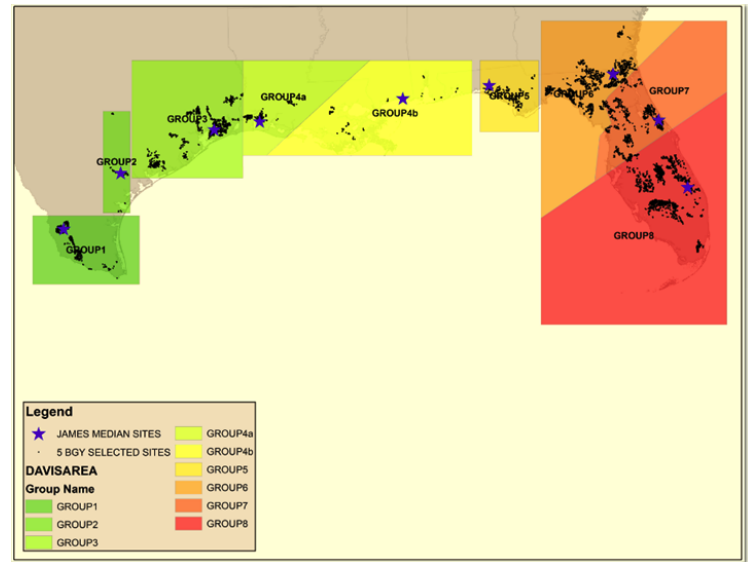


Figure 6.5. Most-feasible algae crude production regions identified by the BAT harmonization analysis.

Table 6.1. Comparison of greenhouse-gas emissions for green jet fuel produced from various feedstocks.⁴

Feedstock	Greenhouse-gas Emissions
Algae (this work)	0.1–4.4
Corn	0.3–0.4
Soybeans	0.4–0.5
Jatropha	0.3
Camelina	0.1–0.3

Replication of SimaPro LCA Software with GREET

NAABB used both the SimaPro LCA⁵ software and GREET⁶⁻⁸ in its biofuels research, so it was important to replicate baseline LCA results from GREET using SimaPro. Doing this assured comparability of results between the two software platforms. Table 6.2 shows a comparison between GREET and SimaPro for the baseline algae-biofuel pathway using harmonized inputs. An in-depth analysis for emission factors of electricity indicated that GREET and SimaPro had significant differences in generation mix, transmission loss, and conversion efficiency of electricity. However, when SimaPro emission factors were changed to the GREET electricity mix, then greenhouse-gas results from SimaPro were much closer to GREET as shown in the right-hand column in Table 6.2.

Table 6.2. SimaPro results for algae renewable diesel.

Item	GREET G CO ₂ eq/MMBTU	SimaPro Using Ecoinvent Emission Factors	SimaPro Using GREET Electricity Emission Factor
Total of all life cycle stages	67,629	81,345	72,482

LCA for Regional Algae Farms

Energy consumption and greenhouse-gas emissions associated with NAABB technologies were analyzed using the GREET model.⁶⁻⁸ GREET has been extended to include algae-biofuel production. The study considered original data from alternative algae strains, cultivation, and fuel production pathways listed earlier.

Algal Strains

Resource assessment data from the BAT model provided productivity and water demand month by month for several thousand locations over 30 years for three cases: generic freshwater, freshwater *Chlorella*, and saltwater *N. salina*. These data were studied with regard to seasonal, monthly, and yearly variability. The greenhouse-gas emissions during winter months were both highly variable

over the 30-year period and large in absolute value compared to emissions associated with petroleum diesel, which has 99,900 gCO₂eq/MMBTU. The amount of variability and the degree of increase in winter greenhouse-gas emissions depends upon the particular site while the spring and summer greenhouse-gas results were fairly uniform year-to-year, month-to-month, and site-to-site within the resource assessment sample.

For each algae species, monthly averaged life-cycle greenhouse-gas emissions were found for each of nine representative sites along the Gulf of Mexico and then averaged over each season (Figure 6.5). Greenhouse gas emissions averaged annually and over three and two seasons are presented in Table 6.3 with standard deviations over the representative site results. Productivity that is suitably high to avoid the high-emissions portion of the greenhouse-gas emissions curve is more important than peak productivity for reducing greenhouse-gas emissions. A robust growth regime over the entire year may be more important to algae greenhouse-gas emissions and energy use than choosing the highest peak value. Overcoming low winter biomass productivity, which leads to large winter emissions and highly variable fall emissions, remains a challenge and is called out as an important research objective for future projects since techno-economic analysis indicates that full-year operation is required for cost reasons.

Note that the focus in this part of the work was to consider fully scaled-up scenarios. Therefore, consideration of site-to-site variation in productivity was required. Although NAABB studied many other strains than those in Table 6.3, only the species shown had validated growth models that could be used for site-by-site growth performance. Future work should produce growth models for key NAABB strains and study LCA results for them at the 5 BGY or larger scale.

Table 6.3. Greenhouse-gas emissions by algae strain with multiple-season averages (gCO₂eq/MMBTU).

	Generic Algae Strain	<i>Chlorella</i>	<i>Nannochloropsis</i>
Annual	82,800 ± 10,500	134,800 ± 34,500	176,400 ± 46,300
Spring, Summer, Fall	65,100 ± 1700	76,100 ± 6000	106,400 ± 9100
Spring, Summer	62,500 ± 1100	65,500 ± 2700	94,800 ± 4700

Cultivation and Fuel-production Pathways

Two NAABB pathways were selected for LCA analysis: the ARID pond design and the hydrothermal liquefaction (HTL) of lipid extracted algae (LEA). ARID was considered because pond-mixing energy is one of the largest contributors to energy demand in the baseline process, accounting for roughly a quarter of the life-cycle fossil energy inputs to produce renewable diesel. The ARID, when using pumps with 60% total efficiency, reduces mixing energy from 48 kWh/ha/d (baseline raceway) to 24 kWh/ha/d and decreases the life-cycle greenhouse-gas emissions by about 30%.

NAABB investigated operations that converted lipid extracted residuals from *N. salina* to diesel blend stock by HTL and subsequent upgrading by hydrotreating. The associated process model was used for a life-cycle analysis to compare HTL processing of LEA with anaerobic digestion. This scenario benefited slightly from the lack of fugitive methane and nitrous oxide emissions assumed in anaerobic digestion models, although it had 15% higher fossil energy use. The following scenarios were considered and analyzed with GREET.

Scenario 1, HTL of LEA—Chlorella sp..DOE 1412 grown in ARID ponds. Lipids are extracted and the LEA is treated with HTL. We assume the same nutrient demand and biomass composition as for *Nannochloropsis* and the same HTL performance. Harvesting and dewatering is unchanged from the baseline system.

Scenario 2, HTL of whole algae—This system repeats the assumption for Scenario 1, but omits lipid extraction and associated energy demands including cell lysis and solvent extraction. We apply the HTL yield for *Nannochloropsis* LEA to the whole biomass. This scenario is testing whether the energy input to lipid extraction is adversely affecting the LCA outcome compared to a rough estimate of HTL performance on whole algae.

The greenhouse-gas emissions for Scenarios 1 and 2 are plotted versus areal productivity in Figure 6.6. The fossil energy and greenhouse-gas emissions are lower for Scenario 2 than for either Scenario 1 or the baseline. Cell lysis accounts for almost one third of the fossil inputs for Scenario 1. By removing cell lysis and solvent extraction, the life-cycle fossil energy decreased in Scenario 2. HTL is the largest fraction of the emissions for Scenario 2. Dissolved-air flotation, settling, and pond mixing are roughly equal portions of the emissions. Pond mixing was already cut in half through the use of ARID.

The two scenarios analyzed here showed that improvements in greenhouse-gas emissions compared to the baseline harmonization process can be made for both scenarios and lower fossil energy use is possible for Scenario 2 (Figure 6.6). Electricity reduction was possible when inefficient paddlewheels were replaced with pumps in the ARID design (both scenarios) and when cell lysis was omitted (Scenario 2). Increased fuel production occurred because of the HTL of LEA⁸

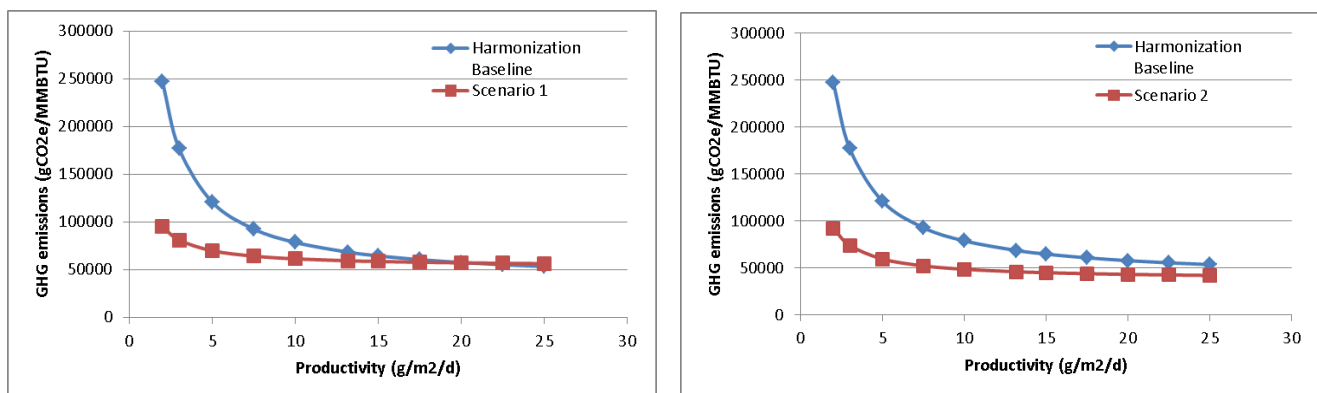


Figure 6.6. Productivity scan for the Scenario 1 (HTL of LEA) and Scenario 2 (HTL of whole algae) improved pathways.

While this analysis compared the performance of alternative and improved processes to the harmonization pathway, many assumptions were made to facilitate the comparison. For both these scenarios the greenhouse-gas emissions are very similar and possibly undifferentiated. The estimates presented here suggest that a species with productivity approximately 15 g/m²/d would have greenhouse-gas emissions roughly half that of petroleum diesel; however, it would be important to sustain the productivity throughout the year.

Additional LCA Studies

Additional LCA work focused on investigating important scenarios in algae life cycle as variations to the NAABB baseline. These were more specific to a particular aspect of production of biofuel from algae and report the variation in greenhouse-gas emissions for the given technology. The following scenarios were modeled in collaboration with NAABB researchers:

- UOP Ecofining™ process to jet fuel or renewable diesel;
- LCA of harvesting and extraction unit operations;
- Land-use change in large-scale algae cultivation; and
- Alternative LEA usage (cattle/mariculture feed).

UOP Ecofining™ process to jet fuel or renewable diesel—Different hydrotreated renewable fuel conversion systems were analyzed using the GREET model, harmonized inputs, and proprietary UOP jet fuel inputs. The life cycle greenhouse-gas emissions for jet fuel are 89,152 g CO₂eq/MMBTU compared to 67,629 g CO₂ eq/ MMBTU for renewable diesel. The largest difference between jet fuel production and diesel production comes at the fuel conversion stage, where jet fuel would result in 30,913 g CO₂eq/MMBTU fuel for conversion, while renewable diesel only results in greenhouse-gas emissions of 10,181 g CO₂eq/MMBTU fuel for conversion.

LCA of harvesting and extraction unit operations—Using NAABB data, the harvesting and extraction processes were all placed on an equivalent basis for comparison and the greenhouse-gas emissions impacts were analyzed using SimaPro LCA software. Table 6.4 contains the harvesting and extraction greenhouse-gas results. Membrane separation and acoustic (ultrasonic) harvesting appear to offer the most pronounced electricity and material input reductions, but these technologies may prove to be the most difficult in terms of scaling up to meet commercial demand. The acoustic (ultrasonic) extraction technology would offer significant greenhouse-gas emissions reductions, only requiring a small amount of electricity to complete the oil extraction.

Table 6.4. Harvesting and extraction technology comparison.

Item	Greenhouse-gas Emissions (g CO ₂ eq/MMBTU)	Percent Improvement over Baseline Technology*
Harvesting Technology**		
Baseline-Flocculation	19,202	--
Aluminum Flocculation	14,560	24%
Chitosan Flocculation	15,298	21%
Electrolytic Flocculation	4220	78%
Membrane Separation	1477	92%
Ultrasonic Harvesting	633	97%
Extraction Technology**		
Wet solvent extraction	51,381	—
Solvent Phase Algal Migration	177,988	-247%
Ultrasonic Extraction	31,652	38%
*Technology and inputs described in harmonized baseline LCA.		
**Electricity use in this comparison was from Ecoinvent database, in order to standardize emissions factors for electricity in all cases.		

Land-use change in large-scale algae cultivation—Land-use-change emissions of CO₂ are routinely neglected in algal biofuel LCA. The analysis of land-use change impacts greenhouse-gas emissions across the range of potential locations deemed suitable for algae cultivation within the NAABB group used an Intergovernmental Panel on Climate Change Tier 1 approach. As a first approximation for this site characterization, the same sites were used as for the BAT model identifying 4492 sites that were modeled for algae raceway facilities. Each 4800 ha site was classified as cropland, grassland, forestland, or marginal/barren according to a 2010 USDA dataset. A NAABB-wide estimate of potential land-use-change impacts for sites under consideration was generated as shown in Table 6.5. Land-use-change emissions of CO₂ from carbon-stock changes on lands converted to algae production is significant and should be included in algal biofuel LCA. A key result from this preliminary study is that clearing of forestland must be avoided when preparing for algal biofuel production.

Table 6.5. NAABB large-scale estimate of potential land use change impacts for algae cultivation.

State / site classification	Number of sites	% of State (or total)	Weighted Land-use-change Greenhouse-gas Emissions (g CO ₂ eq / MMBTU RD)
Texas	1115	24.8%	6752
Cropland	59	5.3%	4220
Pasture/grassland	755	67.7%	5697
Forestland	130	11.7%	18,358
Barren/marginal	171	15.3%	3482
Louisiana	41	0.9%	12,661
Pasture/grassland	41	100.0%	12,661
AL/MS	0	0.0%	0
Georgia	131	2.9%	54,757
Pasture/grassland	14	10.7%	10,023
Forest	117	89.3%	60,033
Florida	3204	71.3%	31,757
Cropland	2	0.1%	6119
Pasture/grassland	1603	50.0%	10,867
Forest	1372	42.8%	60,455
Barren/marginal	227	7.1%	5275
Total	4,492		26,060

Alternative LEA usage (cattle/mariculture feed)—A preliminary screening was performed on LEA usage for animal feed replacements. LEA was assumed to be used as a 1:1 (mass basis) replacement for soybean meal, cottonseed meal, fish meal, or trout feed. All nutrients lost in LEA export would have to be replaced with chemical fertilizers (urea and diammonium phosphate). No anaerobic digestion or use of solid anaerobic digestion byproducts would occur, and electricity or heat previously generated on-site would be replaced with U.S. grid electricity (using GREET assumptions) and with natural gas heat, respectively. Greenhouse-gas intensities for displaced feeds were obtained from the Ecoinvent™ database in SimaPro. Results are shown in Table 6.6. Displacing trout feed with LEA is the only scenario showing lower greenhouse-gas emissions than the anaerobic digestion baseline results.

Table 6.6. Greenhouse-gas emissions for alternate LEA usage scenarios.

LEA Usage Scenarios, for displacing					
	Anaerobic Digestion (g CO ₂ eq/MMBTU RD)	Soybean Meal	Cottonseed Meal	Fish Meal	Trout Feed
Total	72,482	127,662	154,038	102,762	39,987

Value of LEA

NAABB's feed trials with LEA showed that it could be successfully fed to cattle, sheep, poultry, shrimp, and fish as partial replacement for soybean meal in the feed ration. The potential market for LEA as a substitute for soybean meal in animal feed is very large, given the quantity of soybean meal used for feed in the United States (Figure 6.7). The prices of soybean meal and fish meal have varied considerably over the past two years, with the price of soybean meal averaging \$440/ton and fish meal averaging \$1620/ton (Figure 6.7).

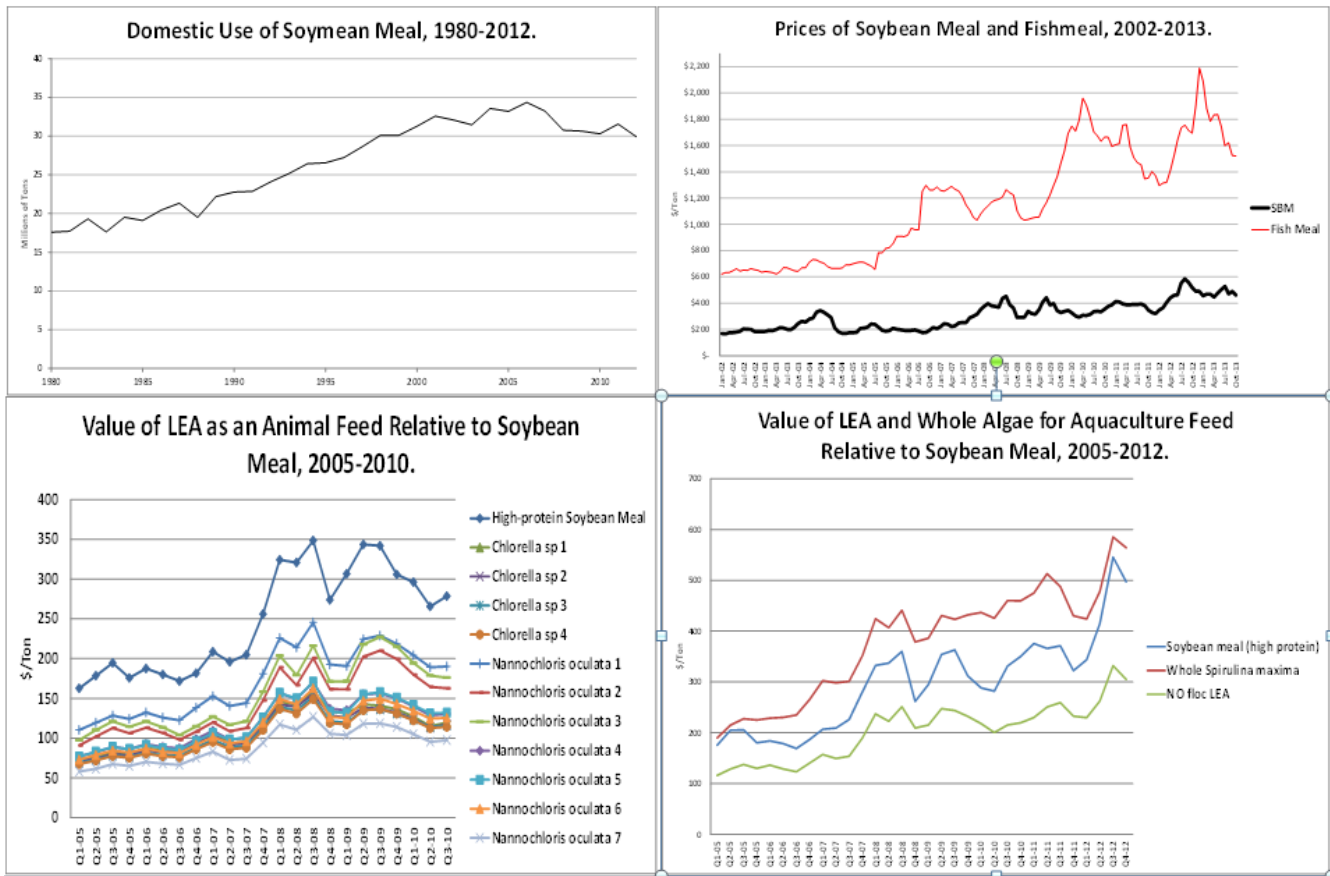


Figure 6.7. Soybean-meal demand, price of soybean meal and fishmeal, and value of LEA and whole algae for animal and aquaculture feed.

The quarterly prices of common livestock and aquaculture feed ration ingredients in 2005–2010 were used to infer the values of constituent nutrients: total digestible nutrients, crude protein, and ether extract (a measure of approximate fat content). The ingredient prices were then used in conjunction with the nutrient content of various LEA samples to infer the potential value that LEA would have had as a livestock and aquaculture ration ingredient from 2005–2010 using a hedonic econometric model⁹.

We found that LEA would have had considerable value as an animal feed ration ingredient, although it is less valuable than soybean meal owing to lower protein content and higher ash content than soybean meal. Changes in LEA value would correspond closely, but not perfectly, to changes in soybean meal value. We found that for most of the 2006–2010 period, LEA would have been valued between \$100 and \$225 per ton (Figure 6.7). In recent periods LEA would be valued at about \$100/ton less than soybean meal.

The value of whole algae and LEA for aquaculture analyses indicated that over the past three years whole algae was worth about \$100/ton more than high-protein soybean meal (Figure 6.7). On the other hand LEA as an aquaculture feed was worth an average of \$130/ton less than high-protein soybean meal.

Projections for 2014 soybean meal price is \$360/ton, which would make LEA for animal feed equal to \$260 to \$230/ton and whole algae fed to aquaculture equal to about \$460/ton. In summary, the value of LEA was deemed low relative to the value of nutrients and energy that can be captured and sold and thus result in lower net costs of production for algal biofuels.

Strain Evaluations

The Sustainability Team evaluated a number of scenarios for strain-specific production cost implications. The harmonized techno-economic analysis model assumptions were left unchanged with the previously published DOE harmonization assumptions for consistency. The updated BAT models were set on a farm size one-tenth of the original harmonization assumption, e.g., 405 ha of total pond area in the updated analyses rather than 4050 ha of pond area. Two strains considered under the NAABB research efforts were evaluated, namely a freshwater *Chlorella* strain and a saltwater *N. salina* strain. The results for both scenarios are presented below in Figures 6.8 and 6.9, respectively. Assuming a 10% return on investment, the *Chlorella* strain resulted in similar diesel selling prices as the updated generic strain (\$20/gal and \$19/gal). Any differences can be explained by the seasonal variability. This is consistent with prior findings from the harmonized techno-economic model.¹⁰ A key conclusion is that seasonal variability should be minimized either through strain selection or site

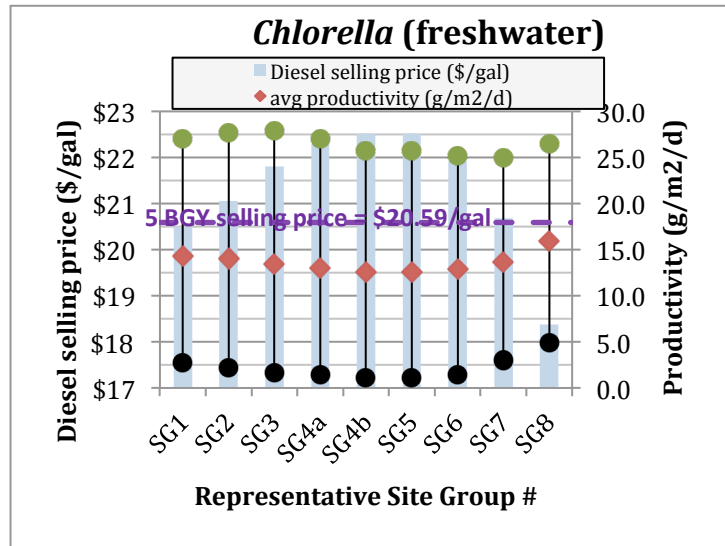


Figure 6.8. Techno-economic analysis results for freshwater *Chlorella* strain. The x-axis refers to the specific site modeled in Figure 6.5

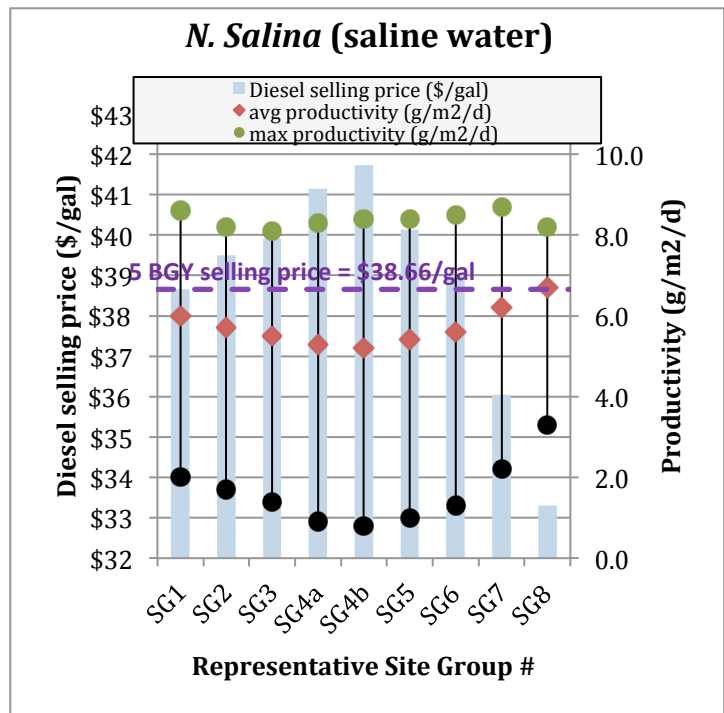


Figure 6.9. Techno-economic analysis results for *N. salina* strain. The x-axis refers to the specific site modeled in Figure 6.5.

selection to reduce production costs, given the high capital-cost dependency of the system and thus high cost penalties incurred during times of low utilization of the installed capital equipment. The *N. salina* scenario was seen to exhibit a considerably higher selling price at an average of \$38/gal, primarily due to much lower productivity values predicted in the BAT model.

Scaling Algae Equipment for Seasonal Production

The Sustainability team used the Algae Logistics Model (ALM)¹¹ for assessing the economic variability of algal systems considering spatial and temporal constraints. Figure 6.10 shows the average cost per gallon of triacylglycerides (TAGs) for the harmonized baseline design for six sites across the Southeast and Southwest. Average daily productivity data was passed into the model, and daily operating costs were assessed based on algae, water, nutrient, and process material throughput. Capital costs were assessed based on the infrastructure required to handle the throughput of each process during peak production of a 30-year simulation.

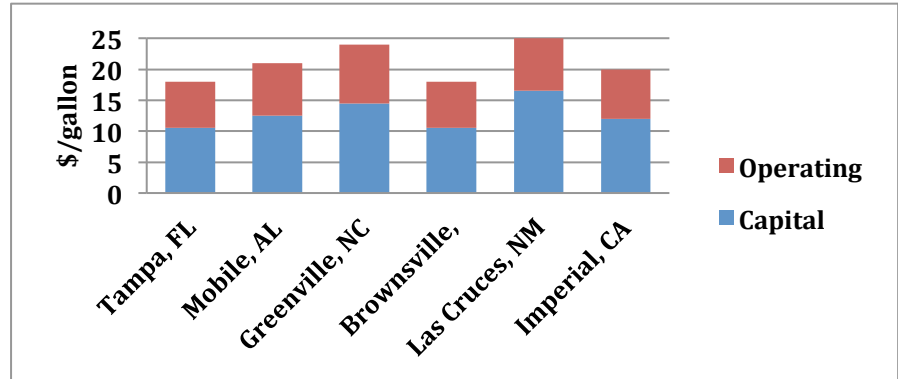


Figure 6.10. Cost assessment of the harmonized baseline design in several locations across the southern United States using respective BAT algal biomass productivity.

Using the scaling assumption of the 30-year peak production can lead to equipment remaining idle for long periods of the year or, in some cases, could lead to equipment not being used at all during the course of the year. To investigate this issue, a simulation was performed assessing costs if the algae-production system was scaled to the annual average productivity instead of the 30-year peak. Results show that if the algae-production system was designed around the 30-year average productivity rather than the peak production level, costs could be reduced by \$0.38 to \$3.48/gallon TAG (Figure 6.11). Due to the potential of lowering costs as much as 17%, further investigation is needed to determine appropriate scaling of algae-production systems based on biomass productivity potential.

Biological factors play a significant role in making algae a viable feedstock for biofuel production. Figure 6.12 shows potential costs of TAG under theoretical biomass productivity and lipid. To drive costs below \$5/gal TAG, the biomass productivity will need to be increased 2.5X over the baseline with a corresponding lipid content to 45%. Engineering advancement to



Figure 6.11. Investigation of appropriate scaling of algae-production systems using the harmonized baseline design and BAT algal-biomass productivity based on a system at 30-year peak biomass productivity or 30-year average biomass productivity.

existing technologies or development of new, innovative technologies will also be needed to decrease the cost below \$5/gal.

Nutrient Availability

The Sustainability team evaluated the nutrient requirements for algae; a baseline of 5 BGY of biofuels was assumed. Compositions of *Nannochloropsis* and *Chlorella* were found and compared to the 2011/2012 global fertilizer supplies of both nitrogen and phosphorus. To produce the target amount of biofuels, *Chlorella* would use almost 20% of the supplies and *Nannochloropsis* almost 40% for nitrogen fertilizer. The same trend is seen for phosphorus with *Nannochloropsis* using most all of the annual commercial fertilizer production. Nutrient recycling scenarios (anaerobic digestion, HTL, and catalytic hydrothermal gasification, CHG) were evaluated to estimate how they could decrease the commercial fertilizer requirement. CHG had the largest potential recycling percentages for nitrogen and phosphorus at 95% and 90%, respectively. For alternative sources of nutrients, concentrated animal feeding operations, animal slaughterhouses, aquaculture, spent coffee grounds, and chicken litter were evaluated. Wastewater provided less than 4% of the nitrogen and 3% of the phosphorus for *Chlorella* if it was grown in the Gulf region. The source with the largest potential was concentrated animal feeding operations, with broiler hen waste providing more than three times the required amount of phosphorus for *Chlorella* in the Gulf region. Combining recycling options with other nutrient sources would lower the nutrient requirements even further.

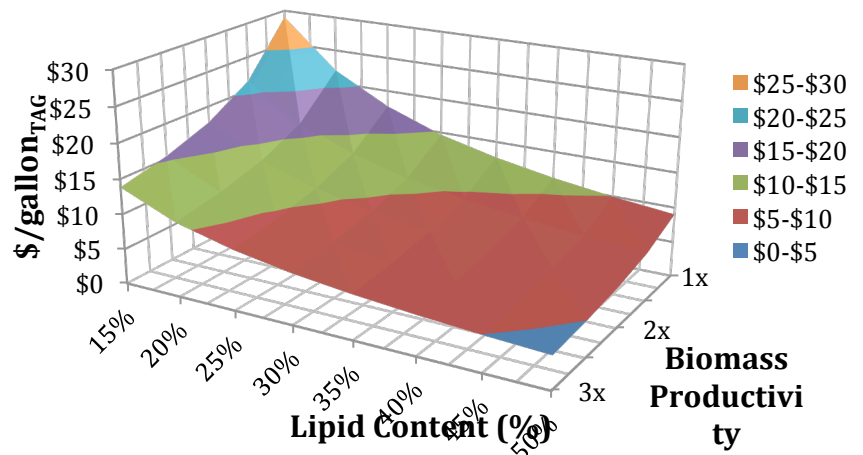


Figure 6.12. Analysis showing that the economic variability of algal biofuels is dependent on both enhanced biological productivity and improvements in engineering technologies.

Technology choices like HTL and anaerobic digestion can recover minerals for potential nutrient recycling and reprocessing into the world supply. HTL can recover 84% of the nitrogen in *Chlorella* and 74% in *Nannochloropsis*. This brings the estimated nitrogen requirement of *Nannochloropsis* down from 33% of the world supply to 9%. There were no results found for phosphorus recycling. Anaerobic digestion recycles 75% of the nitrogen and 50% of the phosphorus for both algal species. The phosphorus requirement for *Nannochloropsis* fell from 101% of the world surplus to 50%. Using additional sources of nutrients, like wastewater or animal waste, could lower the amount of world surplus fertilizers required even further.

Energy-limited Model of Algal Biofuel

The absence of thermodynamic and kinetic rate data for algae has previously limited the validity of computer-aided models. Therefore, NAABB integrated algae-specific data into techno-economic models to better understand the traditional pathway of producing biodiesel from crude lipid. Figure 6.13 shows the generalized block-flow diagram for the energy-limited process, which was

modeled using Aspen Plus¹² For cultivation, the “reactor” is divided into a growth phase and a lipid production phase. The energy-limited model combines the heats from formation of algae and algae-derived compounds, photosynthetic efficiency, incident light, and evaporation rate to estimate the cultivation area through a rigorous solution of mass and energy balances, allowing an analysis of total energy requirements and lost work. A detailed discussion of the initial version of this model has been published¹³ and presentations of the more advanced model were made at the conclusion of the NAABB program¹⁴⁻¹⁶. A separate model of light penetration, using Computational Fluid Dynamics (CFD-COMSOL)¹⁷ provided a range of pond depths, which were then implemented in the Aspen Plus model. The important outcomes of the energy-limited model and areas for additional research include:

1. The importance of recycling water, carbon, and debris and investigating the effects on algal growth;
2. The impact of pumping large amounts of water and developing methods to minimize this;
3. The importance of photosynthetic efficiency and continuing algal biology studies to improve this through genetic engineering; and
6. The value of using an integrated systems approach and computer-aided simulation.

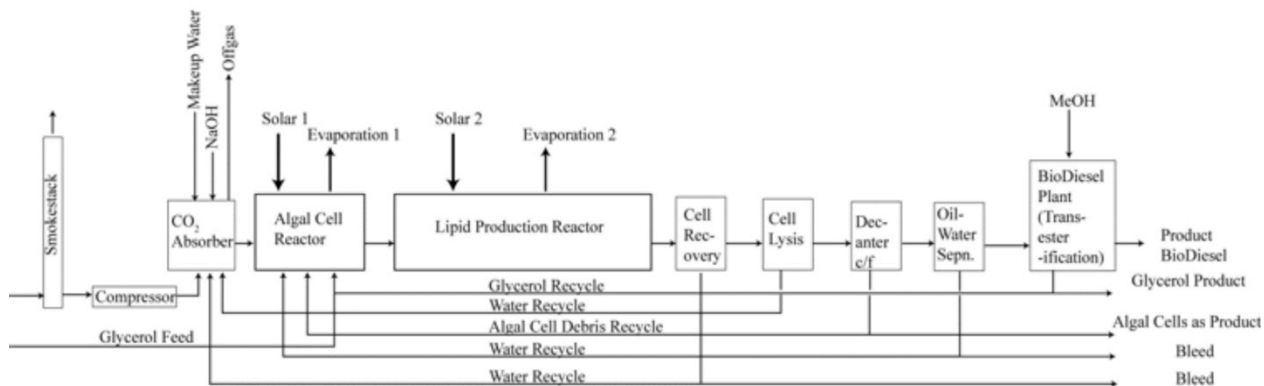


Figure 6.13. Generalized block-flow diagram for the energy-limited model of algal biofuel production.

A techno-economic analysis, based on the results of the energy-limited Aspen process model, was developed. It involved the simple costing of the process using direct industry data and real-world financial modeling based on venture capital practice. Then a techno-economic model combined the energy-limited algae growth model with harvesting and extraction estimates and a rigorously modeled glycerolysis/transesterification process. The harvesting and extraction technologies were all based upon either the NAABB baseline technologies or novel methods developed within NAABB¹⁷ A subsequent study¹⁸ takes into account other technologies that were developed outside NAABB. Harvesting and extraction methods were compared in terms of CAPEX, OPEX, and reliability and the most suitable option was selected in both cases. For the glycerolysis and transesterification processes, conversion experiments were performed with crude algal lipid. Glycerolysis was done to

lower the acid number of the crude lipid and extend catalyst life. Transesterification was done using a solid catalyst that is readily recycled, nontoxic, and nonflammable. The rate constants were regressed to adapt kinetic models to conversion data and then the process was simulated in Aspen Plus.

The model results highlighted that mechanisms existed to reduce the costs substantially from the \$10 to \$20 per gallon range to below \$4 per gallon by the aggressive recycling of key streams. The figure predicted by the techno-economic model was \$4.34/gallon of biodiesel. It should be noted, however, that in the early stages of projects of this type at least $\pm 50\%$ uncertainty would be expected and this should be noted as applying to all predictions. In addition, in the cost and financial models, tax is usually presented as a negative factor. However, in the investment model, tax credits/shields are a powerful, positive factor and are usually overlooked. The impact of these strategies on the process economics deserves closer study.

Overall, these models demonstrate that improvements in cultivation to increase productivity (either through biological or reactor improvements), improved harvesting and extraction methods tested at large scales, as well as maximizing recycle in the production process, are required for optimizing the economics of the algae-to-biodiesel industry,

Financial Feasibility Analysis

The Sustainability Team analyzed the economic feasibility of alternative NAABB technologies for the production of algal biofuels. The technologies that will be discussed were all demonstrated at sufficient scale to provide adequate information, showed promise for reducing costs over baseline, decreased overall energy utilization, and showed potential for scalability (Table 6.7). In addition, an evaluation was included for GMO data from a laboratory-scale strain of algae showing the potential for substantial productivity improvements. The four technologies selected for the financial analysis show significant gains in lowering costs, reducing energy input requirements, increasing production, and receipts. For example HTL-CHG reduces energy consumption 98% by not having to dry LEA, GMO strain increases production 250%, and ARID increases receipts 27%. Richardson, et al.¹⁸ report that HTL-CHG results in greater net cash income than pyrolysis due in part to recycling nutrients, so pyrolysis was not used for the financial analysis.

Methods

Data from NAABB's Algal Biology, Cultivation, Harvesting and Extraction, Conversion, Agricultural Coproducts, and Sustainability teams were used for an economic/financial feasibility study of selected NAABB technologies. The farm-level algae risk model (FARM) is a farm-level Monte Carlo economic/financial simulation model developed by NAABB for analyzing the financial feasibility of algae farms. The model is designed to facilitate analysis of the probability of economic returns and costs of crude oil production for an algae farm under alternative management/technology systems. The model is an integrated systems compilation of several techno-economic models for different phases of a commercial algae farm, but it does not stop there as it includes the financial, marketing, and tax aspects of a farm.

The simulation results provide estimates of the probability of economic success for different pathways, as well as the costs of production for algae crude oil and the sensitivity of the costs of production to changes in CAPEX and OPEX. A detailed description of the FARM model is provided in Richardson and Johnson²

Table 6.7. Comparison of NAABB innovations considered for financial feasibility analysis.

Baseline Technology	Technology Innovation as Demonstrated	Benefit of Innovation	Scalability of Innovation
<u>Centrifugation</u> Ubiquitous use in test beds	<u>Electrocoagulation (EC)</u> Pilot scale validation, 3000 L/h Tested with <i>Chlorella</i> sp.	Produces a low mineral product contamination (flocculation mode) 17% lower CAPEX than centrifuge 3% lower OPEX 9% higher recovery efficiency 9% higher receipts	Available commercially @ 270,000 L/h processed in commercial unit
<u>Open lined ponds</u> Pecos traditional paddle wheel raceway at 23,000 L Seasonal data used	<u>ARID</u> 24,000 L open pond Seasonal data used Validated process model for production	27% increase in receipts 38% increase in annual productivity	Patent available for licensing
<u>Wet-solvent extraction</u> Valicor based technology 10–20% solids used 96% extraction efficiency of crude lipid	<u>HTL-CHG</u> All work done in continuous reaction systems (2 L/h) Used 10–30% solids	68% reduction in OPEX 60% increase receipts Solvent-free process 280% increase in crude yield Methane sold 98% reduction in energy consumption Up to 70% of biomass carbon captured Potential for recycling of water and nutrients	Design and construction of a 1 ton/day processing unit in progress
<u><i>Chlorella</i> sp. DOE1412</u> NAABB prospect strain	<u>GMO</u> Extrapolation of modified laboratory strain of <i>C. reinhardtii</i> cultured in PBRs	240% increase in receipts 250% increase in biomass productivity	Moving genetic traits into <i>Chlorella</i> production strains Permitting requirements to be addressed

Results for analyzing the seven scenarios over a 10-year planning horizon are summarized using a reduced number of key output variables from FARM. The overall profitability of an algae farm scenario is reported using the net present value, probability of economic success, and total cost of production. The probability of economic success is the probability that the farm scenario generates a positive net present value, i.e., that the internal rate of return exceeds the 10% discount rate. Each scenario was simulated for 100 combinations reducing CAPEX and OPEX in 10% increments from 0 to 90%. This results in three matrices

of 100 average net present values, probabilities of economic success, and total costs. The resulting matrices provide a sensitivity analysis indicating the potential profitability if CAPEX and OPEX can be reduced by alternative fractions. The projected average total costs per gallon of algae crude oil and ton of biomass are reported for the 100 combinations of CAPEX and OPEX. Total cost equals the estimated total cash cost of production plus depreciation costs minus credits for byproducts such as LEA and methane. All of the key output variables are presented using the 10x10 matrix for alternative reductions in CAPEX and OPEX. The values in the tables are color-coded using a stoplight scheme of red, yellow, and green for bad, marginal, and good, respectively.

In total, seven scenarios based on combining the four innovations in Table 6.7 are evaluated. Each technology represents a different NAABB work group and contributes to significant decreases in total costs of producing algal crude oil relative to the base NAABB technology (Figure 6.14). In addition to analyzing the economic and financial feasibilities of these technologies, paths forward to further reduce costs and increase the probability of success will be described.

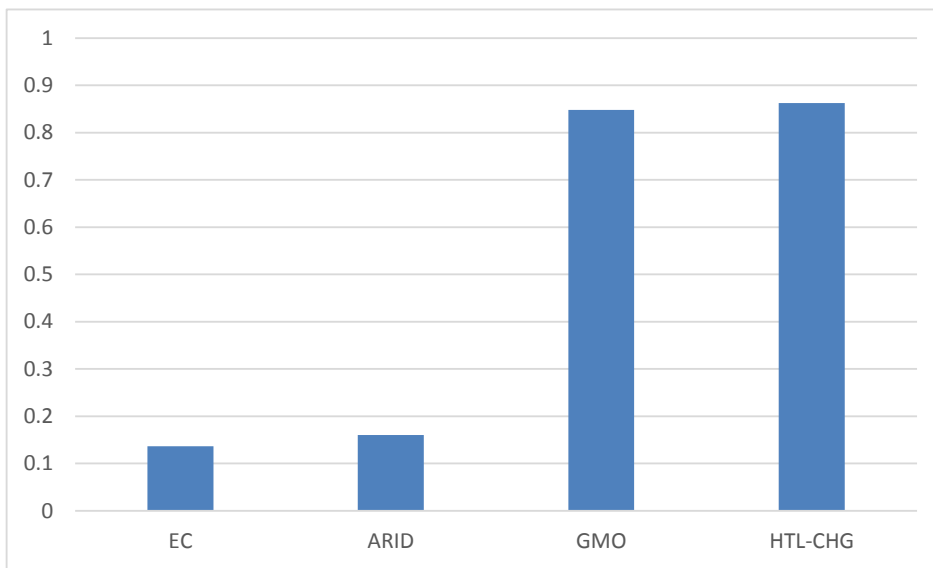


Figure 6.14. Fractional reductions in total costs of production for algae crude oil assuming no CAPEX and OPEX reductions.

Scenarios

The seven scenarios analyzed focused exclusively on fuel production as required by the original Funding Opportunity Announcement. These scenarios show the synergistic effect of new innovations as they are brought to bear on the process of producing algae crude oil. The different combinations of technology improvements from biology, cultivation, harvesting, and extraction are summarized in Table 6.8. Scenario 1 is the NAABB baseline with current algae productivity levels and uses conventional methods for cultivation (lined open ponds) of a *Chlorella* sp., harvesting (centrifugation), and wet-solvent extraction. Scenario 2 highlights the economic contributions of using electrocoagulation (EC) in place of centrifuges for harvesting. Scenario 3 highlights the improvements in economic contributions of the ARID cultivation system and its associated increased productivity. The comparison of Scenario 1 to Scenario 4 allows one to

quantify the economic gains of HTL-CHG over using wet solvent extraction and conventional algae production and harvesting parameters. Scenario 5 combines the improvements in harvesting (EC), extraction (HTL-CHG), and increased algae productivity due to utilization of a GMO strain. The total economic gains in Scenario 5 can be compared to Scenario 1 to evaluate the improvement since the beginning of NAABB. Scenario 6 is used to highlight the economic contributions of the ARID cultivation system with the EC and HTL-CHG systems and their associated increased productivity. Scenario 7 includes all synergistic improvements from the above NAABB innovative technologies.

Each scenario in Table 6.8 was programmed in FARM. For the results provided, we modified the CAPEX and OPEX reported by Davis, et al.¹⁰ based on improvements and data from NAABB innovations. Algae farms for Scenarios 1, 2, 4, and 5 are assumed to be located in Pecos, Texas, while Scenarios 3, 6, and 7 are located in Tucson, Arizona. The ARID scenario algae farms are located in Tucson, Arizona, because that is the only location where the ARID raceway system has been tested.

The monthly biomass production for both farm locations was simulated by the BAT model. BAT produced monthly biomass yields for 30 years based on simulated monthly weather data for the farm sites. The 30 years of monthly biomass production from the BAT model was used to estimate a multivariate probability distribution of monthly biomass, lipid content, and water consumption. The multivariate distributions are used in the FARM model to simulate monthly production of biomass, TAG, HTL bio-oil, LEA, and methane, and their associated cost of production and revenues. The BAT monthly biomass probability distributions were scaled up on a relative basis to accommodate the increased biomass production for the GMO Scenarios 5 and 7.

The EC, ARID, and HTL-CHG technologies highlighted in Scenarios 2–7 are described elsewhere in the report. In the GMO scenarios (5 and 7) biomass production is increased by 50% in the winter (October–February), 100% in the spring and fall (March, July–September), and 200% in the summer (April–June); lipid content is increased to 50% and the probability of pond crashes is reduced 50%.

A summary of the assumptions for the seven scenarios is provided in Tables 6.8a, 6.8b, and 6.8c. Biomass production, harvesting and extraction throughput capacity, and CAPEX differences are highlighted in the tables and reflect information provided by the technology developers.

Table 6-8. Summary of the technologies analyzed for the seven alternative scenarios.

	Scenario 1	Scenario 2	Scenario 3	Scenario 4	Scenario 5	Scenario 6	Scenario 7
Products	Crude TAG & LEA	Crude TAG & LEA	Crude TAG & LEA	Crude HTL oil & methane			
Cultivation	Open pond w/liners	Open pond w/liners	ARID w/liners	Open pond w/liners	Open pond w/liners	ARID w/liners	ARID w/liners
Biology g/m²/d	Generic 7.4	Generic 7.4	Generic 9.3	Generic 7.4	GMO 19.4	Generic 9.3	GMO 23.2
Harvesting	Centrifuge	EC	EC	Centrifuge	EC	EC	EC
Extraction	Wet solvent extraction	Wet solvent extraction	Wet solvent extraction	HTL-CHG	HTL-CHG	HTL-CHG	HTL-CHG
Nutrient Recycling	No	No	No	Yes	Yes	Yes	Yes
Biomass Production (tons/y)	119,900	119,900	152,200	119,900	316,800	152,200	378,600
Crude Oil Production (gallons/y)	4,679,000	5,096,000	6,470,000	13,506,000	42,321,000	20,332,000	51,570,000
Location	Pecos, TX	Pecos, TX	Tucson, AZ	Pecos, TX	Pecos, TX	Tucson, AZ	Tucson, AZ

Table 6-8a. Key input parameters for seven scenarios.

	Scenario 1	Scenario 2	Scenario 3	Scenario 4	Scenario 5	Scenario 6	Scenario 7
	Centrifuge-Wet Solvent	EC-Wet Solvent	EC-Wet Solvent-ARID	Centrifuge-HTL-CHG	EC-HTL-CHG-GMO	EC-HTL-CHG-ARID	EC-HTL-CHG-ARID-GMO
Location	Pecos, TX	Pecos, TX	Tucson, AZ	Pecos, TX	Pecos, TX	Tucson, AZ	Tucson, AZ
Cultivation	Open pond	Open pond	Open pond	Open pond	Open pond	ARID	ARID
Total Hectares of Land	4850	4850	4850	4850	4850	4850	4850
Total Hectares of Ponds	4050	4050	4050	4050	4050	4050	4050
Total Volume of Ponds (AF)	9855	9855	2941	9855	9855	2941	2941
Total Volume of Ponds (millions of liters)	12,156	12,156	3.63	12,156	12,156	3.63	3.63
Days of Operation	330	330	330	330	330	330	330



Table 6-8b. Operating costs, expenses, and capacities for seven scenarios.

	Scenario 1	Scenario 2	Scenario 3	Scenario 4	Scenario 5	Scenario 6	Scenario 7
Harvesting	Centrifuge	EC	EC	Centrifuge	EC	EC	EC
Throughput Capacity (l/hr)	113,560	408,780	408,780	113,560	408,780	408,780	408,780
Capital Cost (M\$\$/unit)	0.275	0.65	0.65	0.275	0.65	0.65	0.65
Number of Units	2231	620	185	2,231	620	185	185
Total Harvesting Capital Cost (M\$)	613.5	403.35	120.6	613.5	403.35	120.6	120.6
% Solids	10%	8%	8%	10%	8%	8%	8%
Harvesting Chemicals OPEX (M\$\$/yr. 5)	0	19.52	6.26	0	19.52	5.83	5.83
Extraction	Wet Solvent	Wet Solvent	Wet Solvent	HTL-CHG	HTL-CHG	HTL-CHG	HTL-CHG
Throughput Capacity (l/hr)	394,300	394,300	394,300	39,500	39,600	39,600	39,600
Capital Cost (M\$\$/unit)	23.57	23.57	23.57	10.20	10.20	10.20	10.20

Table 6-8c. CAPEX differences for seven scenarios.

	Scenario 1	Scenario 2	Scenario 3	Scenario 4	Scenario 5	Scenario 6	Scenario 7
	Centrifuge- Wet Solvent	EC-Wet Solvent	EC-Wet Solvent - ARID	Centrifuge- HTL-CHG	EC-HTL-CHG - GMO	EC-HTL-CHG - ARID	EC-HTL-CHG - ARID - GMO
CAPEX (M\$)							
Land	35.9	35.9	35.9	35.9	35.9	35.9	35.9
Construction	6.7	6.7	158.98	6.7	6.7	158.98	158.98
Liner	205.2	205.2	156.9	205.2	205.2	156.9	156.94
Paddlewheels	138.6	138.6	0	138.6	138.6	0	0
Total CAPEX	1211.9	1001.8	1012.2	1259.8	1059.8	1109.3	1070.3
OPEX (M\$)							
Labor & Overhead	4.9	4.9	6.3	5.0	5.1	6.4	6.5
Natural Gas	418.7	418.7	419.0	4.0	9.0	5.1	10.9
Electricity	64.2	64.0	61.1	64.7	95.1	61.6	92.8
Maintenance	41.6	17.0	18.2	43.2	25.1	18.1	20.4
Insurance	2.4	2.0	2.0	2.5	2.4	2.0	2.1
Interest	263.7	246.5	253.9	133.8	291.7	100.2	102.2
Total OPEX Year 5	820.1	798.7	792.6	263.4	467.0	211.2	261.1

Results

The total economic plus financial costs per gallon of algae crude oil for the seven scenarios and the individual NAABB innovations are summarized in Figure 6.15. The costs reflect the total costs simulated from the FARM model assuming no reductions in CAPEX and OPEX. The pre-NAABB economic plus financial cost of production for a gallon of crude oil is calculated to be more than \$230/gallon. Each NAABB technology analyzed in Scenarios 2–7 contributes to reducing total costs. The combination of the EC, ARID, HTL-CHG, and GMO technologies in Scenario 7 developed and tested by NAABB reduce the total cost from more than \$230/gallon for the base case to less than \$7.40/gallon.

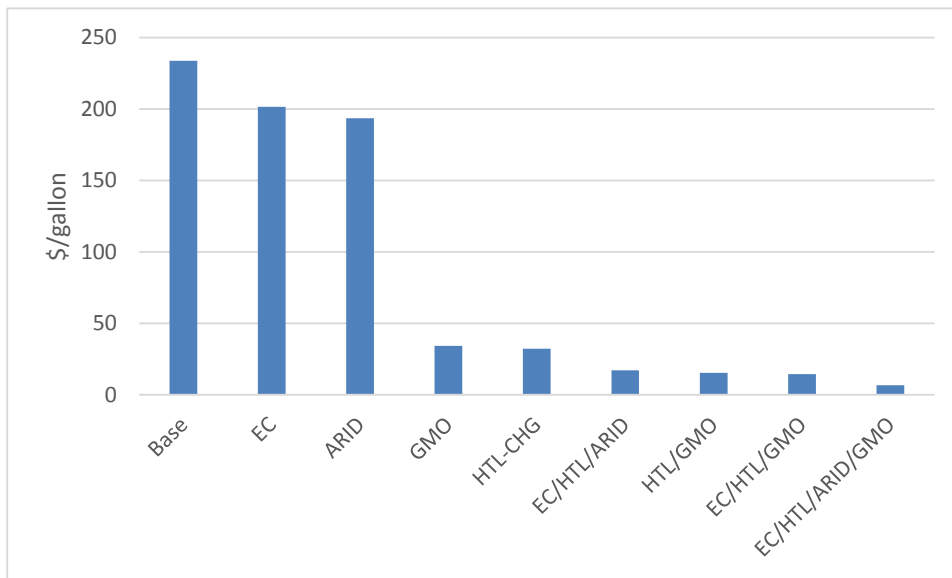


Figure 6.15. Total economic plus financial costs of production for algae crude oil, shown for pre-NAABB technology and for alternative technologies developed by NAABB (\$/gallon).

Table 6.9 summarizes the results of all seven technology scenarios. The reduction in CAPEX and OPEX rows show the respective fractional reductions needed for the algae farm to obtain a reasonable probability of economic success. There are two probabilities of success listed for each scenario, e.g., 0.0–98% (Scenario 5). The first probability of success listed is the probability of economic success for the farm when neither CAPEX nor OPEX is reduced. The second value is the probability of economic success when the reductions in CAPEX and OPEX from the above rows are used. In Scenario 5, for example, when the algae farm does not reduce its CAPEX or OPEX the farm has a probability of success of 0.0. However, when the farm reduces its OPEX by 80% and CAPEX by 70%, the farm has a 98% probability of economic success. The average total costs (\$/gal of crude oil) in Table 6.9 are for the assumed reductions in CAPEX and OPEX. Assuming a 70% reduction in CAPEX and an 80% reduction in OPEX the Scenario 5 total cost (\$/gal of crude oil) averages \$2.10/gallon with a 95% confidence interval of \$1.80/gallon and \$2.70/gallon. The confidence intervals are similar to reporting error bars, but confidence intervals are more robust because they report the 95% confidence interval about the mean rather than a one standard deviation from the mean.

Table 6.9. Summary of results for scenarios 1–7.

	Scenario 1	Scenario 2	Scenario 3	Scenario 4	Scenario 5	Scenario 6	Scenario 7
	Centrifuge Wet Solvent Extraction	EC Harvesting Wet Solvent Extraction	EC with Wet Solvent Extraction & ARID	Centrifuge HTL-CHG Extraction	EC with HTL-CHG & GMO Algae	HTL-CHG EC & ARID Cultivation	EC, ARID, HTL-CHG & GMO Algae
Reduction in CAPEX	90%	90%	90%	80%	70%	70%	50%
Reduction in OPEX	90%	90%	90%	90%	80%	80%	50%
p (Success)	0.0–0.0	0.0–0.0	0.0–0.0	0.0–89%	0.0–98%	0.0–67%	0.0–55%
Average total cost \$/gal	16.40	13.20	8.00	2.10	2.20	3.10	2.80
Lower confidence interval TC \$/gal	13.50	10.60	6.20	1.80	1.80	2.70	2.50
Upper confidence interval TC \$/gal	22.00	18.00	10.80	2.70	2.90	3.80	3.50

In Scenarios 2–6 substantial reductions in CAPEX and OPEX are required to provide a reasonable probability of economic success, as shown in Table 6.9. For example, Scenario 4 would require 80% reduction in CAPEX and a 90% reduction in OPEX to achieve a 89% probability of success. Scenario 7 requires a more reasonable reduction in CAPEX and OPEX of 50% to achieve a 55% chance of economic success. The results for Scenario 7 are highlighted in the next section as it represents the synergies of the four NAABB innovations and has a high probability of economic success at more reasonable cost reduction levels.

The average net present value for each fractional reduction in CAPEX and OPEX for Scenario 7 is summarized in Table 6.10. Average net present value reports the average net increase in wealth and income earned by investing in an algae farm, expressed in 2013 dollars. When net present value is negative the investment failed to return a rate of return in excess of the investor’s discount rate of 10%. There are 41 combinations of CAPEX and OPEX reductions in Scenario 7 that return positive average net present values. Positive net present values are likely if CAPEX and OPEX are reduced 50% or more and if either CAPEX or OPEX is reduced further the algae farm will be even more profitable.

The probability of economic success for each combination of fractional reductions in CAPEX and OPEX for the algae farm in Scenario 7 is reported in Table 6.11. There are 36 combinations of reductions in CAPEX and OPEX that result in probabilities of economic success greater than 75%. Total costs of production for algae crude oil and algae biomass are presented in Table 6.12. The total cost per gallon is \$7.40 with no reductions in CAPEX and OPEX but can be

reduced to \$2.80 per gallon if CAPEX and OPEX are reduced by 50%. If CAPEX and OPEX can both be reduced by 70% the cost of algae crude oil is less than \$2/gallon. The cost of biomass is calculated at \$1033/ton if CAPEX and OPEX are not reduced and the biomass cost is calculated at \$395/ton if both CAPEX and OPEX are reduced 50% and \$205/ton if both CAPEX and OPEX can be reduced 70% (Table 6.10).

Table 6.10. Average net present value for Scenario 7 assuming alternative fractional reductions in CAPEX and OPEX (M\$)

Net Present Value (M\$)

Open Pond Fraction OPEX	Fractional Reductions in the CAPEX									
	0	0.1	0.2	0.3	0.4	0.5	0.6	0.7	0.8	0.9
0	-1078	-967	-856	-745	-634	-523	-412	-302	-191	-81
0.1	-965	-854	-743	-632	-521	-411	-300	-190	-82	25
0.2	-851	-741	-630	-519	-409	-299	-190	-83	22	119
0.3	-738	-627	-517	-407	-298	-191	-85	17	113	205
0.4	-625	-515	-406	-298	-192	-89	11	105	195	285
0.5	-513	-406	-300	-196	-94	3	95	184	273	362
0.6	-407	-303	-201	-102	-6	84	173	261	349	437
0.7	-307	-207	-111	-17	73	161	249	336	424	511
0.8	-216	-121	-29	61	149	236	323	410	497	584
0.9	-133	-41	48	135	222	308	395	481	568	654

Table 6.11. Probability of economic success for Scenario 7 assuming alternative fractional reductions in CAPEX and OPEX.

Probability of Economic Success

Open Pond Fraction OPEX	Fractional Reductions in the CAPEX									
	0	0.1	0.2	0.3	0.4	0.5	0.6	0.7	0.8	0.9
0	0%	0%	0%	0%	0%	0%	0%	0%	0%	7%
0.1	0%	0%	0%	0%	0%	0%	0%	0%	6%	68%
0.2	0%	0%	0%	0%	0%	0%	0%	5%	67%	100%
0.3	0%	0%	0%	0%	0%	0%	4%	65%	100%	100%
0.4	0%	0%	0%	0%	0%	3%	61%	100%	100%	100%
0.5	0%	0%	0%	0%	2%	55%	99%	100%	100%	100%
0.6	0%	0%	0%	1%	45%	99%	100%	100%	100%	100%
0.7	0%	0%	1%	33%	98%	100%	100%	100%	100%	100%
0.8	0%	0%	23%	95%	100%	100%	100%	100%	100%	100%
0.9	0%	13%	90%	100%	100%	100%	100%	100%	100%	100%

Table 6.12. Total cost of production for algae crude oil and biomass for Scenario 7 assuming alternative fractional reductions in CAPEX and OPEX.

Average Total Cost per Ton of Biomass (\$/Ton) and per Gallon of Lipid (\$/Gallon)

ARID Fraction OPEX	Fractional Reductions in the CAPEX									
	0	0.1	0.2	0.3	0.4	0.5	0.6	0.7	0.8	0.9
0	1,033	963	894	825	756	688	620	553	486	420
	7.40	6.90	6.40	5.90	5.40	4.90	4.50	4.00	3.50	3.00
0.1	963	895	826	758	691	624	557	491	426	361
	6.90	6.40	5.90	5.50	5.00	4.50	4.00	3.50	3.10	2.60
0.2	896	828	761	694	628	563	498	433	368	305
	6.40	6.00	5.50	5.00	4.50	4.00	3.60	3.10	2.60	2.20
0.3	831	765	700	634	569	505	440	376	314	256
	6.00	5.50	5.00	4.60	4.10	3.60	3.20	2.70	2.30	1.80
0.4	771	705	641	576	512	447	385	325	270	216
	5.50	5.10	4.60	4.10	3.70	3.20	2.80	2.30	1.90	1.60
0.5	712	647	583	519	455	395	338	284	230	176
	5.10	4.70	4.20	3.70	3.30	2.80	2.40	2.00	1.70	1.30
0.6	654	590	526	464	407	352	298	244	191	137
	4.70	4.20	3.80	3.30	2.90	2.50	2.10	1.80	1.40	1.00
0.7	597	535	475	420	366	312	259	205	151	98
	4.30	3.80	3.40	3.00	2.60	2.20	1.90	1.50	1.10	0.70
0.8	545	488	434	380	326	273	219	165	112	58
	3.90	3.50	3.10	2.70	2.30	2.00	1.60	1.20	0.80	0.40
0.9	501	447	394	340	287	233	179	126	74	35
	3.60	3.20	2.80	2.40	2.10	1.70	1.30	0.90	0.70	0.60

Summary of Scenario Results

The results from simulating a large algae farm with technologies developed by NAABB scientists suggest that algal crude oil could be financially feasible if CAPEX and OPEX can be reduced further. However, the NAABB innovations remain untested in large outdoor raceways. Scenario 1, with the base technology, had a zero probability of economic success, even when CAPEX and OPEX were reduced by 90%. Scenario 7 analyzed the use of all NAABB innovations and shows a high probability of success with a 50% reduction in both CAPEX and OPEX. The commercial production of algae for biofuels is not economically or financially feasible at this time, but, as our modeling shows, the combination of improvements in strain characteristics, cultivation, harvesting, and extraction can increase the likelihood of economic viability. Great strides have been made by the NAABB consortium, but continued enhancements are needed in algal biology, and would be further useful in the areas of cultivation, harvesting, and extraction.

Further research to improve algal biology and crop protection is a pathway to reduced costs of production for algae crude oils. The total costs that may be expected from improved biology and crop protection are summarized in Figure 6.16, assuming no reductions in CAPEX and OPEX. These costs start with the combination of NAABB technologies (Scenario 7) and then decrease in a nonlinear fashion as we increase the biomass productivity to drive costs of algal crude oil to \$2/gallon. This analysis shows that with the NAABB technologies, the biomass productivity to drive total costs to \$2/gallon will need to be more than 150 g/m²/d.

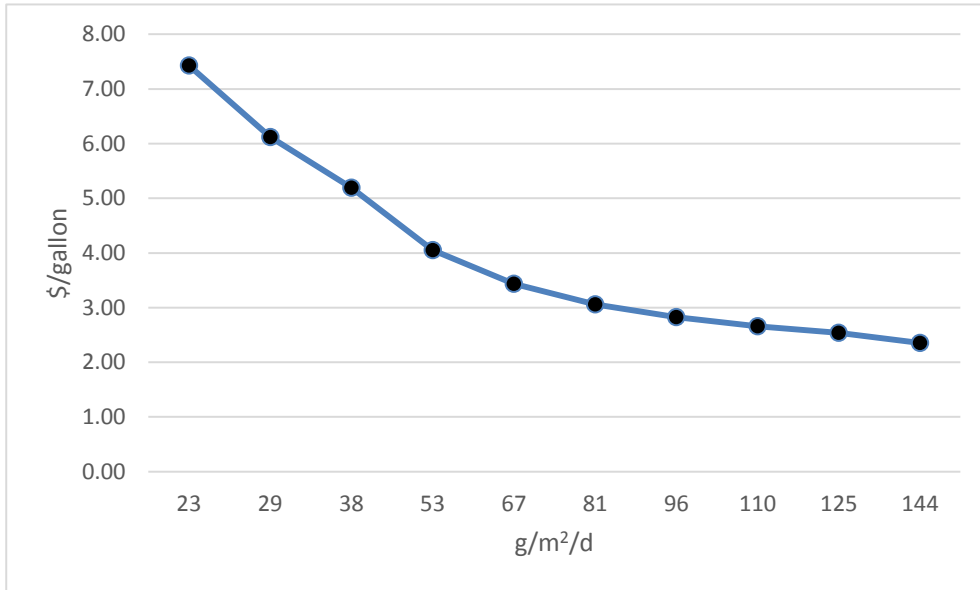


Figure 6.16. Total economic plus financial costs per gallon of algae crude oil assuming alternative rates of biomass productivity and NAABB technologies for harvesting (EC) and extraction (HTL-CHG) without reductions in CAPEX and OPEX.

Global Impacts

A global impacts study evaluated the general equilibrium economic effects of establishing an algal biofuels industry, including effects on agricultural commodity production, commodity prices, and food insecurity. Eleven scenarios with varying biofuels policy assumptions and varying algal technological assumptions were evaluated. All scenarios that forced an increase in consumption of higher priced biofuels resulted in reduced consumption of blended fuels due to the higher price. In the scenarios featuring an algal tax credit, consumer prices for blended fuel are not substantially changed, consumption of blended fuels is not substantially reduced, and U.S. petroleum consumption and imports are reduced only to the extent that a small amount of petroleum is replaced with biofuel.

Land use is minimally affected by introducing large-scale production of algal biofuels. Effects on food insecurity are mediated primarily by changes in U.S. imports of crude oil. Under current technologies, forcing production and consumption of 5 BGY of algal crude oil would tend to increase global food insecurity by between 0.5% to 1.5% in most scenarios due to declines in petroleum exports. Overall, the changes in global food insecurity caused by increasing any U.S. use of any biofuel are small compared to the improvements caused by growing global capital stocks and increases in agricultural productivity.

Conclusions and Recommendations

NAABB's efforts helped bring together the LCA and techno-economic analysis community to develop a harmonized set of assumptions and agree on a baseline comparison for algal fuel production. The experiments and analysis conducted by NAABB indicate that significant technical challenges remain and that algae is

further from technological readiness than previously thought but that algal biofuels can be sustainable if the amount of water and energy used per unit of biomass produced is reduced. Reductions in water in individual process steps is likely to produce nonlinear reductions in CAPEX and OPEX. Reductions in energy consumption and increases in productivity will produce linear reductions in the sustainability metrics of CAPEX, OPEX, and energy consumption.

Summary of Findings

The key findings from the NAABB integrated modeling effort are:

- Algae production appears to be more feasible in the states along the Gulf of Mexico, with *Chlorella* as the best performing algae species and the South Florida region as the most profitable.
- Obtaining year-round advanced biofuels status for algal biodiesel will be an issue unless winter-month net CO₂ emissions can be reduced.
- Year-round algae production will be necessary for algae farming to be profitable.
- Land-use-change emissions of CO₂ from carbon-stock changes on lands converted to algae production is significant and should be included in algal biofuel LCA; clearing of forestland must be avoided when preparing for algal biofuel production.
- Electrocoagulation is a more economical and lower-cost harvesting method than centrifuges.
- Thermal chemical conversion is a more profitable extraction method than either wet solvent extraction or pyrolysis.
- Forty percent reductions in CAPEX and OPEX will be required to provide adequate rates of return to attract investment capital in sufficient quantities to make the industry profitable.
- Significant advances in biology to increase biomass production in open ponds will be required to make the industry economically sustainable.
- The lipid pathway to LEA for feed is not a profitable pathway as the nutrient loss exceeds the value of the LEA as a feed supplement for animals and aquaculture.
- Low CAPEX cultivation systems need to be advanced.
- The total cost per gallon is \$7.40 with no reductions in CAPEX and OPEX but can be reduced to <\$3.00 per gallon if CAPEX and OPEX are reduced by 50% for the NAABB technologies. The biomass productivity to drive total costs to \$2/gallon will need to be increased to 150 g/m²/d.
- Algae crude oil commercialization will require large capital investments and will likely result in a small number of large firms.
- All renewable fuel policy scenarios that forced an increase in consumption of higher priced biofuels resulted in reduced consumption of blended fuels due to the higher price.
- Overall, the changes in global food insecurity caused by increasing any U.S. use of any biofuel are small compared to the improvements caused by growing global capital stocks and increases in agricultural productivity.

Greenhouse-gas Potential Sustainability of Algal Fuels

It is important to provide a path forward for research and development of this important feedstock because algae have the potential to secure the energy future of the United States. As world populations rise out of poverty, the challenge of providing food, energy, and wastewater treatment will become increasingly more difficult. Algae can provide meaningful solutions to these problems.

The relatively high use of physical capital, water, nutrients, energy, and CO₂ per gallon of fuel produced needs to be addressed for the fuel to be sustainable. The following recommendations provide guidance based upon the results of the integrated and separate modeling conducted during the course of NAABB.

Recommendations

- Overcome low winter biomass productivity and variable fall biomass productivity through:
 - Robust winter strains of algae;
 - Crop rotation and protection;
 - Stable storage of algae biomass;
 - CO₂ supply management; and
 - Thermal management of ponds.
- Improve water management strategies through:
 - Coupling local water chemistry with tolerant algae strains for cultivation;
 - Strains that thrive in compromised waters; and
 - New cultivation methods that minimize water use and low capital requirements.
- Recycling of nutrients is required through:
 - Technologies that make nitrogen, phosphorous, and other nutrients bioavailable;
 - Processes that capture nutrients effectively; and
 - Better understanding of nutrient mass balance throughout the whole system and impacts on life cycle.
- The lipid pathway requires higher value for LEA than currently observed through:
 - Higher LEA value;
 - More efficient extraction systems;
 - Higher lipid productivity;
 - New methods to recycle nutrients from LEA and
 - LCA tradeoffs for nutrient recycling.

Based on the research conducted by NAABB, the following broad research areas are important to the sustainability of algal biofuels:

- Reduction of water in the entire production system;
- Stabilization of biomass for processing;

- Robust cultivation systems;
- Improved production stains;
- Cost-effective sourcing of CO₂, water, and nutrients; and
- Improvements in industrial design and logistics.

The work completed by NAABB highlights the need for innovative research into cultivation technologies and the conclusion that this research must be closely linked to the extraction technologies. By considering water in cultivation conjointly with extraction, nonlinear reductions in the environmental and economic impacts of algae-based biofuels can be realized, which will push algal fuels onto a more sustainable pathway.

Team Members

Paul Blowers, University of Arizona
Ryan Davis, National Renewable Energy Laboratory
C. Meghan Downes, New Mexico State University
Eric Dunlop, Pan Pacific
Edward Frank, Argonne National Laboratory
Robert Handler, Michigan Technical University (UOP)
Deborah Newby, Idaho National Laboratory.
Philip Pienkos, National Renewable Energy Laboratory
James W. Richardson, Texas A&M University
Warren Seider, University of Pennsylvania.
David Shonnard, Michigan Technical University (UOP)
Richard Skaggs, Pacific Northwest National Laboratory

Publications

Full-length, Peer-reviewed Publications

Bryant, H., I. Gogichaishvili, D. Anderson, J. Richardson, J. Sawyer, T. Wickersham, and M. Drewery. The value of post-extracted algae residue. *Algal Research* 1 (2012): 185–193.

Dunlop, E.H, A.K. Coaldrake, C.S. Silva, and W.D Seider. An energy-limited model of algal biofuel production: Toward the next generation of advanced biofuels. *AIChE Journal* 59 (2013): 4641–4654.

Handler, R.M, C.E. Canterg, T.N. Kalnes, F.S. Lupton, O. Kholiqovu, D.R. Shonnard, and P. Blowers. Evaluation of environmental impacts from microalgae cultivation in open-air raceway ponds: analysis of the prior literature and investigation of wide variance in predicted impacts. *Algal Research* 1 (2012): 83–92.

Handler, R.M., D.R. Shonnard, T.N. Kalnes, and F.S. Lupton. Life cycle assessment of algal biofuels: Influence of feedstock cultivation systems and conversion platforms. *Algal Research* 4 (2014): 105-115.

Richardson, J.W. and M.D. Johnson. Economic viability of a reverse engineered algae farm (REAF). *Algal Research* 3 (2014): 66-70.

Richardson, J.W., M.D. Johnson, R.Lacey, J.Oyler, and S. Capareda. Harvesting and extraction technology contributions to algae biofuels economic viability. *Algal Research* 5 (2014): 70-78.

Richardson, J.W., M. Johnson, and J. Outlaw. Economic comparison of open pond raceways to photo bio-reactors for profitable production of algae for transportation fuels in the Southwest. *Algal Research* 1 (2012): 93–100.

Richardson, J.W., M.D. Johnson, X. Zhang, P. Zemke, W. Chen, and Q. Hu. A financial assessment of two alternative cultivation systems and their contributions to algae biofuel economic viability. *Algal Research* 4 (2014): 96-104.

Silva, C., E. Soliman,, G. Cameron, L.A. Fabiano, W.D. Seider, E.H. Dunlop, and A.K. Coaldrake. Commercial-scale biodiesel production from algae. *Industrial & Engineering Chemistry Research* (2013): DOI 10.1021/ie403273b.

Sun, A, R. Davis, C. M. Starbuck, A. Ben-Amotz, R. Pate, and P.T. Pienkos. Comparative cost analysis of algal oil production for biofuels. *Energy* 36 (2011): 5169–5179.

Venteris, E.R., R.L. Skaggs, A.M. Coleman, and M.S. Wigmosta. An assessment of land availability and price in the coterminous United States for conversion to algal biofuel production. *Biomass and Bioenergy* 47 (2012): 483e497.

Venteris, E.R., R.L. Skaggs, M.S. Wigmosta, and A.M. Coleman. Regional algal biofuel production potential in the coterminous United States as affected by resource availability trade-offs. *Algal Research* (2014): *In Press*.

Other Important Publications

ANL; NREL; PNNL. Renewable diesel from algal lipids: An integrated baseline for cost, emissions, and resource potential from a harmonized model. (2012): ANL/ESD/12-4; NREL/TP-5100-55431; PNNL-21437. Argonne, IL: Argonne National Laboratory; Golden, CO: National Renewable Energy Laboratory; Richland, WA: Pacific Northwest National Laboratory.

Downes Starbuck, C. M. First principles of technoeconomic analysis of algal mass culture. *Handbook of Microalgal Culture: Applied Phycology and Biotechnology*. Ed. Amos Richmond and Qiang Hu. Wiley and Blackwell. (2013): Chapter 15.

Laur, P. and E.J. Sullivan. Producing algae-based biofuels from produced water. *Water Resources IMPACT* 14 (2012): 15–16.

Richardson, J.W., J.L. Outlaw, and M. Allison. The economics of micro algae oil. *AgBioForum* 13 (2010): Article 4.

Starbuck, C.M. Comment on “Environmental life cycle comparison of algae to other bioenergy feedstocks.” *Environmental Science and Technology* (2010): DOI 10.1021/es103102s.

References

1. Wigmosta, M. S., A. M. Coleman, R. J. Skaggs, M. H. Huesemann, and L. J. Lane. National microalgae biofuel production potential and resource demand. *Water Resources Research* 47 (2011): W00H04.
2. Richardson, J. W. and M. D. Johnson. Algae Income Simulation Model: AISIM. Texas A&M AgriLife Research, Agricultural and Food Policy Center, Research Report (2012): 12–4.
3. Richardson, J. W., M. D. Johnson and J. L. Outlaw. Economic comparison of open pond raceways to photo bio-reactors for profitable production of algae for transportation fuels in the Southwest. *Algal Research* 1 (2012): 93–100.
4. Handler, R.M, C.E. Canterg, T.N. Kalnes, F.S. Lupton, O. Kholiqov, D.R. Shonnard, and P. Blowers. Evaluation of environmental impacts from microalgae cultivation in open-air raceway ponds: Analysis of the prior literature and investigation of wide variance in predicted impacts. *Algal Research* 1 (2012): 83–92.
5. Goedkoop, M., A. D. Schryver, and M. Oele. SimaPro 7.1 Tutorial. PRé Consultants, the Netherlands (2007): <http://www.stanford.edu/class/cee214/Readings/SimaPro7Tutorial.pdf>
6. Argonne National Laboratory. Life Cycle Analysis of Algal Lipid Fuels with the GREET Model. ANL/ESD/11-5. Argonne, IL: Argonne National Laboratory (2011).
7. Frank, E., J. Han, I. Palou-Rivera, A. Elgowainy, and M. Wang. Methane and nitrous oxide emissions affect the life cycle analysis of algal biofuels. *Environmental Research Letters* 7 (2012): 014030.
8. Frank, E., A. Elgowainy, J. Han, and Z. Wang. Life cycle comparison of hydrothermal liquefaction and lipid extraction pathways to renewable diesel from algae. *Mitigation and Adaptation Strategies for Global Change* 18 (2013): 137–158.
9. Bryant, H.L., I. Gogichaishvili, D. Anderson, J.W. Richardson, J. Sawyer, T. Wickersham, and M.L. Drewery. The value of post-extracted algae residue. *Algal Research* 1 (2012): 185–193.
10. Davis, R. et al., Renewable diesel from algal lipids: An integrated baseline for cost, emissions, and resource potential from a Harmonized Model. ANL/ESD/12-4; NREL/TP-5100-55431; PNNL-21437. Argonne, IL: Argonne National Laboratory; Golden, CO: National Renewable Energy Laboratory; Richland, WA: Pacific Northwest National Laboratory (June 2012).
11. Abodeely, J.M., A.M. Coleman, D.M. Stevens, A.E. Ray, K.G. Cafferty, and D.T. Newby. Assessment of algal farm designs using a dynamic modular approach. *Algal Research* (2014): *In press*.
12. Nathanson, R. B., T. A. Adams III, and W. D. Seider. Aspen Icarus Process Evaluator (IPE). University of Pennsylvania (May, 2008): http://higherdbcs.wiley.com/legacy/college/seider/0470048956/pdf/apse_n_IPE_course_notes.pdf

13. Dunlop, E.H., A.K. Coaldrake, C.S. Silva, and W.D. Seider. An energy-limited model of algal biofuel production: Toward the next generation of advanced biofuels. *AIChE Journal* 59 (12) (2013): 4641-54.
14. Dunlop, E.H. and A.K. Coaldrake An energy-limited model for algal biofuel production: A systems engineering approach to techno-economic modeling. Paper presented at 3rd International Conference on Algal Biomass, Biofuels & Bioproducts, Toronto, 2013.
15. Dunlop, E.H. Modeling light penetration in algal bioreactors. 2nd International Conference on Algal Biomass, Biofuels and Bioproducts, San Diego, June 10-13, 2012.
16. Silva, C.S. E. Soliman, G. Cameron, L.A. Fabiano, W.D. Seider, E.H. Dunlop, and A.K. Coaldrake. Design of algae transesterification processes. Oral Presentation delivered at AIChE Annual Meeting, Pittsburgh, PA, 2012.
17. Silva, C., E. Soliman, G. Cameron, L.A. Fabiano, W.D. Seider, E.H. Dunlop, and A.K. Coaldrake. Commercial-scale biodiesel production from algae. *Industrial & Engineering Chemistry Research* (2013): DOI 10.1021/ie403273b.
18. Richardson, J.W., M.D. Johnson, R.Lacey, J.Oyler, and S. Capareda. Harvesting and extraction technology contributions to algae biofuels economic viability. *Algal Research* 5 (2014): 70-78

